Evaluating techniques to improve visual performance with and assessment of premium intraocular lenses

SANDEEP KAUR DHALLU

Doctor of Philosophy

ASTON UNIVERSITY

January 2015

ASTON UNIVERSITY

Evaluating techniques to improve visual performance with and assessment of premium intraocular lenses

SANDEEP KAUR DHALLU
Doctor of Philosophy
January 2015

Summary

Premium Intraocular Lenses (IOLs) such as toric IOLs, multifocal IOLs (MIOLs) and accommodating IOLs (AIOLs) can provide better refractive and visual outcomes compared to standard monofocal designs, leading to greater levels of post-operative spectacle independence. The principal theme of this thesis relates to the development of new assessment techniques that can help to improve future premium IOL design.

IOLs designed to correct astigmatism form the focus of the first part of the thesis. A novel toric IOL design was devised to decrease the effect of toric rotation on patient visual acuity, but found to have neither a beneficial or detrimental impact on visual acuity retention. IOL tilt, like rotation, may curtail visual performance; however current IOL tilt measurement techniques require the use of specialist equipment not readily available in most ophthalmological clinics. Thus a new idea that applied Pythagoras's theory to digital images of IOL optic symmetricality in order to calculate tilt was proposed, and shown to be both accurate and highly repeatable. A literature review revealed little information on the relationship between IOL tilt, decentration and rotation and so this was examined. A poor correlation between these factors was found, indicating they occur independently of each other.

Next, presbyopia correcting IOLs were investigated. The light distribution of different MIOLs and an AIOL was assessed using perimetry, to establish whether this could be used to inform optimal IOL design. Anticipated differences in threshold sensitivity between IOLs were not however found, thus perimetry was concluded to be ineffective in mapping retinal projection of blur.

The observed difference between subjective and objective measures of accommodation, arising from the influence of pseudoaccommodative factors, was explored next to establish how much additional objective power would be required to restore the eye's focus with AIOLs. Blur tolerance was found to be the key contributor to the ocular depth of focus, with an approximate dioptric influence of 0.60D. Our understanding of MIOLs may be limited by the need for subjective defocus curves, which are lengthy and do not permit important additional measures to be undertaken. The use of aberrometry to provide faster objective defocus curves was examined. Although subjective and objective measures related well, the peaks of the MIOL defocus curve profile were not evident with objective prediction of acuity, indicating a need for further refinement of visual quality metrics based on ocular aberrations.

The experiments detailed in the thesis evaluate methods to improve visual performance with toric IOLs. They also investigate new techniques to allow more rapid post-operative assessment of premium IOLs, which could allow greater insights to be obtained into several aspects of visual quality, in order to optimise future IOL design and ultimately enhance patient satisfaction.

Key words: Premium IOL, misalignment, retinal projection, objective accommodation, aberrometry.

Acknowledgements

There are many people I would like to thank for their help during my postgraduate studies. Firstly, I wish to express a sincere thanks to my supervisors Professor James Wolffsohn and Dr Amy Sheppard for their advice, expertise and guidance throughout the course of the thesis. It has been an honour to work alongside you.

I would also like to thank Dr. Raymond Applegate at the University of Houston, USA for his valuable assistance with the image quality metrics used in my aberrometry project, to Dr Toshifuma Mihashi at the University of Tokyo, Japan for his help with the aberrometer, and to both Dr Thomas Drew and Dr Alec Kingsnorth for their time and technical support.

Thank you to Lenstec, Florida for the funding to support my postgraduate studies and all participants who kindly gave up their time to take part in this research – it is very much appreciated.

A warm thank you is extended to my fellow postgraduate friends and colleagues in the Optometry Department, who have provided continual advice and support during my time at Aston University.

And finally, I reserve my biggest thanks for my dear family- to my dad Rajinder, mum Balbir, sisters Barinder and Maninder and nephew Amrit. Thank you for being there for me over the past three years. I am truly grateful to you all for your unfailing support, unconditional love and continuous encouragement.

Contents

CHAPTER 3: Evaluation of a simplified method of measuring intraocular lens tilt

CHAPTER 4: Evaluating long term tilt, decentration and rotation of an implanted IOL

CHAPTER 5: Visual field analysis of two different multifocal and an accommodative intraocular lens

CHAPTER 6: Restoring eye focus- how much additional objective accommodation would we need?

CHAPTER 7: Can Aberrometry Provide Rapid and Reliable Measures of Subjective Depth of Focus following Multifocal Intraocular Lens Implantation?

List of Abbreviations

ACD   -Anterior chamber depth

AFC   -Alternate forced choice

AIOL   -Accommodative intraocular lenses

ANOVA   -Analysis of variance

ANSI   -American National Standards Institute

AS-OCT   -Anterior Segment Optical Coherence Tomography

ATR   -Against the rule

BVD   -Back vertex distance

CCD   -Charged coupled device

CM   -Ciliary muscle

CMOS   -Complementary symmetry metal oxide semiconductor

CSFN   -Neural contrast sensitivity function

dB   -Decibels

DCNVA   -Distance corrected near visual acuity

DOF   -Depth of field/focus

ECCE   Extracapsular extraction

FS   -Femtosecond laser

HOA   -Higher order aberration

HPR   -High pass resolution

IOL   -Intraocular lens

LED   -Light emitting diode

MD   -Mean deviation

MIOL   -Multifocal intraocular lenses

MTF   -Modulation transfer function

Nd: YAG   -Neodymium-doped yttrium aluminium garnet

OBL   -Oblique

OTF   -Optical transfer function

OTFDL   -Diffraction limited optical transfer function

PCO   -Posterior capsular opacification

PMMA   -Polymethylmethacrylate

PSF   -Point spread function

PSD   -Pattern standard deviation

RMS   -Root mean square

SA   -Spherical aberrations

SD   -Standard deviation

SITA   -Swedish interactive threshold algorithm

SLD   -Super luminescent diode

VA   -Visual acuity

VSX   -Visual strehl ratio

WTR   -With the rule

List of tables

List of figures

CHAPTER 1: The ageing eye

1.1. Introduction

Cataracts are a leading cause of readily curable blindness (WHO, 2007) and are estimated to affect over 100 million people worldwide (Pascolini *et al.*, 2012). In developed countries, cataract extraction followed by implantation of an intraocular lens (IOL) is a routine and relatively cost-effective intervention. Standard IOLs, which have a single, fixed focal length, are currently the most commonly implanted lens type (Horvath *et al.*, 2014). However in recent years, there have been rapid advances in IOL design, which have led to the commercialization of 'premium' or advanced technology IOLs such as toric, multifocal and accommodating IOLs. This chapter will provide a review detailing the evolution of intraocular lenses and will also outline the mechanism of action and visual outcomes achievable with premium IOLs.

1.2. Cataract

The crystalline lens is an anteriorly located ocular structure which contributes one third of the eye's refractive power and plays a critical role in accommodation for younger eyes (Gullstrand, 1924). For optimal visual performance it should be transparent. Cataract describes the pathological opacification of the crystalline lens and can be congenital or acquired (Ong *et al.*, 2014). Ageing is typically the most common cause of acquired cataract (Asbell *et al.*, 2005) which occurs as a result of the continual addition of new fibres to the lens mass throughout life; this results in the crystalline lens becoming increasingly more densely packed and less optically clear over time (Al-Ghoul *et al.*, 2001;Asbell *et al.*, 2005). Other causes of acquired cataract include use of certain medications such as corticosteroids, from ocular trauma or secondary to ocular and systemic diseases such as diabetes mellitus (Pollreisz *et al.*, 2010;Ong *et al.*, 2014).

Age-related cataracts can be categorized into three main types: nuclear, cortical and posterior subcapsular and these may occur alone or together in various combinations (Asbell *et al.*, 2005;Michael *et al.*, 2011). Cataract development can impair vision by reducing the amount of light that passes through the increasingly opaque crystalline lens, causing a decrease in retinal image quality (Asbell *et al.*, 2005). Furthermore, they may initiate a change in refractive error, typically a myopic shift with nuclear cataract, as well as an increase in the amount of ocular light scatter, both of which can affect visual performance and may lead to reports of reduced visual acuity, loss of colour discrimination and complaints of glare (Asbell *et al.*, 2005).

Global estimates indicate there to be approximately 285 million visually impaired people across all age groups. Surveys conducted in 39 countries indicated that the leading causes of this visual impairment were uncorrected refractive error followed by cataract, which accounted for 43% and 33% of cases respectively. An estimated 39 million people across the world are blind, with the primary cause in 51% of these cases attributed to cataract (Pascolini *et al.*, 2012). In general, cataract is treatable and it is possible to restore all functions of the natural crystalline lens, except accommodation, with cataract surgery (Ong *et al.*, 2014). Cataract surgery is one of the most commonly performed surgical procedures with an estimated 19 million operations carried out per year globally (Donaldson *et al.*, 2013), it is also one of the most cost-effective procedures (Asbell *et al.*, 2005). In the UK an estimated 300,000 operations are conducted annually by the National Health Service (Trikha *et al.*, 2013). The volume of cataract surgery has increased dramatically since the 1980s (Taylor, 2000) due to growth and ageing of the population (Asbell *et al.*, 2005).

1.2.1. Surgical management of cataract

The first attempts at surgical treatment of cataracts were rather rudimentary and high risk; they involved a surgical technique known as "couching" where a needle was used to displace the cloudy lens into the vitreous body so that it was away from the line of sight (Ridley, 1952;Schemann *et al.*, 2000). This technique has been described as far back as 700BC in Hindu literature, and was also popular in ancient Greek and Roman civilizations. It remained a common procedure up until the 19th century (Bidyadhar, 1955;Saxena, 1965;Raju, 2003). Some of the main post-operative complications associated with couching include: infection, secondary glaucoma, iridocyclitis with or without hypopyon, hyphema, leucoma adherens and retinal detachment (Saxena, 1965). Couching is still performed in some of the world's poorest countries, particularly sub-Saharan Africa (Signes-Soler *et al.*, 2012) and is often the preferred treatment method despite the greater risk and reduced effectiveness compared to more advanced methods of cataract extraction (Saxena, 1965;Schemann *et al.*, 2000). Rabiu *et al.* (2001) conducted a population based cross sectional survey to determine barriers to the uptake of cataract services in rural northern Nigerian communities and determined factors such as an inability to afford treatment, lack of trust, and a greater availability of traditional techniques, such as couching, to be the key influences.

Surgical techniques for cataract management have moved on rapidly from the rather basic procedure of couching and records show that approximately two hundred years ago intracapsular extractions were being performed (Asbell *et al.*, 2005). Intracapsular cataract extraction involves surgical removal of the cloudy lens and capsular bag via a large corneo-scleral incision. Extracapsular cataract extraction (ECCE) developed from this technique and also involved delicate surgical removal of the opacified lens material but not the capsular bag, which was left intact. By this time IOLs were being developed and this capsular bag was left intact with a view to holding this type of artificial lens

22

implant in situ. Keeping the lens capsule was found to be advantageous because of its action as a barrier between the anterior and posterior segments of the eye, which reduced the risk of vitreous problems, retinal detachment and cystoid macular oedema with ECCE (Linebarger *et al.*, 1999;Asbell *et al.*, 2005).

Phacoemulsification, first developed by Charles Kelman in 1967, is a popular surgical method of treatment for cataracts in developed countries such as the UK and has changed little over the past 25 years (Nagy *et al.*, 2009;de Silva *et al.*, 2014). It involves creating a small corneal incision approximately three millimetres in size, through which a probe is inserted. This probe uses high frequency ultrasonic waves to gently liquefy the cataractous lens material so that it can then be aspirated through an irrigation-aspiration system, leaving the capsular bag intact. For this reason, phacoemulsification is sometimes thought of as a modified extracapsular extraction technique.

Although ECCE is associated with a higher incidence of induced astigmatism as well as a longer visual recovery time compared to phacoemulsification, it is the preferred option for cataract removal in economically disadvantaged countries while phacoemulsification predominates in developed countries (Pershing *et al.*, 2011;de Silva *et al.*, 2014). ECCE is favoured in disadvantage countries due to the greater expense associated with purchasing and maintaining phacoemulsification equipment as well as costs associated with surgical training (Khanna *et al.*, 2011). ECCE is also favoured for patients with dense cataracts, as they as more likely to experience post-operative corneal oedema with phacoemulsification (Pershing *et al.*, 2011). Phacoemulsification devices can damage corneal endothelial cells due to mechanical trauma from ultrasound waves as well as from thermal injury (Conrad-Hengerer *et al.*, 2013;Mayer *et al.*, 2014). A greater loss of corneal endothelial cells occurs after

cataract surgery with reported cell losses varying between 4% and 25% (Mencucci *et al.*, 2006). This can give rise to problems such as corneal decompensation and oedema (Mayer *et al.*, 2014).

Recently femtosecond lasers (FS), which generate short pulses of energy at a near infrared wavelength (Roberts *et al.*, 2013), have been introduced to the cataract surgery procedure to increase its automation and potentially improve safety. FS lasers can be used to create precise corneal incisions (Moshirfar *et al.*, 2011;Mayer *et al.*, 2014) without damaging adjacent tissues, One-way, self sealing, water tight FS laser guided corneal incisions that are less prone to leakage and more stable, can be created in order to access the anterior chamber (Moshirfar *et al.*, 2011). FS laser can also be used to create accurate and reproducible capsulotomies. An irregularly shaped capsulotomy can affect IOL position leading to decentration and tilt therefore creating a symmetrical capsulotomy is important in ensuring IOL stability (Kranitz *et al.*, 2011). Additionally, FS lasers can also be used to help break up the lens nucleus prior to removal, although aspiration still requires an inserted probe. Research has shown FS systems decrease the ultrasound energy that is required for phacofragmentation with all levels of cataract (Moshirfar *et al.*, 2011;Naranjo-Tackman, 2011). In a porcine eye study conducted by Nagy *et al.* (2009), FS laser was found to reduce the required phacoemulsification power by 43% and to shorten phacoemulsification time by 51%. There is therefore less likely to be damage to surrounding ocular structures with FS lasers since the shock and acoustic waves they produce dissipate within 100μm of the lens tissue targeted (Nagy *et al.*, 2009). Conrad-Hengerer *et al.* (2013) found that use of FS lasers led to significantly lower endothelial cell loss compared to standard phacoemulsification, which is a key advantage in patients with known corneal endothelial cell dysfunction, such as Fuchs endothelial dystrophy (Mayer *et al.*, 2014). Additionally, less corneal oedema can speed up visual recovery post-operatively

(Conrad-Hengerer *et al.*, 2013). Early studies suggest FS lasers to have a good record of safety, with a low incidence of post-operative complications (Nagy *et al.*, 2009;Moshirfar *et al.*, 2011) although published studies have not yet evaluated their long term safety (Conrad-Hengerer *et al.*, 2013). Possible disadvantages of FS laser assisted cataract surgery include an increased rate of anterior capsule tears (Bali *et al.*, 2012). Some early studies comparing FS laser assisted cataract surgery with conventional surgery have reported similar visual acuity outcomes with both procedures (Nagy *et al.*, 2012;Donaldson *et al.*, 2013) while others found better refractive outcomes with FS laser cataract surgery compared to conventional cataract surgery (Filkorn *et al.*, 2012). Uy *et al.* (2011) compared refractive results in eyes undergoing FS laser anterior capsulotomy with those receiving a manual continuous curvilinear capsulorhexis and found a spherical equivalent closer to the target refraction in the laser group. After removal of the cataract, a foldable artificial intraocular lens is placed into the intact capsular bag to restore vision back to satisfactory levels. Such procedures are carried out on a routine basis in developed countries such as the UK (Apple *et al.*, 1996;Donaldson *et al.*, 2013;Roberts *et al.*, 2013;Trikha *et al.*, 2013).

1.3.   History of Intraocular lenses

IOLs were first developed by Sir Harold Ridley over sixty years ago. Ridley witnessed the inert nature of polymethylmethacrylate (PMMA) imbedded inside the eye whilst serving as a RAF ophthalmologist during the Second World War and this observation inspired the invention of the first intraocular lens. At the time, routine cataract operations only involved removal of the cloudy lens material, leaving patients with a refractive error in the region of +20D. As a result of this, patients were forced to wear thick and unsightly aphakic spectacles to restore vision. Ridley was one of the first to suggest that surgically removing the opacified lens material provided only a partial

solution to the problem of cataract. It was believed that subsequent implantation of a suitably calculated IOL offered a more complete cure as it removed this post-operative need for thick aphakic spectacles, leaving only a requirement of spectacles for near tasks (Ridley, 1952;Apple *et al.*, 1996;Kershner, 2003;Bhartiya *et al.*, 2009).

The first IOL operation was carried out by Ridley in 1949 using an IOL composed of a modified PMMA material, otherwise known as Perspex. Ridley was concerned about the purity of commercially available PMMA and so to minimise any unforeseen risk requested a purer form to be made specifically for the purpose of ocular implantation (Apple *et al.*, 1996). Ridley carried out an extracapsular cataract extraction procedure on the patient and successfully implanted an IOL some weeks later. However, IOLs implanted in this way were found to be prone to displacement which spurred the development of new IOLs that were designed to sit in the anterior as opposed to posterior chamber, tethered at the irido-corneal angle. Although these lenses were easier to insert, initial anterior chamber IOLs produced undesirable corneal effects such as corneal decomposition and oedema (Jaffe, 1996). Iris supported IOLs were subsequently developed to overcome the problems that occurred with these earlier IOLs and these were relatively successful, although there were some reports of pupil deformation and iris chafing (Bhartiya *et al.*, 2009). The vulnerability of the anterior chamber prompted a return to posterior chamber IOLs development. IOLs have since undergone vast improvements in both their design and optical quality. Developmental milestones include the invention of foldable IOLs which enabled smaller corneal incisions to be made and thus facilitated faster recovery time post-operatively (Apple *et al.*, 1996;Kershner, 2003;Bhartiya *et al.*, 2009). The lenses described above were all of a spherical design. Present IOLs include toric, multifocal, and accommodating designs often referred to as "premium" or "advanced technology" IOLs (Ale *et al.*, 2012; Mingo-Botin *et al.*, 2010; Mendicute *et al.*, 2009) as well as those intended for a more niche

market such as telescopic lenses for patients with age-related macular degeneration (Bhogal et al., 2011).

Toric IOLs are used to correct astigmatism, a common refractive disorder, in order to improve post-operative visual outcomes. Multifocal and accommodating IOLs are designed to provide excellent uncorrected acuity at near as well as far distances in the pseudophakic eye (Leyland et al., 2003). As a result of the enhanced visual performance achievable with premium' IOLs compared to standard monofocal designs (Leyland et al., 2003), they are becoming an increasingly popular choice amongst surgeons and patients and are discussed in more detail in the next section (van der Linden et al., 2012). It is important for premium IOLs to be correctly positioned within the capsular bag following cataract surgery given their more complex optics. Malposition of an IOL can introduce unwanted aberrations, such as astigmatism which is induced by lens tilt (Chang et al., 2007;Sheppard et al., 2008).

1.4.   Astigmatism

Pre-surgical corneal astigmatism of more than 1.50DC exists in approximately 18-22% of patients awaiting cataract surgery (Ferrer-Blasco et al., 2009;Ahmed et al., 2010;Buckhurst et al., 2010a;Mingo-Botin et al., 2010).   With increasing levels of uncorrected astigmatism, lower visual acuities are observed (Wolffsohn et al., 2011a;Kobashi et al., 2012) therefore in order to optimise post-operative visual acuity this corneal astigmatism should be corrected (Mingo-Botin et al., 2010). Currently, astigmatic correction can be achieved through implantation of a toric IOL (Wang et al., 2003b;Ferrer-Blasco et al., 2009;Buckhurst et al., 2010b;Ale et al., 2012b) or incisional surgery (Bayramlar et al., 2003;Wang et al., 2003b;Kaufmann et al., 2005;Muftuoglu et al., 2010).

1.4.1. Toric IOLs

A study comparing toric IOLs and limbal relaxing incisions found that the former produced residual astigmatism of less than or equal to 1.00DC in approximately 90% of subjects, compared to just 40% with limbal relaxing incisions. Additionally there was a trend towards better contrast sensitivity under mesopic with glare conditions with toric IOLs compared to limbal relaxing incisions (Mingo-Botin *et al.*, 2010). Therefore toric IOLs are considered to be the superior form of correction in patients with mild to moderate astigmatism.

The invention of intraocular lenses represented a significant shift in modern cataract surgery techniques and allowed great advances in the distance acuity that could be reached after surgery. The success of cataract surgery is influenced greatly by the ability of an implanted IOL to maintain a fixed and steady position within the capsular bag over the long term. However, once implanted, all IOLs are prone to tilt and decentration within the capsular bag, which can affect vision (Visser *et al.*, 2011a) as the subject is no longer looking through the optimum part of the lens (Kim *et al.*, 2010). With toric IOLs, lens misalignment due to rotation or inaccurate positioning becomes an additional source of concern and is a frequently reported complication (Ale *et al.*, 2012b;Packer, 2014). IOL rotation is influenced by many factors including capsular bag shrinkage, IOL material and haptic design (Prinz *et al.*, 2011). Recent toric IOL development has focussed on methods to increase lens stability (Buckhurst *et al.*, 2010b;Ale *et al.*, 2012b) such as with improved lens haptic designs. Despite this, the issue of lens rotation persists. Thus an alternative idea is to focus on techniques to compensate for the effects of toric IOL rotation, in order to increase patient tolerance to lens misalignment. It would be an attractive proposition to develop a lens optical design which is less susceptible to reduced refractive error on rotation away from the intended axis.

While toric IOL rotation has been studied at length and there is extensive literature measuring tilt and decentration, there are currently no studies that have examined the link between rotation, tilt and displacement of an implanted IOL. Tilt can have a detrimental impact on quality of vision (Taketani *et al.*, 2004;Kumar *et al.*, 2011;Madrid-Costa *et al.*, 2012); however it is commonly overlooked as a potential source of reduced vision. While IOL rotation is commonly evaluated using digital slit lamp image analysis, current tilt measurement techniques require the use of specialised expensive equipment not commonly found in most optometric consulting rooms. Therefore a simpler technique using similar image analysis would be a useful way of rapidly measuring tilt in clinical practice.

1.4.2. Incisional surgery

There are a several different approaches relating to the use of incisional surgery in reducing astigmatism during cataract surgery. Options include placing a clear corneal incision along the steep corneal meridian in order to utilise the effects of wound induced corneal flattening (Wang *et al.*, 2003b;Kaufmann *et al.*, 2005). Alternatives include opposite clear corneal incision where two standard cataract incisions are made along the steep meridian, limbal relaxing incisions or peripheral corneal relaxing incisions (Wang *et al.*, 2003b). Incisional surgery relies heavily on the corneal healing response which can vary significantly between individuals, leading to greater unpredictability in refractive outcomes post-operatively (Wang *et al.*, 2003b;Buckhurst *et al.*, 2010b). Peripheral corneal relaxing incisions preserve much of the cornea's optical qualities, leading to fewer complaints of post-operative glare or discomfort (Bayramlar *et al.*, 2003;Wang *et al.*, 2003b). However, a complication of more peripheral incisions is the need for longer incisions to achieve the required power which can have a greater impact upon corneal innervation and therefore healing time post-operatively (Mingo-Botin *et al.*, 2010) Limbal relaxing incisions are thought to be

superior to corneal relaxing incisions because they can correct greater levels of astigmatism and do not encroach as much onto the central cornea (Buckhurst *et al.*, 2010a). They therefore rely less upon the subjects' specific corneal healing pattern meaning surgical outcomes can be predicted with comparatively greater accuracy (Bayramlar *et al.*, 2003). However there are reports of under corrected astigmatism with some types of incisional surgery (Bayramlar *et al.*, 2003;Wang *et al.*, 2003b)

1.5.   Presbyopia

Ocular accommodation describes an increase in the dioptric power of the eye when changing focus from distance to near (Wold *et al.*, 2003;Ostrin *et al.*, 2004;Glasser, 2006). The most widely accepted theory of the mechanism of accommodation is based on Helmholtz's theory which suggests accommodation is achieved by the change in shape of the crystalline lens secondary to ciliary muscle (CM) contraction. When viewing a distant object, the CM relaxes allowing the lens zonules and suspensory ligaments to pull on the lens, thereby flattening it. When a near object is viewed, the CM contracts to accommodate and this reduces the tension on the lens zonules which therefore slacken; this allows the elastic capsule surrounding lens to mould it into a thicker, more convex form (Gilmartin, 1995).

The ability to accommodate decreases gradually with age, in a process commonly referred to as presbyopia. This starts to hinder near vision from around 40 years of age and by age 55 years, little or no accommodation remains (Ostrin *et al.*, 2004;Ong *et al.*, 2014). The exact cause of presbyopia development is not fully understood although several theories have been proposed (Atchison, 1995;Pierscionek *et al.*, 1995;Charman, 2008). One theory suggests that a gradual age-related increase in crystalline lens size reduces zonular tension, causing a reduction in accommodative amplitude (Gilmartin, 1995;Schachar, 2006;Charman, 2008) while an alternative theory

proposed that a progressively weakening CM initiated this presbyopic change (Duane, 1925). The latter has largely been disproven by research, which demonstrates that the CM retains most of its contractility throughout life (Strenk *et al.*, 1999;Strenk *et al.*, 2006). Generally speaking, the majority of recent research suggests that an increase in crystalline lens size coupled with changes to lens capsule elasticity, are the principle causes behind this loss in accommodative amplitude with age (Glasser *et al.*, 1998;Glasser *et al.*, 1999)

Several strategies have evolved in order to compensate for the loss of accommodation following cataract surgery including presbyopia correcting IOLs such as multifocal and accommodating forms (Ong *et al.*, 2014).

1.5.1. Multifocal and Accommodating IOLs

It is estimated that several million IOLs are routinely implanted into the eye following cataract extraction every year (Simpson, 1992). Standard single focus IOLs, commonly known as monofocal IOLs, provide good uncorrected vision at only one focal point, typically the distance, leaving patients with inadequate uncorrected near and intermediate vision (Ong *et al.*, 2014). Consequently, patients must wear some form of refractive corrective appliance, most often spectacle lenses, in order to aid with close visual tasks.

Multifocal IOLs (MIOLs) have been around since the 1980s (Keates *et al.*, 1987;Gimbel *et al.*, 1991;el-Maghraby *et al.*, 1992) and are designed to provide clear vision at a range of focal points (Packer, 2014) thus reducing the need for spectacles postoperatively. Several design strategies have been developed in order to confer multifocality onto an IOL. Multi-zonal lens designs incorporate a concentric ring pattern into the lens design and may utilize refractive, diffractive or combined refractive-

diffractive principles in order to create multiple focal points from distance to near. However there are reports of optical side effects such as dysphotopsia with MIOLs (Packer, 2014). Dysphotopsia, sometimes referred to as entopic or photic phenomena, describes undesirable light related images such as streaks, haze, haloes, glare (Davison, 2000;Tester *et al.,* 2000). The MIOL design will affect the incoming light distribution, the number of focal points as well as image quality (Buckhurst *et al.,* 2012).

More recently, within the last five years, segmented lenses have been developed in which the near portion is confined to a specific area of the IOL, much like in a bifocal spectacle lens, although their mechanism of action is, like all MIOLs, simultaneous rather than translating. The first commercially available segmented IOL was evaluated in 2011 by Alio *et al.* (2011a) who concluded that this IOL improved distance, intermediate and near vision but was more susceptible to tilt and decentration. However, it is not understood how the near segment light is distributed across the retina and this knowledge is needed to optimise the shape, design and power profile of this near addition. Such sectorial IOLs rely on good IOL alignment. Materials used in such advanced technology IOLs include hydrophobic acrylic, hydrophilic acrylic, poly (methyl methacrylate) (PMMA) and silicone (Morris *et al.,* 2014).

Accommodative IOLs (AIOLs) were developed in the 1990s (Cumming *et al.,* 1996) in order to overcome the problem of photic phenomena experienced with MIOLs (Alió *et al.,* 2012). There are a range of AIOLs designs currently available, which use different mechanisms in order to provide functional near vision. AIOLs are based upon the optic shift principal and are designed to imitate the natural change that occurs in a young crystalline lens during accommodation, by moving anteriorly within the capsular bag to

allow clear vision during near tasks (Nanavaty *et al.*, 2010;Sheppard *et al.*, 2010). Single optic AIOLs can theoretically achieve a maximum of 1.5D of near power (Schor, 2009). Dual optic accommodative IOLs are relatively new and consist of a mobile, high powered positive anterior optic and a stationary, negative posterior optic which are held close in the unaccomodated eye by a spring haptic. Stimulation of accommodation initiates compressive forces resulting in an anterior lens movement. The effectiveness of dual optic AIOLs is uncertain with reports suggesting similar near and intermediate vision between single and dual optic lenses (Alió *et al.*, 2012) therefore more studies are required (Bohorquez *et al.*, 2010). Additional concepts include curvature changing AIOL devices (Schwiegerling *et al.*, 2013) and emerging technologies such as magnetically driven implants which utilise magnetic force fields in order move the IOL optic anteriorly during accommodation (Ford *et al.*, 2014).

There is a higher incidence of posterior capsular opacification (PCO) with accommodating IOLs. PCO is a common, multi-factorial complication of cataract surgery that is caused by the retention of lens epithelial cells in the capsular bag which then migrate, proliferate and transform to produce Elschnig's pearls and capsular fibrosis (Spalton, 1999). This causes light scatter leading to a reduction in visual performance. PCO can be treated with neodymium-doped yttrium aluminium garnet (Nd:YAG) laser capsulotomy (Spalton, 1999) and this has been shown to be effective in improving or maintaining visual acuity in 96% of cases (Ang *et al.*, 2013)

The reported rates of PCO vary depending on follow up period, definition of PCO, research design and method of reporting (Schaumberg *et al.*, 1998). Milazzo *et al.* (2014) reported the rate of incidence of PCO to be 30%, while Spalton (1999) stated up to 50% of patients developed PCO 2 or 3 years after surgery. Schaumberg *et al.* (1998) conducted a systematic review followed by meta-analysis to determine the

proportion of eyes developing PCO at 1 year, 3 years and 5 years postoperatively and reported pooled estimates of 11.8%, 20.7% and 28.4% respectively.

PCO is influenced by surgical technique, IOL design and patient factors such as age and intraocular or systemic diseases including uveitis and diabetes (Hancox *et al.*, 2007). The design of an IOL design is plays an important role in the incidence of PCO, for example it has been shown that a 360 degree square edge barrier to the optic can help reduce the incidence of PCO, as can sharp-edged optics (Hancox *et al.*, 2007). Additionally, PCO rate is influenced by IOL biomaterial with acrylic IOLs being associated with less PCO compared to silicone and PMMA IOLs (Ursell *et al.*, 1998) and hydrogel lenses linked to a significantly higher degree of PCO compared to PMMA and silicone (Hollick *et al.*, 2000).

As AIOLs are designed to move within the posterior chamber, unlike multifocal and monofocal IOLs, they are unable to provide an effective barrier against the migration and proliferation of cells over the posterior capsule and this is thought to result in a higher incidence of PCO with this IOL type. Hancox et al (2007) compared PCO and Nd:YAG capsulotomy rates in patients implanted with an accommodating IOL versus monofocal IOL and found that after 2 years, 50% of eyes implanted with the AIOLs developed clinically significant PCO with symptoms that required Ng:YAG capsulotomy compared to no eyes with the monofocal IOL. A study comparing PCO rates in monofocal IOL versus multifocal IOL patients found no significant difference between the two groups (Elgohary *et al.*, 2008). This is corroborated by a study comparing visual performance in children implanted bilaterally with either monofocal or multifocal IOLs which found no difference in PCO rates between the two groups (Ram *et al.*, 2014). A larger study with a sample size of 225 eyes showed an higher PCO rate among a multifocal spherical IOL group versus a monofocal spherical however this

difference was not found to be statistically significant (Biber *et al.*, 2009). Alio *et al.* (2012) a dual optic AIOL and found a significantly higher rate of PCO in the single optic group with an PCO incidence rate of 40% in the single optic group versus 11.5% in the dual optic group.

Horvath *et al.* (2014) reported that in 2011 7.8% of European cataract surgery patients opted to receive a premium IOL, defined as multifocal, multifocal toric and accommodative IOLs, compared to 14.7% in the United States. Thus standard monofocal IOLs are the most commonly implanted IOL type currently. However, it is envisaged that while standard monofocal IOL implantation will continue to increase at a steady rate in the coming years, the trajectory of premium IOLs, specifically multifocal and accommodating IOLs, will increase at a significantly faster rate in comparison. Current AIOLs provide some increase in depth of field, but in general not enough accommodative amplitude is provided by these lenses (Wolffsohn *et al.*, 2010b). Correction of presbyopia is a major driving force in IOL development and it is believed that continued innovation and improvement of AIOLs will increase the accommodative amplitude that is achievable with these lenses to beyond ten dioptres, which will lead to a rise in their popularity. New accommodating lens designs are currently in development, such as the NuLens shape-changing accommodating IOL which early studies have shown can provide up to 10 dioptres of accommodative amplitude in human subjects (Alió *et al.*, 2009) and active change of more than 40D in the monkey eye (Ben-nun *et al.*, 2005). It is postulated that a fully functioning AIOL could, in future, represent the gold standard of presbyopia correction (Chang *et al.*, 2008). Other developments include light-adjustable lenses in which the optic consists of a flexible silicon polymer matrix containing a photoreactive macromer, a photoinitiator and UV absorbers (Charman, 2014). The lens can be adjusted noninvasively after implantation using a light delivery device in order to first correct myopia, hypermetropia and

astigmatism to emmetropia (Hengerer *et al.*, 2011). Following this, a small near add zone can be added with further adjustment, which can be customised according to the patient's visual axis and pupil diameter (Lichtinger *et al.*, 2012). Early studies indicate it is possible to induce controlled amounts of negative spherical aberration and defocus in order to enhance near vision (Villegas *et al.*, 2014) indicating the potential of this as a presbyopia correcting strategy.

1.5.2. Key aspects of Multifocal and Accommodating IOL

Presbyopic correcting IOLs have been examined using both subjective and objective methods. Visual acuity at different distances, contrast sensitivity, defocus curve measurement, assessment of reading ability, dysphotopsia evaluation and subjective quality of life questionnaires are all examples of tests that can be performed to evaluate visual performance post-operatively.

1.5.2.1. Retinal Projection of IOL optical focus

Visual field tests are conducted routinely in Optometric practices and hospital eye departments across the UK primarily to assess optic nerve function but also to investigate retinal and neurological disorders (Kocabeyoglu *et al.*, 2013;Horvath *et al.*, 2014). As mentioned MIOLs provide good vision at more than one focal point; depending on whether the patient is viewing a distant or near target, there will be corresponding blur at the other focal length as a result of the mechanism of action of that MIOL. Retinal light sensitivity, as measured during visual field testing, is affected by blur (Anderson *et al.*, 2001).

By comparing visual field plots in MIOL patients for both near and far distances, it may be possible to investigate how incoming light is distributed across the retina. To the author's knowledge there have been no comparisons of visual field plots at different

focal distances for newer types of MIOLs such as segmented IOLs or with accommodating IOLs. Furthermore there have been no comparisons between the retinal thresholds in different regions of the same MIOL. This information could provide useful insight into the optimal design features of different MIOLs.

1.5.2.2. Range of Clear Focus Created by Multifocal and Accommodating IOLs

MIOL and AIOL performance may also be assessed by measuring distance corrected near visual acuity (DCNVA), subjective amplitude of accommodation from the reported closest distance of clear focus (push-up test), using subjective defocus curves, or from objective autorefractor or aberrometry measures of optical refraction when viewing targets at different distances. A defocus curve consists of the subjective measurement of visual acuity at different distances or with different levels of trial lens induced defocus and can be used to evaluate range of clear vision (Gupta *et al.*, 2007;Wolffsohn *et al.*, 2013). There is general agreement that subjective measures such as the push-up test tend to overestimate accommodation compared to objective measures of true optical refractive changes (Marcos *et al.*, 1999b;Wold *et al.*, 2003;Wang *et al.*, 2006a;Wolffsohn *et al.*, 2006a;Vasudevan *et al.*, 2007;Win-Hall *et al.*, 2009). Additionally, subjective measures may be more influenced by a range of factors such as contrast, pupil size, higher order aberration, visual acuity, age, chromatic aberration, retinal eccentricity and target detail (Wang *et al.*, 2006a). The precise factors which influence the difference between subjective and objective depth of focus measures are currently unknown. As some patients seem to cope without the need for a separate near correction after cataract surgery with standard spherical IOLs (Bradbury *et al.*, 1992;Nanavaty *et al.*, 2006) this depth of focus could identify which patients would benefit most from current AIOLs with their limited objective accommodation (Wolffsohn *et al.*, 2010b).

There is no universally accepted, standardised procedure for measuring defocus curves in terms of the range and step sizes between trial lenses (Wolffsohn *et al.*, 2013).Traditional defocus curve testing is subjective and slow to perform. As IOL near additions can be as high as 4D and measurements of visual acuity must be taken every 0.5D including into the positive curve range for adequate curve fitting, typically around 14 separate measures of visual acuity are needed for each eye. To fully assess presbyopic correction strategies, defocus testing would ideally be performed multiple times to assess the range of clear vision with binocularity, with different target contrasts and under different lighting conditions. However subjectively measured defocus curves can be quite lengthy, leading to patient fatigue and variability in results. Hence conducting repeated subjective defocus curves in different testing conditions is unlikely to be feasible. There is therefore a need for shorter defocus curve testing times which cannot be achieved by increasing step sizes between lenses as this has been shown to decrease the quality of results obtained (Wolffsohn *et al.*, 2013). Objective techniques may enable faster defocus curve testing to be performed thereby allowing more time for repeated examinations under a range of different conditions. However their relative accuracy compared to more traditional subjective measures is uncertain.

1.6. Aims of thesis

In the last sixty years, much research has been undertaken to improve IOL design with a view to enhancing post-operative visual outcomes. Such premium IOLs have reduced or even eliminated spectacle dependence leading to an increase in patient satisfaction (Packer, 2014). However, methods of evaluating these lenses have not developed as rapidly.

The literature review has drawn attention to two areas concerning premium IOLs. The first concerns toric IOL misalignment, while the second relates to the need for faster techniques to assess visual performance with premium IOLs in order to acquire a greater understanding into different aspects of their optical performance.

The aim of the thesis is therefore to address topics related to these two aspects in order to improve optical performance with and assessment of premium IOLS. The specific hypotheses to be investigated in this thesis are listed below.

1. Hypothesis: Patient tolerance to toric IOL misalignment is increased using a novel, split surface design.
2. Hypothesis: A new, simplified method of measuring IOL tilt is valid and repeatable.
3. Hypothesis: There is an association between IOL rotation, tilt and decentration.
4. Hypothesis: Perimetry is an effective tool for mapping the retinal projection of different presbyopia correcting IOLs.
5. Hypothesis: How much additional objective accommodation is required in order to restore the eye's focus with AIOLs?
6. Hypothesis: Aberrometry can provide rapid and reliable measures of subjective depth of focus following multifocal IOL implantation.

CHAPTER 2: Reducing the effect of toric intraocular lens misalignment using a split surface approach

2.1. Introduction

Astigmatism is a visually debilitating refractive condition of the eye that occurs in relatively low amounts in a large proportion of the population (Read *et al.*, 2007;Ferrer-Blasco *et al.*, 2009;Ahmed *et al.*, 2010;Buckhurst *et al.*, 2010a;Mingo-Botin *et al.*, 2010). Increasing levels of uncorrected astigmatism are associated with corresponding reductions in visual acuity and therefore should be compensated for where possible (Wolffsohn *et al.*, 2011a;Kobashi *et al.*, 2012). Environmental factors, eyelid pressure, extraocular muscle forces and nutrition are thought to influence the development of astigmatism (Read *et al.*, 2014). Astigmatism can be classified as with the rule (WTR), against the rule (ATR) or oblique (OBL). WTR astigmatism is characterised by a steeper vertical meridian and ATR astigmatism is characterised by a steeper horizontal meridian. Vertical lines dominate the visual world; it is believed that WTR astigmatism aids with distance vision because vertical lines at far are focused on the retina while ATR astigmatism improves reading vision because vertical lines from near objects are more in focus at the retina (Novis, 2000;Read *et al.*, 2014). While WTR astigmatism is more common amongst young adults, with age there is an axis shift resulting from a change in corneal curvature such that in the older population ATR astigmatism predominates (Ferrer-Blasco *et al.*, 2009;Read *et al.*, 2014). The nature of this corneal change was examined and an age related steepening of the horizontal corneal meridian, possibly resulting from an associated reduction in eyelid tension, was thought to account for the majority of the observed astigmatic axis shift (Read *et al.*, 2007).

Ferrer-Blasco *et al.* (2009) found an increase in both the prevalence and mean astigmatism with age in their study. Prevalence of astigmatism was found to increase from 10% in 0 to 10 year olds up to 64% in 81 to 90 year olds. Similarly, the mean amount of astigmatism increased from -0.94DC in 0 to 10 year olds, to -1.86DC in 81 to 90 year olds. A cross-sectional study found that 45 percent of the total population had more than 0.50 dioptres of corneal astigmatism, while only 4.7 percent exhibited more than 1.50 dioptres (Fledelius *et al.*, 1986). In those awaiting cataract surgery on the other hand, pre-surgical corneal astigmatism of more than 1.50DC has been reported in approximately 18-22% of patients (Ferrer-Blasco *et al.*, 2009;Ahmed *et al.*, 2010;Buckhurst *et al.*, 2010a;Mingo-Botin *et al.*, 2010). With increasing levels of astigmatism, lower visual acuities are observed (Buckhurst *et al.*, 2010a;Wolffsohn *et al.*, 2011a;Kobashi *et al.*, 2012;Sheppard *et al.*, 2013) therefore in order to optimise post-operative visual acuity (VA) this corneal astigmatism should be corrected (Mingo-Botin *et al.*, 2010). In order to achieve post-operative spectacle independence, it has been suggested that astigmatism greater than or equal to 0.75 dioptres should be corrected (Rubenstein *et al.*, 2013).

Astigmatic correction can be achieved during cataract surgery via the use of incisional surgery as discussed in chapter 1 (Bayramlar *et al.*, 2003;Wang *et al.*, 2003b;Kaufmann *et al.*, 2005;Muftuoglu *et al.*, 2010) or the implantation of a toric IOL (Wang *et al.*, 2003b;Ferrer-Blasco *et al.*, 2009;Buckhurst *et al.*, 2010b;Ale *et al.*, 2012b). Incisional surgery relies heavily on the corneal healing response which can vary significantly between individuals, leading to greater unpredictability in refractive outcomes post-operatively (Wang *et al.*, 2003b;Buckhurst *et al.*, 2010b). Peripheral corneal incisions can produce up to 1.0D of corneal astigmatic change, while additional incisions such as opposite clear corneal incisions or limbal relaxing incisions can produce larger amounts of astigmatic change, typically up to 2.0D (Read *et al.*, 2014).

Research has shown toric IOLs to be the better form of correction, both in terms of predictability of visual outcomes and improved healing times due to their reduced surgical impact (Horn, 2007;Buckhurst *et al.*, 2010a;Mingo-Botin *et al.*, 2010). They are commonly used in patients with more than 1.0D of corneal astigmatism. Most commercially available toric IOL can correct less than 3.0D of astigmatism (Iovieno *et al.*, 2013). Correcting higher levels of corneal astigmatism over 3.0D is more challenging. Current methods include combining toric IOL implantation with limbal relaxing incisions, use of piggyback toric IOLs, or implantation of high powered toric IOLs (Read *et al.*, 2014). The Acrysof IQ toric IOL is available in cylinder powers of up to 6.0D, which corresponds to approximately 4.0D at the corneal plane. Higher toric IOL powers are available such as the Rayner T-flex toric IOL which is available in cylinder powers of up to 11.0D and the Acri.Comfort toric IOL, which is available in up to 12.0D (Visser *et al.*, 2011b;Iovieno *et al.*, 2013). Customised high powered toric IOLs can be ordered for special cases, for instance Luck (2010) used a toric IOL with a cylinder power of 16.0D in a patient with pellucid marginal degeneration. Thus much greater amounts of astigmatic correction are possible with toric IOLs compared to incisional surgery.

2.2. Toric IOLs

Spectacle correction of astigmatism can give rise to meridional magnification (Guyton, 1977) leading to asymmetrically magnified and distorted retinal images which can be challenging to adapt to (Buckhurst *et al.*, 2010a). Astigmatic correction at the corneal or IOL plane is believed to negate this effect due to the reduced vertex distance (Buckhurst *et al.*, 2010a), and for this reason toric IOLs are the favoured form of astigmatic correction. Toric IOLs are also thought to provide a more stable correction compared to alternatives such as relaxing incisions with less of a corneal impact. All IOL manufacturers must follow the standards set out by the International Organisation

for Standardisation in ISO 11979-2. A part of this defines the tolerances that IOLs must meet (International Organisation for Standardisation, 2014).

Visual outcomes with toric IOLs are however reliant upon accurate alignment of the lens (Buckhurst *et al.*, 2010a;Sheppard *et al.*, 2013) and once implanted all IOLs are prone to misalignment, which can affect vision (Visser *et al.*, 2011a;Visser *et al.*, 2011b). With toric IOLs, lens rotation becomes an additional source of concern and is a frequently reported complication (Ale *et al.*, 2012b). Reports indicate that toric rotation induces a hyperopic spherical change in addition to reducing the power of the astigmatic correction (Langenbucher *et al.*, 2009;Jin *et al.*, 2010). Kim *et al.* (2010) found that a loss in astigmatic power of up to 3.3% occurred for every degree of IOL rotation; therefore even small amounts of rotation can reduce the corrective power of a toric IOL. Ma *et al.* (2008) reported a sinusoidal relationship between residual astigmatism and misalignment of a toric IOL indicating that smaller rotations result in a proportionately greater loss in cylindrical effect. If an IOL rotates off axis by more than 30°, nearly no astigmatic correction occurs, however there will be a shift in the resultant astigmatic axis (Shimizu *et al.*, 1994;Novis, 2000). At more than 45° of rotation, the IOL can add to the existing ocular astigmatism leading to greater levels of astigmatism post-surgically (Novis, 2000). The greater the cylinder power, the more essential accurate IOL placement becomes (Ale *et al.*, 2012a). With newer lens designs, such as multifocal toric IOLs, the impact of rotation on visual performance may be greater as a result of the precise nature of the refractive correction. A study comparing a monofocal toric IOL with a multifocal toric IOL found that uncorrected distance visual acuity was more affected by IOL rotation in the multifocal group one month post-operatively (Garzón *et al.*, 2015). However, other studies evaluating multifocal toric IOLs have reported good predictability of refractive results and rotational stability (Alió *et al.*, 2011;Ferreira *et al.*, 2013;Mojzis *et al.*, 2013;Venter *et al.*,

2013). Currently available toric IOLs, including multifocal toric IOLs are detailed in table

2.1.

Toric IOL	Type	Spherical Power	Near	Cylinder Power (D)	Material	Haptic	Aspheric
Staar Toric IOL, Staar Surgical Company	Monofocal	+9.5 to +28.5	-	2.0, 3.5	Silicone	Plate	No
Acrysof IQ toric, Alcon	Monofocal	+6.0 to +34.0	-	1.5 to 6.0 in 0.75 steps	Hydrophobic acrylic	Loop	Yes
Tecnis , Abbott Medical Optics	Monofocal	+5.0 to +34.0	-	1.00, 1.50, 2.25, 3.00 and 4.00	Hydrophobic acrylic	Loop	Yes
MicroSil/Customised Torica, HumanOptics	Monofocal	-3.5 to +31.0	-	2.0 to 12.0 in 1.0 steps (available in higher customised cylinder powers)	Silicone, PMMA haptic	Loop	No
Lentis Tplus/ Tplus X customised, Oculentis GmbH	Monofocal	-10.0 to +35.0 in 0.5/0.01D steps	-	+0.25 to +12.0 in 0.75/0.01D steps	Hydrophilic acrylic with hydrophobic surface	Loop/Plate	Yes
Morcher 89A, Morcher GmbH	Monofocal	+10.0 to 30.0	-	0.5 to 8.0 in 0.25 steps	Hydrophilic acrylic	Bag in the lens	No
AF-1 toric, Hoya	Monofocal	+6.0 to +30.0	-	1.5 to 3.0 in 0.75 steps	Hydrophobic acrylic with PMMA haptic tips	Loop	Yes

Acri.Comfort/ AT Torbi, Carl Zeiss Meditec	Monofocal	-10.0 to +32.0	-	1.0 to 12.0 in 0.50 steps	Hydrophilic acrylic with hydrophobic surface	Plate	Yes
T-flex, Rayner	Monofocal	-10.0 to +35.0	-	1.0 to 11.0 in 0.25 steps	Hydrophilic acrylic	Loop	Yes
Light Adjustable Lens, Calhoun Vision	Monofocal	+17.0 to 24.0	-	0.75 to 2.0	Silicone with PMMA haptics	Loop	Yes
Acrysof IQ ReSTOR toric, Alcon	Multifocal Diffractive & Refractive	+6.0 to +34.0	+3.00D	1.0 to 3.0 in 0.5/0.75 steps	Hydrophobic acrylic	Loop	Yes
Acri.Lisa Toric, Carl Zeiss Meditec	Multifocal Diffractive & Refractive	-10.0 to +32.0	+3.75D/+4.00D	1.0 to 12.0 in 0.50 steps	Hydrophilic acrylic with hydrophobic surface	Plate	Yes
M- flex T, Rayner	Multifocal Refractive	+14.0 to +32.0	+3.00/+4.00D	+1.5 to +6.0 in 0.50 steps	Hydrophilic acrylic with hydrophobic surface	Loop	Yes
Lentis Mplus toric, Oculentis GmbH	Refractive sectorial shaped near zone	0.0 to +36.0	+3.00D	+0.25 to +12.0 in 0.75 steps	Hydrophilic acrylic with hydrophobic surface	Plate	Yes

Table 2.1: List of currently available toric intraocular lenses.

2.3. Factors affecting toric IOL rotation

Misorientation can occur for a number of reasons, for example surgical error resulting in inaccurate positioning of the IOL at the time of surgery (Watanabe *et al.*, 2012) or post-operative rotation of the implanted IOL within the capsular bag (Ale *et al.*, 2012a;Shah *et al.*, 2012). When implanting a toric IOL, reference markers, usually on opposite sides of the pupil, must be determined to ensure correct placement of a toric IOL during surgery (Buckhurst *et al.*, 2010a). However these must be established prior to rather than during surgery, since low to moderate amounts of eye rotation have been reported to occur when changing from a seated to supine position (Chernyak, 2004). Techniques to apply these markers include using ink (Graether, 2009) or specific toric axis marking instruments (Buckhurst *et al.*, 2010a). A commonly used 3 step ink-marker system (Ma *et al.*, 2008;Visser *et al.*, 2011a) for toric IOL implantation was found to have a mean alignment error rate of approximately 5°(Visser *et al.*, 2011a). In this system the horizontal 0° to 180° axis of the eye is marked pre-operatively with the patient sitting upright. The desired alignment axis for the toric IOL is ascertained and then marked intra-operatively using a device with angular graduations. Following this the toric IOL is implanted and rotated until the IOL and reference markers match (Ma *et al.*, 2008;Visser *et al.*, 2011a). Precisely orientating the toric IOL during surgery is therefore essential in order to achieve optimum correction of astigmatism.

The majority of IOL rotation is thought to occur within the first month of surgery (Mingo-Botin *et al.*, 2010) due to factors such as capsular bag size, capsulorhexis size and capsular fusion (Shimizu *et al.*, 1994;Prinz *et al.*, 2011). There is a gradual reduction in capsular bag size in the weeks following surgery. While this shrinkage can help to secure the IOL, it is also possible for lens rotation to occur as a result of this contraction because of the compressive effect on the IOL haptics. Capsular bag

shrinkage is the most commonly reported source of late IOL rotation in uncomplicated cataract cases, with most of the resulting rotation occurring in the first three months after surgery (Kim *et al.*, 2010;Prinz *et al.*, 2011). Capsular fibrosis, which normally occurs in the weeks after surgery (Mamalis *et al.*, 1996) can also help to anchor the IOL. However it is possible for lens rotation to occur before this fibrosis stabilises the IOL (Buckhurst *et al.*, 2010a). The presence of certain ocular or systemic diseases, such as glaucoma or diabetes, are thought to influence capsular fibrosis leading to a greater likelihood of rotation in these patients (Ale *et al.*, 2012a).

Interestingly, there appears to be a refractive element to lens rotation with myopes being more susceptible to early toric IOL rotation (Shah *et al.*, 2012). This effect may occur as a result of the correlation between increased axial lengths and a greater capsular bag diameter, which is thought to cause greater IOL instability (Novis, 2000) as a result of reduced equatorial friction (Shah *et al.*, 2009). Hence, maximising the resistance between the IOL haptic and capsular bag can help to reduce lens rotation soon after surgery; IOL material is crucial for this (Kim *et al.*, 2001b). Polymethylmethacrylate (PMMA) has been found to be the best in terms of creating the most friction with the capsular bag and silicon the worst (Oshika *et al.*, 1998;Yoshida *et al.*, 1998;Taketani *et al.*, 2004). IOL size is also important as smaller IOLs have less contact and therefore less resistance with the capsular bag which can lead to increased lens rotation (Buckhurst *et al.*, 2010a). IOL haptic design can also impact upon the degree of rotation (Kim *et al.*, 2010;Prinz *et al.*, 2011). Plate haptic IOLs are more stable in the long term as they seem to be less vulnerable to the effects of capsular bag compression, whereas open loop haptic lenses show good rotational stability initially, but are more likely to rotate later on with capsular compression (Patel *et al.*, 1999;Buckhurst *et al.*, 2010a). Early research into closed loop haptics indicates better overall rotational stability with this IOL haptic as a result of good initial friction

between the IOL and capsular bag coupled with greater resistance to capsular compression (Buckhurst *et al.*, 2010b). Surgical factors can also influence IOL rotation as discussed earlier, therefore ensuring accurate IOL alignment at the time of implantation as well as careful wound construction is imperative (Buckhurst *et al.*, 2010a).

Shimizu *et al.* (1994) suggested the maximum acceptable shift in toric IOL axis to be no more than 30°. This is worrying since Leyland *et al.* (2001) determined that 18% of early plate haptic IOLs rotated by more than 30° three to six months after surgery, meaning that in theory, up to one fifth of patients implanted with this type of toric IOL would receive inadequate astigmatic correction. In the case of significant toric IOL rotation, repositioning surgery is advised to try and achieve re-alignment, however there is a time frame of approximately two weeks from the date of initial surgery in which this should be carried out, after this the risk of capsule rupture increases (Novis, 2000;Ale *et al.*, 2012b).

There is therefore a need to improve the rotational stability of toric IOLs or to introduce a mechanism to compensate for the effect of toricity caused by lens rotation, as this would give patients better vision and allow surgeons greater flexibility. Several design strategies have been developed in order to increase lens stability and therefore reduce intracapsular lens rotation (Buckhurst *et al.*, 2010b;Ale *et al.*, 2012b), however there is still uncertainty as to which type of IOL design confers better rotational stability (Prinz *et al.*, 2011).

In this chapter a novel idea for compensating for the rotational effects of a toric IOL is evaluated. This involves splitting the toric power of an IOL over both the front and back

surfaces of an IOL, as opposed to across just one surface, and misaligning their axes slightly to determine whether this provides a beneficial effect that could be incorporated into toric IOLs. In theory with such a design the maximum toric power would be spread over a wider angular subtense, perhaps reducing the power loss with rotation away from the axis of peak astigmatism. Most toric IOLs are made with one spherical surface and one toric surface. It has been suggested that this can cause a disparity between the images and object magnifications in different meridians in the case of corneal astigmatism. Bitoric IOLs may have the additional advantage of eliminating this image distortion and therefore offer an advantage over standard toric IOLs (Langenbucher *et al.*, 2009). The effectiveness of this new toric IOL design idea on improving patient tolerance to lens rotation will be evaluated for each of the three main types of astigmatism. Additionally differences in the potential benefit of this correction in moderate compared to high astigmats will be investigated, as will the influence of adaptation.

2.4. Method

Thirty-one healthy subjects with a mean age of 26.4 ± 8.3 years and with best corrected Snellen acuity of 6/9 or better gave informed consent to take part in the study. The study was approved by the Institutional Ethics Committee and the research conformed to the tenets of the Declaration of Helsinki.

The patients were split into two subgroups, an induced astigmatism group made up of 16 subjects with limited astigmatism <-0.75D and an adapted astigmatic group of subjects (n=15) with ocular toricity from -1.00 to -3.00 DC (mean -1.27 ± 0.54DC). Contact lens wearers were required to remove their lenses at least twelve hours before having any tests carried out.

In order to participate in the study, participants were required to:

- Be aged at least 18 years

- Have no more than three dioptres of astigmatism

- Be free of any active eye disease

- Not currently taking ocular or systemic medications with known ocular side effects

- Have no history of ocular surgery within the previous three months

- Have best corrected visual acuity of at least 6/9 in the eye being tested

- Be willing to participate in the study.

2.4.1. Induced Astigmatism Cohort

Patients underwent a refractive examination to ensure they were wearing the most accurate sphero-cylindrical distance prescription, maximising the positive power while retaining the best possible distance visual acuity and a measurement of their best corrected visual acuity was taken at this point. In order to induce astigmatism, a low

(1.50DC) and high (3.00DC) cylinder was added to the distance prescription, compensated for with sphere. The 1.50DC lens was assessed at 90°, 135° and 180 in a random sequence, in order to test the effectiveness of this new toric IOL design idea with the three main types of astigmatism. The 3.00DC was examined at 90° only in order to keep testing times to within reasonable limits.

The induced cylinder was then corrected using two forward facing lenses of either -0.75DC for the low cylinder, or -1.50DC for the high cylinder. These were added to the trial frame either aligned with each other or misaligned from each other by 5° or 10°, again in a randomized order. Finally, these two correcting lenses were misorientated from the angle of the induced astigmatism in 5° steps up to a maximum of 15°, in a clockwise direction and in a randomised order. Misalignment refers to the separation of the two individual correcting cylinder lenses relative to each other by up to 10°, while misorientation describes rotation of the correcting system, comprising these two cylindrical lenses, away from the induced astigmatism axis by up to 15° as illustrated in figure 2.1A and 2.1B.
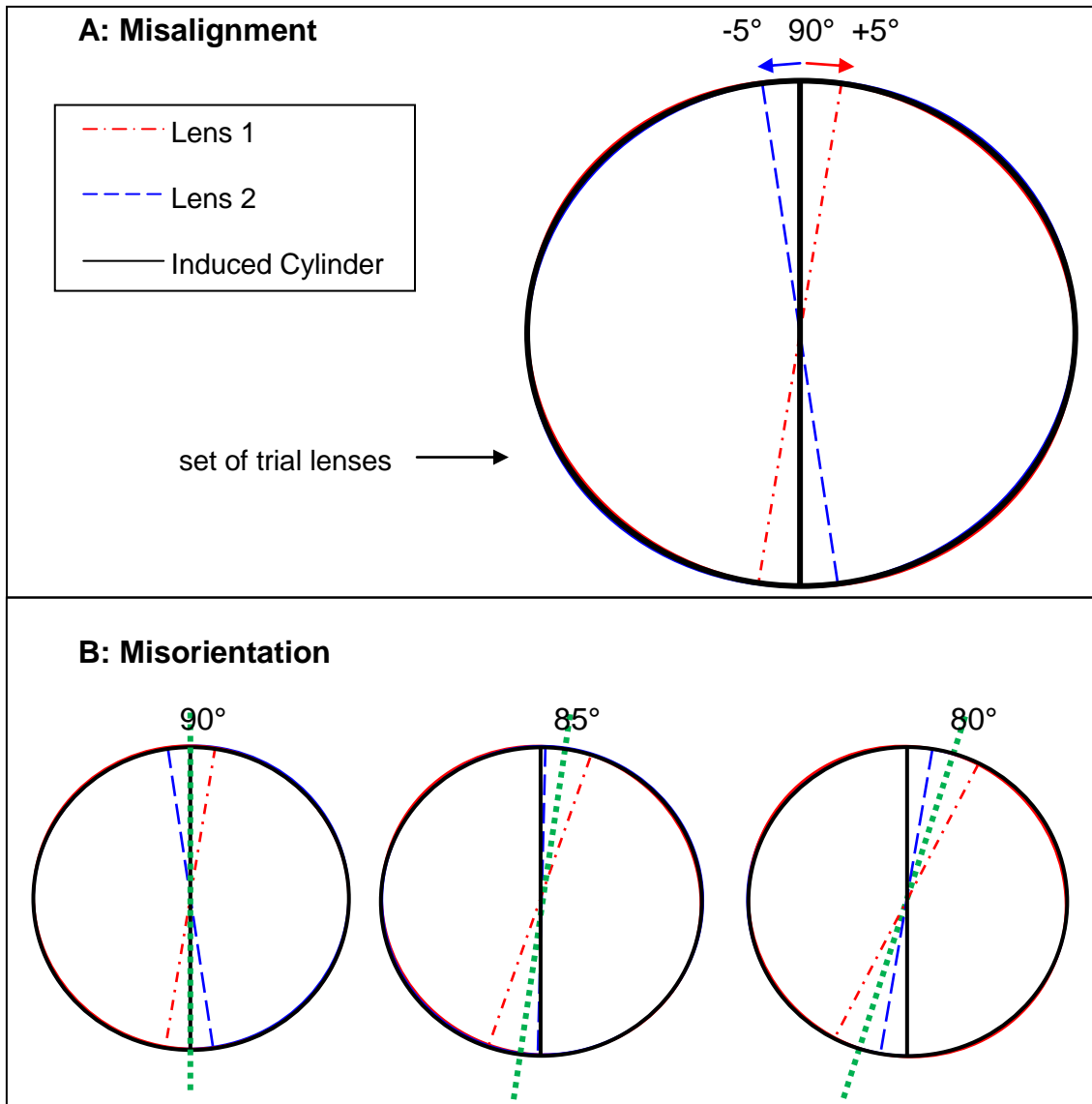
Figure 2.1A: illustrates lens misalignment. Two correcting lenses (blue dash and red dot-dash) of equal power, either 0.75 or 1.50DC depending on the induced cylinder power (black solid) were misaligned by up to 10°. 2.1B: illustrates lens misorientation. The two misaligned lenses were rotated clockwise in the trial frame by up to 15°. The green line dotted represents the central axis direction of the two corrective lenses.

The position of the two -0.75DC/-1.50DC lenses for each lens misalignment and each misorientation is detailed in table 2.2.

Axis	Correcting lens power	Misorientation (°)	Misalignment of split cylinders (°)	Lens 1 (°)	Lens 2 (°)
VERTICAL (90°)	-0.75DC / -1.50DC	0	0	90	90
			5	87.5	92.5
			10	85	95
		5	0	85	85
			5	82.5	87.5
			10	80	90
		10	0	80	80
			5	77.5	82.5
			10	75	85
		15	0	75	75
			5	72.5	77.5
			10	70	80
OBLIQUE (135°)	-0.75DC	0	0	135	135
			5	132.5	137.5
			10	130	140
		5	0	130	130
			5	127.5	132.5
			10	125	135
		10	0	125	125
			5	122.5	132.5
			10	120	130
		15	0	120	120
			5	117.5	122.5
			10	115	125
HORIZONTAL (180°)	-0.75DC	0	0	180	180
			5	177.5	182.5
			10	175	185
		5	0	175	175
			5	172.5	177.5
			10	170	180
		10	0	170	170
			5	167.5	172.5
			10	165	175
		15	0	165	165
			5	162.5	167.5
			10	160	170

Table 2.2: Axis positions of the two correcting toric lenses at each misalignment and misorientation with induced astigmatism of 1.50/3.00DC.

2.4.2. Astigmatic Cohort

Patients with astigmatism between -1.00 and -3.00DC had their own astigmatism corrected using two cylindrical lenses of half the power each. The two cylindrical lenses were placed into the trial frame such that the axes of these two cylindrical lenses were misaligned from each other by 0°, 5° or 10°. These correcting lenses were then orientated to coincide with the angle of the patients' astigmatism and randomly misorientated by as much as 15° in 5° steps in both the clockwise and anticlockwise direction. This was done to enable evaluation of the effects of adaptation on rotational tolerance by comparing patients with a moderate toric component to their prescription against those in whom the astigmatism had just been induced. All measurements were taken on one eye only.

Distance visual acuity was measured on a digital logarithmic progression chart on all patients (TestChart 2000Pro, London, UK) with the letters randomised between presentations. Each letter read correctly was scored as 0.02 logMAR and subjects were encouraged to guess if unsure.

2.5. Statistical Analysis

All data were collected in an Excel database (Microsoft Office 2007) and analysed using SPSS for Windows (version 20.0, SPSS Inc.). A one-sample Kolmogorov-Smirnov test revealed that the visual acuity data were normally distributed (Kolmogorov-Smirnov Z = 1.206, P=0.109). Therefore visual acuity with each axis and astigmatic power misalignment was compared by repeated measure analysis with posthoc tests applied when the overall significance was p <0.05.

2.6. Results

2.6.1. Induced Astigmatism cohort

Misorientation of the split toric lenses when 1.50 dioptres of astigmatism was induced at 90°, 135° and 180° caused an anticipated reduction in visual acuity (F = 70.341; p<0.001; Figure 2.2). There was a statistically significant change in VA with axis (F = 3.775; p=0.035). Comparatively worse visual acuities were recorded when astigmatism was induced at 90° than at 180° as expected. Splitting and misaligning the toric power did not result in a statistically significant better visual acuity compared to no separation with the low 1.50DC lens (F=2.190, P=0.129).

Misalignment of the toric power split between the two lenses when induced with a high 3.00DC lens at 90° also produced no statistically significant benefit in VA retention with axis misorientation (F = 0.491, p=0.617; Figure 2.3).
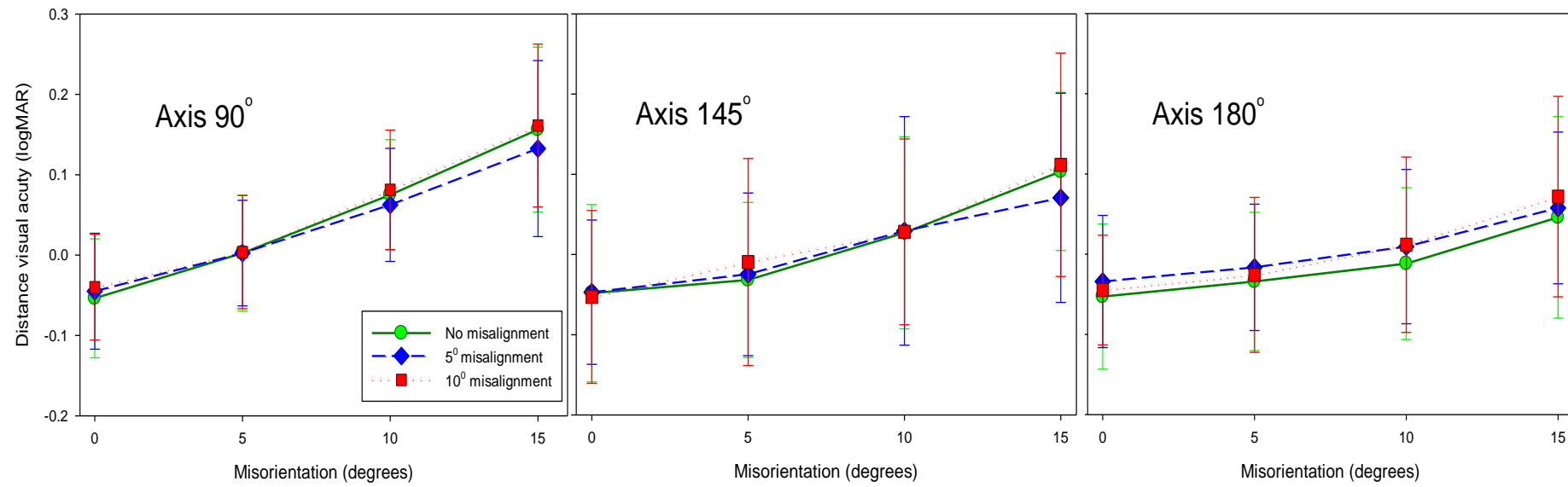
Figure 2.2: The effect of misaligning split toric power on distance VA with lens misorientation when +1.50DC is induced at 90°, 135° and 180°. N = 16. Error bars = 1 standard deviation (S.D.).
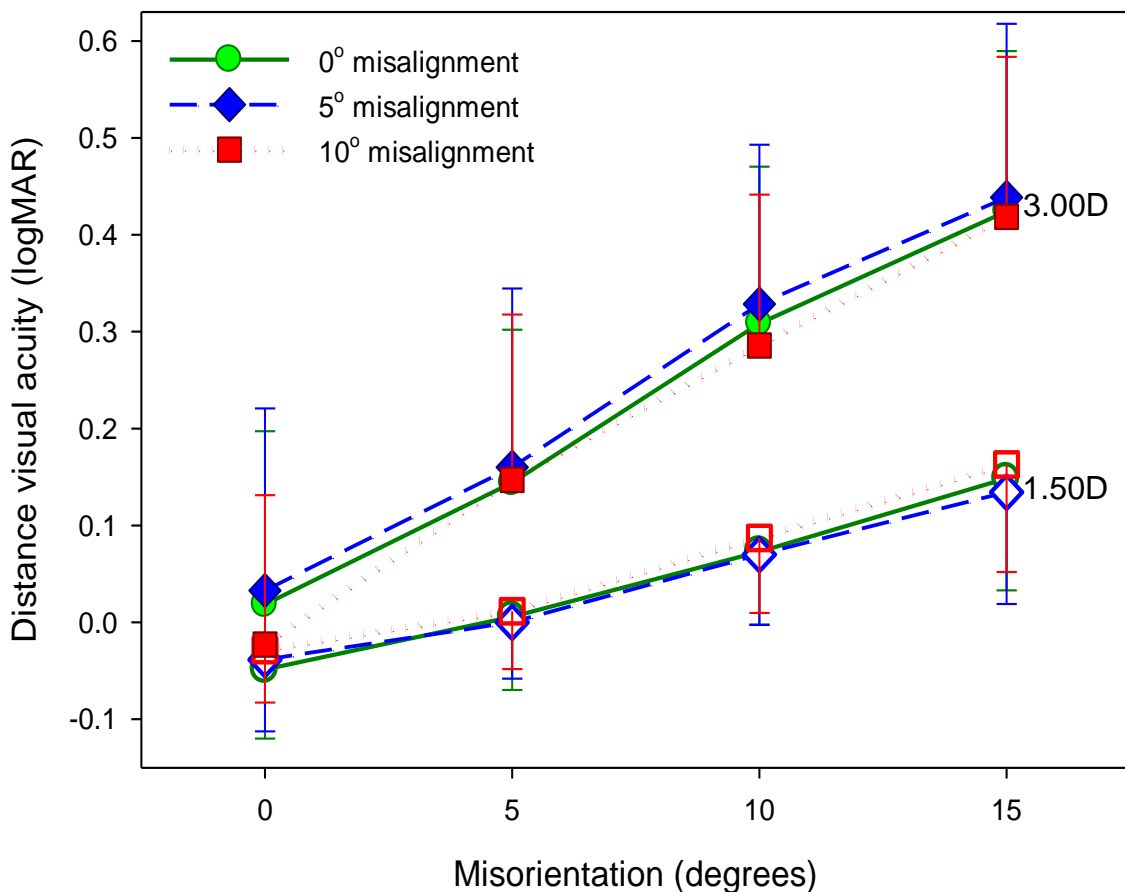
Figure 2.3: The effect of misaligning split toric power on distance visual acuity for 1.50DC and 3.00DC lenses induced at 90° with misorientation. N = 16. Error bars = 1 S.D.

2.6.2. Adapted Astigmats

Patients with habitual astigmatism of between -1.00 and -3.00DC at any axis were recruited for this part of the study. A breakdown of the quantity, axis and classification of the astigmatism present in these subjects is shown in Table 2.3. Most subjects had either with the rule (n=7) or against the rule astigmatism (n=7); there was one patient with oblique astigmatism.

Patient number	Astigmatism (DC)	Axis (°)	Type
1	1.00	70	ATR
2	1.50	70	ATR
3	1.00	70	ATR
4	1.00	85	ATR
5	2.00	85	ATR
6	1.00	95	ATR
7	1.00	110	ATR
8	1.00	165	WTR
9	3.00	170	WTR
10	1.50	175	WTR
11	1.50	175	WTR
12	1.00	180	WTR
13	1.00	5	WTR
14	1.50	5	WTR
15	1.00	25	OBL

Table 2.3: Details the astigmatic prescriptions present in the adapted subgroup. An axis of 90±22.5° was classed as against the rule, 0±22.5° as with the rule and 135±22.5° or 45±22.5° as oblique astigmatism.

Adapted astigmats had a similar decline in visual acuity with misorientation to non-astigmatic subjects in whom toricity was induced using cylindrical lenses (F = 4.412, p = 0.054). When the subjects own astigmatism was corrected using two cylinders of half the power, splitting and misaligning the power of the astigmatic correction did not

produce a statistically significant benefit in visual acuity preservation with axis misorientation (F=0.120, p=0.887; Figure 2.4).
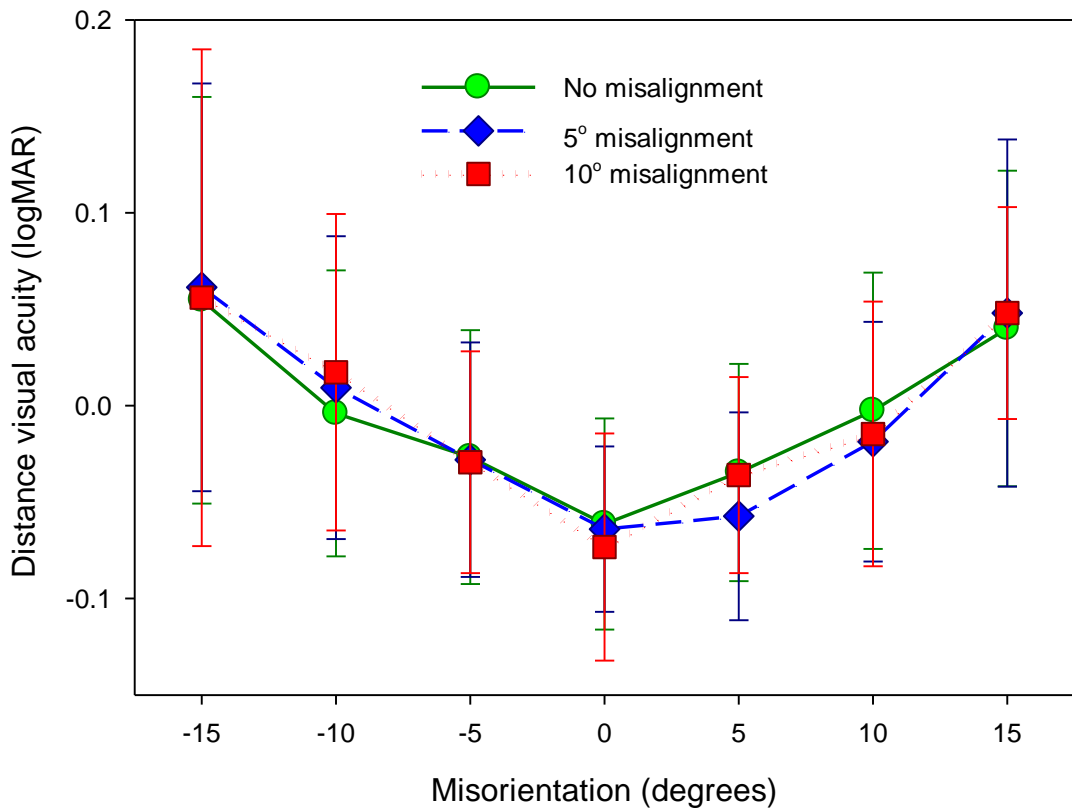
Figure 2.4: The effect of misaligning split toric power on distance visual acuity in adapted astigmats, with misorientation. N = 15. Error bars = 1 S.D.

2.7.   Discussion

The purpose of this study was to investigate whether splitting the toric power across the front and back surfaces of a toric IOL misaligned by either 5° or 10° had the potential to increase patient tolerance to small shifts in lens rotation without significantly detracting from distance visual acuity. This was not found to be the case and splitting toric power had no statistically significant impact on maintaining better distance visual acuity when a lens was misorientated away from the intended axis.

Visual acuity dropped with toric lens misorientation, as expected, and this happened regardless of whether the toric power was split and misaligned or not. While the magnitude of any benefit observed with spectacle lenses would have to be adjusted for the difference in location of a contact lens or intraocular lens in relation to the ocular optics, the lack of effect seen with spectacle lenses is unlikely to be altered by the back vertex distance of the visual correction or with a bitoric compared to two toric lenses used to simulate the effect.

In the low astigmatic cohort, the best visual acuities were observed when the toric lens was induced at 180°. As previously mentioned, patients that have with the rule astigmatism are thought to see better at distance while those with against the rule astigmatism see better at near and since all visual acuities in this study were recorded at a six metre testing distance better acuities were expected to occur at 180° compared to 90° and 135°.

There did not appear to be a symmetrical reduction in VA for clockwise (-5°,-10° and -15°) and anticlockwise (+5°, +10° and +15°) misorientation in the astigmatic cohort, as shown in figure 2.4.   Instead VA seemed slightly better with anticlockwise misorientation, particularly for 5° and 10° separations, probably because most of the

patients had a cylinder axis slightly clockwise of the horizontal and vertical meridians, however this difference was not found to be statistically significant (F=1.488, P=0.243).

As has been previously demonstrated (Wolffsohn *et al.*, 2011a) a faster drop in visual acuity occurred with lens misorientation for the high cylinder (3.00D) compared to the low cylinder (1.50D), which illustrates how accurate IOL placement becomes increasingly important with rising levels of astigmatism.

It has been reported that differences in neural image processing may negatively affect visual acuity in patients with simulated astigmatism compared to those with habitual astigmatism (Ohlendorf *et al.*, 2011b). The study compared adapted astigmats with non astigmatic patients in whom toricity was induced using cylindrical lenses and found there was no statistically significant effect of adaptation on visual acuity with both groups experiencing comparable drops in visual acuity with increasing lens misorientation. This indicates that adaptation to astigmatic correction may occur rapidly at least in the young as has been suggested previously (Sawides *et al.*, 2010;Ohlendorf *et al.*, 2011a)

High contrast visual acuity was used to evaluate visual performance in this study, which may have masked some of the more sensitive measures of vision and visual function such as low contrast acuity and reading speed (Watanabe *et al.*, 2013). However, adding these measures to the assessment could also have increased the result variability due to fatigue. Further studies incorporating other visual assessment tests may provide a better understanding of the visual impact of a split surface approach to toric correction.

Verification strategies to ensure the trial frame was consistently orientated with the eye, perhaps through use of eye reference markers, should have been employed for each lens power and axis change to ensure consistency of the testing procedure. This lack of verification is a potential limitation of the current study.

In conclusion, this study simulated the effect of splitting and misaligning toric power across more than one IOL surface and found spreading the toric power of the lens in this way had no beneficial effect on distance high contrast visual acuity with misorientation, but also had no detrimental effect. It may not therefore be an advantage to incorporate this technique into toric refractive corrections such as IOLs. Despite the rotational issues encountered with toric IOLs, clinical studies have reported good visual outcomes in patients with low to moderate astigmatism between 1.0D and 2.5D (Visser *et al.*, 2013;Read *et al.*, 2014). However, as small shifts in intraocular lens rotation have been shown to produce proportionately larger drops in cylindrical effect (Ma *et al.*, 2008;Buckhurst *et al.*, 2010b) the need to compensate for toric misorientation, especially with higher powered toric IOLs, remains imperative in order to avoid the associated drop in acuity.

CHAPTER 3: Evaluation of a simplified method of measuring intraocular lens tilt

3.1. Introduction

The success of cataract surgery is greatly influenced by the ability of an implanted IOL to maintain a fixed and steady position within the capsular bag over the long term. IOLs may rotate, tilt or decentre such that the subject is no longer looking through the optimum part of the lens and this can lead to reduced visual performance (Kim *et al.*, 2010). Good IOL alignment is important in achieving post-operative success especially with newer IOLs such as aspheric and multifocal designs.

3.2. IOL tilt

Research into IOL misalignment has focussed mainly on investigating the impact of IOL rotation, and measurement techniques have been developed to enable accurate assessment of rotation as discussed later in chapter 4. IOL tilt is often overlooked as a potential cause of reduced vision post-operatively; however lens tilt, like rotation, can have a detrimental impact on quality of vision (Taketani *et al.*, 2004;Kumar *et al.*, 2011;Madrid-Costa *et al.*, 2012). While IOL rotation is more of a concern with toric and some multifocal IOLs, lens tilt can affect the success of all types of IOL. Spherical IOL tilt, for example, has been shown to induce unwanted refractive astigmatism (Auran *et al.*, 1990;Kozaki *et al.*, 1991b;Oshika *et al.*, 2005) and coma-like aberrations (Oshika *et al.*, 2005;Taketani *et al.*, 2005b), while tilt of an aspheric IOL may produce a loss in its spherical aberration neutralising capability (Nishi *et al.*, 2010) and tilt of an accommodating IOL may limit its corrective ability (Rosales *et al.*, 2010). For this reason it is important to measure lens tilt.

Uozato *et al.* (1988) investigated the tolerable limits of IOL tilt and decentration and concluded that decentration of more than 1.0mm or tilt of more than 5° would impair

visual quality. Hayashi *et al.* (2001) investigated the correlation between IOL decentration and tilt on visual acuity at all distances with a multifocal and monofocal IOL and found tilt of 2.38±1.18 in the monofocal group and 2.94±1.58 in the multifocal group. They found significant correlations between the degree of IOL decentration and logMAR visual acuity, with greater decentrations associated with worse far and intermediate acuity. No correlation was found between tilt and visual acuity in either group. However, the IOLs tilted by less than 5° in all but one participant, and so the impact of severe IOL dislocation on visual function could not be assessed. The amount of tilt reported to occur after surgery varies; some authors have found average tilt of 2.45° (Hayashi *et al.*, 1997), 2.69° (Kim *et al.*, 2001a) and 3.43° (Taketani *et al.*, 2004), which would have a negligible impact on vision, while others have documented as much as 28.87° (Oshika *et al.*, 2005), which would have a significant effect.

Differences in IOL tilt have been shown to occur in patients with ocular pathology. There are greater amounts of IOL tilt resulting from capsular shrinkage in patients with diabetes, retinitis pigmentosa and pseudoexfoliation syndrome compared to otherwise healthy eyes (Hayashi *et al.*, 1999). The key findings of IOL tilt studies from the past three decades are detailed in table 3.1. According to Sivak (1985) lens tilt of more than 20° is needed to induce a significant level of unwanted astigmatism, whereas Nishi (2010) stated that even minor variations in IOL tilt could impact on visual acuity.

While IOL rotation can occur as soon as a few hours after surgery and again in significant amounts several months afterwards (chapter 4), research into changes in tilt over time indicates no such pattern. Taketani *et al.* (2004) assessed IOL position using Scheimpflug images on patients 4 to 48 months after the phacoemulsification and IOL implantation procedure, and found no correlation between time after surgery and level of tilt. Hayashi *et al.* (1997) evaluated lens position using a Scheimpflug imaging

system at six different intervals between 1 week and 1 year after implantation and concluded that as long as the IOL was placed correctly within the capsular bag at the time of surgery, there would be no significant progression in lens tilt and decentration in the 12 months following surgery, and this was true for any lens material including PMMA, silicone and soft acrylic. It therefore appears that capsular bag shrinkage, which is a leading source of late IOL rotation, does not affect lens tilt in the same way (Kim *et al.*, 2010;Prinz *et al.*, 2011). The relationship between lens tilt, rotation and decentration is unclear. It is not certain whether IOL tilt occurs as a consequence of other lens movement, such as rotation or decentration, and so should be investigated further.

3.3. Current IOL tilt measurement techniques

There are various methods of measuring lens tilt (Nishi *et al.*, 2010;Rosales *et al.*, 2010;Kumar *et al.*, 2011;Grewal *et al.*, 2012), however there is currently no gold standard technique (de Castro *et al.*, 2007). Common methods of IOL tilt measurement include Scheimpflug imaging, Purkinje reflections and Anterior Segment Optical Coherence Tomography, each of which are discussed in more detail next.

3.3.1. Scheimpflug imaging

In standard cameras, the image and object planes are usually parallel to each other, as well as to the plane of focus. Therefore an object that is placed parallel to the image plane of a camera will coincide with the plane of focus and the whole object will be imaged sharply (figure 3.1a). If the object is not parallel, image distortion may occur and the image will only be focussed along a small region where it intersects with the plane of focus as illustrated in figure 3.1b.

In Scheimpflug systems, the image and object planes are not parallel, but at an angle to each other (Wolffsohn *et al.,* 2007;Grewal *et al.,* 2012). A tangent from both the image plane, object plane and plane of focus will intersect at a point, known as the Scheimpflug intersection (figure 3.1c). In this way all sections of non-parallel objects can be focussed sharply and completely with a large depth of focus. As a result of tilt of the object plane in respect to the optical axis of the instrument, image magnification will vary over the image resulting in geometrical distortion, thus correction factors need to be applied to account for this as this can produce a discrepancy in tilt and decentration measurements (Coppens *et al.*, 2005;de Castro *et al.*, 2007). What's more, because each succeeding optical surface is viewed through the preceding refracting ocular surface, this introduces optical distortion, which must also be accounted for (de Castro *et al.*, 2007;Rosales *et al.*, 2010). Commercially available Scheimpflug instruments such as the Pentacam system typically only correct for the anterior and posterior corneal surface and not the crystalline lens (Rosales *et al.*, 2009). Ray tracing techniques can be utilised to attain accurate information about crystalline lens geometry in order to fully correct optical distortion (Coppens *et al.*, 2005). Limitations of Scheimpflug imaging include a need for adequate pupil dilation (de Castro *et al.*, 2007;Nishi *et al.*, 2010) in order to be able to visualize the posterior surface of the lens, as well as excellent patient co-operation in remaining still and maintaining good fixation during measurement (de Castro *et al.*, 2007).
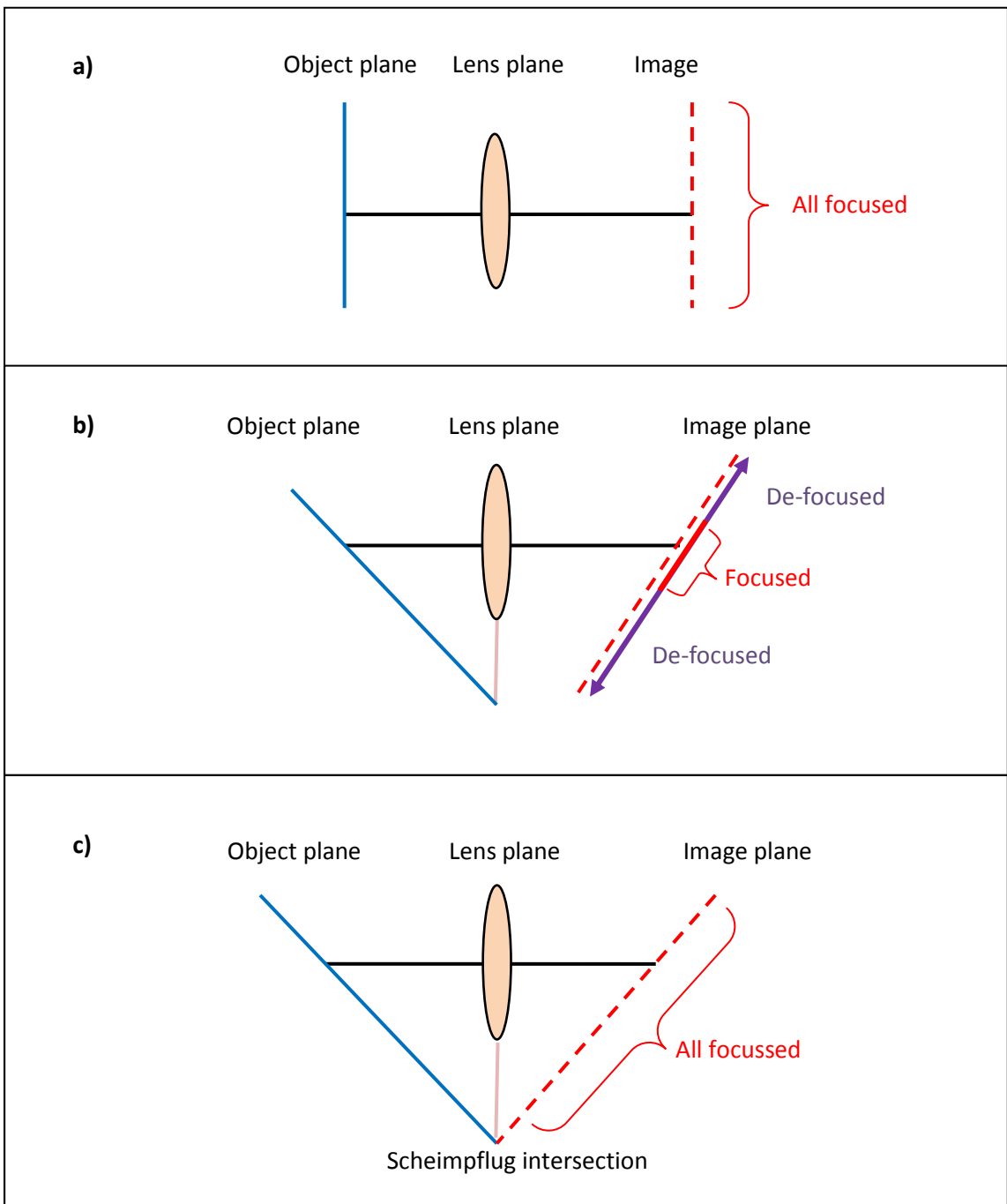
Figure 3.1a: the object, lens and image plane are parallel to each other producing a sharp image. 3.1b: the object and image planes are not parallel leading to peripheral image distortion. 3.1c: the object and image planes are not parallel, however use of the Scheimpflug principle renders the whole image in sharp focus.

3.3.2. Purkinje imaging

Purkinje imaging is another method which can be used to assess *in vivo* IOL alignment. Purkinje images are named after Johannes Purkinje who first described them in 1832. They are reflections from all interfaces of ocular media with different refractive indices (Nishi *et al.*, 2010). Purkinje reflexes from the corneal and lenticular surfaces of the eye can be used to assess IOL tilt (de Castro *et al.*, 2007).
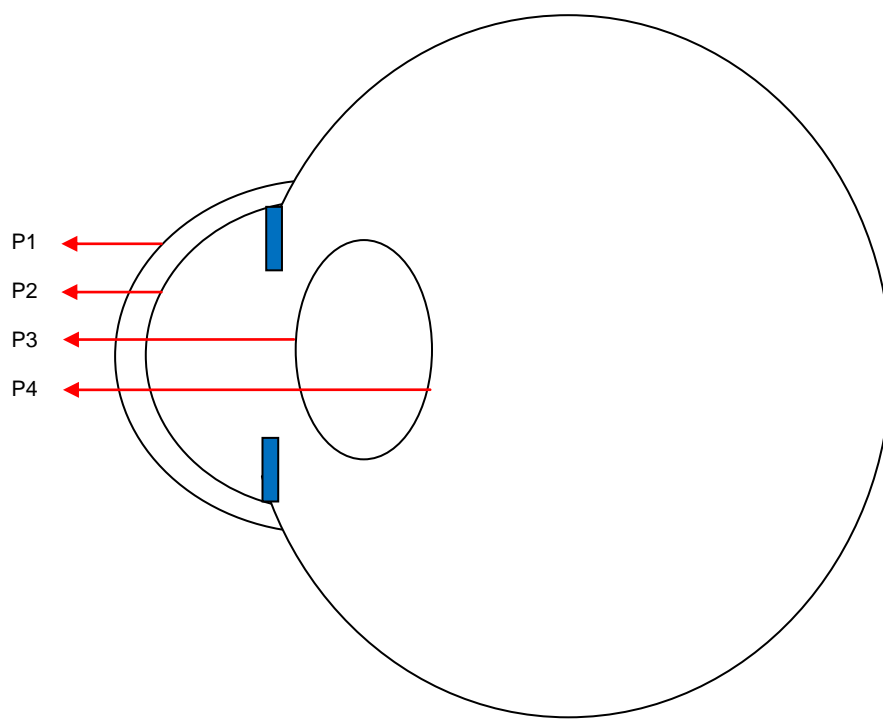
Figure 3.2: Purkinje images are formed as a result of reflections from the eye's refractive surfaces. Purkinje 1 comes from the anterior cornea/tear film, Purkinje 2 from the posterior cornea, Purkinje 3 from the anterior lens and Purkinje 4 from the posterior lens.

Clinical studies have used purkinje images to assess lens alignment (Phillips *et al.*, 1988;Auran *et al.*, 1990;Guyton *et al.*, 1990).This method of measuring lens tilt and decentration in dilated eyes, assumes a linear relationship between the location of Purkinje images 1, 3 and 4 relative to a central reference point such as the pupil centre, as a function of ocular rotation in addition to lens tilt and decentration (de Castro *et al.*, 2007;Rosales *et al.*, 2010).

However there are some reports of low reproducibility with this technique (Kim *et al.*, 2001b) as well as limitations in its use in certain instances, such as with very flat lenses, which can produce unreliably large values for Purkinje 3 (de Castro *et al.*, 2007).

3.3.3. Anterior Segment Optical Coherence Tomography

IOL tilt can also be measured using Anterior Segment Optical Coherence Tomography (AS-OCT). OCT is a high resolution imaging technique in which a light source is split into two beams. One, called the reference beam, is reflected by a mirror and the second, a measurement beam, is reflected by ocular structures. These beams are recombined and the distance travelled by the reference beams can be scanned to allow interferometry to build a 2D or 3D image. Tilt angle can be ascertained using the software that is supplied with the instrument (Wolffsohn *et al.*, 2007;O'Donnell *et al.*, 2011).
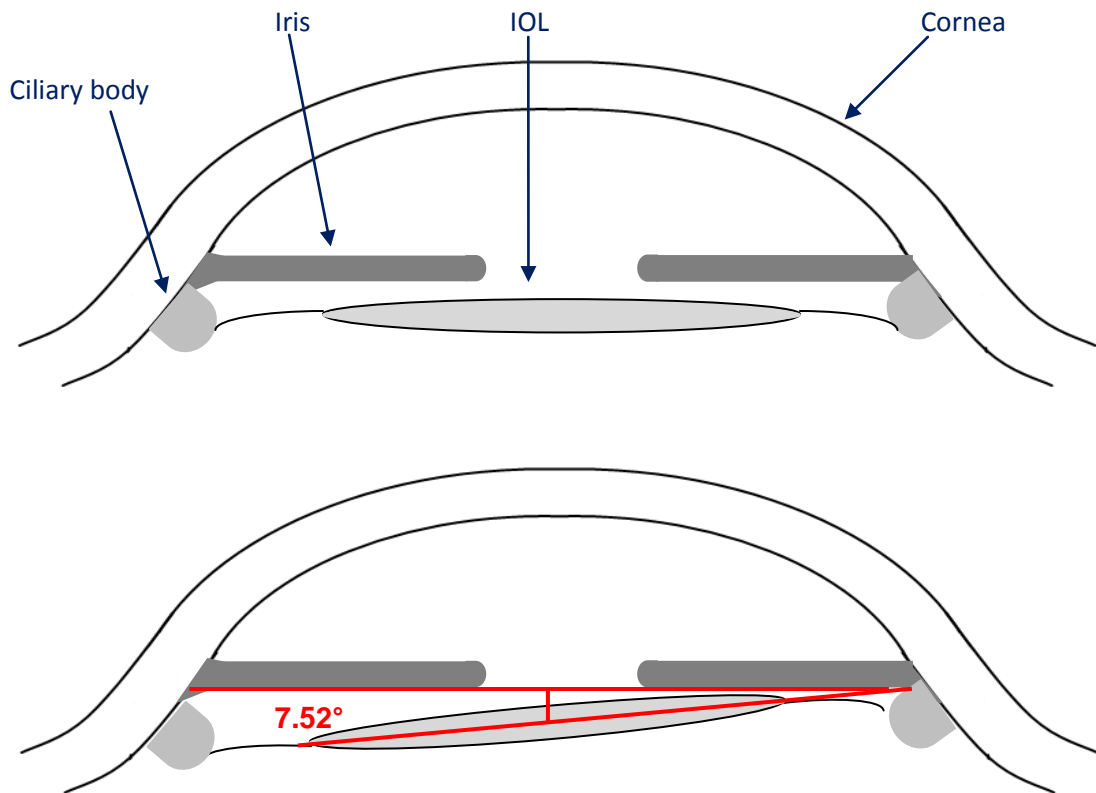
Figure 3.3: AS-OCT can be used to image the anterior segment of the eye and the supplied software tools used to measure tilt angle of an implanted IOL.

AS-OCT can be used for a number of different functions from measurement of corneal thickness and anterior chamber depth to non-invasive *in vivo* evaluation of IOL alignment (Kumar *et al.*, 2011). As with Scheimpflug imaging, AS-OCT is prone to optical distortion as a result of differences in the refractive index of ocular structures and the curved nature of the eye's surfaces, and so a correction factor must be applied (Dunne *et al.*, 2007). Some instruments, such as the Visante (Carl Zeiss Meditec Inc., Dublin, CA, USA) use built-in software to help reduce the effect of distortion, however some error still remains. While it is possible for AS-OCT devices to measure the posterior crystalline lens surface without dilation (O'Donnell *et al.*, 2011) pupil dilation is recommended to ensure adequate assessment of tilt with this technique (Kumar *et al.*, 2011).

IOL name	No. of eyes	Post-op visit	Analysis method	Tilt ±SD (°) about X axis	Tilt ±SD (°) about Y axis	Decentration (mm)	Rotation ±SD (°)	Visual Outcomes	Study
Posterior chamber IOL	-	-	Purkinje imaging	7.53±3.03	-	0.68±0.33	-	-	Kozaki *et al.* (1991a)
PMMA Posterior chamber IOL	13	-	Purkinje	7.8	-	0.7	-	-	Phillips *et al.* (1988)
PC IOL	56	variable, up to 3years	Purkinje	Mean: 6.09±3.80	-	Mean: 0.67±0.43 (range 0 to 2.5mm)	-	-	Durak *et al.* (2001)
Alcon MA30BA	40	4-48months	Scheimpflug	3.43±31.55	-	0.303 ± 0.168	-	Best corrected VA at time of exam of better than 20/25	Taketani *et al.* (2004)
un-specified	1	5years	Scheimpflug	28.87	-	1.78	-	Visual acuity 25/20	Oshika *et al.* (2005)
Group I: sharp optic edge one eye, rounded optic edge in other eye	Group I:50	1 week, 6+12 months	Scheimpflug	At12months: Group I- sharp edge: 3.03±1.79, rounded edge: 3.26±1.69	-	At 12months: Group I- sharp edge: 0.24±0.13, rounded edge: 0.23±0.13	-	-	Baumeister *et al.* (2005)

Group II: silicone sharp optic edge one eye, acrylate sharp edge in contralateral eye	Group II: 56			Group II- silicone:2.34± 1.81, acrylate:2.32 ±1.41		Group II- silicone 0.29±0.21, acrylate: 0.24±0.10			
1 piece vs. 3 piece hydro-phobic acrylic IOL	88	1,7,14,30 days and 6 months	Purkinje reflection and photos	1 piece: 2.70±0.84 3 piece: 2.72±0.55	-	1 piece: 0.39±0.13 3 piece: 0.34±0.08	-	-	Mutlu *et al.* (2005)
Acryfold 60BB and Acrysof MA60AC	64	6months	Scheimpflug	Acryfold 60BB : 2.22± 1.44 Acrysof MA60AC: 3.18±1.84	-	Acryfold 60BB : 0.345± 0.208 Acrysof MA60AC: 0.370±0.171	-	All patients had best corrected VA better than 20/25 at the time of exam	Taketani *et al.* (2005a)
Aspheric IOL	21	≥6months	Scheimpflug and Purkinje imaging	S: 1.17±0.75 P: 1.89±1.00	S: 1.56±0.82 P: 2.34±0.97	Horizontal S: 0.23± 0.19 P: 0.34± 0.19 Vertical - S: 0.19± 0.20 P: 0.17± 0.23	-	-	de Castro *et al.* (2007)

Young group with their natural crystalline lens (CL) and Tecnis ZCB00 IOL	40 each group	≥6 weeks	Purkinje	Crystalline lens: 2.2±0.7 (up) IOL group: 2.5±1.4 (up)	CL: 3.1±1.5 (temporal) IOL group: 2.6±1.5 (temporal)	CL: 0.16 down 0.07 temporal IOL group: 0.06 nasal and 0.02 upward of pupil	-	-	Mester *et al.* (2009)
Tecnis, AMO, Acrysof	21	-	Scheimpflug and Purkinje imaging	S: 1.17±0.75 P:1.89±1.00	S: 1.56±0.82 P:2.34±0.97	Horizontal- S: 0.23 ± 0.19 P:0.34±0.19 Vertical- S: 0.19±0.20 P:0.17±0.23	-	-	Rosales *et al.* (2010)
Part I: Akreos Adapt Plate haptic OU one vertical and the other horizontal Part 2:Acrysof 3 piece MA60AC one eye, Acrysof 1 piece SA60AT in other eye	Part 1: 15 eyes Part 2: 15 eyes	1 + 3 months	Purkinje *-ve= upward & temporal tilt	At 3months: Part 1- Vertical:-1.5±1.1, Horizontal: 2.9±0.9 Part 2- 1 piece: 2.2±7.2, 3 piece: 5.3±2.4	At 3months: Part 1- Vertical: 1.6±1.2, Horizontal: 1.9±1.4 Part 2- 1 piece: 1.9±0.3, 3 piece: 2.6±4.1	At 3months: Part 1- Vertical: 0.4±0.2, Horizontal: 0.4±0.2 Part 2- 1 piece: 0.4±0.3, 3 piece: 0.6±0.8	-	-	Crnej *et al.* (2011)

3 IOLs: 1-piece foldable acrylic (Appasamy), 1-piece non-foldable PMMA (Appasamy) and 1 piece foldable acrylic (Akreos)	123	6±1.2 months	AS-OCT	Mean: 1.52±0.9 Range: 0.04-3.6	-	no data	-	Best corrected visual acuity ≥20/20 in 88 eyes out of 123, 20/30 in 23 eyes and ≤20/40 in 12 eyes	Kumar *et al.* (2011)
1 piece : Tecnis ZCB00 3 piece Tecnis ZA9003	100	1 day, 1month, 3 months, 12 months and 24 months	Purkinje meter (prototype)	Vertical 12months- 1 piece: 2.28±1.80, 3 piece 4.12±5.08	Horizontal 12months- 1piece: 2.27±3.07, 3 piece: 2.71±2.73		-	Mean **un-corrected** distance logMAR visual acuity at 24 months- 1piece: 0.11±0.09, 3 piece: 0.13±0.04	Findl *et al.*(2015)

				24months- 1 piece: 3.04±2.13, 3 piece 3.41±2.66	24months- 1 piece: 2.02±2.36, 3 piece: 2.79±2.40			Mean **corrected** distance logMAR VA at 24 months- 1piece: 0.02±0.02, 3 piece: 0.02±0.10.	

Table 3.1: Table of important findings from IOL tilt studies from the last three decades. Tilt about the X axis refers to movement of the superior edge of the IOL forward (positive number) or backward (negative) relative to the inferior IOL, while tilt about the y axis refers to temporal tilt constituting movement of the nasal IOL edge forwards (positive) or backwards (negative) relative to the temporal IOL (de Castro *et al.*, 2007).

3.3.4. New tilt evaluation technique

The previously used techniques of rotating Scheimpflug, Purkinje analysis and m ti-axis ASOCT involve additional non-standard consulting room equipment which is generally expensive. Hence, a simpler technique using standard en-face photography would be useful in clinical practice, even if it had limited resolution, as a screening tool.

IOLs have a circular optic which, when imaged, should have major and minor axes of equal length. When tilted these axes will no longer be equivalent and the central optic will appear elliptical as opposed to circular. For example, if the IOL is tilted outwards about the horizontal meridian, the lower part of the IOL will be more anteriorly located compared to the top half of the IOL. Therefore the width of the IOL will remain unchanged, however the height will decrease (figure 3.4). It is proposed that by applying Pythagoras's theorem, the relationship between the height and width of the central IOL optic can be used to mathematically determine IOL tilt in relation to the visual axis.

While the direction of tilt cannot easily be determined, the orientation and magnitude should be determinable with simple current slit-lamp image capture technology
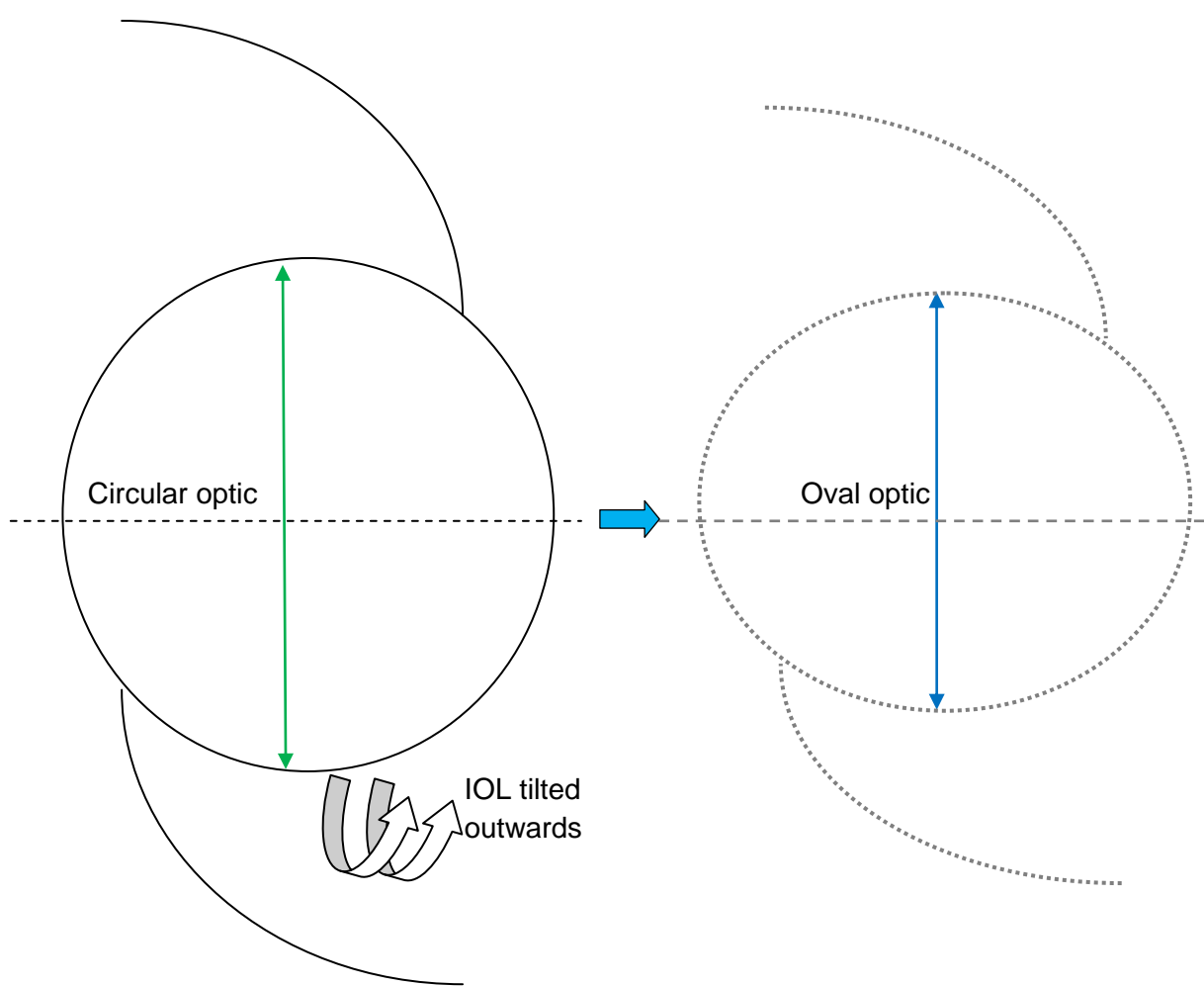
Figure 3.4: As an IOL with a circular optic (black, solid) is tilted, it appears more elliptical (grey, dotted).

Pythagoras's theorem defines the relationship between the three sides of a right angled triangle and states that in a right angled triangle, the square of the hypotenuse is equal to the sum of the squares of the other two sides (figure 3.5, equation 3.1)

$$a^2+b^2=c^2$$

Equation 3.1
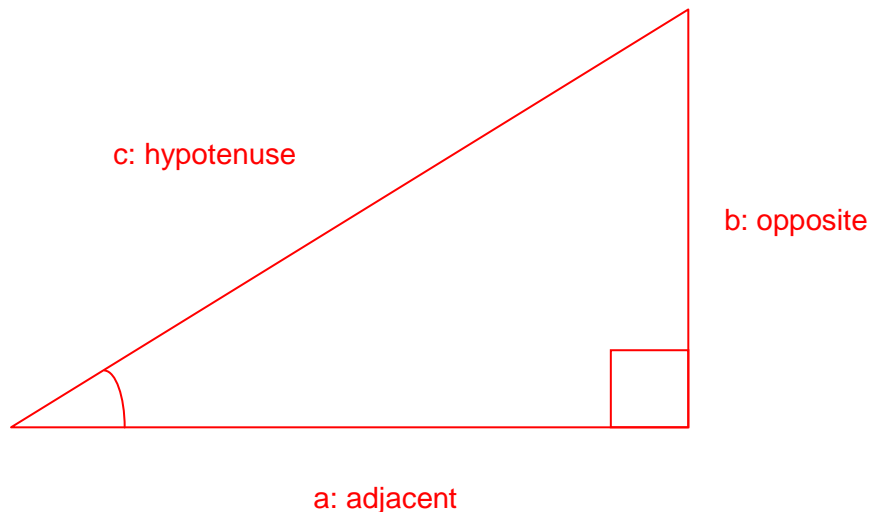
Figure 3.5: Pythagoras's theorem.

The Pythagorean trigonometric identity expresses Pythagoras's theory in terms of trigonometric functions. The cosine of an angle gives the ratio of the length of the adjacent side, to the length of the hypotenuse. Given this, the projection of an IOL can be defined so that the axial ratio of the ellipse, as measured by dividing the minor axis by the major axis, is used to calculate angle of tilt (Ө) (figure 3.6, equation 3.2, 3.3):

$$\mathbf{Cos}\ \square = \frac{\mathbf{adjacent}}{\mathbf{hypotenuse}} = \frac{\mathbf{minor\ axis}}{\mathbf{major\ axis}}$$

Equation 3.2

$$\mathbf{\theta} = \mathbf{cos}^{-1}\frac{\mathbf{minor\ axis}}{\mathbf{major\ axis}}$$

Equation 3.3
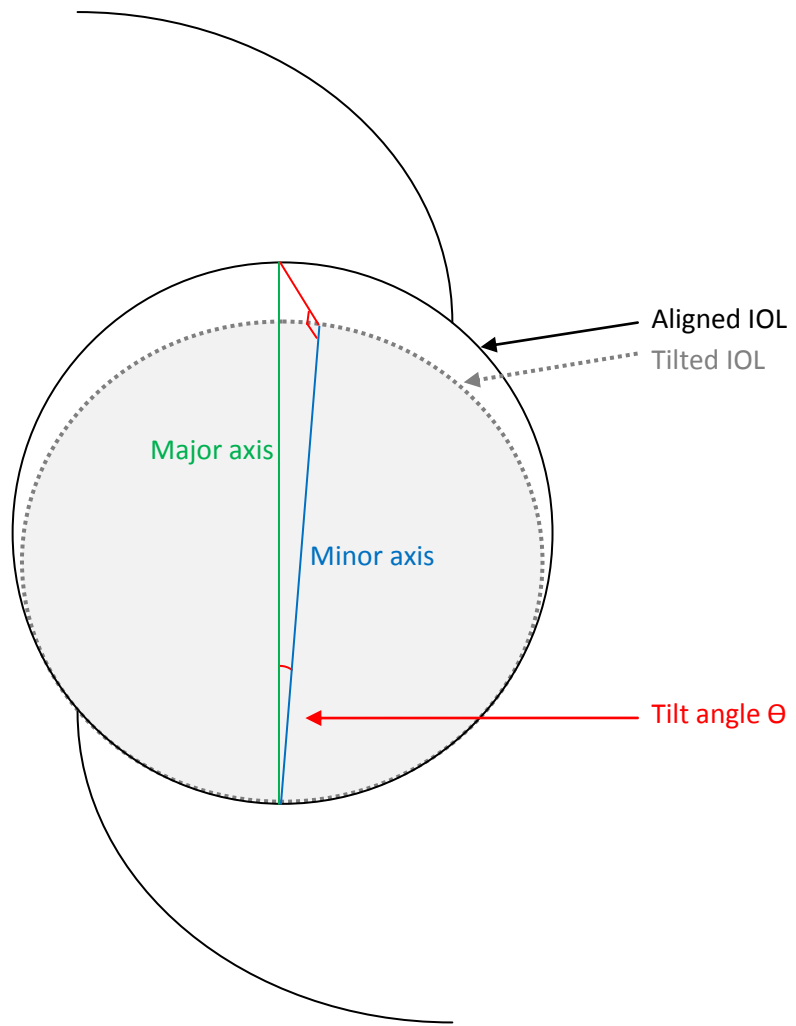
Figure 3.6: illustrates the use of Pythagoras's theorem to determine the IOL tilt angle.

This technique could potentially enable tilt to be measured rapidly using equipment that is readily accessible in most ophthalmic clinics; the accuracy and repeatability of this new IOL tilt technique is evaluated next.

3.4. Methods

A multifocal IOL (AcrySof Restor, Alcon) was carefully placed on a bespoke tilt stand (figure 3.7) which enabled vertical tilt and horizontal tilt. This custom built stand was constructed in the engineering department at Aston University. Following a pilot study, a flat platform on which to place the IOL was constructed to minimise potential alterations in the lens tilt between measurements. Goniometers, which enable an object to be accurately rotated about a fixed point, were stacked on top of each other to enable both vertical and horizontal tilt to be adjusted. A GNL 10/M goniometer which allowed tilt of ±10 ° was firmly fastened on top of a GNL 18/M goniometer which allowed tilt of ±5°, at 90 degrees to each other (Thorlabs, Munich, Germany). The IOL platform was then securely attached on top of this stack of goniometers (figure 3.7).

The IOL was placed flat on the IOL platform and the stand tilted horizontally, both in the leftward and rightward direction as well as vertically in both the upward and downward direction by up to 10° in 1° steps. An image of the IOL was captured after each degree of tilt using a high resolution Nikon digital camera (figure 3.8). The camera used was a Nikon D5200 24.1 megapixel camera with a Nikon 60mm f/2.8G ED AF-S Macro. Camera resolution is related to the sensor size, with bigger sensors producing higher quality images. In this case the sensor size was 23.5mm by 15.6mm, giving a resolution of 255.3 pixels per millimetre. Good alignment of the IOL relative to the camera is crucial in obtaining accurate tilt measurements and so IOL centration was carefully monitored to ensure the IOL remained on-axis during photography.
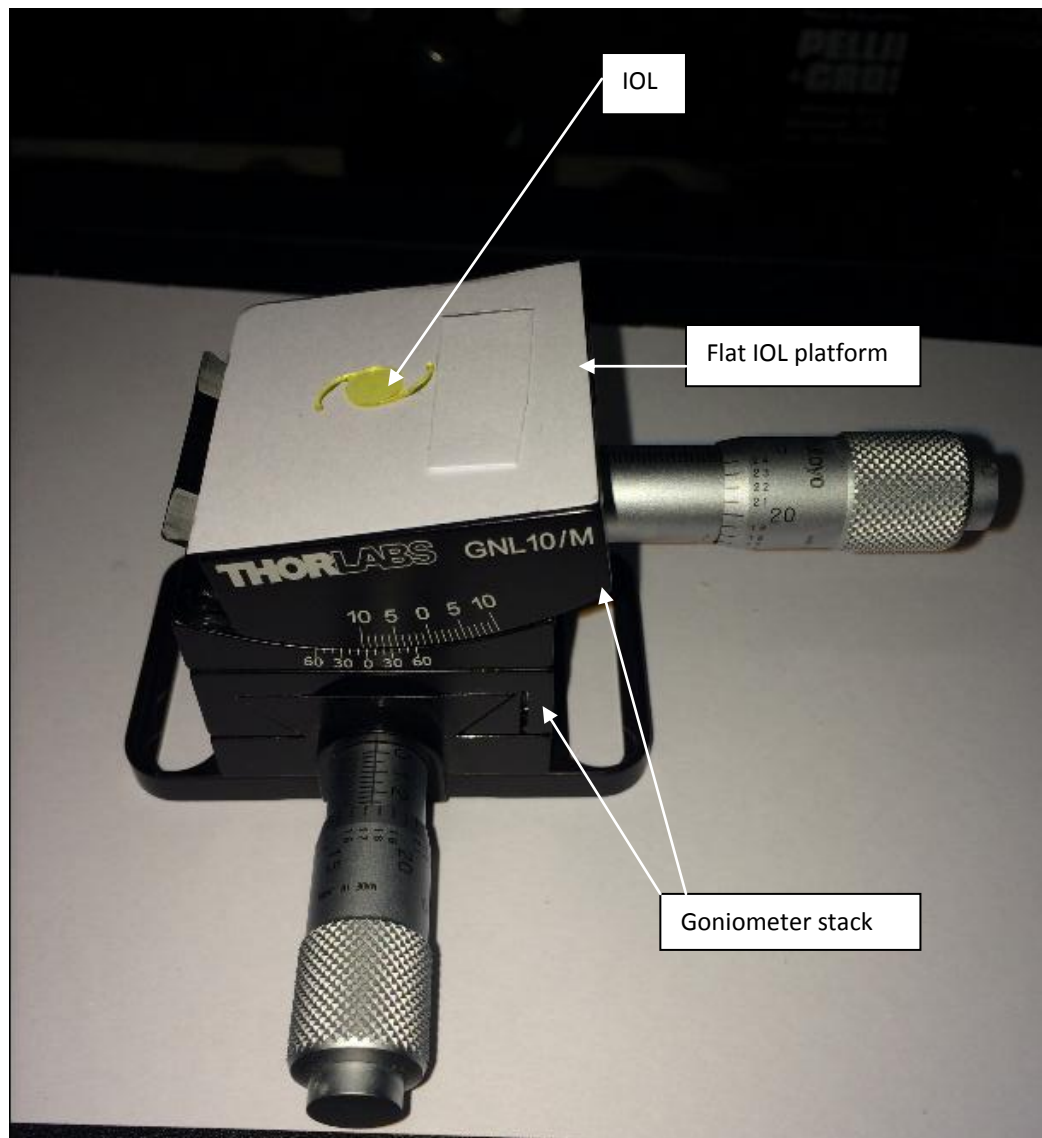
Figure 3.7: custom tilt stand on which the IOL was placed during the study.
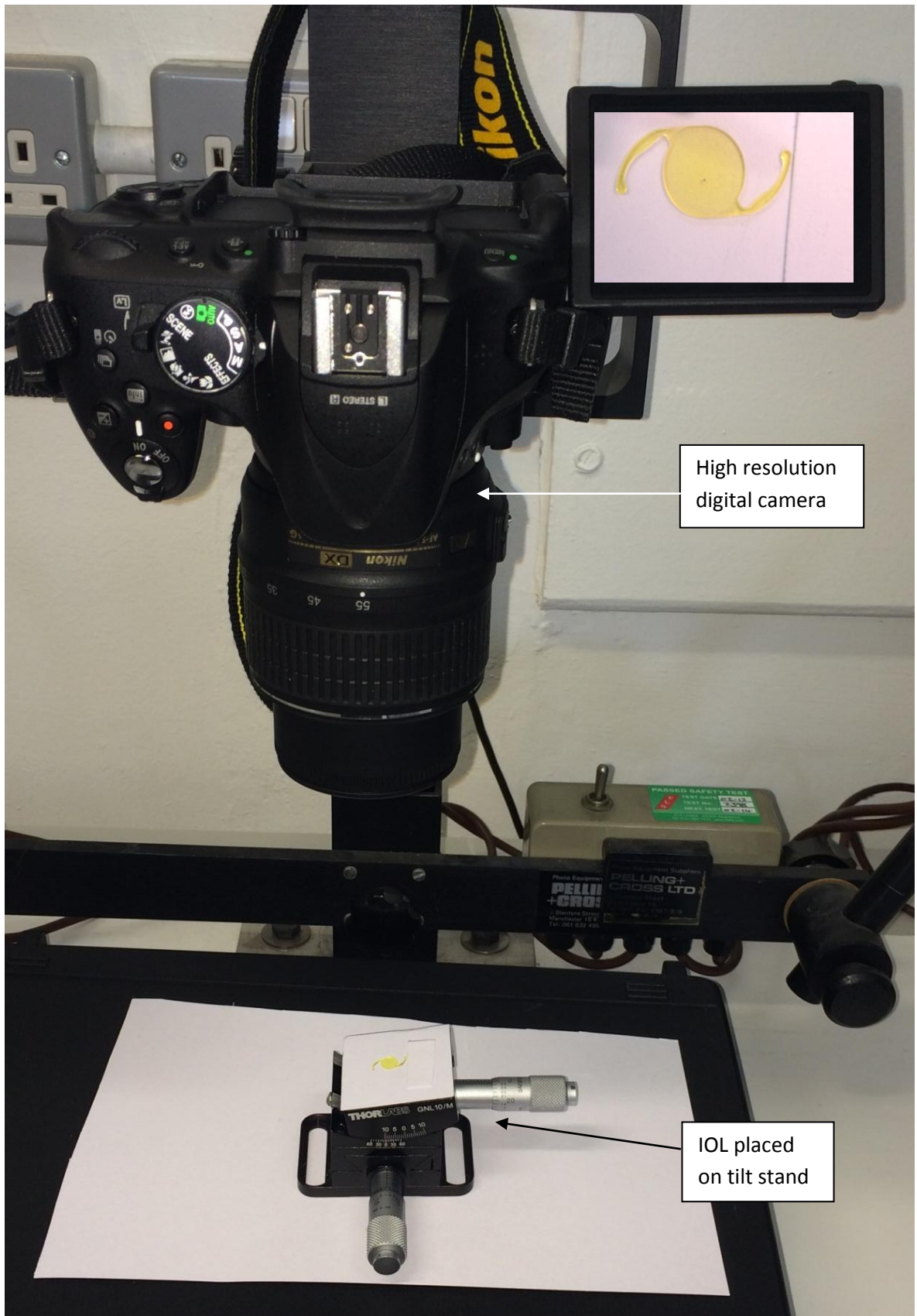
Figure 3.8: image showing the setup of the camera in relation to the IOL. The digital camera was placed vertically above the IOL which was placed centrally on the stand.

The images were extracted and analysed using an imaging programme called ImageJ (figure 3.9) available at: http://imagej.nih.gov/ij/.
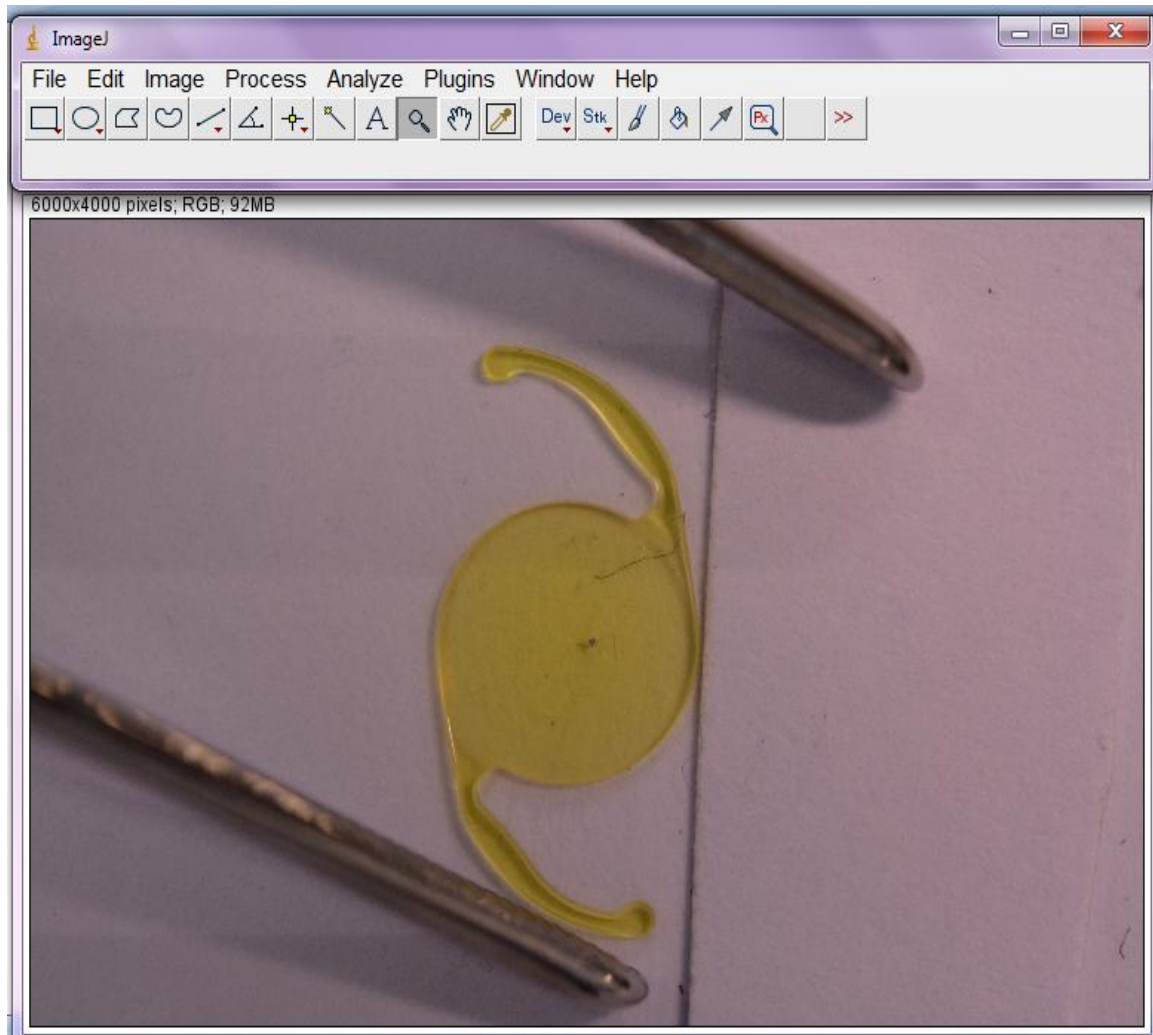
Figure 3.9: screenshot of an IOL tilt image extracted into ImageJ.

An ellipse was superimposed over the central IOL optic (figure 3.10 and 3.11) in order to obtain measurements of the IOL width and height in pixels; from this IOL tilt could then be calculated using equation 3.3. This was done in order to determine how accurately width and height measurements from digital imaging related to actual IOL tilt and thus whether this technique could be used to accurately evaluate IOL tilt *in vivo.*
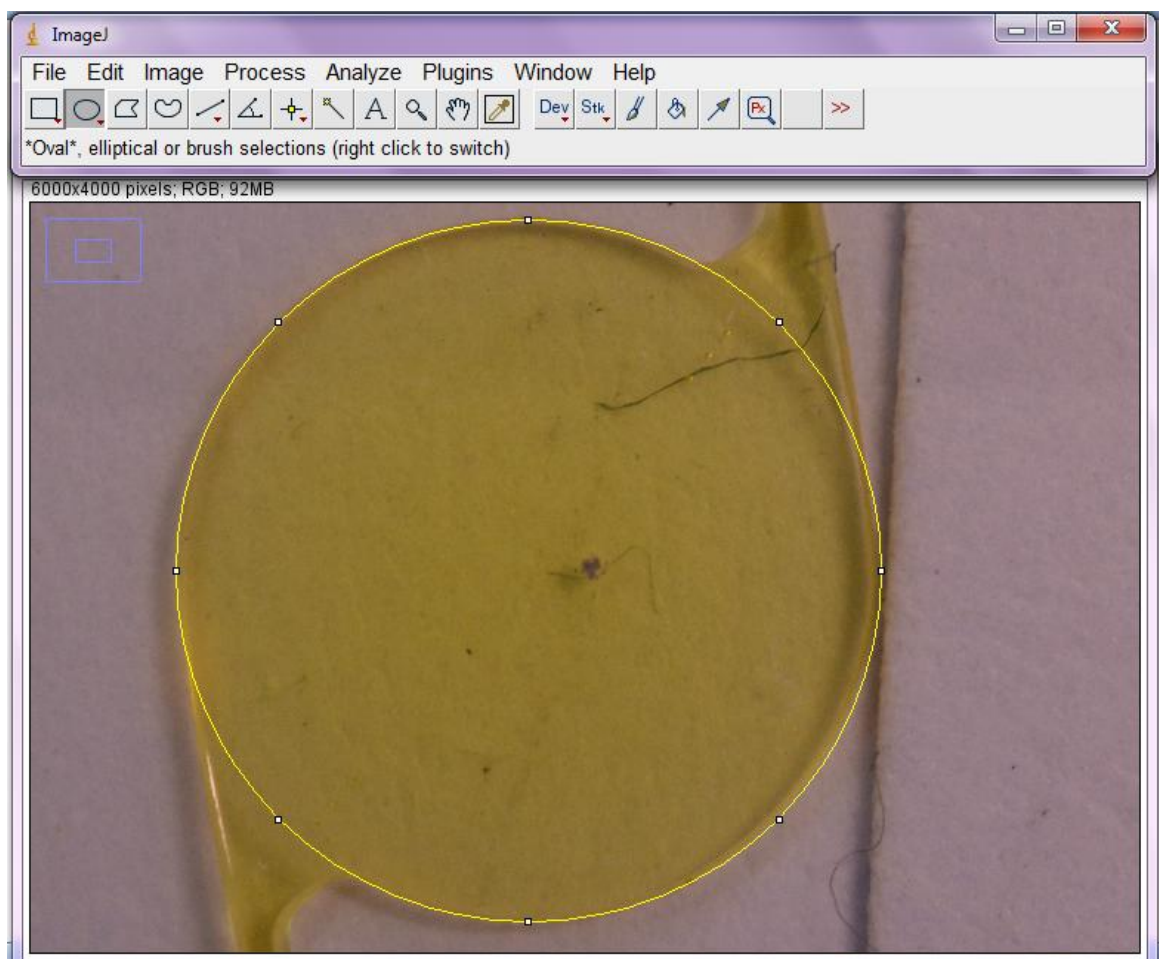
Figure 3.10: An oval tool is selected in ImageJ and superimposed over the central IOL optic.
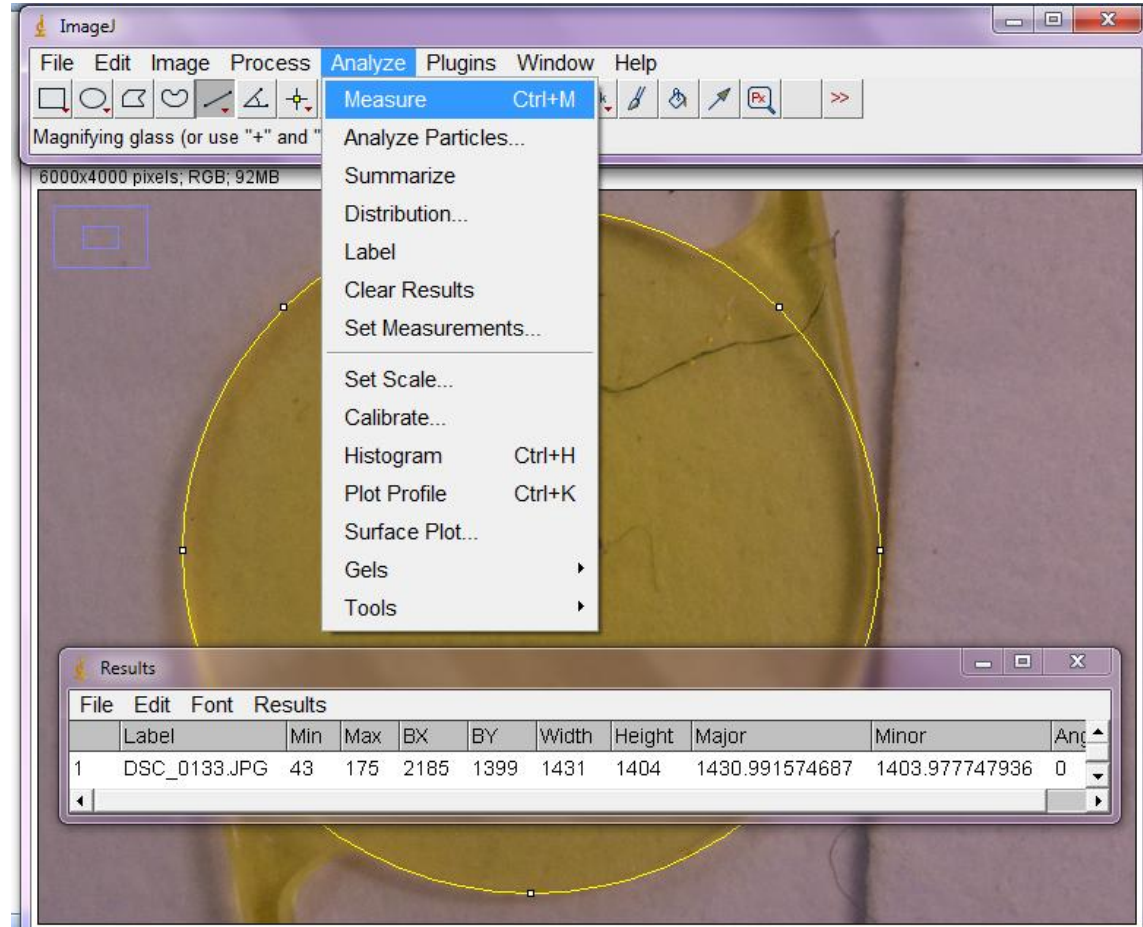
Figure 3.11: The dimensions of this oval in pixels can then be evaluated using the "Analyze" menu function.

Resolution describes the ability to distinguish between two adjacent spots. It is an important factor to consider when using digital imaging and is influenced by pixel number (Peterson *et al.*, 2005). The Nikon camera had a resolution of 6000 x 4000 and was viewed on a 15 inch monitor with a screen resolution of 1280 x 1024 pixels. Viewing higher resolution images on a monitor of lower resolution can lead to a reduction in the perceived image quality and this can be a potential source of inaccuracy (Peterson *et al.*, 2005). The number of pixels across the lens will affect ability to detect tilt. In this study, the images were scaled using the known IOL dimensions and it was determined that in order to reliably distinguish 1° of tilt, a difference between IOL width and height of 0.0009 ± 0.00002mm, which s equivalent to 0.211 ± 0.006 pixels, was required. Given that 0.205 to 0.217 pixels are required to

detect a 0.0009mm difference, a pixel resolution of between 227.78 to 230.00 pixels per millimetre is required, as shown below. Therefore a minimum resolution of 227 pixels per millimetre is recommended equivalent to around 1400 across a 6mm IOL optic or 2724 pixels across the typical 12mm iris.

0.205 - 0.207pixels = 0.0009mm

x 1111.1111

227.78 -230.00pixels = 1.00 mm
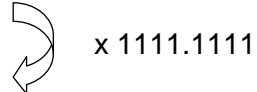
3.5. Repeatability

The repeatability of the new tilt evaluation technique was analysed in order to assess its reliability. To investigate this, ten images of increasing IOL tilt in the horizontal rightward direction were assessed again using image J software in the same measurement session (intrasession), on a different session day by the same observer (inter-session) and then also with a different observer (inter-observer). To assess intra-session repeatability the same observer measured the ten horizontal rightward tilt images, continued measuring the other tilt direction images and then re-measured the first ten horizontal rightward images within the same testing session. The observer was masked to the previous measurement values. The same observer also re-analysed the same ten horizontal rightward images in the same way on a different day in order to assess inter-session repeatability. Finally inter-observer repeatability was evaluated using an individual with no prior knowledge of the research and with no previous experience of this type of image analysis. The measurement procedure was explained to them using a demonstration image and the individual asked to record their findings on a separate spreadsheet.

3.6. Statistical analysis

A one-sample Kolmogorov-Smirnov test revealed that the data exhibited a normal distribution (Kolmogorov-Smirnov Z = 0.576, P >0.05). Tilt calculated using the new method was compared to actual tilt using paired two-tailed t-tests. Agreement between the two methods of tilt assessment was evaluated by calculating the mean of the differences, or the bias, between the two techniques and the 95% confidences limits, as described by Bland and Altman (1986), and presented graphically.

3.7. Results

Tilt values were calculated and compared against actual tilt (table 3.2; 3.3).

IOL tilt direction	Actual tilt (°)	Width (pixels)	Height (pixels)	W/H ratio	IOL tilt (°)	Change in tilt angle (°)
horizontal rightward	0	1412.982	1413.991	0.999	2.16	0
	1	1412.014	1414.010	0.998	3.04	0.88
	2	1412.020	1415.995	0.997	4.29	2.13
	3	1414.009	1422.010	0.994	6.08	3.92
	4	1402.020	1411.971	0.993	6.81	4.64
	5	1407.997	1422.028	0.990	8.06	5.89
	6	1407.006	1425.017	0.987	9.12	6.95
	7	1396.019	1415.012	0.987	9.40	7.23
	8	1397.972	1418.013	0.986	9.64	7.48
	9	1377.967	1401.001	0.984	10.40	8.24
	10	1386.013	1413.037	0.981	11.22	9.06
horizontal leftwards	0	1410.025	1412.006	0.999	3.04	0
	1	1410.038	1414.014	0.997	4.30	1.26
	2	1409.028	1416.023	0.995	5.70	2.66
	3	1393.995	1402.026	0.994	6.14	3.10
	4	1396.000	1406.025	0.993	6.85	3.81
	5	1395.015	1407.000	0.991	7.48	4.45
	6	1378.027	1390.992	0.991	7.83	4.79
	7	1385.994	1400.997	0.989	8.39	5.36
	8	1374.013	1392.994	0.986	9.47	6.43
	9	1382.016	1405.019	0.984	10.38	7.35
	10	1373.012	1401.996	0.979	11.67	8.64

Table 3.2: Actual versus calculated horizontal IOL tilt. The change in tilt angle column refers to the difference in calculated tilt relative to the preceding tilt value

IOL tilt direction	Vertical tilt (°)	Width (pixels)	Height (pixels)	W/H ratio	IOL tilt angle (°)	Change in tilt angle (°)
vertical upward	0	1355.016	1353.012	0.999	3.12	0
	1	1359.023	1356.008	0.998	3.82	0.70
	2	1356.018	1350.021	0.996	5.39	2.27
	3	1360.017	1351.958	0.994	6.24	3.12
	4	1356.000	1343.984	0.991	7.63	4.52
	5	1359.997	1346.016	0.990	8.22	5.11
	6	1360.016	1344.001	0.988	8.80	5.69
	7	1362.017	1343.992	0.987	9.33	6.22
	8	1365.986	1344.005	0.984	10.29	7.18
	9	1368.009	1342.025	0.981	11.18	8.07
	10	1374.020	1341.005	0.976	12.59	9.47
vertical downward	0	1342.997	1341.976	0.999	2.23	0
	1	1343.997	1342.023	0.999	3.11	0.87
	2	1346.983	1344.005	0.998	3.81	1.58
	3	1346.998	1341.010	0.996	5.40	3.17
	4	1350.020	1340.991	0.993	6.63	4.40
	5	1354.018	1343.992	0.993	6.98	4.74
	6	1350.990	1337.997	0.990	7.95	5.72
	7	1350.021	1335.998	0.990	8.27	6.03
	8	1356.015	1338.021	0.987	9.34	7.11
	9	1355.998	1332.003	0.982	10.79	8.56
	10	1348.999	1322.998	0.981	11.27	9.03

Table 3.3: Calculated versus actual IOL tilt in the vertical meridian.
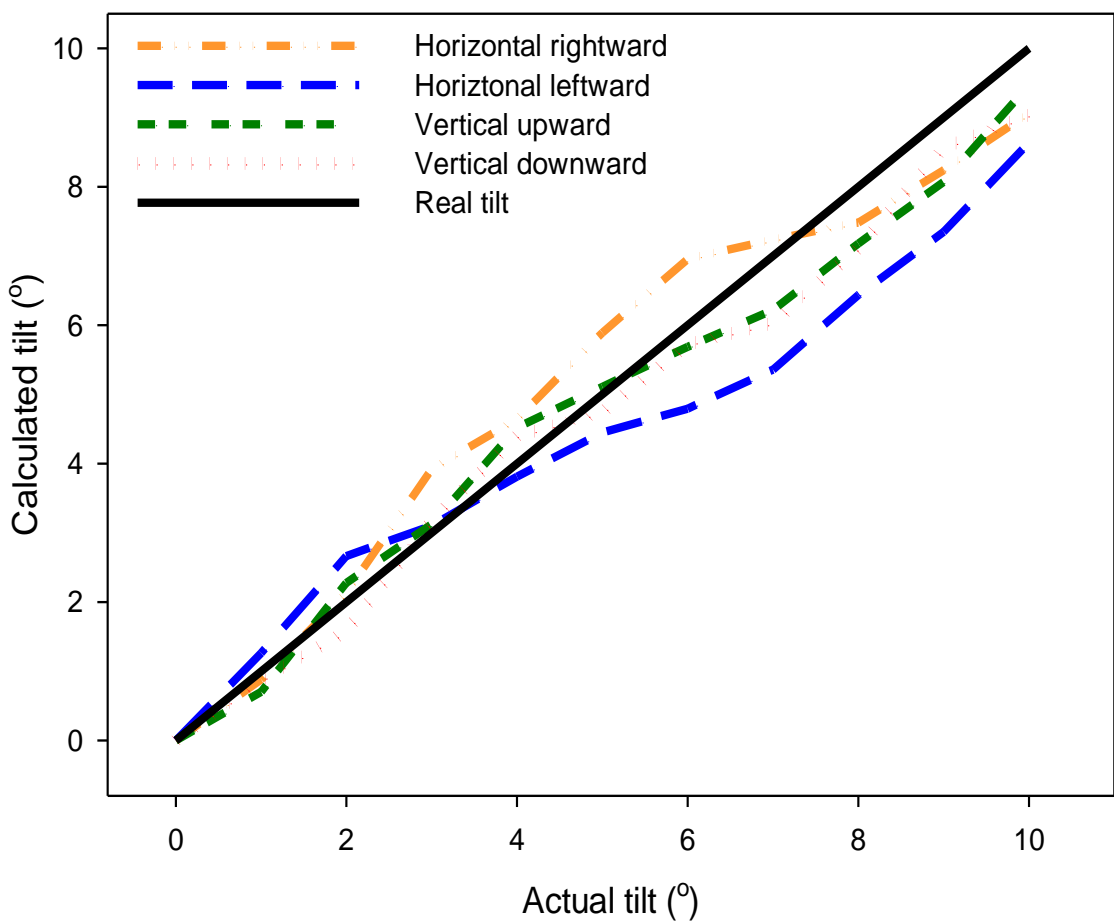
Figure 3.12: plot comparing calculated tilt in the four directions with actual tilt.

Calculated and actual tilt values were found to be highly correlated (figure 3.12; 3.13). Paired t-tests showed there to be no statistically significant difference between actual and average calculated tilt (paired t-test t=-1.739, p=0.113) indicating good agreement between the two techniques.

3.8. Validity of new IOL tilt evaluation:

Agreement between the new method of calculating IOL tilt and actual tilt was plotted graphically using Bland and Altman plots (figure 3.13-3.16). There was a slope to the

data with the difference between actual and calculated tilt changing from positive to negative with increasing tilt indicating proportional bias, therefore regression based limits of agreement were used (Bland *et al.*, 1999). Since the data showed homoscedasticity as opposed to heteroscedasticity the 95% prediction intervals were used to represent the limits of agreements, and are indicated by the black dashed lines. The regression line is indicated by the solid black line (Bland *et al.*, 1999;Ludbrook, 2010). Inspection of the Bland Altman plot indicates good agreement between actual and calculate tilt, more so for vertical tilt than horizontal tilt, since the mean difference is close to 0 and the limits of agreement narrow.
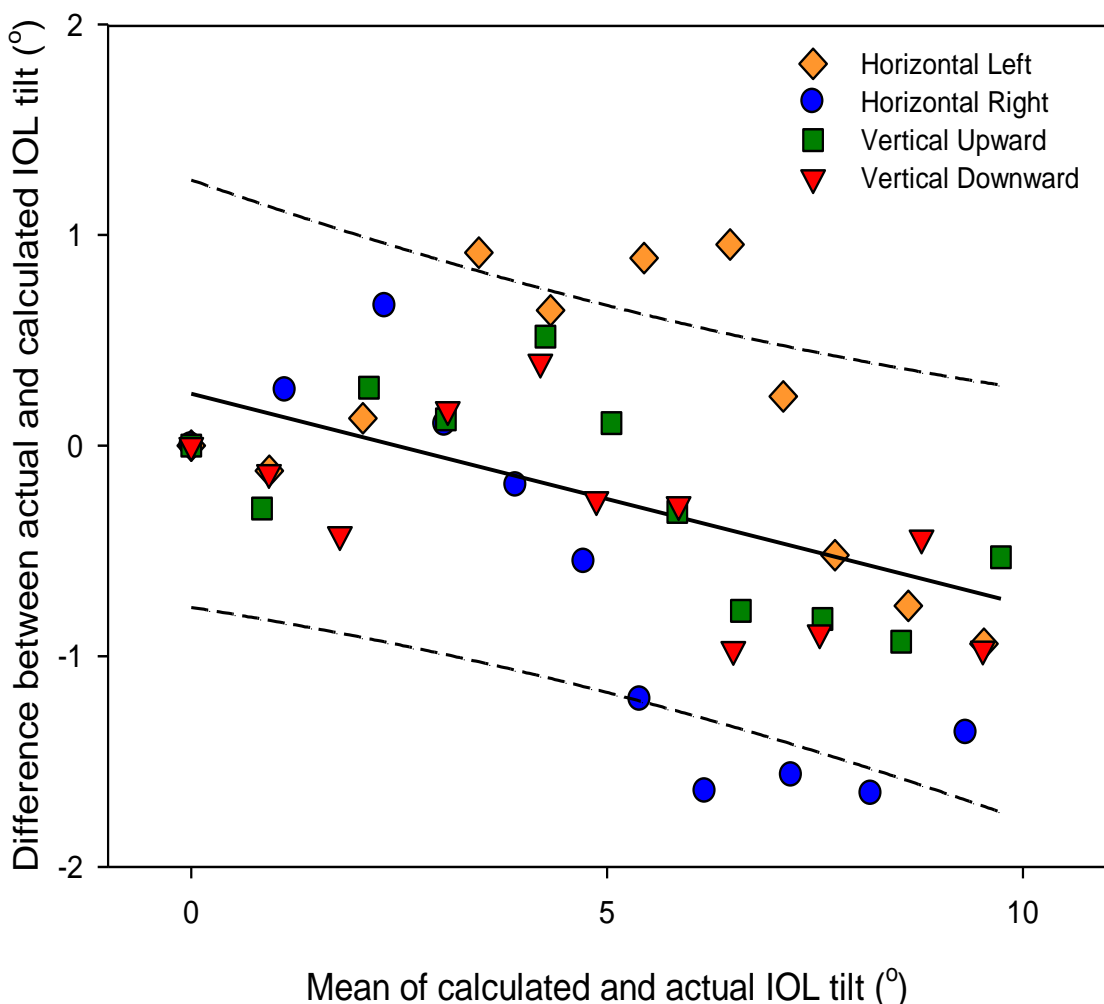
Figure 3.13: Bland and Altman plot comparing calculated versus actual tilt.

3.9. Repeatability of new IOL tilt calculation method

3.9.1. Intra-session

Test-retest intersession repeatability is presented in Bland-Altman graphical format (Figure 3.14). The average difference between calculated tilt measured by the same observer within the same measurement session at the 95% confidence interval was -0.12° ± 0.62°. This demonstrates good intra-session repeatability of the new tilt technique since the mean difference was close to 0 with narrow limits of agreement.
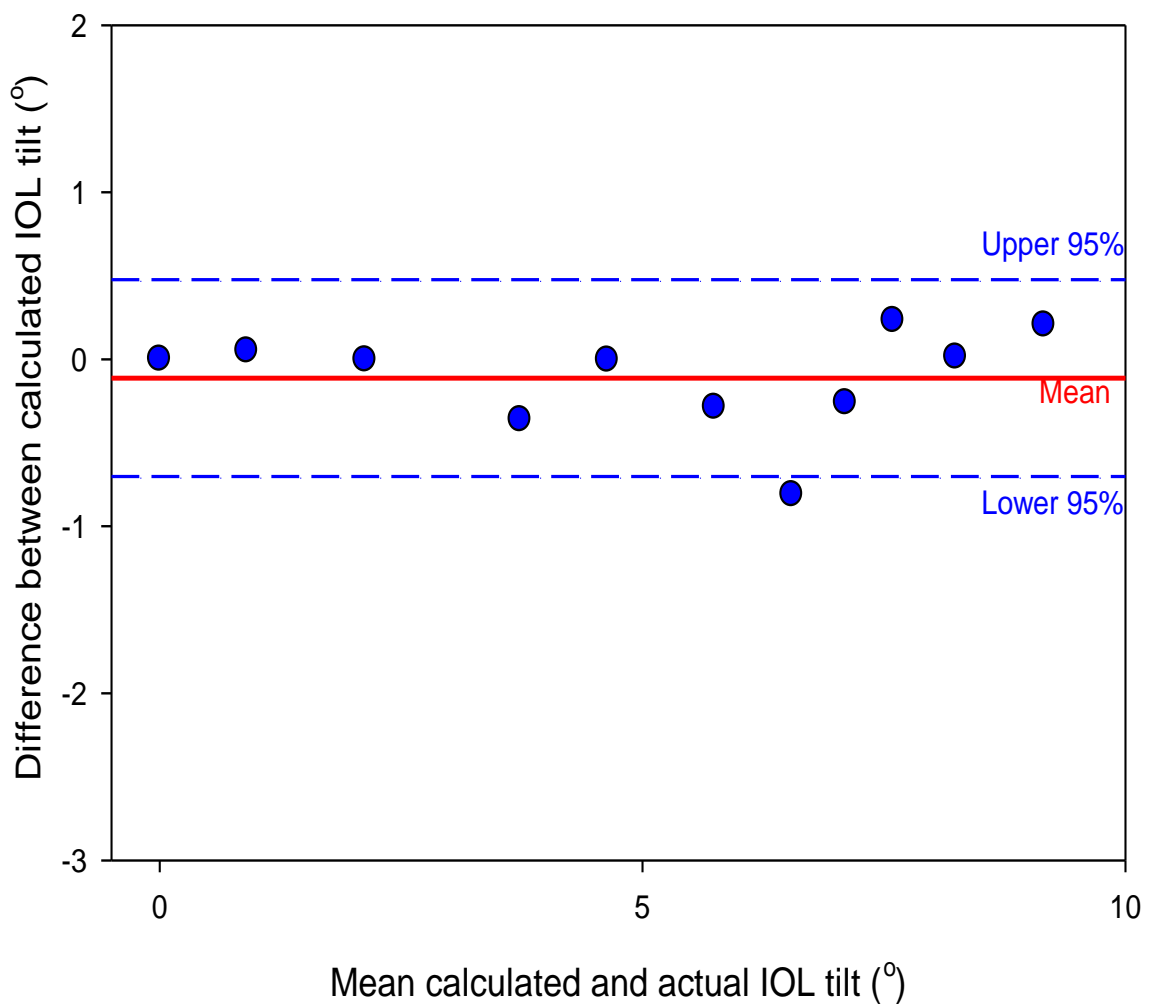
Figure 3.14: Bland and Altman plot comparing intra-session repeatability of the new tilt calculation method.

3.9.2 Intersession

The average difference between calculated tilt measured on the same images by the same observer on different days at the 95% confidence interval was -1.24° ± 0.99° (figure 3.15). This mean difference is relatively small which demonstrates the relative repeatability of this new tilt technique with the same observer at different measurement sessions.
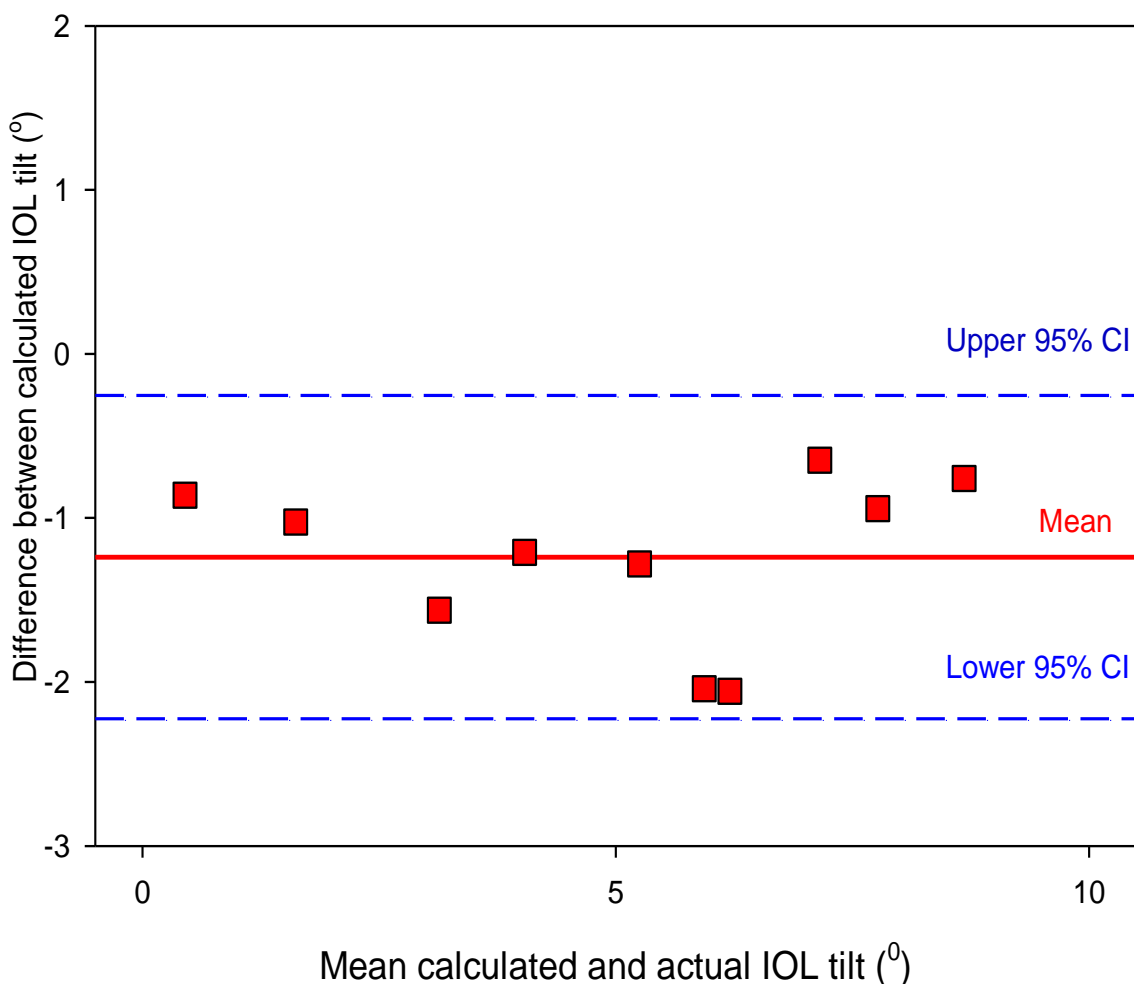
Figure 3.15: Bland and Altman plot comparing the intersession repeatability of the new calculated tilt method.

3.9.3   Inter-observer

The average difference between calculated tilt from two different observers assessing the same images at the 95% confidence interval was -2.08° ± 1.28° (figure 3.16). Repeatability of the technique between different observers was lower than for intra and inter-session measurements with the same observer. This may have occurred due to a learning curve with the first examiner, who had more opportunity to practice their measurement technique in ImageJ compared to the second observer. Thus this mean difference could potentially be reduced by addressing this limitation; however the mean difference in tilt measurements found between observers is acceptable for the intended purpose of this new tilt measurement technique as a screening tool to detect large amounts of lens tilt.
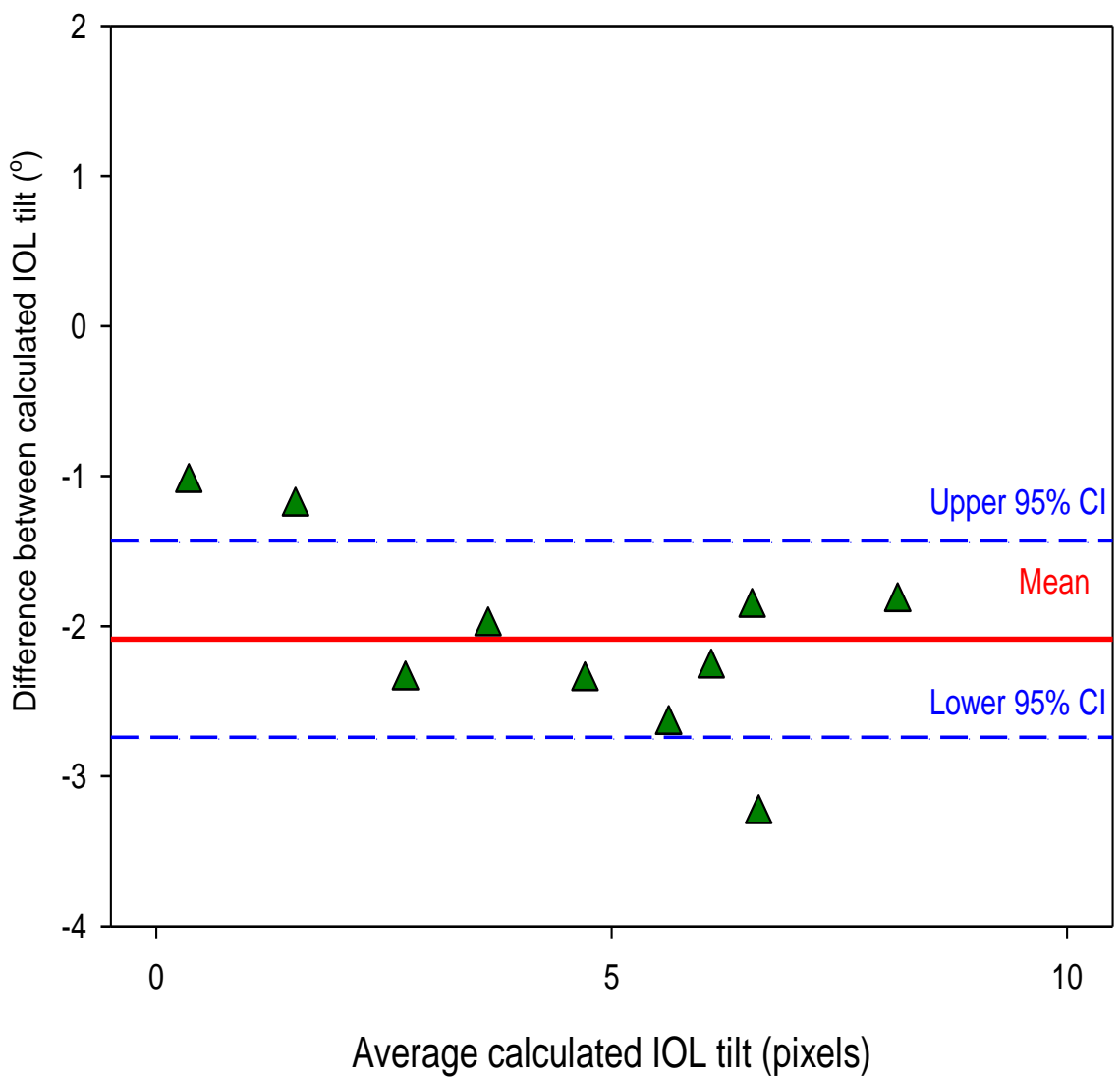
Figure 3.16: Bland and Altman plot comparing inter-observer repeatability of the new tilt calculation method.

3.10. Discussion

Accurate alignment of an implanted IOL is important in achieving post-operative success, particularly with toric and multifocal designs. IOL tilt is frequently disregarded when evaluating lens fit, but can have an equally damaging effect on visual quality as other measures of malposition such as IOL rotation and decentration (Taketani *et al.*, 2004;Kumar *et al.*, 2011;Madrid-Costa *et al.*, 2012). Tilt and decentration are commonly evaluated together and can influence the eye's optical properties by contributing to the myopic shift of the post-operative refractive error and inducing oblique astigmatism (Korynta *et al.*, 1999;Durak *et al.*, 2001). Large decentrations and tilts can produce considerable post-operative refractive errors. The relationship between the geometrical axes of decentration and tilt influences the extent of the refractive error. Korynta *et al.* (1999) found that the least favourable combination of 12° tilt and 3mm decentration generated a refractive error of up to -7.00DS and +4.00DC. IOL shape can also influence decentration and tilt, with biconvex lenses found to be least affected by decentration and tilt compared to planoconvex and meniscus designs, and so considered the superior choice for IOLs (Kozaki *et al.*, 1995). IOL haptic design may also influence decentration and tilt, with 3 piece IOLs showing a tendency to tilt and decentre more than 1 piece IOLs in a study by Crnej *et al.* (2011) although the difference was not found to be statistically significant.

The purpose of this study was to develop a new, objective method of rapidly measuring IOL tilt. Most, if not all optometry and ophthalmology clinics have access to a slit lamp and even if a camera system is not integrated into the system, images can be captured by smart phones or other cameras through the eyepiece optics. An advantage of the new technique is the speed with which the images can be captured, especially if the patient has already been set up behind the slit lamp for other post-operative tests,

since there is no need to rotate the camera or analyse multiple images as with Scheimpflug imaging and AS-OCT.

Absolute calculated tilt values appeared to compare well with actual tilt and the technique has been shown to be repeatable (figure 3.13-3.16). This new tilt measurement method was assessed against actual, known tilt of an un-implanted IOL to ensure more accurate evaluation, as opposed to comparing directly with other tilt evaluation methods such as Purkinje and Scheimpflug imaging, each of which have their own range of measurement error. Grewal *et al.* (2012) found that Scheimpflug imaging used in conjunction with ImageJ software was highly repeatable. Similarly, de Castro (2007) found both Purkinje and Scheimpflug imaging to be highly repeatable, with a mean standard deviation of repeated tilt measures of 0.61° for Purkinje and 0.20° for Scheimpflug imaging. The mean standard deviation of repeated tilt measures for the new tilt evaluation technique was comparable at 0.92°. The impact of these typical measurement errors on visual performance would be expected to be minimal given that no correlation was found between visual acuity and mean IOL tilt levels of between 2.39° and 2.94° (Hayashi *et al.*, 2001). There may have been a learning curve with the new, simplified tilt method in terms of the process of superimposing the oval onto the IOL optic in ImageJ, which could have lead to an improvement in calculated tilt values with repeated testing. Development of an automated mechanism to determine this would be advantageous to make the technique more objective.

The cornea and crystalline lens greatly influence the optical quality of the human eye, with the cornea accounting for two thirds of the eye's refractive power and the crystalline lens contributing one third of the power (Gullstrand, 1924). It is therefore

important to measure corneal shape and correct for any associated distortion effects in order to obtain more accurate measurements. This is especially the case when imaging the crystalline lens, or an implanted IOL, given the numerous refraction changes that occur imaging through the multiple preceding ocular surface layers (Dubbelman *et al.*, 2001;Ortiz *et al.*, 2012). The new method of calculating IOL tilt presented here is susceptible to the effects of corneal astigmatism. If significant amounts of corneal astigmatism are present in a subject, the imaged lens may appear more tilted that it actually is. The impact of this on measurement accuracy is not currently known but was predicted as follows.

Mean corneal astigmatism is estimated to be in the region of 1.00D (Hoffer, 1980;Ferrer-Blasco *et al.*, 2009;Hoffmann *et al.*, 2010) in the average population, ranging up to 6.75DC (Ferrer-Blasco *et al.*, 2009). The meridional magnification effects associated with uncorrected astigmatism can be calculated using equation 3.4 (Atchison, 1996;Rosen *et al.*, 2011).

$$\mathbf{SM} = \frac{\mathbf{1}}{\mathbf{1} - \mathbf{dF}}$$

Equation 3.4

Where d refers to the vertex distance and F, the lens power.

This formula can be adapted to the current scenario by entering the power of the corneal astigmatism as F, and using the anterior chamber depth as the vertex distance. Estimates of mean anterior chamber depth have been given as 3.11mm (Hoffmann *et al.*, 2010), 3.32mm (Hoffer, 1980) and 3.59mm (Queiros *et al.*, 2005). A ratio of the associated magnification effects can be determined using equation 3.4, which can then be converted into a magnification percentage. Using averaged anterior chamber depth values an approximate meridional magnification effect of 0.3% was found for 1 dioptre of uncorrected corneal astigmatism, which translated to apparent tilt of 4.59°. Apparent tilt for every dioptre of astigmatism up to 7.00DC was calculated and is shown in figure 3.17.
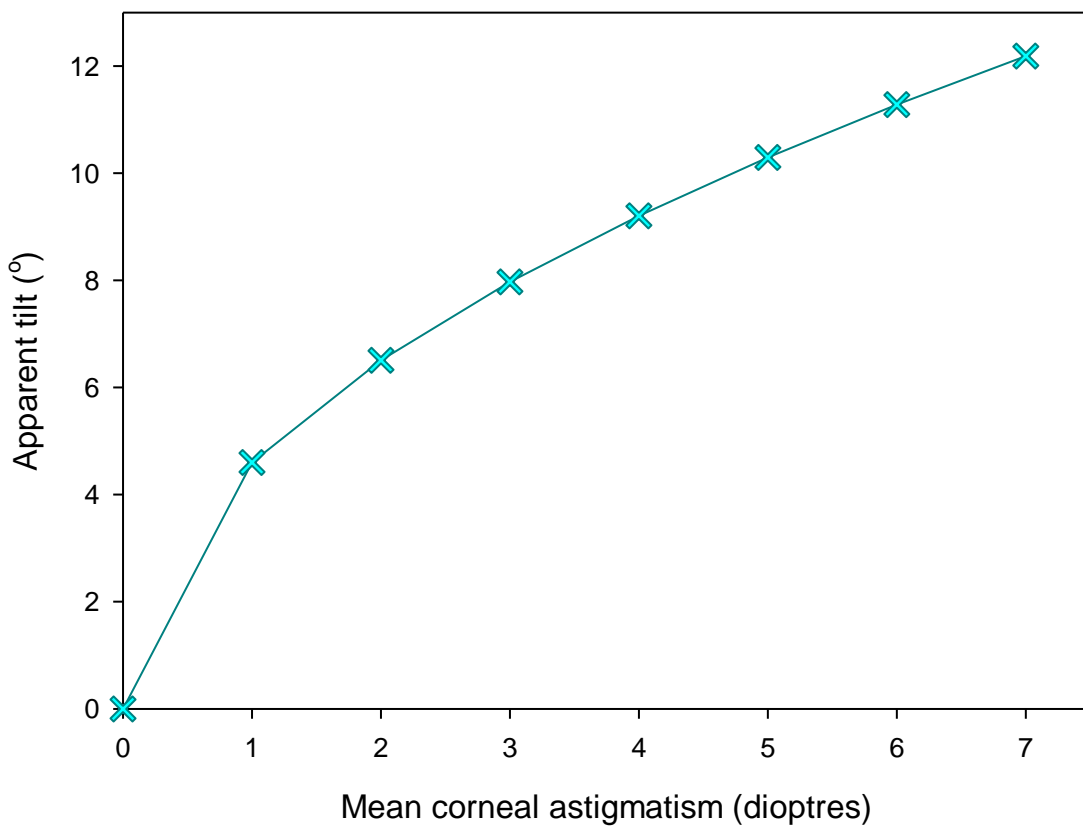
Figure 3.17: the effect of corneal astigmatism on apparent IOL tilt.

Curve fitting in Matlab using the rational fit model (r^2=0.999) gave the following equation with which to predict the effect of uncorrected corneal astigmatism on apparent tilt:

$$\textbf{Apparent tilt}\,(°) = \frac{(\mathbf{0.8498x^2 + 7.88x + 0.002778})}{\mathbf{x + 0.9185}}$$

<div align="right">Equation 3.5</div>

Where x= uncorrected corneal astigmatism in dioptres.

Uncorrected corneal astigmatism can mask true tilt therefore use of corneal topography is recommended so that the effect of any corneal astigmatism can be measured and accounted for using equation 3.5. Alternatively, the effect of corneal astigmatism on measurement error may be eliminated by insertion of an appropriately calculated toric contact lens. This will ensure enhanced accuracy of IOL tilt evaluation using this new, simplified method in patients with varying degrees of corneal astigmatism.

This new method of mathematically calculating IOL tilt has been shown to be accurate and repeatable and as such could be useful as a rapid alternative to more costly methods of tilt assessment such as Scheimpflug imaging, Purkinje imaging or AS-OCT. This technique has been used to assess tilt in a large cohort of subjects implanted with an IOL in the next chapter.

CHAPTER 4: Evaluating long-term tilt, decentration and rotation of an implanted IOL

4.1. Measurement of IOL position

For maximum effect, an IOL must remain correctly orientated in the capsular bag after surgery (Prinz *et al.*, 2011) as malposition can negatively impact upon visual performance (Kim *et al.*, 2010;Wolffsohn *et al.*, 2010a;Visser *et al.*, 2011a). Previous research in this thesis (chapter 2) has confirmed a statistically significant decrease in visual acuity with increasing amounts of toric rotation with a larger and faster drop in acuity observed for greater amounts of uncorrected astigmatism (figure 2.3). Therefore accurate IOL placement becomes even more crucial with greater IOL powers (Ale *et al.*, 2012b).

Previous chapters have evaluated a new idea for improving patient tolerance to toric IOL rotation (chapter 2) and also developed a relatively simple, new technique that can be used to measure tilt of an IOL (chapter 3). IOL malposition can be characterised by a third type of misalignment- decentration (Baumeister *et al.*, 2005). A review of the literature has revealed there to be a paucity of available information regarding the association between lens tilt, rotation and decentration. Given the similarity in their possible causes, the link between these factors should be examined in more depth to determine whether they arise together or occur independently of each other.

4.2. Lens Decentration

Accurate IOL placement is a key determinant of patient success after IOL implantation. A recent study investigated the effect of decentration by laterally displacing a wavefront corrected IOL by 1mm and found an increased incidence of higher order aberrations,

mainly coma, with increasing decentration. Thus it was concluded that excellent centration was necessary to maximize visual performance (Wang *et al.*, 2005b).

IOL decentration describes a difference in the IOL centre relative to another reference point, commonly the centre of the pupil or limbus. Subjective decentration assessment of an implanted IOL requires the pupil to be dilated and is examined by measuring the position of the edge of the IOL optic within the pupil. It is susceptible to the effects of parallax since the IOL lies in a different plane.

Lens decentration can reduce optical quality, especially when coupled with lens tilt (Eppig *et al.*, 2009). Tilt and decentration are often evaluated together as the actual combination of the two will influence the optical quality (de Castro *et al.*, 2007) and can influence the refractive error that is induced; they will either enhance or lessen this refractive error depending upon the relationship between their geometrical axes (Korynta *et al.*, 1999). IOL decentration, like tilt, can reduce retinal image quality and thus visual performance (Taketani *et al.*, 2004). IOL tilt greater than 5° and decentration of over 1mm may induce a myopic shift as well as oblique astigmatism thereby impairing visual quality (Uozato *et al.*, 1988;Yang *et al.*, 2000;Baumeister *et al.*, 2005). There is an estimated reduction in effective optical zone power of 11% when a 6.0mm IOL is decentred by 0.5mm (Hansen *et al.*, 1988). Possible causes of tilt and decentration include an asymmetric capsulorhexis causing unequal capsule shrinkage as well as capsule tear (Jung *et al.*, 2000). Lens centration may be related to IOL factors such as design, length and material (Jung *et al.*, 2000). Significantly higher amounts of decentration have been found with a silicone 3-piece IOL compared to a plate haptic silicone IOL (Cumming, 1993;Hwang *et al.*, 1998), although Hwang *et al.* (1998) reported no difference in the rate at which this decentration occurred. This increased resistance to decentration with the plate haptic IOL was attributed to an

increased rigidity together with differences in the ability of each IOL to resist the force of capsular fibrosis (Cumming, 1993;Hwang *et al.*, 1998). There is considered to be no significant difference in the progression of tilt or decentration in the 12 months following IOL implantation, provided the IOL was placed correctly in the capsular bag at the time of surgery (Hayashi *et al.*, 1997;Yang *et al.*, 2000;Taketani *et al.*, 2004). In some instances, an IOL may be deliberately decentred so that the associated prismatic effect that this induces can be used to treat strabismus (Nishimoto *et al.*, 2007).

Concentric ring design IOLs rely on a precise distribution of light in order to create multiple focal points from distance to near. While diffractive MIOLs are believed to be less sensitive to IOL movement, the success of refractive designs are dependent upon good centration as well as minimal tilt (Hayashi *et al.*, 1997).

IOL position can be measured in a number of ways (Baumeister *et al.*, 2005). Purkinje imaging, Scheimpflug images corrected for optical distortion (Phillips *et al.*, 1988;Baumeister *et al.*, 2005;de Castro *et al.*, 2007) and AS-OCT also corrected for distortion (Dunne *et al.,* 2007) can be used to measure decentration. An alternative technique uses digital image analysis together with comparison of the centres of an oval fitted over the central IOL optic and limbus but relies upon good retroillumination images (Becker *et al.*, 2004). The magnifying effect of the cornea should also be compensated for by using the known size of the IOL optic (Buckhurst, 2011).

4.3.   Methods of assessing IOL rotation

A key aspect of assessing premium IOL misalignment is the use of accurate assessment techniques. There are several ways of measuring IOL rotation such as through use of a slit lamp protractor, however subjective techniques such as this depend upon the patient maintaining an identical head position every time a

measurement is taken and are only accurate to the nearest 1 to 5 degrees (Buckhurst *et al.*, 2010a;Wolffsohn *et al.*, 2010a;Shah *et al.*, 2012).

Differences in eye and head inclination between visits must also be accounted for when evaluating the degree of total postoperative toric IOL rotation, as this can be a source of measurement inaccuracy. The reproducibility of the eye's orientation during standard fundus photography was evaluated in order to assess the effect of autorotation on measurement accuracy and it was shown that the eye's rotational stability changed by an average of 2.3°±1.7° over the 6 month measurement period (Viestenz *et al.*, 2005). This difference in eye position was attributed to a number of factors including head rotation, cyclotorsion as well as errors in equipment alignment (Wolffsohn *et al.*, 2010a). Eye rotation was generally found to be higher in females, older patients, those with greater amounts of astigmatism and worse visual acuity (Viestenz *et al.*, 2005). There have been several attempts to compensate for this head and eye rotation. Shah *et al.* (2009) first calculated the centre of the toric IOL over which they superimposed a radial grid to enable measurement of the axis of the toric markings to within 0.1°. Head and eye rotation was compensated for by measuring the axis of an additional line joining the IOL centre to a single prominent episcleral blood vessel.

Use of ocular reference markers, such as conjunctival vessels (Wolffsohn *et al.*, 2010a), can be used to account for the effect of eye and head rotation thereby increasing the accuracy of toric IOL rotation measurement. Iris features can also be used as reference points instead of ocular blood vessels as they are more stable, especially in cases when certain topical mydriatic agents are used, such as phenylephrine which also has a vasoconstrictive action (Wolffsohn *et al.*, 2010a). However iris features are susceptible to change during pupil dilation and it has

therefore be suggested that a combination of both iris features and blood vessels be used for greater accuracy (Visser *et al.*, 2011a). For instance Buckhurst *et al.* (2011) used either two consistent conjunctival vessels or iris features on opposite sides of the pupil. Alternatively the use of peripheral iris features, which are unaffected by iris movement during dilation, can be used to overcome issues with iris stability (Buckhurst *et al.*, 2010a).

Other IOL alignment measurement techniques include use of Scheimpflug imaging (Sasaki *et al.*, 1989;Jung *et al.*, 2000;Kim *et al.*, 2001b), Purkinje reflections (Phillips *et al.*, 1988;Auran *et al.*, 1990) and anterior-segment optical coherence tomography (Kumar *et al.*, 2011) each of which have been discussed in more detail in chapter 3.

Several studies have investigated IOL rotation using a range of the techniques described. IOL rotation values obtained, along with short study summaries including assessment methods, have been summarised below in table 4.1.

IOL name	No. of eyes	No. of patients	Follow up visit (months)	Analysis method	Rotation±SD (°)	Rotation information	Tilt (°)	Study
Nidek Nt-98B	47	47	3	Image analysis	21% > 30		no data	Shimizu *et al.* (1994)
STAAR 4203TF	37	30	20±17	Slit-lamp protractor	21.6%>5	2.7% ≥ 40	no data	Ruhswurm *et al.* (2000)
STAAR 4203TF	22	16	4	Slit-lamp protractor		22%>10, 13.6%>20, 9% >30	no data	(Leyland *et al.*, 2001)
Custom IOL (600TW)	26	24	12-48	Slit lamp	46%>5,	23%>10	no data	Gerten *et al.* (2001)
STAAR 4203TF and 4203TL	25	19	2 weeks- 26.2 months	Image analysis	1.36±1.85, 0% > 5		no data	Jampaulo *et al.* (2008)
AcrySof SN60T	17	-	6	Image analysis	0.1-1.8, 0% > 5		no data	Weinand *et al.* (2007)
AcrySof SN60T	53	43	4	Slit lamp	3.5 ± 1.9		no data	Bauer *et al.* (2008)
AcrySof SN60T	30	15	3	Slit lamp	3.63 ±3.11, 19% > 5,	3% > 10	no data	Mendicute *et al.* (2008)
AcrySof SN60T	44	33	1 week-3 months	Slit lamp integrated eye piece	2.2±2.2 , 5% > 5		no data	Zuberbuhler *et al.* (2008)
AcrySof SN60T	20	3	3	Slit lamp integrated eyepiece	3.53 ± 1.97, 5% > 5		no data	Mendicute *et al.* (2009)

Akreos Adapt and AcrySof SA60AT	64 and 58	-	24 months	Retro-illumination images	Akreos:2.53±2.40 6months, 3.2±2.57 at 24 months Adapt: 3.2±2.57 at 6 months, 3.33±3.06 at 24 months	Akreos: 10%≥5 at 6months, 9%≥5 at 12 months and 20%≥5 at 24 months Adapt: 11%≥5 at 6months, 25%≥5 at 12 months and 19%≥5 at 24 months	no data	Kwartz *et al.* (2010)
Acrysof toric	30	24	1 day to 13.3±5.0months	Digital image analysis using ImageJ software	3.45±3.39,	3.3%> 10.3	no data	Kim *et al.* (2010)
Acri.Smart 46S and Acri.Lyc 53N	80	40	1 hour, 1 week & 1,6,12 months	Retroillumination images and Adobe Photoshop	Acri.Smart: 2.6±1.9 Acri.Lyc:3.1±2.4	<4° in 71%, <2° in 29% of eyes in both groups	no data	Prinz *et al.* (2011)
Acrylic toric IOL	29	22	1 week & 1 month	Anterior segment optical coherence tomography	1week:3.2±2.2 1month: 3.2±2.4	1 week: range 0–8 1 month: range 0–9 < 5° from target in 72.4%, <10 in 100%	no data	Watanabe *et al.* (2012)
Arysof Toric IOL	168	168	1 day, 1 week & 1,3,6months	Retroillumination images and purpose-designed software	6months: 1.6±0.5	6 months: 0.61%<0.5, 66.7% = 1.1-2.0, 15.9%>2.1	no data	Shah *et al.* (2012)
Bi-Flex toric IOL	30	22	1 day, 1 week, 1 and 3 months	Retroillumination images	2.12±3.45	range: -2 to +5 (+= clockwise, - =anticlockwise)	no data	Bachernegg *et al.* (2013)
AcrySof Cachet	50	28	2 weeks & 12months	Digital overlay of ocular photographs	11.0±15.1	range 0-60	no data	Kermani *et al.* (2013)

Tecnis toric IOL	67	60	4-8weeks	Dilated slit lamp examination	3.4	range 0-12	no data	Sheppard *et al.* (2013)
Tecnis toric IOL Randomised control study: ZCT150 Open label study: ZCT225, ZCT300 or ZCT400	Randomised control group: ZCT150 (102) Open label group: ZCT225 (17), ZCT300 (25) or ZCT400 (30)	Randomised control group: ZCT150 (102) Open label group: ZCT225 (17), ZCT300 (25) or ZCT400 (30)	1 day, 1 week, 1 and 3 months	High resolution digital retroillumination photographs	mean <3	7.1%≥5 between 1 and 3 months 5.9%≥5 between 3 and 6 months	no data	Waltz *et al.* (2014)
Tecnis 1-piece IOL	30	30	1 hour, 3 month	Retroillumination photographs	Mean difference between visits 2.7±3.0	62% < 3, 95%< 6	no data	Hirnschall *et al.* (2014)

Table 4.1: Studies from the past two decades which have assessed toric IOL rotation, listing the methods used to quantify rotation along with results obtained. In general, although the range of reported rotation varied between studies, mean rotation was <5° in most cases.

4.4. Study Purpose

A new technique, described in chapter 3, to measure IOL tilt from static images using a mathematical equation was tested and calculated tilt values appeared to correlate well with actual tilt. Few clinical studies have measured IOL tilt and to the author's knowledge, none have objectively measured tilt, rotation and decentration in the same subjects (table 4.1).Therefore, an aim of this study was to put the technique developed in chapter 3 into clinical use in order to quantify long term IOL tilt of an aspheric monofocal IOL with toric orientation markings (Bausch and Lomb, Rochester, NY, USA) and also to determine whether there is any relationship between IOL tilt, rotation and decentration.

4.5. Study design

A retrospective analysis of previously collected data was carried out. Data had been collected in an earlier study by Buckhurst *et al.* (2010b) who evaluated the long term rotational stability of the Akreos AO IOL with a simulated toric design. Objective analysis of digital retroillumination images was undertaken and the purpose of that study was to determine whether the platform would be suitable for correcting astigmatism through application of a toric optical surface. In the present study this previously collected raw data was re-analysed to calculate IOL rotation and decentration. Calculated mean rotation and decentration values differ slightly from those found in this earlier work perhaps as a result of the elimination of different outliers from the analysis. For the current study, IOL tilt was additionally calculated for each post-operative visit using the new simplified tilt technique described in chapter 3 and the correlation between these measures of IOL rotation, decentration and tilt assessed.

4.6. Sample size

The American National Standards Institute (ANSI) provides guidance on standards for the clinical investigation of toric IOLs. According to the current American national standard, known as ANSI Z80.30-2010 approved in March 2010, a minimum of 100 subjects should be recruited when assessing IOL rotation. A sample size calculation showed that in order to achieve a power of 80% for a correlation coefficient of 0.3 at a 0.05 significance level, a minimum of 75 subjects were required.

4.7. Methods

A prospective, non-randomised study had previously been conducted on 107 subjects (mean age 69.9 ± 7.7 years) implanted with the Akreos AO aspheric monofocal IOL (Bausch & Lomb, Rochester, NY). The Akreos lens is a single piece, aberration neutral, aspheric lens with toric orientation markers to enable rotation assessment. It is made from an acrylic material, features a central 6mm optic and a closed loop haptic design. Data had been collected at the following six European sites: Universitat Rostock Germany, Umea University Hospital Sweden, University Hospital Sweden, University Medical Centre Ljubljana, Universitat Niederrhein Germany and Uppsala University Hospital Sweden (Buckhurst *et al.*, 2010b). Aston University acted as a reading site for this multi-centre study by collating and analysing the data. For the current study, a retrospective analysis was conducted on this previously collected data.

Digital slit lamp images were taken of the implanted IOL at pre-determined intervals over a six month period. In order to fully image the IOL, pupils were dilated using phenylephrine 2.5 % and tropicamide 1.0 %. Peripheral iris features were used as stability markers in order to account for head and eye rotation.

Subjects were assessed over four visits. Visit 1 occurred 1 to 2 days after surgery, the second visit occurred 1 to 2 weeks after, patients were seen for the third time 1 to 2 months after implantation and then for the fourth and final time between 4 and 6 months post operatively. Informed consent was obtained from all participants prior to lens implantation and ethical approval obtained.

Inclusion criteria for this study were:

- The absence of ocular pathology such as Fuch's endothelial dystrophy.

- Presence of clinically significant cataract treatable with standard phacoemulsification and IOL implantation.

- Ability to meet the minimum dilation level of 5.5mm.

- Best corrected visual acuity projected to be better than 0.2 logMAR.

- Aged between 50 and 80 years.

- A willingness participate in the study and attend the agreed post-operate visits.

The presence of any of the following conditions served as exclusion criteria:

- Anterior segment pathology such as chronic uveitis and corneal dystrophy

- Uncontrolled glaucoma

- Previous intraocular and corneal surgery

- Diabetic retinopathy

- Very shallow anterior chamber

- Traumatic cataract

- Aniridia

- Microphthalmos

- Amblyopia

- Degenerative visual disorders

4.7.1. Image capture

At each visit retroillumination images of the posterior capsule were taken using a digital slit lamp. The SL-990 digital slit lamp biomicroscope was used to image the IOL at a 10X magnification with the eye externally illuminated. The illumination arm of the slit lamp was decoupled, the IOL retro-illuminated by the fundus and then imaged (Buckhurst *et al.*, 2010b).

4.7.2. IOL rotation measurement

The digital images were analysed using bespoke computer software written in *Labview* (National Instruments, Texas, USA). Using this software the axis of IOL rotation was determined by constructing a line between the two IOL orientation markers as has been described in greater detail by Buckhurst (2011) . Eye rotation between visits was accounted for by comparing the axis of a line joining two conjunctival vessels or iris features on opposing sides of the pupil (Shah *et al.*, 2009).

4.7.3. IOL tilt measurement

IOL tilt was calculated mathematically (equation 3.3) from the given height and width measurements of the IOL as described in chapter 3 using ImageJ software. A pixel to mm conversion factor was obtained by imaging an object of known size.

4.7.4. IOL decentration measurement

Centration was measured by overlaying ovals over the IOL optic, pupil margin and also the limbus using the same computer software programme and measuring the centre of these ovals (Buckhurst *et al.*, 2010b;Wolffsohn *et al.*, 2010a). Scheimpflug systems use the central of the pupil as a reference point for decentration measurements

therefore IOL position relative to the pupil was used in this study for decentration evaluation (de Castro *et al.*, 2007). Measurements were given in pixels and converted into mm using this pixel conversion factor. Corneal magnification effects were compensated for by using the known size of the IOL optic (Buckhurst, 2011). The distance between the centre of the IOL and the centre of the pupil was calculated using equation 4.1 below.

$$h = \sqrt{x^2 + y^2}$$

Equation 4.1

Where h= distance between centres, x= horizontal distance between centres and y= vertical distance between the centres.

4.8. Statistical Analysis

IOL data were assessed for normality using the Kolmogorov-Smirnov test and were not normally distributed (Kolmogorov-Smirnov: Rotation $Z=5.632$, $P<0.001$; Tilt $Z=4.491$, $P<0.001$). Therefore, non-parametric tests were performed. The Friedman Chi-Square test was used to determine if there was a difference in level of IOL rotation over time. If a difference was detected then post-hoc testing was conducted using the Wilcoxon signed-rank test to establish which post-operative visits showed this difference. As multiple comparisons were made using the Wilcoxon signed-rank test, a compensating Bonferroni adjustment was made.

Stepwise linear regression analysis was performed to determine the relationship between IOL rotation and post-operative visit. Statistical analysis was performed using SPSS version 21.0 (SPSS Inc., Chicago, IL., USA.)

4.9.   Results

4.9.1. IOL rotation

IOL rotation was assessed at four intervals over a six month period. The average total rotation that occurred from visit 1 to visit 4 as given by the median, was 1.25°°. The average change in rotation at each visit is detailed in figure 4.2.

A breakdown of the percentage of early, mid and late rotation is shown in figure 4.1. Over 80% of IOL rotation that occurred between each visit was below 5°, and over 90% rotated by less than 10° between each of the four visits. This illustrates the relative rotational stability of the Akreos AO lens. The current standard for toric IOL manufacturers is known as ANSI Z80.30-2010, and states that ≥90% of eyes should experience a change in axis of ≤5° between two consecutive visits that are approximately three months apart. Analysis of the change in rotation from visit 3 which took place 1 to 2 months post-operatively, and visit 4 which occurred between 4 and 6 months after surgery, showed that ≤5° rotation occurred in 90% of subjects (figure 4.1).
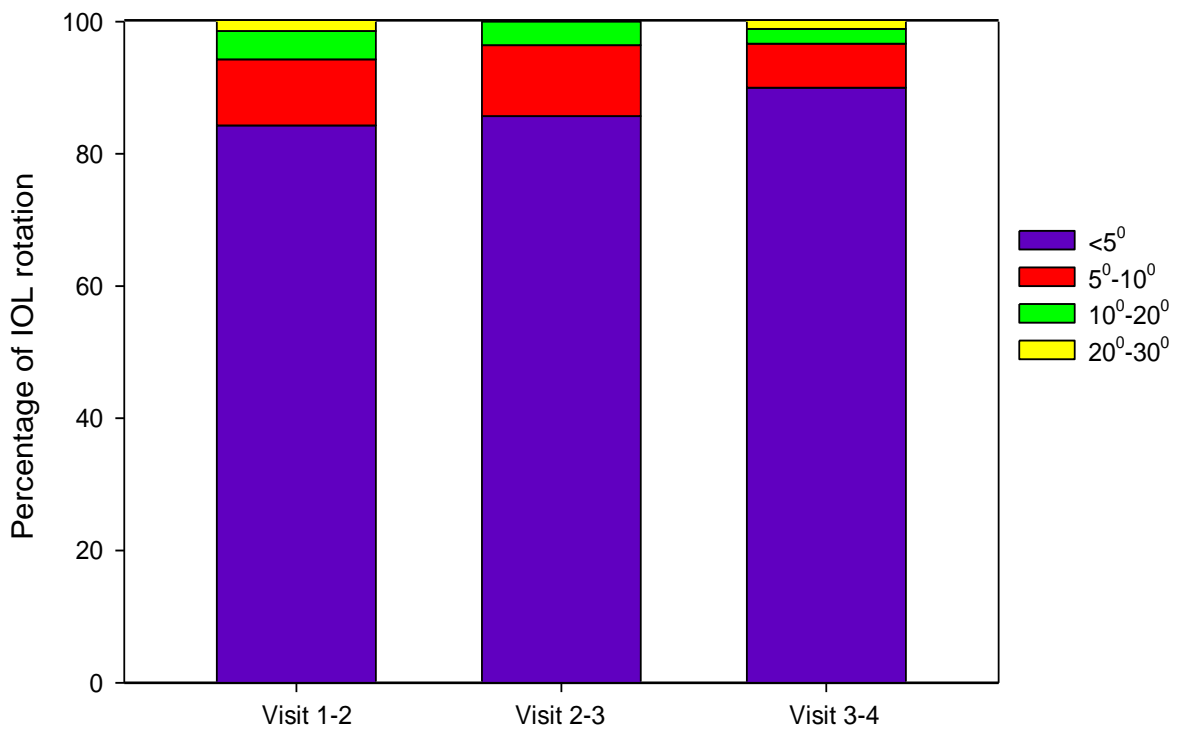
Figure 4.1: Comparative breakdown of the amount of IOL rotation that occurred between visits.

The Freidman test confirmed there was a significant ($\chi2(3)$ = 18.120, P <0.001) difference in the amount of rotation that occurred between visits. Post hoc tests were conducted to determine whether this difference in IOL rotation occurred for early, mid or late IOL rotation by comparing visit 1 with 2, visit 2 with 3 and visit 3 with 4; a bonferroni adjustment was made to compensate for the effect of multiple comparisons. A greater amount of IOL rotation occurred soon after lens implantation corresponding to the time between visit 1 and 2 (Z=-2.782, P=0.005) while similar levels of rotation occurred between visit 2 and 3 (Z=-1.612, P=-0.107) and between visit 3 and 4 (Z=-1.049, P=-0.294). This indicates the lens is more likely to rotate in the first 2 weeks

after surgery, but after this period maintains a more stable position within the capsular bag.

This was confirmed by linear regression analysis. This was performed to establish which of the post-operative visits contributed most to total IOL rotation at the final visit. Total IOL rotation from visit 1 to 4 was entered as the dependent variable and rotation from visit 1 to 2, visit 2 to 3 and visit 3 to 4 were entered as the independent variables. Analysis showed that the majority of total IOL rotation at 6 months was influenced by rotation that occurred between visit 1 and 2, which accounted for 50.6% of the variance. A further 33.3% occurred due to late rotation from visit 3 to 4 and 16.1% due to rotation between visit 2 and 3.
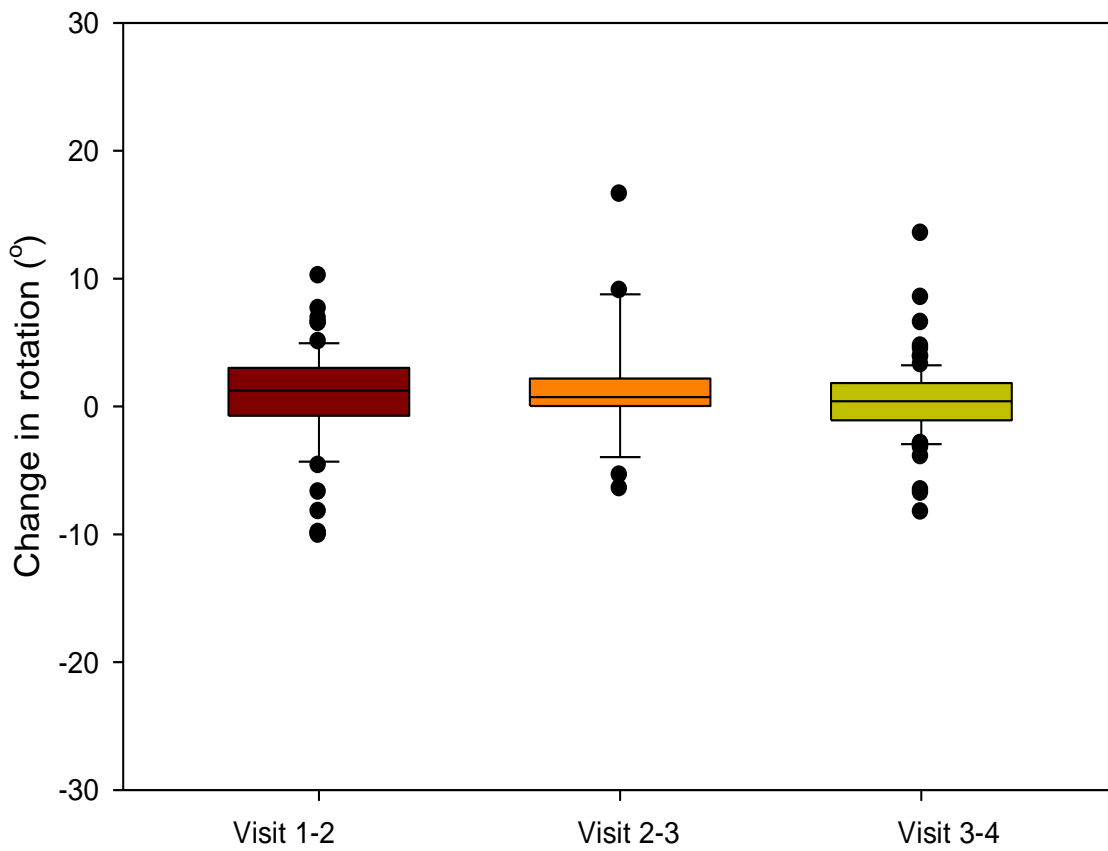
Figure 4.2: Box plot of the mean change in rotation between visits. The line in the centre of the box represents the median or 50th percentile, while the upper and lower limits of the box indicate the 25th and 75th percentile respectively. The bars show the maximum and minimum rotations values and the dots indicate outliers. The average change in rotation was within 5° between visits.

4.9.2. IOL tilt

IOLs were found to have tilted on average by 3.67°° between the first and last follow up visit, with a maximum recorded tilt at 6 months of 22.84°. A breakdown of the median tilt at each visit is given in table 4.2.The absolute tilt values at each post-operative visit were relatively high. Refractive information was not available and so the effects of uncorrected corneal astigmatism could not be accounted for, which may have artificially increased calculated tilt values.

	Visit 1	Visit 2	Visit 3	Visit 4
Median tilt (°)	13.60	10.99	12.15	12.29
Range (°)	19.62	15.21	13.53	15.99

Table 4.2: The average, absolute IOL tilt values at each post-operative visit. There was comparatively less IOL tilt at visit 3 corresponding to 1-2 months after surgery.
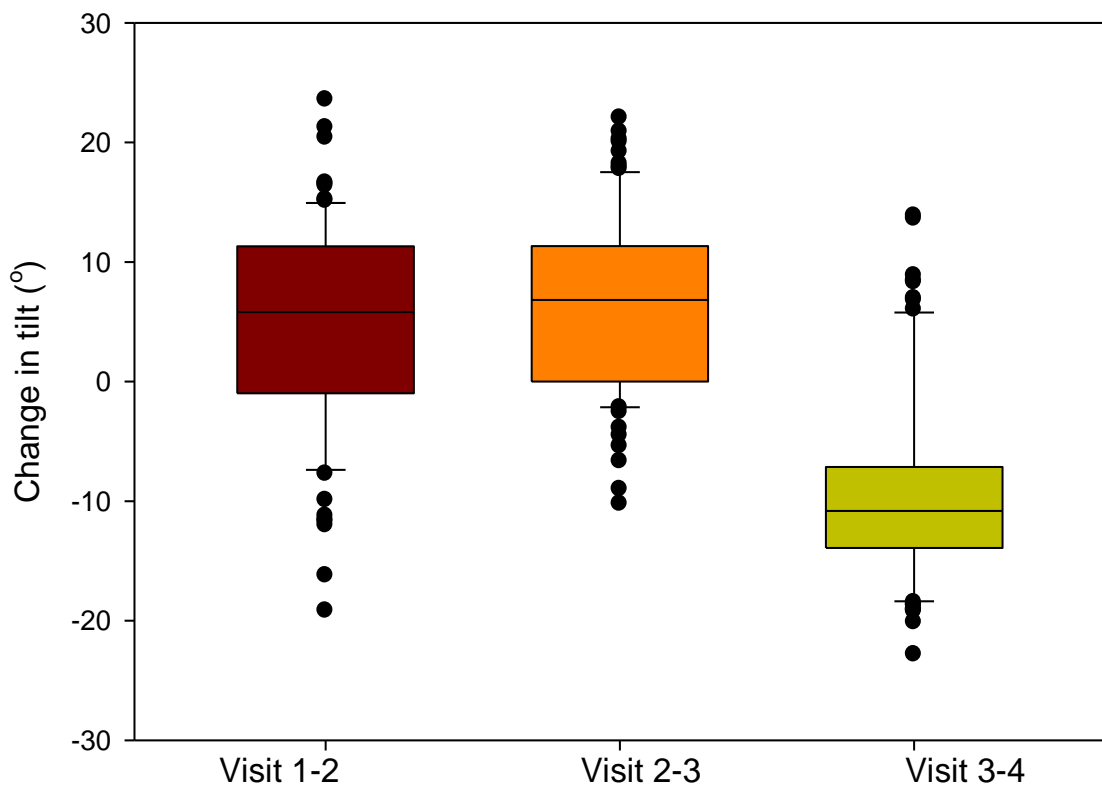
Figure 4.3: Box plot of the mean change in tilt between visits. The median is shown by the central line in each box; the upper and lower limits of the box indicate the 25th and 75th percentile respectively. The maximum and minimum tilt values are represented by the bars and outliers indicates as dots.

The difference in lens tilt between visits was analysed using the Freidman test, which showed a statistically significant ($\chi2(3) = 71.667$, P <0.001) difference in the amount of tilt that occurred between visits. Post hoc tests revealed a statistically significant difference in IOL tilt between visits 1 and 2 (Z=-4.218, P<0.0016), between visit 2 and 3 (Z=-5.495, P<0.0016) and also between visit 3 and 4 (Z=-6.528, P<0.0016) indicating the pattern of IOL tilt is less predictable compared to lens rotation.

Linear regression analysis was performed to establish which post-operative visits influenced IOL tilt position at the final post-operative visit. Total IOL tilt from visit 1 to 4 was entered as the dependent variable. Tilt from baseline (taken as 0°) to visit 1, from visit 1 to 2, visit 2 to 3 and visit 3 to 4 were entered as the independent variables. Analysis showed that the majority of IOL tilt was influenced by initial tilt corresponding to 1-2 days following implantation, which accounted for 73.9% of the variance. A further 15.2% occurred due to late tilt corresponding to 4-6 months after surgery. Intermediate tilt was not a greatly influencing factor with 1.1% of total IOL tilt due occurring between 1 and 2 weeks and 9.1% between 1 and 2 months after surgery.

4.9.3. IOL decentration

IOLs were found to have decentred on average by 0.016mm (IOL versus pupil) between the first and last follow up visit, with a maximum recorded decentration at 6 months of 0.34mm. The change in decentration at each visit is shown in figure 4.4.

4.9.3.1. Decentration: IOL versus pupil

The difference in decentration between visits, with IOL position measured relative to the pupil (figure 4.4), was analysed using the Freidman test, which showed a difference in the amount of decentration that occurred between visits($\chi 2(3) = 60.503$, P <0.001). Post hoc tests revealed a statistically significant difference in IOL decentration between visits 2 and 3 (Z=-5.718, P<0.0167) and between visit 3 and 4 (Z=-6.575, P<0.0167).
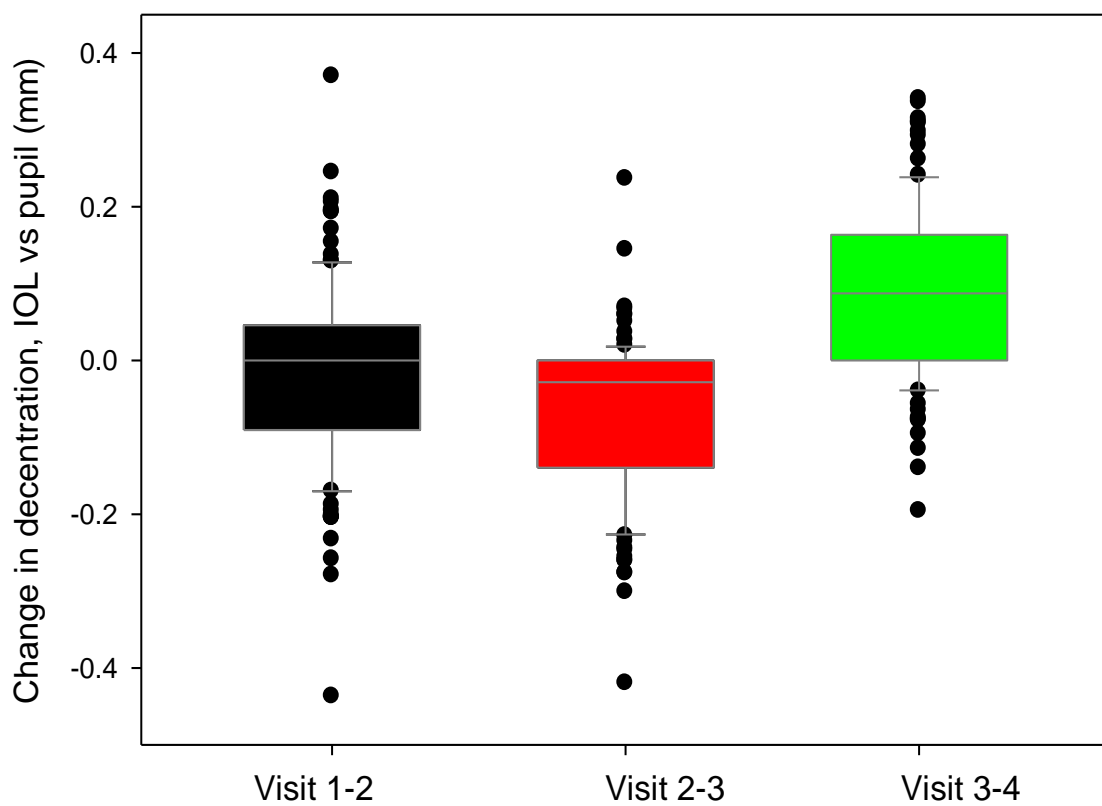
Figure 4.4: Box plot of the mean change in decentration between visits (IOL vs. pupil).

Linear regression analysis was performed to establish which post-operative visits most influenced IOL decentration position at the final visit. Total IOL decentration from visit 1 to 4 was entered as the dependent variable and decentration that occurred from visit 1 to 2, visit 2 to 3 and visit 3 to 4 were entered as the independent variables. Analysis showed that the IOL decentration was influenced by initial decentration between visit 1 and 2 corresponding to 1-2 days following implantation, which accounted for 36.5% of the variance. A further 23.1% occurred due to late decentration from visit 3 and 4 corresponding to 4-6months after surgery and 40.4% due to intermediate decentration between visit 2 and 3, corresponding to 1-2 weeks post-operatively.

4.9.4. Association between tilt, rotation and decentration

The relationship between total IOL tilt, rotation and decentration from visit 1 to 4 was examined and revealed correlations between visits for each IOL misalignment type, such as between tilt at visit 2 and visit 3, between rotation at visit 1 and 2 and so on. However, no statistically significant correlations were found between the different types of IOL misalignment (table 4.3).

Spearman's rho				TILT(DEG)				ROTATION(DEG)				DECENTRATION			
				V1	V2	V3	V4	V1	V2	V3	V4	V1	V2	V3	V4
TILT	V1	Correlation Coefficient			.192	.015	.118	.046	.080	-.120	.051	-.125	-.099	-.147	-.124
		Sig. (2-tailed)			.058	.886	.243	.666	.451	.256	.629	.218	.332	.146	.223
	V2	Correlation Coefficient				.233*	.145	-.013	.023	-.106	-.005	.095	.194	.165	.187
		Sig. (2-tailed)				.020	.151	.899	.826	.319	.960	.351	.055	.104	.065
	V3	Correlation Coefficient					-.023	-.009	-.047	-.055	-.030	-.144	.061	.174	.094
		Sig. (2-tailed)					.823	.931	.656	.602	.774	.152	.544	.084	.352
	V4	Correlation Coefficient						.113	.087	-.083	.128	.069	.029	-.026	-.054
		Sig. (2-tailed)						.280	.408	.431	.221	.498	.774	.801	.592
ROTATION	V1	Correlation Coefficient							.885**	.401**	.935**	-.032	.133	-.072	-.096
		Sig. (2-tailed)								.000	.000	.000	.762	.204	.493	.359
	V2	Correlation Coefficient								.483**	.822**	-.001	.050	.081	-.030
		Sig. (2-tailed)									.000	.000	.994	.635	.443	.777

	V3	Correlation Coefficient				.357**	-.099	-.061	-.145	-.172
		Sig. (2-tailed)				<mark>.000</mark>	.344	.563	.164	.100
	V4	Correlation Coefficient					.009	.096	-.066	-.121
		Sig. (2-tailed)					.935	.358	.529	.250
DECENTRATION	V1	Correlation Coefficient						.181	.233*	.177
		Sig. (2-tailed)						.072	<mark>.020</mark>	.078
	V2	Correlation Coefficient							.361**	.792**
		Sig. (2-tailed)							<mark>.000</mark>	<mark>.000</mark>
	V3	Correlation Coefficient								.760**
		Sig. (2-tailed)								<mark>.000</mark>
	V4	Correlation Coefficient								
		Sig. (2-tailed)								

Correlation is significant at the 0.05 level (2-tailed) **Correlation is significant at the 0.01 level (2-tailed)

Table 4.3: Correlation between tilt, rotation and decentration at each post-operative visit. Significant correlations are highlighted in yellow.

4.10. Discussion

The success of an implanted toric IOL is not determined solely by its ability to correct refractive astigmatism, long term lens stability with minimal misalignment is equally, if not more important (Kim *et al.*, 2010). IOL tilt, although often overlooked as a potential source of reduced vision following cataract surgery, can induce additional unwanted refractive astigmatism (Auran *et al.*, 1990;Kozaki *et al.*, 1991b;Oshika *et al.*, 2005) and coma-like aberrations (Oshika *et al.*, 2005) and so should be evaluated. There is a paucity of literature investigating lens rotation, tilt and decentration together and so the aim of this study was to assess the link between the three in greater detail.

The stability of the Akreos AO IOL was assessed at set intervals over a six month period. The lens showed good rotational stability, both in the short and long term, with less than 5° rotation present in the majority of subjects at each visit. Lens position was calculated from retro-illumination images and showed relatively little rotation over the six month period. This observed rotational stability may have occurred in part due to the closed loop haptic design of the IOL. Narendran *et al.* (2009) reported no more than 5° of lens rotation occurred between 1 week and 2 years after surgery in a study they conducted with the T-flex toric (Rayner, Hove, UK) closed loop haptic design IOL. Closed loop designs tend to be longer than other haptic designs (fig 4.6a-c), which may improve friction between the lens and capsular bag early on. Additionally, capsular bag shrinkage is a chief source of IOL rotation in uncomplicated cataract cases (Kim *et al.*, 2010;Prinz *et al.*, 2011) and closed loop designs are believed to benefit from a greater tolerance to the effects of capsular contraction as a result of a second insertion between the haptic and IOL (Buckhurst *et al.*, 2010a).
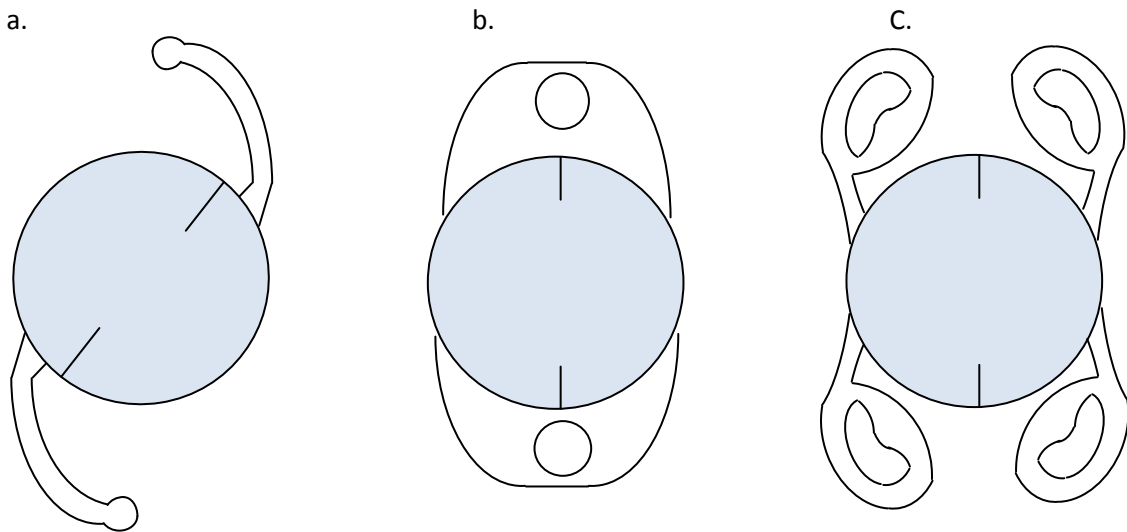
Figure 4.5a: Example of an open loop haptic design such as the Acrysof toric 6N60TT. 4.5b: Example of a plate haptic design such as the STAAR toric IOL. 4.5c: Example of a closed loop haptic design like the Akreos AO toric IOL.

Total IOL rotation at 6 months was influenced mostly by early rotation occurring between visit 1 and 2. This too may have been due to IOL haptic design and capsular compression effects. Previous research has shown that plate haptic design lenses are more resistant to capsular bag compression and thus have better long term stability while open loop designs are more vulnerable to capsular shrinkage and therefore show better stability early on (Patel *et al.*, 1999;Buckhurst *et al.*, 2010a;Kim *et al.*, 2010;Prinz *et al.*, 2011). Closed loop haptics are relatively new compared to plate and open loop haptic designs and there is comparatively less literature available on the long term stability of this haptic design. However, like the plate haptic design, it appears that closed loop designs show poor initial stability but may be less prone to capsular compression effects resulting in better long term stability.

IOL tilt was evaluated using a new mathematical technique, described in chapter 3, in conjunction with digital retroillumination images. The new method of evaluating IOL tilt,

which had previously been evaluated using digital images of an IOL *in vitro* related well with retroillumination images taken of an IOL *in vivo* indicating its potential for use in rapidly assessing post-operative IOL tilt in patients. Using this new technique, significant mean IOL tilt was measured six months after surgery. Hayashi (1997) assessed tilt using Scheimpflug imaging and a computer software package at six intervals over a 12 month period with three different lens materials and found average IOL tilt of between 1.95 and 2.71°.A later study by de Castro *et al.* (2007) found mean Scheimpflug and Purkinje imaging tilt values of 0.26°± 2.63° about the x axis, and 1.54°±1.50° around the y axis, while Rosales *et al.* (2006) found tilt of 0.87°± 2.16° about the x axis and 2.3° ± 2.44° about the y axis using Purkinje imaging. In this study, relative tilt of 1.83° ± 7.03° occurred between the first visit, conducted 1 to 2 days after surgery, and the final visit four to 6 months later. The average, absolute tilt present at the first visit was 13.60°, whereas by the final visit this had reduced to 12.28° indicating potential compensatory tilt movements in the intervening months.

The effect of corneal astigmatism was not accounted for in this study, which is a limitation as uncorrected astigmatism may have artificially increased measured values of absolute tilt. As described in chapter 3, uncorrected astigmatism of even 1 dioptre could cause an error in tilt measurement of approximately 4.59° and so the effects of this should have been accounted for. Uozato *et al.* (1988) stated tilt of more than 5° would impact upon quality of vision; given this, the possible impact of 13.60° of tilt on visual performance would be significant. Possible causes of this tilt may include asymmetric capsular fibrosis and the presence of viscous-elastic between the lens and capsule (Cazal *et al.*, 2005). While total lens rotation was mostly influenced by late rotation occurring in visits 3 and 4, regression analysis showed most IOL tilt occurred within 48 hours of surgery with smaller amounts of tilt occurring in the weeks and

months that followed. In view of this, it may have been useful to have had information on intra-operative IOL tilt during surgery.

The association between tilt, rotation and decentration was investigated and a poor correlation was found between each of these factors indicating they occur independently from each other. One might have expected a link due to the similarity of possible causes in lens fibrosis and shrinkage as well as surgical skill factors. However, the interaction between these factors and the natural history of the biological changes in the anterior chamber after cataract surgery are not well understood.

Hence the chapters so far have focussed on toric IOLs and have shown the importance of correcting even low levels of corneal astigmatism in order to optimise vision. Objective analysis of digital retro-illumination images following surgery can allow IOL stability to be assessed relatively easily and precisely using equipment that is readily available in clinical practice. The remaining chapters will examine the other principal form of premium IOLs, those designed to overcome presbyopia.

CHAPTER 5: Visual field analysis of two different multifocal and an accommodative intraocular lens

5.1. Introduction

Surgery for cataract extraction and subsequent IOL implantation is carried out on a routine basis in developed countries such as the UK (Bhogal *et al.*, 2011;Trikha *et al.*, 2013;Horvath *et al.*, 2014).Traditional monofocal IOLs are designed to provide good vision at a single focal point, typically the distance, often leaving patients with poor unaided near and intermediate vision, thus corrective lenses must be worn. Multifocal IOLs (MIOLs) on the other hand are designed to give clear vision at more than one focal point thus reducing this need for spectacles postoperatively. As a result they have become increasingly popular amongst patients (Davison *et al.*, 2006;Alfonso *et al.*, 2008;van der Linden *et al.*, 2012;Aychoua *et al.*, 2013).

5.2. Multifocal and Accommodating IOLs

Several different design strategies have been developed in order to bestow multifocal capability onto an IOL (Alio *et al.*, 2011a;Alio *et al.*, 2011b;Alfonso *et al.*, 2012;Alio *et al.*, 2012b). These include refractive, diffractive or combined refractive-diffractive concentric ring design IOLs, segmented designs and also accommodating IOLs (AIOLs) which are designed to imitate the action of a young crystalline lens during accommodation. Numerous studies comparing the efficacy of most of these lenses have been conducted (Wolffsohn *et al.*, 2006a;Alfonso *et al.*, 2008;Barisic *et al.*, 2008;Zelichowska *et al.*, 2008).

5.3. Concentric ring design MIOLs

MIOLs may incorporate a central concentric ring optic (figure 5.1) made up of steps of differing heights, and so would look similar in appearance, but not in action to a Fresnel lens. The inclusion of an apodized concentric ring pattern into the IOL optic

that utilizes either refractive, diffractive or combined refractive-diffractive principles to create multiple focal zones from distance to near, is a popular means of achieving multifocality (Alio *et al.*, 2011b;Bhogal *et al.*, 2011;McAlinden *et al.*, 2011;Alio *et al.*, 2012b).
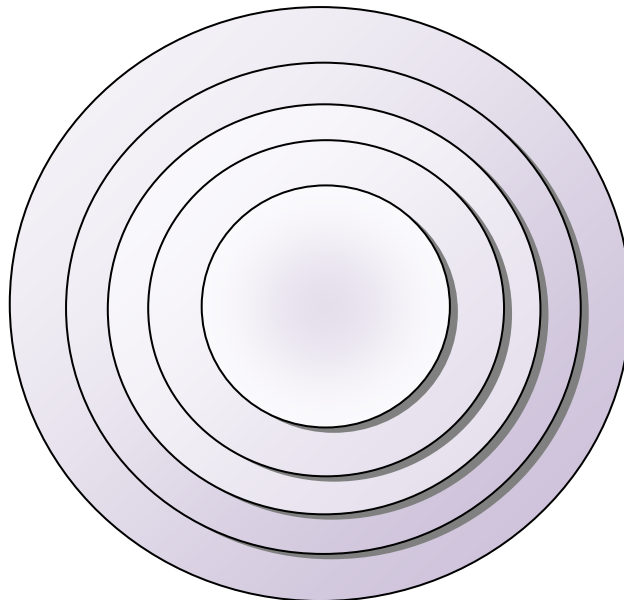
Figure 5.1: typical ring pattern of concentric MIOLs.

Concentric refractive MIOLs consist of concentric zones of varying curvatures to create more than one refractive power; they are sensitive to lens decentration as this can reduce the portion of the near segment within the pupil margin.

Diffractive designs use diffraction of light at a boundary to create multiple focal points, with the separation between ring edges determining the effective near addition power of the IOL. In fully diffractive MIOLs the concentric ring covers the entire central IOL optic and so the splitting of light is not affected by pupil size. Partially diffractive MIOLs only incorporate this diffractive pattern over a specific area of the optic.

5.3.1. Rayner Mflex

The Rayner Mflex IOL (Rayner Intraocular Lenses, Ltd, Sussex, England) is a biconvex aspheric refractive MIOL made from a hydrophilic acrylic copolymer with a central optic diameter of 6.25mm, a haptic angulation of 0° and a 360° square edge to impede lens epithelial cell migration and therefore minimise posterior capsule opacification (PCO) (Cezon Prieto *et al.*, 2010). The anterior surface of the IOL features the multifocal optic, which consists of five refractive zones that alternate between the base and add power of the lens in order to create dual focal points (figure 5.2). The lens is available with an add power of +3.00D or +4.00D at the IOL plane equivalent to 2.25 or 3.00D at the spectacle plane (Rabsilber *et al.*, 2013). A greater portion of incident light is focussed at the distance focal point compared to near, as a result of the central distance zone which is surrounded by the alternating distance and near zones, thus the design can be described as "distance dominant" (Cezon Prieto *et al.*, 2010).
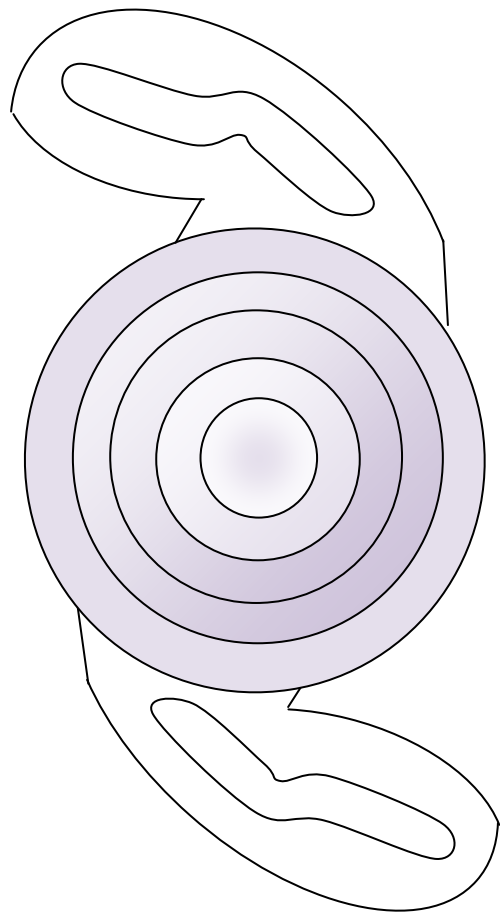
Figure 5.2: An illustrated example of the Rayner Mflex IOL.

5.3.2. Acrysof ReSTOR

The Acrysof ReSTOR lens (figure 5.3) is a one piece hydrophobic acrylic, hybrid lens as it incorporates both diffractive and refractive technologies in its optic. The central 3.6mm of the lens contains the diffractive optic and is made up of 12 concentric rings of gradually decreasing heights. This is surrounded by a refractive region which directs any additional incoming light, for example from larger pupils, to the distant focal point (Alfonso *et al.*, 2008).
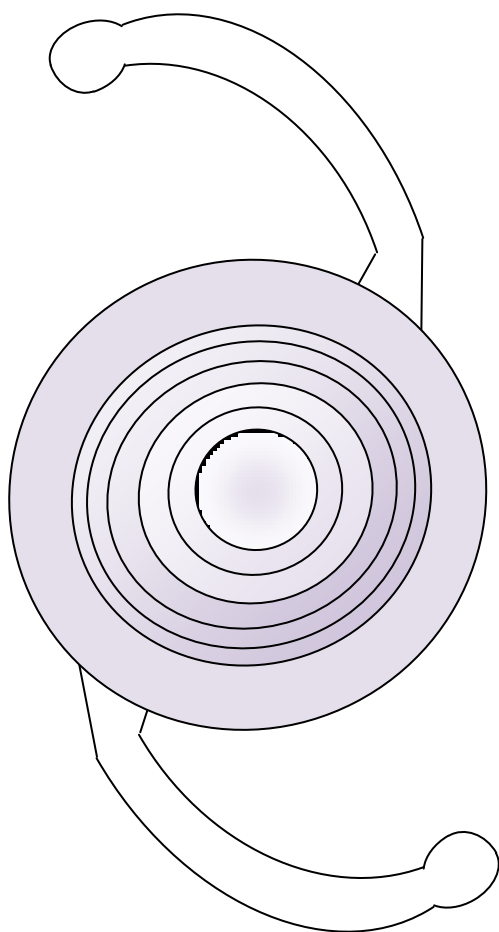
Figure 5.3: An illustrated example of the Acrysof ReSTOR IOL.

Both the Rayner Mflex and Acrysof Restor lenses incorporate a concentric ring design in the central optic and so will be referred to as concentric ring IOL for this study.

It has been hypothesised that because incoming light is split across two foci in multifocal IOLs wearers, they may experience a reduced quality of vision despite demonstrating good visual acuity (Ravalico *et al.*, 1998). Concentric ring design IOLs are more prone to photic phenomena like glare and haloes as a result of the numerous optical transitions present within the pupil area (Bhogal *et al.*, 2011;van der Linden *et al.*, 2012). Dysphotopsia can affect quality of vision, resulting in patient dissatisfaction. The aspheric optic of the Rayner Mflex lens helps minimise these visually troublesome phenomena (Alfonso *et al.*, 2008). Cezon Prieto *et al.* (2010) evaluated the level of dysphotopsia following implantation of the Rayner Mflex lens by showing patients pictures representing halos and glare and asking them to rate their experience of such unwanted visual phenomena with a score of 1, meaning no glare or haloes, to 4 indicating severe halos or glare. At the 1 month post-operative visit, no halos were reported in 21.9% of eyes and no glare in 28.1%, at 6months this had improved to no halos in 78.1% and no glare in 100% of eyes and by 12months there were no reports of halos or glare in all eyes, thus the experience of glare and halos does not appear to be permanent. They were no reports of severe or moderate glare and no reports of severe haloes at any of the post-operative visit with this IOL. Similarly, there were no reports of photic symptoms in a study by Aslam *et al.* (2009) who evaluated the same IOL; they speculated that the relatively low refractive index hydrophilic acrylic material could have been an influencing factor, in addition to the blended surface design at each zonal interface which was thought to reduce light scatter. Another study assessing subjective visual symptoms found that in patients with the apodized diffractive Acrysof ReSTOR lens, 38% reported no glare, and 34% reported no haloes three months post-operatively. Moderate glare was reported in 17% of eyes, moderate halos in 13% and severe halos in 3% of eyes. Despite this, overall satisfaction with this lens was good with dissatisfaction reported in only 4% of patients (Chiam *et al.*, 2007).

5.4. Segmented MIOL

Segmented IOLs are rotationally asymmetric MIOLs which incorporate the near prescription into a particular segment of the lens, much like in a bifocal lens (figure 5.4), although the mechanism of action is still simultaneous rather than translating (Alio *et al.*, 2011a;Alio *et al.*, 2012a;van der Linden *et al.*, 2012).
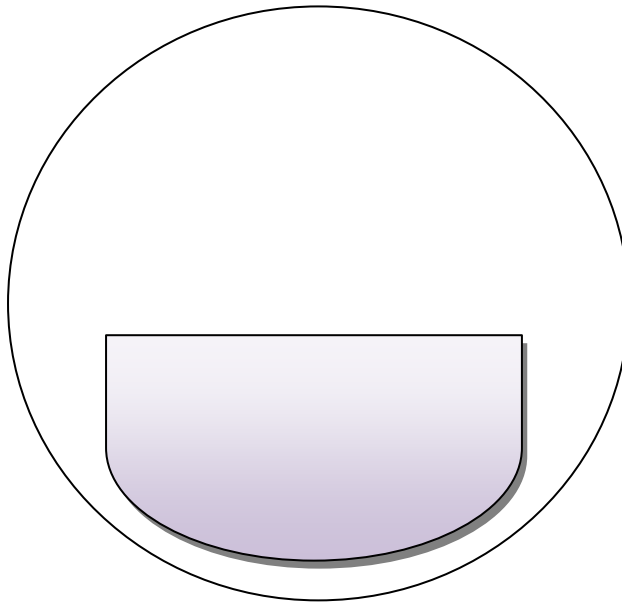
Figure 5.4: Example of a segmented IOL optic.

Segmented IOLs such as the Oculentis Mplus IOL (Oculentis GmbH, Berlin, Germany) are a relatively new MIOL design. The 6mm lens optic of the Oculentis IOL features an aspheric distance correction with a sectorial addition incorporating the near correction embedded on the posterior surface. The near addition is available with a +3.00D (model LS-313 MF30), +2.00D (model LS-313 MF20) or +1.50 D (model LS-313 MF15) addition power at the IOL plane (McAlinden *et al.*, 2011;van der Linden *et al.*, 2012;Wolffsohn *et al.*, 2013) as well as in toric forms. The model used in this study had an add power of +3.00. The IOL is designed to reflect any incoming light between the near and far zones of the IOL away, in order to prevent super-imposed images or diffraction in the optical axis. The optic is enclosed by a 360° square edge to reduce the incidence of PCO (van der Linden *et al.*, 2012) and is made from a hydrophilic

acrylic material with a hydrophobic surface (figure 5.5). Segmented IOLs rely on good IOL centration as the distribution of light to the near segment depends upon the proportion of near segment within the pupil.
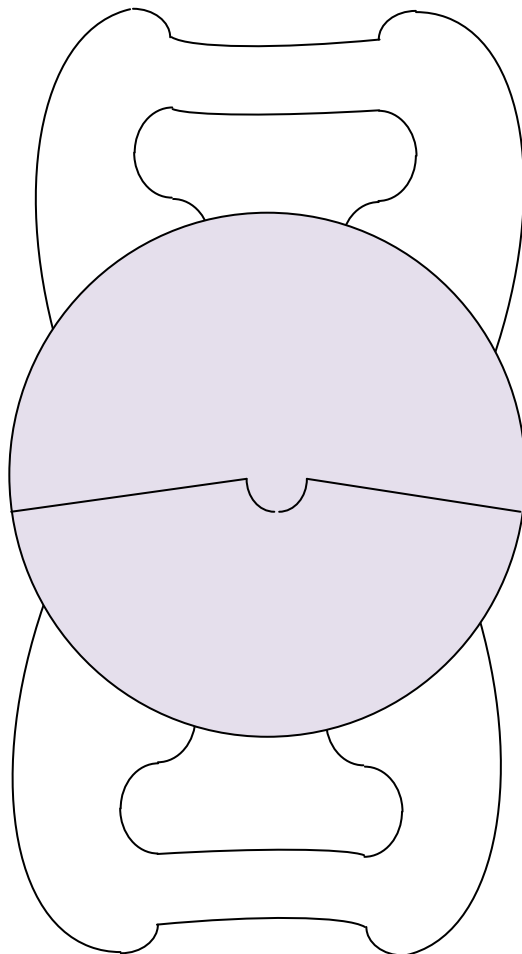
Figure 5.5: An illustrated example of the Oculentis Mplus IOL.

5.5. Accommodating IOLs

The Tetraflex KH-3500 IOL (Lenstec, St Petersburg, Florida, USA) is a one piece, hydrophobic acrylic 'accommodating' lens (figure 5.6), which is designed to move anteriorly within the capsular bag upon ciliary muscle contraction (Nanavaty *et al.*, 2010;Sheppard *et al.*, 2010;Wolffsohn *et al.*, 2010b). However, studies have shown that any improvement in near vision with this lens results from flexure rather than a change in position (Wolffsohn *et al.*, 2010b). It is a single-piece acrylic IOL with a spherical optic measuring 5.75mm (Wolffsohn *et al.*, 2010b) and unlike concentric ring

designs, does not feature a refractive or diffractive optic which helps minimise the rate of halo and glare post-operatively (Zhe *et al.*, 2010).
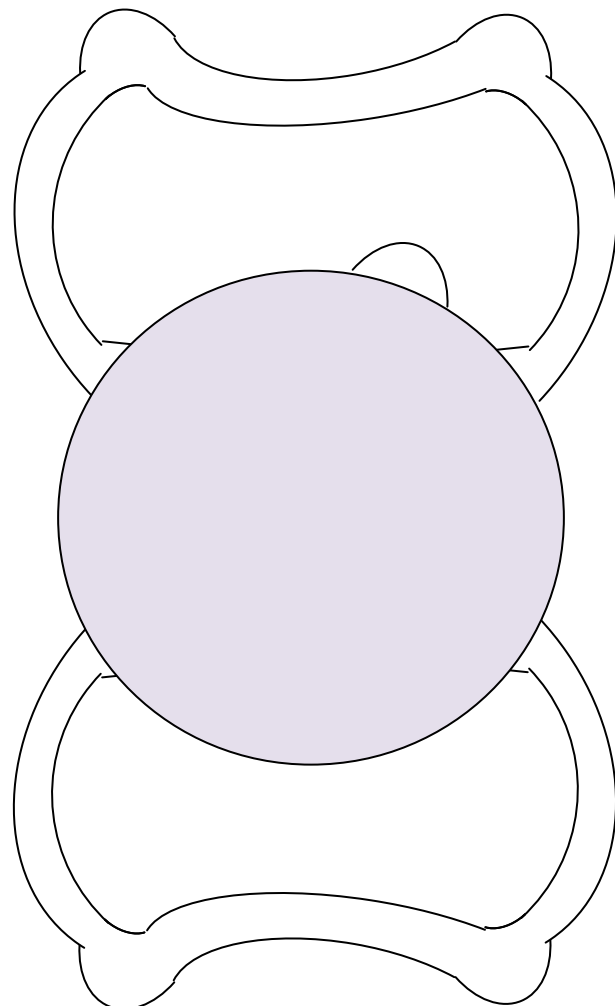
Figure 5.6: illustrated example of the Tetraflex accommodating IOL.

As incoming light passing through the pupil is focussed at more than one focal point by MIOLs, this light must be split between these points; the precise distribution of light varies with each type of MIOL due to their differing optical properties. Consequently, a greater proportion of light should theoretically reach each focal point with the AIOL than in the MIOLs. However, the way in which light from these focal planes is distributed across the retina with MIOLs is currently unknown. It would be useful to map the retinal projection of different types of MIOL and compare with an AIOL, as this information could be used to optimise future MIOL design.

5.6. Visual field testing

Visual field tests are conducted routinely in Optometric practices and hospital eye departments across the UK primarily to assess optic nerve function as well as to investigate retinal and neurological disorders (Kocabeyoglu *et al.*, 2013). Visual field machines measure the differential light sensitivity in decibels (dB) using a log scale of sensitivity whereby 0dB represents the brightest stimulus and 51dB the dimmest (Rosenfield *et al.*, 2009). There are several different ways of mapping a subjects' field of vision using perimetry; these range from rather basic screening tests to comprehensive examinations designed to test the threshold sensitivity at various retinal points.

5.6.1. The Nidek MP-1 microperimeter

The MP-1 microperimetry is a relatively new piece of equipment designed to test threshold sensitivity at precise points on the retina (Crossland *et al.*, 2012). It is highly customisable such as in terms of stimulus position and target size.

The MP-1 utilises a 4-2-1 step strategy which is more precise than the 4-2 strategy used in the Humphrey Visual field analyzer (Carl Zeiss Meditec, USA), however this more accurate testing strategy has been found to measurably increase testing time with this machine compared to other perimeters (Springer *et al.*, 2005). Patient fixation is directly monitored by the MP-1 (Springer *et al.*, 2005) via an integrated infrared camera which displays a fundus image in real -time (Charbel Issa *et al.*, 2007). The MP-1 is highly sensitive to small shifts in fixation, testing stops whenever the patient appears to lose fixation and does not resume until tracking has been re-established (Charbel Issa *et al.*, 2007). In other perimeters such as the Humphrey Visual field analyzer, fixation is tracked from the first Purkinje image relative to the pupil centre or monitored via camera by the examiner who can pause the test as necessary in order to re-establish fixation; field testing does not stop unless instigated by the examiner. This

helps keep testing times to within reasonable limits, which is important as longer testing times can cause patient fatigue which in turn can lead to erroneous results (Johnson *et al.*, 1988;Hudson *et al.*, 1994;Bengtsson *et al.*, 1998b).

5.6.2. **Humphrey visual field analyzer**

The Humphrey visual field analyzer attempts to provide a balance between conducting an accurate test and keeping testing times to within acceptable limits. The testing method itself is relatively straightforward; numerous flashes of light of varying intensity are shown against a defined background and the patient is required to click a button every time they see the spot of light. Almost all aspects of the field test are customisable in order to adapt to the individual being tested, allowing a more meaningful examination to be conducted.

Several different testing programs are included which allow specific parts of the visual field to be examined as required. Common programs include central 40, 24-2 which tests the central 24 degrees, 10-2 and the peripheral 60 test. The size of the stimulus can also be changed to cater for patients with low vision, as can stimulus colour. A stimulus size III, which has an angular subtense of 0.43°, is most widely used in routine visual field assessment. The Humphrey visual field analyser, and indeed most perimeters, traditionally measure light using the old European unit of luminance, the apostilb (asb); most perimeters use a uniform background luminance of 31.5 asb as standard (Rosenfield *et al.*, 2009).

The 24-2 test program compares threshold values for each test point with normative data from aged-matched subjects and classifies each threshold value as either normal or abnormal based on four different probability levels. The mean deviation (MD) is also worked out by averaging all data points and comparing to others of a similar age and race, a positive score signifies better overall sensitivity than normal while negative

values mean a brighter stimulus was required before detection and is thus indicative of lower sensitivity. The pattern standard deviation (PSD) measures the level of irregularity in the visual field with lower PSD scores indicating less variability.

5.7. Threshold Estimation

There are several different testing strategies each with differing levels of accuracy and examination time. The specific sensitivity of every test point can be determined using a full threshold test in which threshold values from previously tested points are used to determine the brightness of successive test points. On the Humphrey visual field analyzer a 4-2 double reversal staircase procedure is used so at each test point stimulus brightness is gradually reduced in 4dB steps to begin with, until it can no longer be detected by the patient; after this the intensity is increased and then decreased, this time in 2dB steps, until reversal occurs again. The dimmest light that can be seen by the patient, in other words the last stimulus seen before the second reversal, corresponds to the threshold value at that point (Anderson *et al.*, 1992). This is done for every test location and so is useful for mapping any visual field loss or reduction, due to its increased accuracy. However as expected this test can be time consuming, for example examination of the central 30° of vision using this 4-2 double staircase strategy on both eyes can take up to forty five minutes (Schaumberger *et al.*, 1995;Schimiti *et al.*, 2002). This introduces the possibility for patient fatigue, which as mentioned previously can affect test reliability.

Supra-threshold tests on the other hand use pre-set stimulus intensities for each test location and provide estimated visual field plots, which are more useful as a screening tool.

5.7.1. Swedish Interactive Threshold Algorithm (SITA)

The Humphrey visual field analyzer includes the SITA testing strategy, which enables a full threshold visual field test to be completed in a shorter time interval (Bengtsson *et al.*, 1998a;Bengtsson *et al.*, 1998b;Chandra Sekhar *et al.*, 2000) thus minimizing fatigue effects. The SITA standard (Swedish Interactive Threshold Algorithm) analyses the patients' previous responses in order to predict the threshold values (Bengtsson *et al.*, 1997), this reduces testing time considerably without reducing the repeatability of the data (Bengtsson *et al.*, 1999;Chandra Sekhar *et al.*, 2000). The SITA fast test allows even quicker assessment (Bengtsson *et al.*, 1998a;Artes *et al.*, 2002) and is ideally used on reliable patients. This testing strategy calculates the threshold sensitivity of one primary point located in each of the four quadrants of the patient's visual field, and uses this information to estimate the starting stimulus intensity of adjacent test points. To determine the threshold of these four primary points, the stimulus intensity is altered in 4dB steps until the first reversal occurs, and then in 2dB steps until the second reversal. For all neighbouring points on the other hand, the stimulus intensities are altered in 4dB steps until a single reversal occurs (Bengtsson *et al.*, 1998a). Such threshold estimating procedures in conjunction with a lower level of testing accuracy compared to the SITA standard mean fewer stimuli need to be presented to the patient leading to a reduced testing time (Bengtsson *et al.*, 1998a;Artes *et al.*, 2002).

5.8. Use of visual field testing to determine IOL retinal light distribution

Since MIOLs provide good vision at more than one focal point, depending on whether the patient is viewing a distant or near target, there will be corresponding blur at the other focal length as a result of the mechanism of action of that MIOL. Retinal light sensitivity is affected by blur (Anderson *et al.*, 2001). By comparing visual field plots in MIOL patients for both near and far distances, it may be possible to investigate how

incoming light is distributed across the retina. Psychophysical measures of visual function, such as perimetry, provide a subjective assessment of retinal sensitivity to incremental changes in luminance at different locations in the visual field (Lung *et al.*, 2012). An alternative way of assessing visual function is through the use of electrophysiological assessment techniques such as multifocal electroretinography. Here electrical responses to visual stimuli at different retinal locations are recorded using electrodes, thus the light sensitivity of retinal cells as well as the spatial distribution of this sensitivity can be evaluated (Jimenez *et al.*, 2008;Lung *et al.*, 2012;Messias *et al.*, 2013). Electroretinography provides an objective assessment about the function of the retina (Sample *et al.*, 2001;Lung *et al.*, 2012;Gualtieri *et al.*, 2013;Messias *et al.*, 2013) however it requires the use of suitable equipment to capture the low amplitude signals that are generated as well as signal processing algorithms to ensure clinically useful results are produced (Jimenez *et al.*, 2008).

Visual field examinations have previously been conducted on patients implanted with multifocal and monofocal IOLs primarily to determine whether there is a significant difference in threshold sensitivity caused by the implantation of an IOL (Steinert *et al.*, 1999). A study conducted high-pass resolution (HPR) perimetry on subjects. This test represents thresholds by displaying the scaled threshold target size at each location, which would increase with eccentricity in a normal subject (Frisen, 1993). Some authors believe HPR perimetry to be superior to standard differential light sensitivity perimetry in certain instances such as for estimating the number of functioning retino-cortical channels (Frisen, 1993), in assessing the function of MIOLs (Ravalico *et al.*, 1998) and identifying visual field loss earlier in subjects already displaying glaucomatous progression (Chauhan *et al.*, 1999). Ravalico *et al.*, (1998) performed HPR perimetry on patients implanted with either a one-piece near dominant aspheric MIOL, a distance dominant concentric ring design MIOL or a diffractive MIOL. The test was conducted at three different distances and the diffractive MIOL was found to give

higher spatial resolution at distance and the best performance at near. However to the author's knowledge there have been no comparisons of visual field plots at different focal distances for newer types of MIOLs such as segmented IOLs and AIOLs. Furthermore there have been no comparisons between the retinal thresholds in different regions of the same MIOL.

A reduction in foveal sensitivity, as measured by perimetry, occurs with increasing amounts of dioptric blur (Weinreb *et al.*, 1986;Herse, 1992;Anderson *et al.*, 2001;Rosenfield *et al.*, 2009). The effect of retinal blur differs according to stimulus size, with more pronounced blur effects occurring for smaller stimuli (Anderson *et al.*, 2001;Rosenfield *et al.*, 2009). Anderson *et al.* (2001) found a loss in sensitivity of 0.43dB per dioptre of refractive blur for a 0.4 degree stimulus corresponding to Goldman III on the Humphrey perimeter, while Weinreb *et al.*, (1986) found a reduction in averaged macular sensitivity of -1.26dB with every dioptre of blur in dilated (>4mm) pupils for the same stimulus size. Herse *et al.* (1992) determined the reduction in average sensitivity with blur was related to pupil size as they found a greater -1.84dB/D drop with an 8mm pupil compared with -1.10dB/D for a 3mm pupil. Sensitivity was also found to decrease with eccentricity with Herse *et al.* (1992) finding a reduction of approximately -0.34db/degree for an 8mm pupil. This is consistent with Weinreb *et al.*, (1986) who found a reduction of -0.377dB/ degree. Anderson *et al.* (2001) stated the effect of blur on peripheral vision was less severe compared to central vision. They found that peripheral sensitivity was initially unaffected by blur but then showed a sharp deterioration similar to that which occurs centrally. This difference is thought to occur as a result of differences in the size of the ganglion cell receptive field centrally and peripherally (Johnson *et al.*, 1978;Anderson *et al.*, 2001).

5.8.1. Expected outcomes

As mentioned, there are three types of presbyopia correcting IOL, each with a different mechanism of action. As a result, differences retinal sensitivity thresholds are expected with each.

When viewing a close object, the near portion of an MIOL will be stimulated in order to give the patient good vision at near and there will be retinal blur corresponding to the distance portions of the lens. Thus MIOLs incorporating a concentric ring in the optic would be expected to reduce the overall light sensitivity from distance and increase it at near and so would be expected to have a lower average threshold value at distance compared to a distance corrected IOL such as an AIOL. Providing the IOL had an equal number of near and distance focussed optical zones, a comparable threshold average would be expected between both near and distant corrected threshold sensitivity values with this MIOL type and no regional difference in sensitivity is expected.

Since AIOLs do not incorporate multiple focal zones into the optic, a greater proportion of light should theoretically reach each focal point with this IOL compared to a concentric ring design or segmented MIOL where incoming light is split between each focal point. Additionally, if the AIOL truly accommodates, the retinal sensitivity for distance and near viewing will be similar.

It is uncertain what form the retinal projection a segmented IOL such as the Oculentis lens would take. If this IOL projects discrete areas of distance and near onto the retina, the retinal sensitivity at these locations should reflect this by showing an intra-lens regional difference in retinal sensitivity between the inferior and superior portions that is reversed depending on the focal distance for which the subject is corrected. This is important to understand as it might have implications as to the optimal size, location

143

and shape profile of the near segment. The distance segment is expected to give sensitivity similar to the AIOL and better than the concentric ring IOL for distance viewing while the near portion is anticipated to give sensitivity comparable to the accommodating and better than the concentric IOL for the near target.

5.9. Study Purpose

This study will therefore assess the threshold sensitivity across the central 24° of the retina in eyes that have been implanted with either a diffractive multifocal, segmented multifocal or hinge -optic accommodating IOL in order to determine whether perimetry is an effective tool for mapping the retinal projection of these different presbyopia correcting IOLs. If so, this could provide valuable information relating to optimal IOL design features such as the most effective near segment size and shape for segmented MIOLs like the Oculentis Mplus. Earlier studies have performed perimetry on different presbyopia correcting IOLs at difference distances in order to compare them to each other (Ravalico *et al.*, 1998) however none, to the author's knowledge, have compared newer MIOLs such as the segmented IOL and none have attempted to compare differences in threshold sensitivity across different locations of the retina for the same IOL. This will therefore be investigated in the current study.

5.10. Method

A prospective, comparative clinical study was conducted on 30 eyes (mean age 64.5 ± 9.32years). Thirteen eyes implanted with an Oculentis MPlus segmented intraocular lens (Oculentis, Berlin, Germany), 10 with a Tetraflex accommodating intraocular lens (Lenstec, Florida, USA), and 7 with either a Rayner Mflex or Acrysof Restor lens were recruited approximately 1 year following implantation.

All surgeries were carried out by the same experienced surgeon at Solihull Hospital and the Midland Eye Institute (Solihull U.K.) and all patients gave informed consent to participate in the study following explanation of the procedures and the risks involved.

The study adhered to the tenets of the Declaration of Helsinki and was approved by the Local Research Ethics Committee.

To take part in this study, participants were required to:

- have post-operative corrected Snellen visual acuity of at least 6/7.5

- be free of any active ocular or systemic disease with ocular side effects

- not be on ocular or systemic medications with known ocular side effects

- Have no history of eye surgery within the last 3 months.

All patients had pre-operative ocular health checks prior to surgery to ensure the absence of any active ocular pathology that could impact upon the post-operative visual outcome; there were no complications with the surgeries in any of the patients.

Microperimtery using the MP-1 microperimeter (NIDEK, Japan) was initially used to try and map the multiple transition zones and near segment area of the two implanted multifocal IOLs. However the MP-1 was found to be unsuitable for the patient demographic as the equipment was especially sensitive to small movements in head and/or eye movement and this increased testing times to unacceptable levels (figure 5.7).
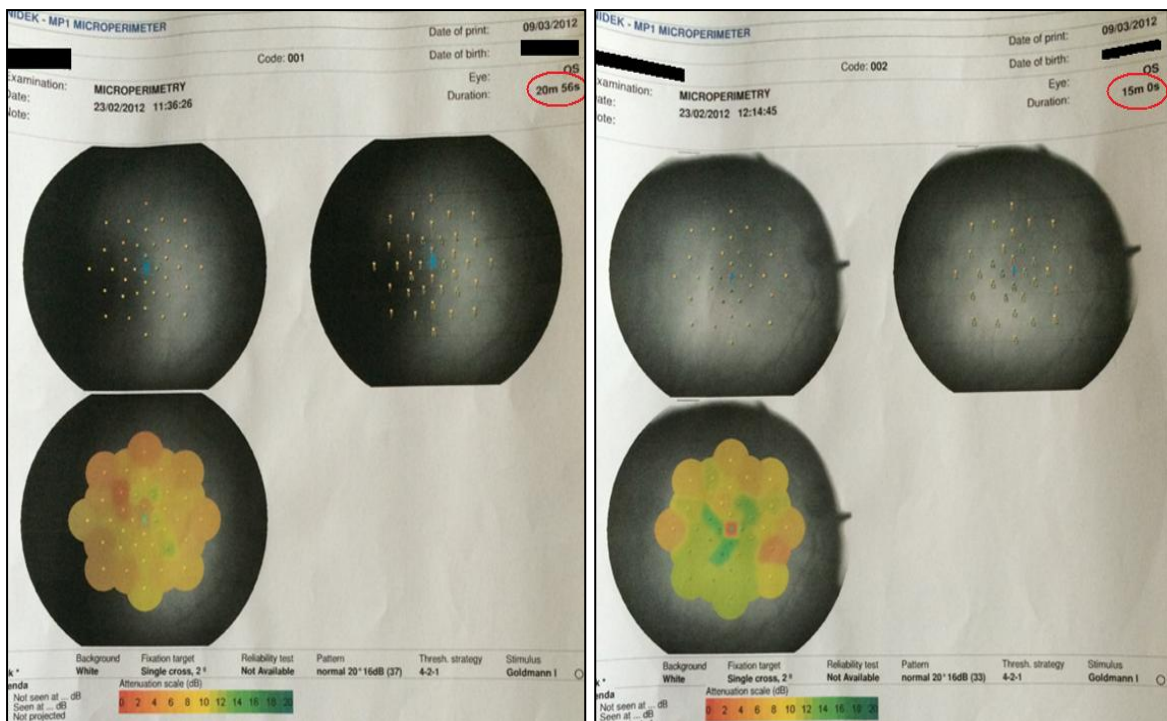
Figure 5.7: Microperimetry data for one eye, from two different subjects. This technique was found to be unsuitable for our patient demographic and resulted in unacceptably long testing times (red circle).

Therefore the use of the MP-1 Microperimeter was abandoned in favour of the Humphrey visual field analyser (Carl Zeiss Meditec, USA). A SITA FAST strategy was chosen as it provided the best balance between conducting a detailed threshold examination and testing within a reasonable time frame to minimise fatigue; a 24-2 testing pattern was selected for similar reasons. A standard stimulus size III was used.

Once the patients were familiarised with the visual field testing procedure, they were asked to perform the 24-2 SITA Fast exam twice with each eye, four times in total, once corrected for optimal distance viewing and once optimised for near viewing to correspond with the focal demand of the visual field target hemisphere distance.

The total deviation of each of the 52 plots for the patients' right and left eyes were collated according to figure 5.8, so that values for right and left eyes would coincide.

		1	2	3	4					4	3	2	1			
	5	6	7	8	9	10			10	9	8	7	6	5		
	11	12	13	14	15	16	17	18	18	17	16	15	14	13	12	11
19	20	21	22	23	24	25		26	26		25	24	23	22	21	20	19
27	28	29	30	31	32	33		34	34		33	32	31	30	29	28	27
	35	36	37	38	39	40	41	42	42	41	40	39	38	37	36	35
		43	44	45	46	47	48		48	47	46	45	44	43		
		49	50	51	52				52	51	50	49				

Figure 5.8: Diagram showing how total deviation results were recorded so that values coincided for both eyes.

Visual field results were averaged by location in two different ways, as indicated in figures 5.9 and 5.10 and then analysed for all IOLs, for both near and distance viewing.

5.10.1. Division of visual field test points by region

In the first analysis, shown in figure 5.9, the field data was divided regionally along the 45° and 135° meridians to create central, superior, inferior, nasal and temporal sections. An attempt to distribute visual field data points equally amongst each section was made, meaning some data points were merged into a different quadrant from that in which they would normally fall. For example, points 22 and 25 were included in the

"superior" quadrant rather than temporal and nasal quadrants, and points 30 and 33 in the "inferior" quadrant.
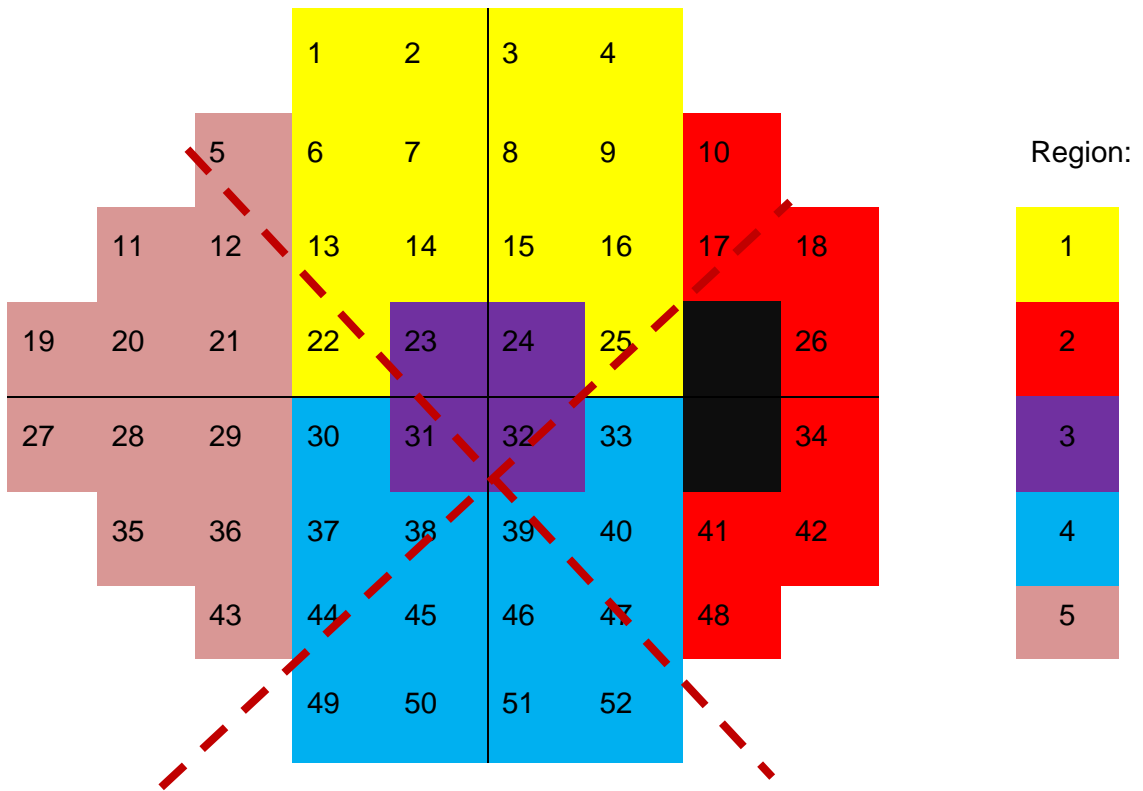
Figure 5.9: A diagram illustrating a regional division of the visual field plot. The red dashed line shows the approximate regional distribution of test points.

5.10.2. Division of test points by quadrant

In the second analysis, shown in figure 5.10, the field plot was divided along the horizontal and vertical meridians with the two meridians intersecting at the fovea thus creating quadrants corresponding to the superior temporal, superior nasal, inferior temporal, inferior nasal and central field.
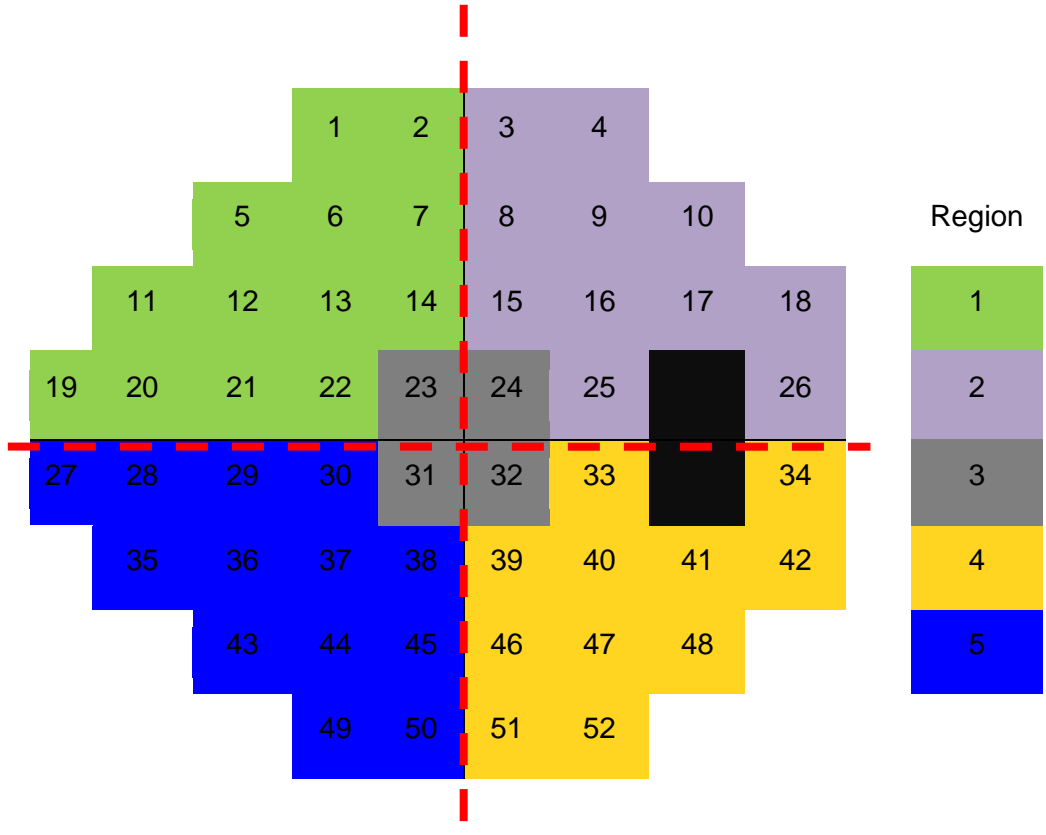
Figure 5.10: An illustration showing the visual field plot divided into quarters. The red dotted line demonstrates the quadrant division of test points.

5.11. Statistical analysis

5.11.1. Sample size calculation

A sample size calculation carried out using Sigma Plot statistical and graphing software (Version 11, Systat Software Inc., Chicago, Illinois, USA) showed a minimum of 30 subjects was required to achieve a power of 80% for a correlation coefficient of 0.5, at a 0.05 significance level.

5.11.2 Testing for Normality

A one-sample Kolmogorov-Smirnov test revealed that the visual acuity data were normally distributed (Kolmogorov-Smirnov Z = 1.678, P=0.07). Therefore threshold

sensitivity across regions with the different IOLs was compared using parametric analysis.

5.11.2. Analysis method

The 52 retinal sensitivity thresholds of the 24-2 visual field examination were grouped together in two different ways (figure 5.9 and 5.10) and collected in an Excel database (Microsoft Office 2007). All data were analysed using SPSS for Windows (version 20.0, SPSS Inc.) using repeated measures analysis, with posthoc tests applied when the overall significance was p <0.05.

5.12. Results

Data were analysed in the same way for the two different test point distributions and results are detailed below.

5.12.1. Regional division

Analysis of variance of data that was split into regions according to figure 5.9 showed no significant difference in retinal sensitivity between the three lenses (ANOVA: F=1.936, P=0.187) or between the two distances (ANOVA: F=5.646, P=0.055), but did show a statistically significant difference between different regions (ANOVA: F=5.267, P=0.003) and an interaction between distance and region (ANOVA: F=7.122, P=0.001).

Tests of Within-Subjects Effects					
Source	Type III Sum of Squares	df	Mean Square	F	Sig.
lens	45.455	2	22.728	1.936	.187
distance	14.895	1	14.895	5.646	.055
region	23.380	4	5.845	5.267	.003
lens * distance	11.463	2	5.731	.490	.624
lens * region	10.346	8	1.293	1.289	.272
distance * region	17.297	4	4.324	7.122	.001
lens * distance * region	1.470	8	.184	.213	.987

Table 5.1: ANOVA of visual field data divided by region.

Further testing using student's t-tests to compare mean threshold sensitivity by region for all IOLs showed that threshold sensitivity in region 1, corresponding to the superior portion of the lenses, differed from the other four regions (table 5.2).

Student's T-test (p value)					
	region 1	region 2	region 3	region 4	region 5
region 1		0.016	0.003	0.014	<0.001
region 2			0.42	0.98	0.27
region 3				0.23	0.73
region 4					0.16
region 5					

Table 5.2: Further analysis of the regional differences within the lenses.

Threshold loss appeared greatest in region 1 for both near and far distances with the Oculentis and Concentric MIOLs, and at near for the Tetraflex lens. There was a larger standard deviation for threshold loss with the Oculentis lens at near for all regions, indicating the data is more widely spread (figure 5.11). The standard deviation was also relatively large for the Tetraflex IOL at distance for all regions as well as for other more specific regions such as region 1 of the Oculentis lens at distance and region 3 of the Tetraflex lens for near. Higher standard deviations may have occurred as a result of the relatively small sample size or possibly due to other factors such as subject head movements during testing, despite the fact that subjects were instructed to keep their heads still and to fixate on a central target.
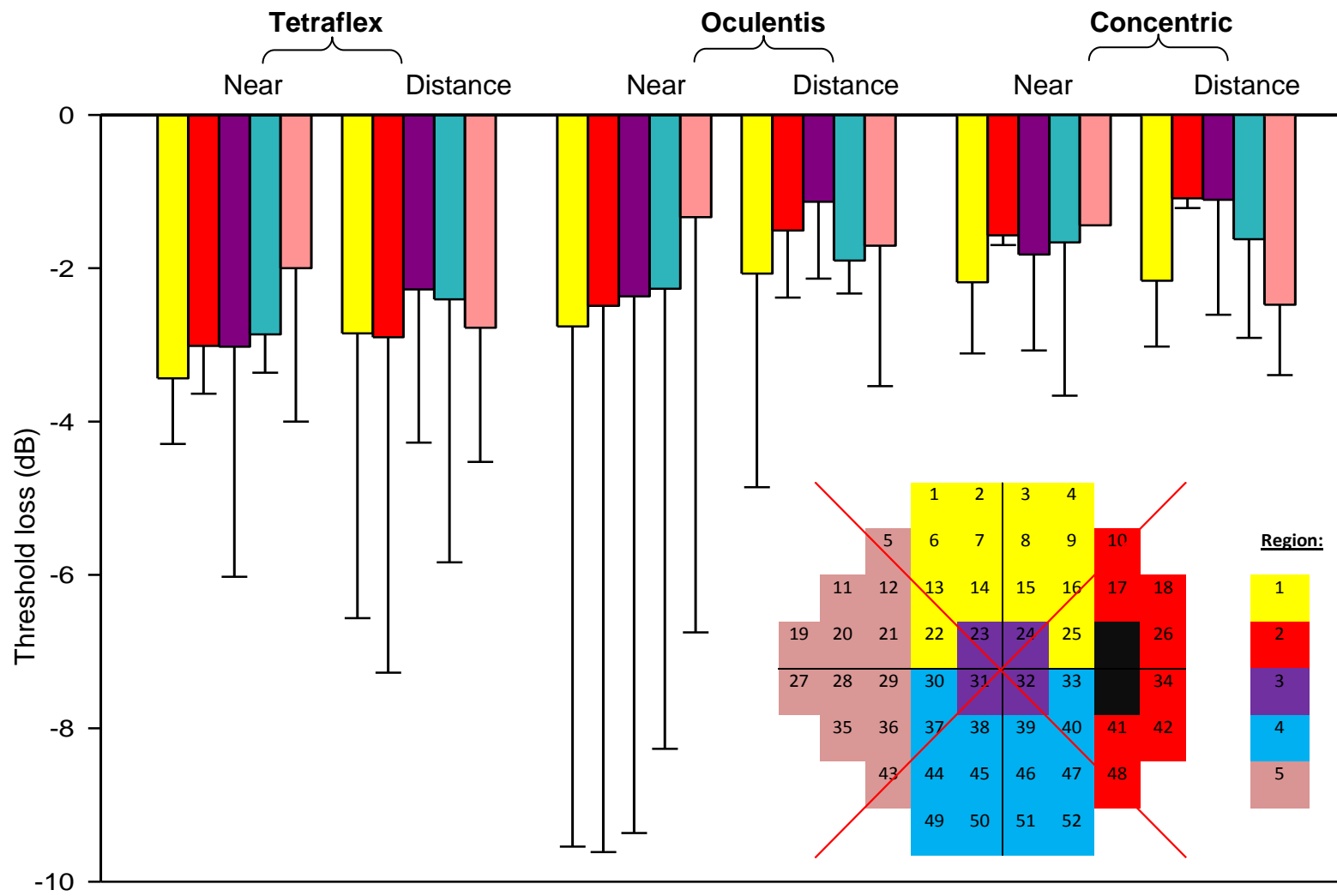
Figure 5.11: Comparative retinal sensitivity loss, divided regionally, at each region for each distance and lens.

5.12.2. Quadrant division

Analysis of variance of data that was split by quadrant according to figure 5.10 showed a statistically significant difference in retinal sensitivity between the three lenses (ANOVA: F=5.470, P=0.020) but no difference between regions (ANOVA: F= 1.701, P=0.183) or distance (ANOVA: F=0.169, P=0.695), although again there was an interaction between distance and region (ANOVA: F=3.610, P=0.019; figure 5.9).

Tests of Within-Subjects Effects					
Source	Type III Sum of Squares	df	Mean Square	F	Sig.
lens	129.538	2	64.769	5.470	.020
dist	.245	1	.245	.169	.695
region	10.256	4	2.564	1.701	.183
lens * dist	12.377	2	6.189	3.702	.056
lens * region	11.836	8	1.480	1.260	.287
dist * region	9.725	4	2.431	3.610	.019
lens * dist * region	4.318	8	.540	1.053	.411

Table 5.3: ANOVA of visual field data split into quadrants.

Further analysis using student's t-tests comparing retinal threshold sensitivity between IOLs revealed that the Tetraflex accommodating lens differed from both the Oculentis segmented and concentric ring design MIOLs (table 5.4).
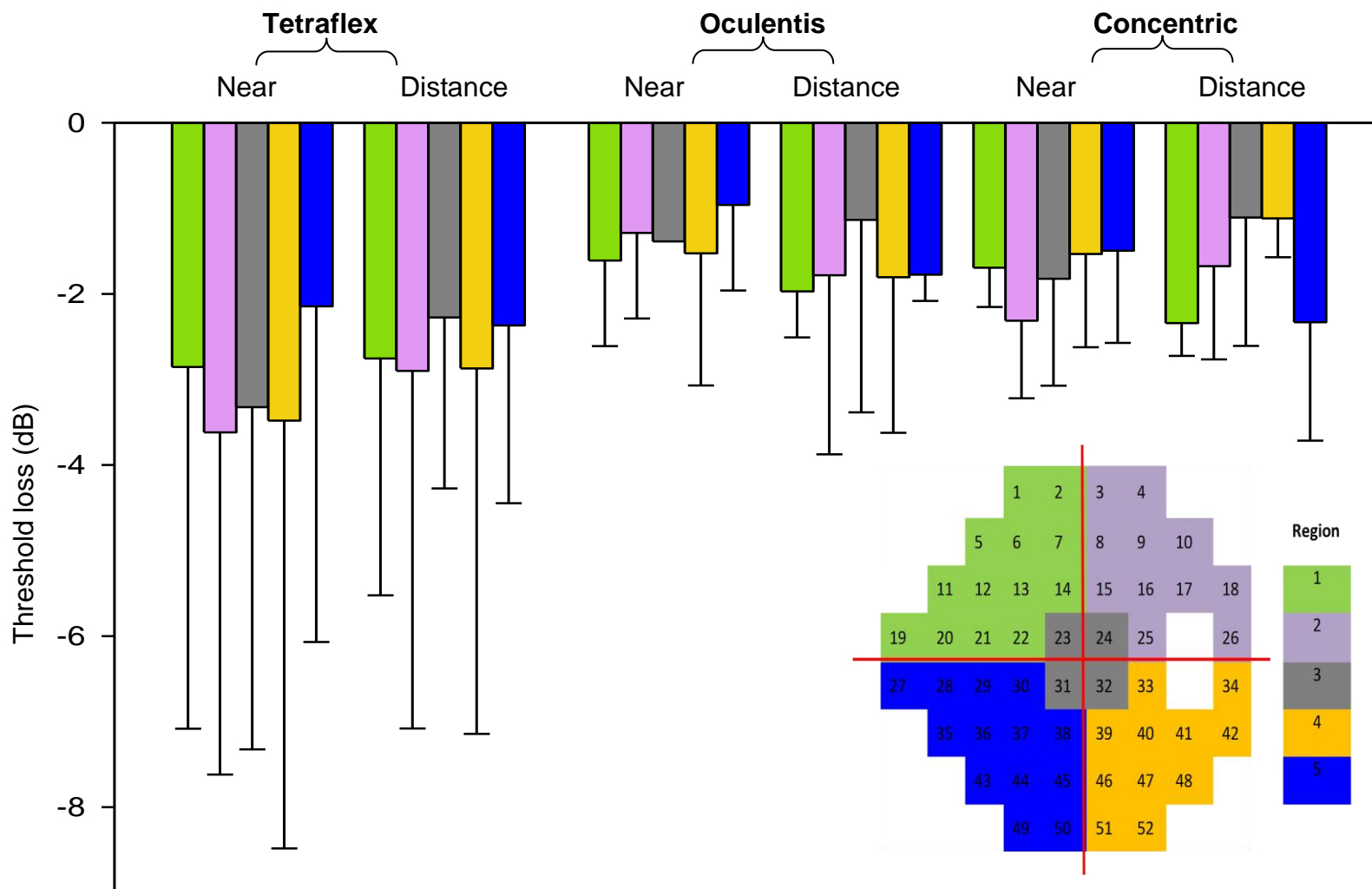
Figure 5.12: Comparative retinal sensitivity loss, divided by quadrant, at each region for each distance and lens.

Student's T-test (p value)			
	Accommodating	**Segmented**	**Concentric**
Accommodating			
Segmented	<0.001		
Concentric	<0.001	0.26	

Table 5.4: Differential threshold sensitivity between IOLs with test points divided by quadrant.

5.12.3. Other analyses

There was no regional difference between the inferior and superior portions of the Oculentis lens when corrected for near (Student's t-test: p=0.52) or distance (p=0.77).

5.13. Discussion

This study assessed the retinal threshold sensitivity of two different types of MIOL and an AIOL in order to determine whether the retinal projection of light from the IOL optics led to a measureable difference between lenses. A reduction in perimetric sensitivity occurs with increasing blur (Weinreb *et al.*, 1986). While the reports in the literature vary, it can be expected that defocus of a light source on the retina will cause between a 0.4db (Anderson *et al.*, 2001) and 1.8dB (Herse, 1992) change in sensitivity per dioptre. Therefore a visual field examination using the Humphrey visual field analyzer was undertaken to determine whether this test was able to identify retinal threshold differences created as a result of the mechanism of action of each lens type. If so, it was hoped that this could provide valuable insight into the optimal design features of a segmented MIOL.

There was a statistically significant difference between lenses depending on how the visual field plot was divided for analysis. Data divided regionally appeared better suited to picking up differences in sensitivity between different areas of a lens (table 5.2; figure 5.12), compared to data divided into quadrants.

It was thought that the near segment of the Oculentis MPlus IOL would project onto the retina resulting in a regional difference in sensitivity, the superior region having better sensitivity than the lower region for the distance visual field and vice versa for the near focused visual field. While there was an interaction between region and distance of visual field analysis across all lenses for both analyses, this did not result specifically from the predicted pattern of retinal sensitivity with the segmented IOL compared to the other IOLs. This lack of regional difference in threshold sensitivity between the inferior and superior portions of the Oculentis lens could suggest that simultaneous images are

spread over the central retina as opposed to being located in discrete areas. This may be because of a blending zone, which results in a more gradual power change across the lens from distance to near, much like in a varifocal spectacle lens, as opposed to the abrupt power change that had been anticipated. Additionally the Oculentis lens is designed to reflect any light that hits the transition zone away from the optical axis (Alio *et al.*, 2011a) which could also have contributed to the masking of the near segment during perimetry. Interestingly, the superior region was depressed in retinal sensitivity for the regional analysis compared to the other regions in the regional analysis, and this was true for all lenses (table 5.2; figure 5.11). This could have occurred because of differences in visual performance between the inferior and superior portion of the visual field (Danckert *et al.*, 2003;Silva *et al.*, 2008). Previc *et al.* (1990) believed the upper and lower visual fields were specialised for differing functions with the lower field being optimised for near vision and the upper field optimised for distant visual tasks such as scanning a visual scene. Research has shown the lower visual field to provide better contrast sensitivity and spatial resolution compared to the upper field (Abrams *et al.*, 2012;Petrova *et al.*, 2012). A potential reason for this disparity is thought to be an increased number of ganglion and cone cells in the upper half of the retina, which receives its input from the lower visual field compared to the inferior hemiretina, which receives it input from the superior field (Curcio *et al.*, 1990;Silva *et al.*, 2008). This therefore could explain the observed reduction in upper visual field sensitivity.

If AIOLs truly accommodated, there should be no blur at distance or near, hence the retinal sensitivity should be superior to the concentric and segmented MIOLs at both visual field distances. However, AIOLs are known to provide limited objective accommodation by six months after implantation (Kriechbaum *et al.*, 2005;Wolffsohn *et al.*, 2006b;Saiki *et al.*, 2010;Takakura *et al.*, 2010;Wolffsohn *et al.*, 2010b) and instead any 'accommodative' mechanism results from lens flexure (Hancox *et al.*,

2006;Wolffsohn *et al.*, 2010b). In this case, as light is not split in focus, the accommodating IOL should provide better retinal sensitivity for distance visual fields than the concentric or segmented MIOLs, but worse retinal sensitivity for near focused visual fields. However, quadrant analysis showed the AIOL to provide poorer retinal sensitivity at both distance and near compared with the concentric and segmented multifocal IOLs (table 5.4; figure 5.12). This could be the result of the patients implanted with AIOLs having more posterior capsular opacification, a known side effect of these lenses (Hancox *et al.*, 2006;Hancox *et al.*, 2007;Saiki *et al.*, 2010;Takakura *et al.*, 2010) although this was not apparent from slit lamp examination. Alternatively greater retinal deterioration in this group compared to the MIOL groups may have been a contributory factor, though again this was not evident through ophthalmoscopy. Lastly, the IOL material and fibrosis could also have influenced this result. A reduction in IOL transparency, referred to as "glistenings" can occur with all materials including silicone, PMMA and acrylic. However, the frequency of glistenings has been found to be greatest in 1 piece hydrophobic acrylic IOLs such as the Tetraflex IOL (Xi *et al.*, 2014), which may explain the poorer retinal sensitivity observed with this IOL.

As subjects were required to complete the visual field test twice, once when corrected for distance and the other when near-corrected, there was potential for fatigue to occur which may have reduced test reliability. While the impact on average distance and near visual field results was balanced by randomising the order of the tests, patient fatigue can result in a general depression of the visual field (Bengtsson *et al.*, 1998b) thus making it more difficult to pick on up small variations in retinal sensitivity. For this reason, the SITA-fast strategy was selected in order to provide a balance between accurate threshold evaluation and testing time. However in hindsight this test may not have been adequate enough to detect subtle differences in sensitivity between regions of a MIOL in order to identify the near segment of the Oculentis lens. In order to

counteract for the effect of fatigue a longer break should perhaps have been introduced between tests and the more accurate SITA-standard test used (Bengtsson *et al.*, 1997;Chandra Sekhar *et al.*, 2000).

Despite perimeters being readily accessible by most eye-care practitioners to assess light sensitivity across the visual field, perimetry does not appear to be a useful technique to map and compare the retinal projection of different MIOLs and AIOLs in order to gain greater insight into the mechanism of action of these relatively new lenses.

CHAPTER 6: Restoring eye focus- how much additional objective accommodation would we need?

6.1. Accommodation

Accommodation describes the dioptric increase in ocular power when focussing on near objects (Wold *et al.*, 2003;Ostrin *et al.*, 2004;Glasser, 2006). The most widely accepted theory of accommodation suggests accommodation is achieved by a change in shape of the crystalline lens secondary to ciliary muscle (CM) contraction. Accommodative ability decreases gradually with age in a process commonly termed presbyopia.

Pseudophakic patients implanted with monofocal IOLs are sometimes able to demonstrate relatively good near ability, an occurrence that is generally termed pseudo accommodation (Nakazawa *et al.*, 1984;Glasser, 2006). True accommodation and pseudo-accommodation are fundamentally different. True accommodation occurs due to a change in the optical power of the eye. Pseudoaccommodation on the other hand, refers to the achievement of functional near vision through non accommodative means, such as an extended depth of focus produced as a result of higher order aberrations, such as coma (Wolffsohn *et al.*, 2010b), pupil constriction or from using implants and corneal inlays that produce a simultaneous image, like multifocal contact lenses or IOLs (Glasser, 2006).

AIOLs take advantage of the continued flexibility of the CM and are designed to mimic a young crystalline lens during accommodation in order to provide pseudophakes with better vision during near tasks (Wolffsohn *et al.*, 2006a;Cleary *et al.*, 2010). There are several different AIOLs designs available; single optic devices use CM contraction

during near vision stimulation to produce forward movement in order to increase the effective power of the IOL. Dual optic AIOLs are designed to increase the power change with accommodative effort and also use forward shift with CM contraction to achieve this (Marchini *et al.*, 2007;Cleary *et al.*, 2010;Sheppard *et al.*, 2010). Wavefront technology has shown the forward shift feature of AIOLs induces myopia associated with spherical aberrations and coma, which aids with near vision (Macsai *et al.*, 2006).

AIOL performance can be assessed in a number of ways; these may include measurement of distance corrected near visual acuity (DCNVA), or subjective defocus curves, using the push up test or measuring objective refractive changes to target over a range of vergences with an autorefractor or aberrometer (Vasudevan *et al.*, 2007;Yi *et al.*, 2010;Atchison, 2012). Such focus-shift AIOLs have been found to produce little objective accommodation (Wolffsohn *et al.*, 2006a;Wolffsohn *et al.*, 2006b;Cleary *et al.*, 2010). The subjectively reported range of clear focus results principally from pseudo-accommodative factors such as pupil size and aberrations, which increase the subjective depth of focus. Many agree that amplitude of accommodation is best measured using objective methods since true accommodative amplitude is overestimated during subjective measurement (Wold *et al.*, 2003;Ostrin *et al.*, 2004;Macsai *et al.*, 2006;Cleary *et al.*, 2010).

Research has indicated that the objective accommodative performance of such focus shift AIOLs is limited with only a small benefit to near vision (Cleary *et al.*, 2010;Sheppard *et al.*, 2010;Takakura *et al.*, 2010;Wolffsohn *et al.*, 2010b). Macsai *et al.* (2006) compared an AIOL with a standard monofocal IOL and reported superior uncorrected distance and near vision with the AIOL. However subjects with AIOLs perceived greater eye focusing ability than was measured, which they hypothesised could have occurred as a result of several pseudo-accommodative factors such as

pupil size and aberrations increasing subjective depth of focus. Cleary *et al.* (2010) too attributed the observed near vision performance with an implanted AIOL to depth of focus rather than true pseudophakic accommodation of the IOL.

The amount of accommodation AIOLs need to provide in order to restore equivalent near vision will depend upon how much pseudo-accommodation patients already have. Therefore the ability to determine how these factors contribute to pseudo-accommodation is of interest, especially until AIOLs can provide greater levels of true accommodation.

6.2. Depth of field and focus

Depth of field is key component of the accommodative process. If an object that is in focus is moved closer to or further away from the eye, there will be a drop in image sharpness producing a blurred retinal image. However for a given range of object distances, the observer will not perceive this blurring and the object will still appear clear even without a change in ocular accommodation. The depth of field describes this range of object distances that does not produce a detectable reduction in image focus and is represented in figure 6.1 (Nakazawa *et al.*, 1984;Glasser, 2006). When focusing a near target, the visual system utilises the depth of focus in order to alter the refractive state by the minimum amount in order to form a paraxial image at the retina (Bernal-Molina *et al.*, 2014).

The depth of focus on the other hand, describes the range of image distances in front of and behind the focal point or retina over which the image may be focused without causing an objectionable reduction in image sharpness, as illustrated in figure 6.1 (Hung, 2001;Wang *et al.*, 2006a;Gupta *et al.*, 2007;Vasudevan *et al.*, 2007;Millodot, 2009;Atchison, 2012).
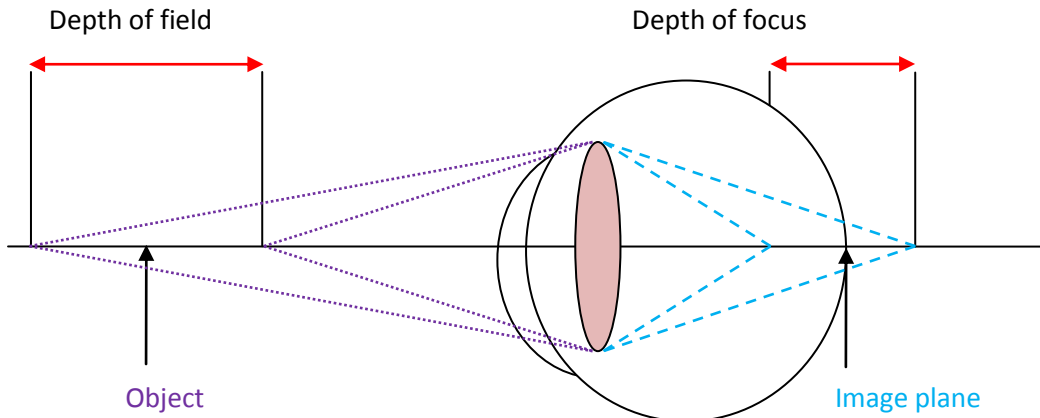
Figure 6.1: Schematic representation of the depth of field and depth of focus of an eye.

Depth of field and depth of focus are closely related but can be distinguished by the fact that the former is an object quantity while the latter, an image quantity (Atchison *et al.*, 1997;Millodot, 2009). Atchison *et al.* (1997) did not differentiate between depth of field and depth of focus and instead defined them as the greatest range in dioptric focusing error that does not produce an objectionable drop in retinal image quality. This is a practice that shall be followed here by use of the acronym DOF. So long as an image remains within the DOF space it will be perceived as clear thus the DOF effectively provides a perceptual tolerance for small errors in ocular focus (Ciuffreda *et al.*, 2007b).

6.3. Objective versus subjective measures of accommodation

6.3.1. Objective

Accommodation can be measured both subjectively and objectively. Objective measures of accommodative amplitude require the use of instrumentation such as autorefractors or aberrometers, which measure the optical power of the eye. In an eye with accommodation, an increase in optical power will be observed as the near target is moved closer to the eye. In absolute presbyopes with no accommodation on the other hand, no change in power will be recorded (Glasser, 2006).

6.3.2. Subjective

Two key ways of subjectively measuring accommodation are discussed below. The first technique relates to using push-up to blur to determine accommodative ability while the second method evaluates acuity loss with changing stimulus vergences.

6.3.2.1.   Push-up test

With subjective measures, such as the push up test, the distance corrected subject is required to report when text that is moved gradually closer to the eye can no longer be sharply focused. In young adults as the near target moves closer, the eyes will accommodate to increase the optical power of the eye, converge to direct the eyes onto the near target and the pupils will constrict increasing the DOF (Kasthurirangan *et al.*, 2006).

In young adults the subjective near point during the push-up test is achieved as a result of true accommodation as well as pseudo-accommodation. In presbyopes with no accommodation, when focusing on a near object there will be no accommodative increase in the optical power of the eye however the eyes will still converge as part of the near vision triad and, more importantly, the pupils will still constrict leading to an increased DOF. Glasser *et al.* (2006) concluded that this increase in DOF during subjective measurement could lead to the incorrect assumption that some accommodation was present in absolute presbyopes when it is not. For example, MIOL patients tested using the push-up test could appear to have functional accommodation when in reality none exists (Ostrin *et al.*, 2004). Subjective tests like the push up test can overestimate accommodation compared to objective measurements (Marcos *et al.*, 1999b;Wold *et al.*, 2003;Wang *et al.*, 2006a;Wolffsohn *et al.*, 2006a;Vasudevan *et al.*, 2007;Win-Hall *et al.*, 2009). According to Ostrin *et al.* (2004) the push up test

overestimates accommodation even more in patients with poor visual acuity and those with a reduced ability to detect blur.

Wold *et al.* (2003) stimulated and measured accommodation using four different techniques, two of which were subjective and two objective. They found more consistent results when accommodation was stimulated with negative trial lenses, a finding corroborated by Ostrin *et al.* (2004), and concluded this was an effective way of stimulating maximum accommodation. Objective measurements were less variable than results obtained with subjective measurements. However, there are relatively few studies which have directly compared subjective and objective methods (Marcos *et al.*, 1999b;Wold *et al.*, 2003) in the same cohort using the same target, and in the same test conditions.

6.3.2.2. Defocus curve testing

The subjective measurement of visual acuity at different distances or with different levels of trial lens induced defocus can also be used to evaluate range of clear vision (Gupta *et al.*, 2007;Wolffsohn *et al.*, 2013). There is currently no universally accepted standardised procedure for measuring defocus curves in terms of the range and step sizes between trial lenses. A key aspect of the testing procedure is randomisation of either the trial lenses, letter sequences or both in order to counteract for memory effects. Gupta *et al.* (2007) investigated the importance of randomisation when measuring defocus curves in pre-presbyopes and found there was no statistically significant difference between randomising the order in which trial lenses are presented compared to randomising the letter sequences when measuring visual acuity. Furthermore they found no difference between randomising just one of these factors compared to randomising both factors in eliminating learning effects and

reducing unwanted bias, although randomising both factors was considered ideal. It has been suggested that the use of negative lenses to stimulate accommodation causes pupil miosis through the near triad, which can artificially increase DOF thus masking true accommodative ability (Gupta *et al.*, 2007). However Wold *et al.* (2003) and Ostrin *et al.* (2004) compared several different methods of assessing accommodation and concluded that the use of negative lenses was most effective in stimulating maximum accommodation and produced more consistent results, and so the effect of pupil miosis in falsely increasing DOF appears to be minimal under these conditions.

Defocus curve testing is commonly used to compare presbyopia correcting strategies (Wolffsohn *et al.*, 2013) such as MIOLs, but is subjective and slow to perform. To fully assess presbyopic correction strategies defocus testing would ideally be performed multiple times to assess the range of clear vision with binocularity, under different lighting conditions as the optics of the eye change and with different target contrasts. However subjectively measured defocus curves can be quite lengthy, leading to patient fatigue and variability in results. Therefore conducting repeated subjective defocus curves in different testing conditions is unlikely to be feasible. There is a need for shorter defocus curve testing times which cannot be achieved by increasing step sizes between lenses as this has been shown to decrease quality of results obtained (Wolffsohn *et al.*, 2013).

6.4.   Factors affecting DOF

Subjective DOF is influenced by many ocular and patient factors and these are thought to partly contribute to the difference between subjective and objective DOF. For example target factors (Marcos 1999) such as luminance, colour, size and shape (Atchison *et al.*, 1997), as well as subject factors such as pupil size, age and higher

order aberrations (Atchison *et al.*, 1997;Wang *et al.*, 2006a) can affect subjective DOF as summarised in table 6.1.

Factors increasing Depth of Focus	Study
Luminance ↓	(Campbell, 1957;Ciuffreda *et al.*, 2007b;Cufflin *et al.*, 2007)
Target contrast ↓	(Campbell, 1957;Atchison *et al.*, 1997;Ciuffreda *et al.*, 2007b;Cufflin *et al.*, 2007)
Spatial frequency ↓	(Legge *et al.*, 1987;Marcos *et al.*, 1999b)
Pupil size ↓	(Campbell, 1957;Nakazawa *et al.*, 1984;Atchison *et al.*, 1997;Ostrin *et al.*, 2004;Cufflin *et al.*, 2007)
Retinal eccentricity ↑	(Ronchi *et al.*, 1975;Ciuffreda *et al.*, 2007b)
Target detail ↓	(Atchison *et al.*, 1994;Atchison *et al.*, 1997;Marcos *et al.*, 1999b;Ostrin *et al.*, 2004;Wang *et al.*, 2006b)
Visual acuity ↓	(Green *et al.*, 1980;Legge *et al.*, 1987)
Chromatic aberration ↑	(Ciuffreda *et al.*, 2007b)
Blur sensitivity ↓	(Ciuffreda *et al.*, 2007b)

Table 6.1: list of factors which are thought to increase subjective depth of focus.

Presbyopes have a higher DOF compared to young subjects and this most likely occurs due to pupil miosis, an increase in ocular aberrations with age (McLellan *et al.*, 2001;Yi *et al.*, 2010;Atchison, 2012) and reduced sensitivity to blur (Kline *et al.*, 1999b).

6.4.1. Pupil size

As pupil size varies, so too does the level of incoming light, ocular aberrations and DOF. Pupil size influences retinal image size and shape (Atchison *et al.*, 2005). With a decreasing pupil, the size of the retinal blur circle decreases to below the eye's blur threshold meaning a sharp image is still perceived over a wider range and this raises

the range of clear focus. Therefore as pupil size decreases, DOF increases (Nakazawa *et al.*, 1984). However, there is some disparity as to the direction of the change in DOF with pupil size depending on whether DOF is measured subjectively or objectively. Marcos *et al.* (1999a) found that as pupil size increased from 2mm to 4mm DOF decreased, as expected, for both subjective and objective measurement techniques. However for larger pupils, specifically 4mm to 6mm subjective DOF decreased, but the objective DOF increased in some cases. This suggests cues other than perception of blur are used to achieve best focus. Due to the paucity of data in this area, the discrepancy between subjective and objective DOF and pupil diameter should be investigated further.

6.4.2. Tolerance to blur

Human blur perception is multifaceted and complex. Blur detection, which is an important part of blur perception, describes the ability to detect when an image is just noticeably blurred compared to a blur-free target (Atchison *et al.*, 2005). A reduced sensitivity to blur from ocular disease or trauma for example, is believed to be associated with an increased DOF (Ciuffreda *et al.*, 2007a) and so blur detection ability may be an important contributor to the difference between objective and subjective measures of accommodation (Vasudevan *et al.*, 2007).

The ability of observers to resolve fine detail decreases gradually with age (Kline *et al.*, 1999a). Legge *et al.* (1987) found that individuals with reduced visual acuity were more tolerant to defocus compared to those with normal vision. Given this, ability to tolerate blur should increase with age. Kline *et al.* (1999b) investigated the effect of ageing on ability to correctly identify blurred text signs by measuring photopic and mesopic legibility threshold in a group of young and older adult observers. They found the older observers were better at correctly identifying the defocused text compared to young observers indicating young people with better vision are less tolerant to blur, which is

consistent with the findings of Legge *et al.* (1987). The superior performance of older observers in this task was later attributed by Jung and Kline (2010) to age related optical factors, specifically pupil miosis, as well as experience-mediated neural compensation. There is also thought to be a link between personality and tolerance to blur (Woods *et al.*, 2010).

Interestingly, myopes were reported to have larger objective blur thresholds compared to emmetropes and were therefore believed to be less sensitive to defocus blur (Campbell, 1957). However later studies have found no statistically significant difference in the blur thresholds of myopes compared to non myopes (Schmid *et al.*, 2002).

Blur thresholds also increase with pupil size (Campbell, 1957) and retinal eccentricity (Hess *et al.*, 1989;Ciuffreda *et al.*, 2007a). This increase with retinal eccentricity is thought to occur due to a combination of anatomical, physiological, optical and perceptual factors (Ciuffreda *et al.*, 2007a). Blur detection varies with stimulus exposure time; ability to detect blur improves with longer stimulus durations in both central and peripheral vision (Hess *et al.*, 1989).

6.4.3. Higher order aberrations

Ocular aberrations arise from imperfections in the eye's structures, particularly the cornea and crystalline lens, and can affect the clarity of the retinal image (Liang *et al.*, 1997;He *et al.*, 2000;McLellan *et al.*, 2002;Charman, 2005). They are dynamic and change with pupil size, age and accommodation (Artal *et al.*, 2002;Holladay *et al.*, 2002;Artal *et al.*, 2004;Li *et al.*, 2011). HOAs such as spherical aberration are thought to act as cues for best focus and can also increase DOF (Wang *et al.*, 2006a).

Ocular aberrations can be measured in a number of ways. The more popular method of measurement is through the use of an aberrometer (Vandenberg *et al.*, 1993;Liang *et al.*, 1997;Porter *et al.*, 2001;Kuroda *et al.*, 2002). There are several types of aberrometer currently available to measure ocular aberrations; all are based upon slightly different measurement principles. Aberrometers based on the Hartmann-Shack principle are currently preferred since it is thought they allow faster and more accurate evaluation of the eye's higher order aberrations (Prieto *et al.*, 2000;Cheng *et al.*, 2003;Miranda *et al.*, 2009;Bueno *et al.*, 2010;Yu *et al.*, 2010).

6.5. Study purpose

Together, pupil size, HOAs and tolerance to blur are thought to cause the observed difference between subjective and objective depth of focus measurements although the relative contribution of each factor to the observed difference is not currently known. Hence these features should dictate how much additional optical power change an AIOL should need to overcome presbyopia. To the author's knowledge, this has not been confirmed previously. Therefore the purpose of the study is to investigate the factors affecting subjective range of clear focus in pre-presbyopes in greater detail.

6.6. Method

The study was approved by the Institutional Ethics Committee and the research conformed to the tenets of the Declaration of Helsinki. Written, informed consent was obtained from all participants.

To take part in this study, participants were required to:

- be aged between 20 and 45 years

- have no more than 0.75 dioptres of uncorrected astigmatism

- be able to wear contact lenses for the duration of the study rather than spectacles unless they were emmetropic

- have corrected visual acuity in the eye being tested of at least 6/7.5

- be free of any active eye disease

- not be on ocular medications or systemic medications with known ocular side effects

- Have no history of eye surgery within the last 3 months.

6.6.1. Blur detection test

There is no standard way of measuring blur tolerance and so to investigate if and how much a person's sensitivity to blur influenced subjective range of clear focus variance, a blur detection test was developed. There are different ways of measuring a subject's blur sensitivity. One method consists of a bipartite target in which one half of the target is movable relative to the other fixed half and the observer is asked to find the position of just noticeable blur (Cufflin *et al.*, 2007). Other methods include alternate-forced choice spatial tasks in which one target differs from the others and the subject is requested to identify this target (Hess *et al.*, 1989). A test for measuring a subject's ability to distinguish blur was devised based on this second type of blur detection test. Blur discrimination is affected by target size. As target size increases, blur thresholds

increase and so blur sensitivity decreases (Ciuffreda *et al.*, 2007a). Thus a target close to the limit of the subject's acuity was required. GIMP software (version 2.6) which is an image manipulation program, was used to blur the image by differing levels using a Gaussian blur filter. Initially a linear blur progression was envisaged in order to determine blur detection capability to greater levels of accuracy. However this resulted in an excessive number of test slides, which would have increased testing time and could have resulted in subject fatigue. Therefore a logarithm blur progression was chosen as this was thought to provide a better balance between accurate blur discrimination assessment (Hammett *et al.*, 1998) and testing time.

Subjects were asked to view the high contrast computerised visual target monocularly, which was placed two metres away, through a 1.5mm pinhole in order to neutralise aberration and pupil size effects. The test was conducted in a room that received solely artificial illumination which provided a background luminance that fell within the photopic range (85 cd/m2).The visual target comprised of four shortened logMAR charts placed in each corner of the screen. This shortened chart comprised three lines of black letters equivalent to 6/5 (bottom line), 6/6 (middle line) and 6/9 (top line) against a white background (figure 6.3). A shortened logMAR chart was chosen to prevent subjects using cues such as the blurred edges of larger letters or the reduced contrast of smaller letters to aid in their subjective assessment of blur as this could produce inaccurate results. For this reason a chart consisting of only small letters was used.

6.6.1.1. Calculating equivalent letter size at a reduced working distance

The following mathematical calculation (equation 6.1) was used to calculate the correct letter size needed to equate to 6/9, 6/6 and 6/5 from this shorter working distance.

$$\tan A = \frac{L}{D}$$

Where: A= angular subtense in degrees of arc, L= letter height in millimetres and D= working distance in millimetres.

In order to determine the equivalent letter height for use in the blur detection test using equation 6.1, angular subtense first needs to be calculated. The approach used to ascertain this value is detailed next.

Visual acuity is generally recorded according to the following Snellen fraction.

$$\text{Snellen notation} = \frac{\text{test distance (m)}}{\text{Distance (m) letter subtends 5mins of arc}}$$

Therefore a 6/6 Snellen letter will subtend 5minutes of arc at 6 metres(Rosenfield *et al.*, 2009). This value can be used as the standard from which the angular subtense of other Snellen letters can be calculated, in minutes of arc (equation 6.3).

$$\text{Angular subtense (6m)} = \left(\frac{\text{distance (m) letter subtends 5mins of arc}}{\text{test distance (m)}} \times 5 \right)$$

A 6/9 Snellen letter will subtend 5 minutes of arc at 9 metres, so using equation 6.3, the angular subtense of a 6/9 letter at 6 metres is 7.5 minutes of arc. This method was used to calculate the angular subtense of Snellen letters from 6/60 to 6/5 (table 6.2).

Snellen Notation		Decimal	Angular subtense (mins of arc)
20/200	6/60	0.10	50
20/100	6/30	0.20	25
20/70	6/21	0.29	17.5
20/60	6/18	0.33	15
20/50	6/15	0.40	12.5
20/40	6/12	0.50	10
20/30	6/9	0.67	7.5
20/25	6/7.5	0.80	6.25
20/20	6/6	1.00	5
20/17	6/5	1.18	4.17

Table 6.2: Snellen notation in metres and feet with the calculated angular subtense.

After calculating angular subtense, it is then possible to work out the equivalent height of a letter for a reduced testing distance using equation 6.1. To calculate letter size at a 2 metre testing distance, all angular subtense values were converted into degrees of arc by dividing these values by 60, since there are 60 minutes of arc in one degree of arc (Rosenfield *et al.*, 2009). So a 6/9 letter with an angular subtense of 7.5 minutes of arc would be equivalent to 0.125 degree of arc. The height of this 6/9 letter at 2 metres could then be calculated by rearranging equation 6.1 to find L (equation 6.4).

$$\mathbf{L = \ tan\,A \ \times D}$$

Where letter height L= unknown, angular subtense A=0.125 deg of arc and test distance D= 2 metres, which is equivalent to 2000millimetres.

Inputting this into equation 6.4 gave an equivalent letter height of 4.36mm. The same procedure was followed for 6/6 and 6/5 letters to give letter heights of 2.91mm and 2.43mm respectively.

In blur detection tasks, subjects must identify blur so for example subjects may be required to indicate in which alternative location they are able to detect a blur target (Jakel *et al.*, 2006). A blur discrimination task, on the other hand, relates to just noticeable difference in perceived blur (Wang *et al.*, 2005a). The test used in this study comprised one blurred image and three sharply focussed images with subjects required to identify the blurred image and so is best described as a blur detection test. The number of alternatives presented to the patient can impact on test accuracy. A four alternate forced choice (AFC) method was adopted in our blur detection test, as opposed to a 2 AFC since a greater number of alternatives have been shown to produce more reliable results. A study comparing a 2, 4 and 8AFC method found that naive observers showed the highest sensitivity and reliability with a 4AFC test for detection tasks (Jakel *et al.*, 2006). This was not found to be true for discrimination tests, however, and this was attributed to the fact that discrimination tasks require more of the participant's attention compared to detection tasks. Increasing the number of choices in a blur discrimination test will therefore cost more attentional resources, leading to a poorer performance.

Subjects were given thirty seconds to identify the blurred chart by indicating whether it was the top right, top left, bottom right or bottom left image that was blurred (figure 6.3). A demonstration practice plate was placed at the beginning of the test and consisted of a blurred chart with a 5.5 Gaussian filter applied. The purpose of this was to allow subjects to familiarise themselves with the task and make it easier for them to understand the aim of the test before starting. Subsequent plates had decreasing amounts of Gaussian blur applied to them using this computer software. The level of

176

Gaussian blur applied to the blurred image decreased logarithmically in 1.2log steps until the final plate, which had no blurred image. A log as opposed to linear step change was used to minimise the number of test slides and therefore limit the effect of fatigue on results. A blank black page was inserted between each test page and shown for five seconds to allow subjects to recover before seeing the next image and also to stop patients from potentially identifying the blurred image by the change in letter clarity from one slide to the next rather than recognising the blurred image out of the four on the screen. A staircase method of assessment, much like in visual field testing, was adopted for better accuracy.

6.6.1.2.   Staircase strategy

Blur tolerance ability was assessed with a double-reversal staircase strategy. Use of this bracketing strategy ensured greater end point accuracy. Subjects were required to identify the blurred image out of the four displayed, a correct answer resulted in the examiner moving onto the next test slide. An incorrect response, on the other hand, prompted a reversal of 1 Gaussian blur filter step. If this was correctly answered the examiner continued on with the test, in which the blur level applied to each slide decreased in logarithmic steps. Another incorrect answer instigated the second reversal whereby the examiner went back to preceding test slide. After a correct response was given, the examiner continued with the test until the observer gave a final incorrect response in which case this last correctly identified blur level was recorded as the final blur tolerance as illustrated in figure 6.2.
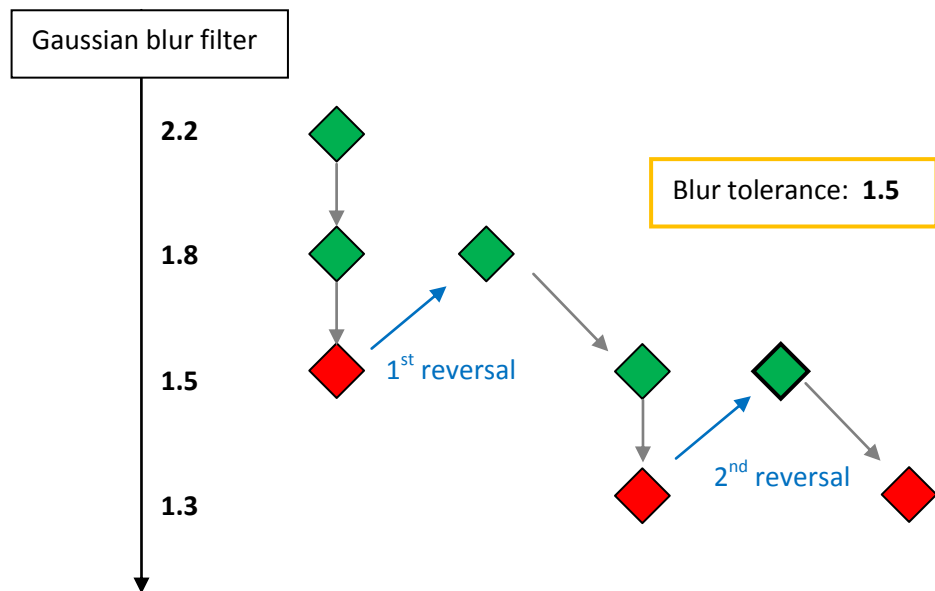
Figure 6.2: Example of the double-reversal staircase procedure used to accurately determine blur tolerance in subjects. Green diamonds represent when the blurred image was correctly identified and red diamonds when an incorrect answer was given.
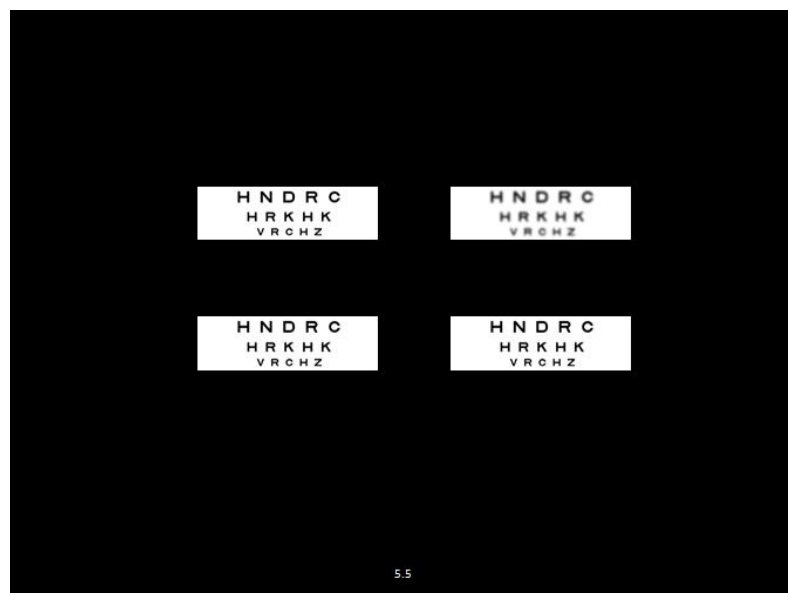
Figure 6.3: Example of one of the blur detection test slides where subjects were asked to identify which of the four images was blurred (the top right image is blurred in this case).

6.6.2. Experimental protocol

50 subjects mean age 32.98 ± 6.42 years (range 23- 45 years; 30 female) attended the Ophthalmic Research Group's laboratories where a basic refractive examination was conducted in order to ensure they were wearing the most accurate distance prescription; a measurement of the best corrected visual acuity (VA) for each eye was taken at this point. To minimise reflections, subjects with uncorrected VA below 6/7.5 were fitted with a contact lens in the eye under test. Spherical daily disposable lenses were given to subjects with astigmatism up to -0.75DC while toric contact lenses were fitted to those with more than -0.75DC astigmatism.

After allowing the contact lenses to settle for 10 minutes, tolerance to blur and amplitude of accommodation were measured on the eye being tested. To investigate if and how much a person's sensitivity to blur influenced subjective and objective range of clear focus variance, blur detection ability was assessed using the 4AFC test described earlier in which subjects were required to identify the blurred image out of the four displayed on the screen. Subjective amplitude of accommodation was measured in all subjects using a push-up test to confirm subjective range of focus in subjects with greater than 10 dioptres of accommodation.

After this, subjective and objective defocus curves were measured simultaneously using full aperture trial lenses from +2.00 to -10.00DS in -0.50 steps and in a randomised order. Objective measurements were taken using the Aston open field aberrometer. Wavefront sensing using a Hartmann-Shack wavefront sensor is commonly used to objectively measure the ocular aberrations of the human eye. The Hartmann-Shack aberrometer is designed to measure along the eye's primary optical axis and so is ideally used in the assessment of central vision (Wei *et al.*, 2010). The

Aston aberrometer is a miniaturised slit-lamp mountable aberrometer based on the Hartmann-Shack principle (Bhatt *et al.*, 2013) and is described in more detail in chapter 7. The aberrometer measured pupil size and higher order aberrations in addition to HOAs at each level of defocus. Distance visual acuity was measured on a digital logarithmic progression chart placed four metres away (TestChart 2000Pro, Thomson Software Solutions, Hatfield, UK) with the letters randomised between presentations in order to reduce learning effects (Wolffsohn *et al.*, 2013).

Each letter read correctly was scored as 0.02logMAR and subjects were encouraged to guess if unsure. Trial lenses were held approximately 40mm from the corneal plane so they were not in the aberrometer path and were powered to create the traditional defocus step sizes of 0.50D at a back vertex distance (bvd) of 12mm using equation 6.5. The original and equivalent lens powers at the greater bvd have been listed in table 6.3.

$$\mathbf{Fc} \; = \; \frac{\mathbf{F}}{\mathbf{1 + xF}}$$

Equation 6.5

Where Fc= power corrected for vertex distance, F=original lens power and x=the difference in bvd in metres.

Lens power (bvd:12mm)	Equivalent Lens (bvd:40mm)
+2.00	+2.00
+1.50	+1.50
+1.00	+1.00
+0.50	+0.50
plano	plano
-0.50	-0.50
-1.00	-1.00
-1.50	-1.50
-2.00	-2.00
-2.50	-2.75
-3.00	-3.25
-3.50	-400
-4.00	-4.50
-4.50	-5.25
-5.00	-5.75
-5.50	-6.50
-6.00	-7.25
-6.50	-8.00
-7.00	-8.75
-7.50	-9.50
-8.00	-10.25
-8.50	-11.25
-9.00	-12.00
-9.50	-13.00
-10.00	-14.00

Table 6.3: original power alongside equivalent defocus lens power at a 40mm bvd.

All subjective acuities were corrected for magnification effects associated with this increased back vertex distance using equation 6.6 and 6.7 (Aaron *et al.*, 2010;Rosen *et al.*, 2011).

$$\textbf{Spectacle Magnification} = \frac{\textbf{1}}{\textbf{1} - (\textbf{bvd} \times \textbf{F})}$$

<div align="right">Equation 6.6</div>

Where bvd refers to the back vertex distance in metres and F is the lens power in dioptres.

$$\textbf{Change in acuity} = \textbf{log}(\textbf{SM}) \qquad \text{Equation 6.7}$$

6.7.   Analysis

6.7.1. Objective accommodation range

All aberrometry values were normalised. The objective defocus range was then calculated for each subject in Sigma Plot 11.0 using dynamic curve fitting to find the initial point of plateau of the aberrometer-predicted Z4 spherical defocus values. A Sigmoidal 3, parameter equation was selected to fit the data (equation 6.7) with an average rsqr goodness of fit value of 0.953±0.08.

$$y = \frac{a}{1 + e^{-\left(\frac{x - x0}{b}\right)}}$$

<div align="right">Equation 6.7</div>

Where e= the base of the natural logarithm, a= the curve's maximum value, b= the slope of the curve and x0= the x-value of the sigmoid's midpoint.
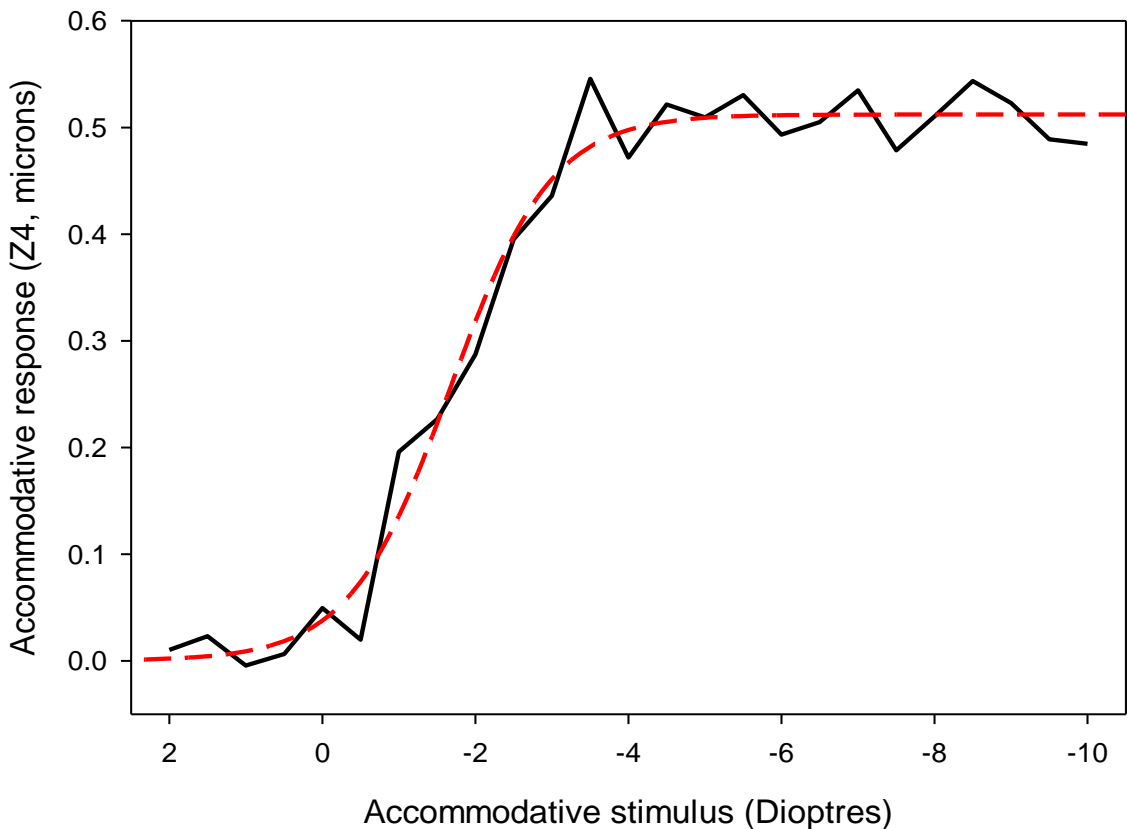
Figure 6.4: Example of a subject's accommodative response to various defocus trial lenses as measured objectively using aberrometry. The raw aberrometry data was normalised and curve fitting applied to determine the initial point of plateau. Measuring the point when maximum accommodation is first reached gives us the objective focussing range which can then be directly compared with the subjectively measured range.

6.7.2. Subjective accommodation range

There are two different criteria, relative and absolute, which can be used to determine subjective range of accommodation from defocus curves, as summarised by Gupta *et al.* (2008).The absolute criterion refers to the first point at which visual acuity passes a certain level, for instance +0.3logMAR. The relative criterion on the other hand states that best visual acuity plus an allowance to account for variance with repeated visual acuity measurements of 0.04logMAR, gives the subjective range of focus. The two can give very different values for the range of focus as illustrated in figure 6.5 and so both

were employed in the analysis. Gupta *et al.* (2008) recommended the best VA plus 0.04 relative criterion as this was found to have the strongest correlation and smallest Bland-Altman limit of agreement to the subjective push up test, though they acknowledged that this criterion had been used in relatively few studies.
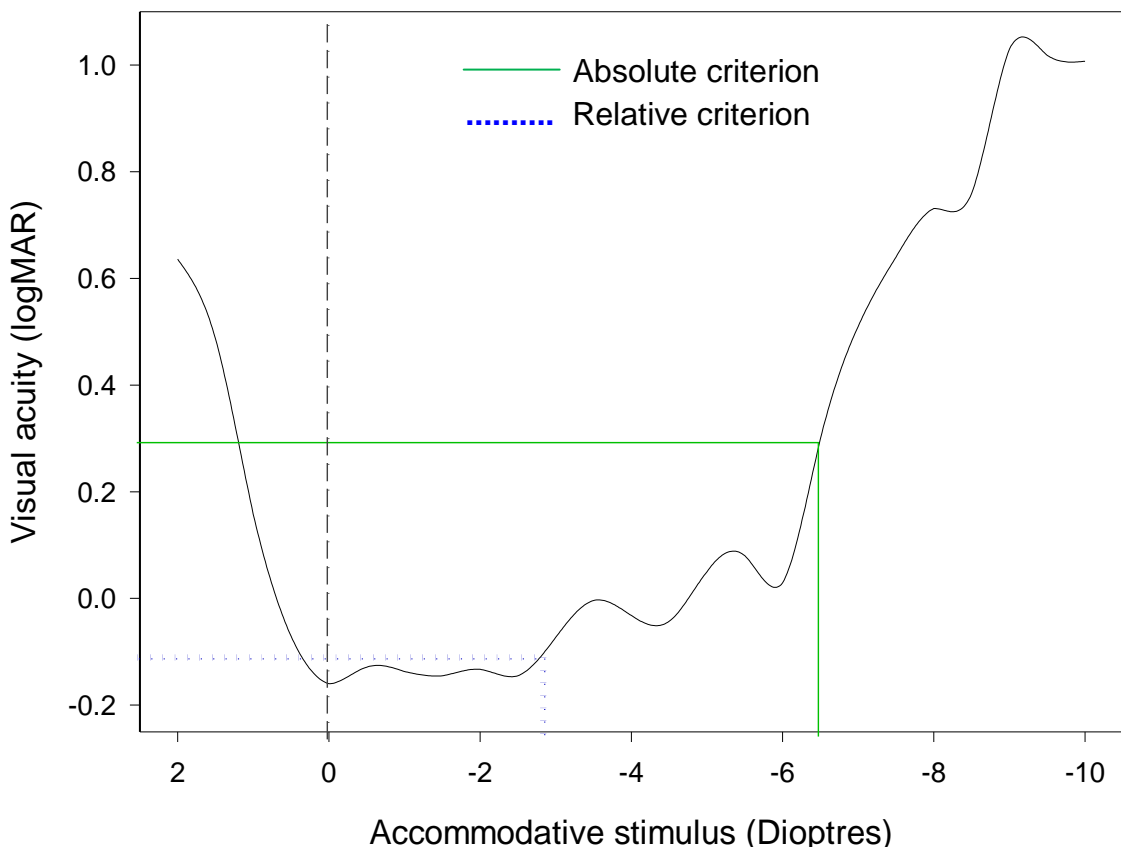
Figure 6.5: A subject's subjective defocus curve. The subjective range of accommodation was determined using both absolute (green, solid) and relative (blue, dotted) criteria which gave varying ranges of approximately 6.50D (absolute) versus 2.75D (relative).

6.8. Statistical analysis

6.8.1. Sample size calculation

A sample size calculation was carried out with Sigma Plot statistical and graphing software (Version 11, Systat Software Inc., Chicago, Illinois, USA) which showed a minimum of 30 subjects was required to achieve a power of 80% for a correlation coefficient of 0.5 with a significance level of 0.05.

6.8.2. Testing for Normality

A one-sample Kolmogorov-Smirnov test was used to test for normality and revealed that the data was normally distributed (Kolmogorov-Smirnov Z = 0.661, P=0.775), therefore parametric analysis was used.

6.8.3. Analysis method

Stepwise linear regression analysis was performed using Sigma plot 11.0 (Systat Software Inc., Chicago, Illinois, USA) in order to identify the key factors influencing the difference between subjective and objective defocus curves and to determine their relative contribution to this difference.

6.9. Results

Subjective range of focus was principally accounted for by the change in spherical lens power (67.4% of the variance) with an additional 6.2% determined by the blur tolerance accounting for 73.6% of the variance in total ($F=17.751, p<0.001$). This was confirmed by analysis of the difference between objective accommodation and the subjective range of clear focus where 20.3% of the variance could be accounted for by the subject's blur tolerance. Tolerance to blur was correlated with the difference between objective accommodation and the subjective range of clear focus ($r=0.464$, $p=0.007$; figure 6.6) and spherical aberrations ($r=0.366$, $p=0.036$). Spherical aberrations were also related to average pupil size ($r=0.367$, $p=0.011$).The power of the statistical tests performed was 0.8 or above.
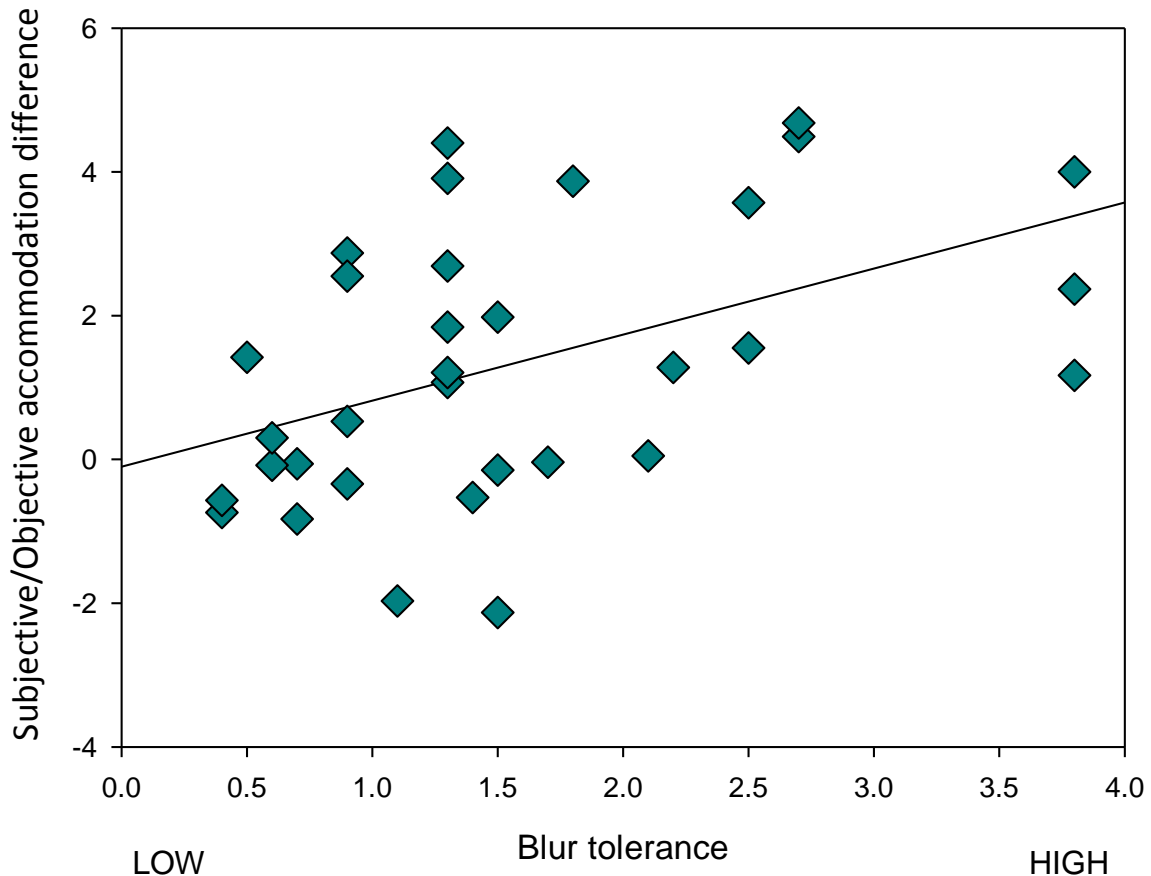
Figure 6.6: Subjective/objective difference in accommodation increased with the subjects' ability to tolerate blur.

Age was correlated to objective accommodation and the subjective range of clear focus (p<0.001; figure 6.7), but not pupil size, aberrations or tolerance to blur in the pre-presbyopes (p>0.05).
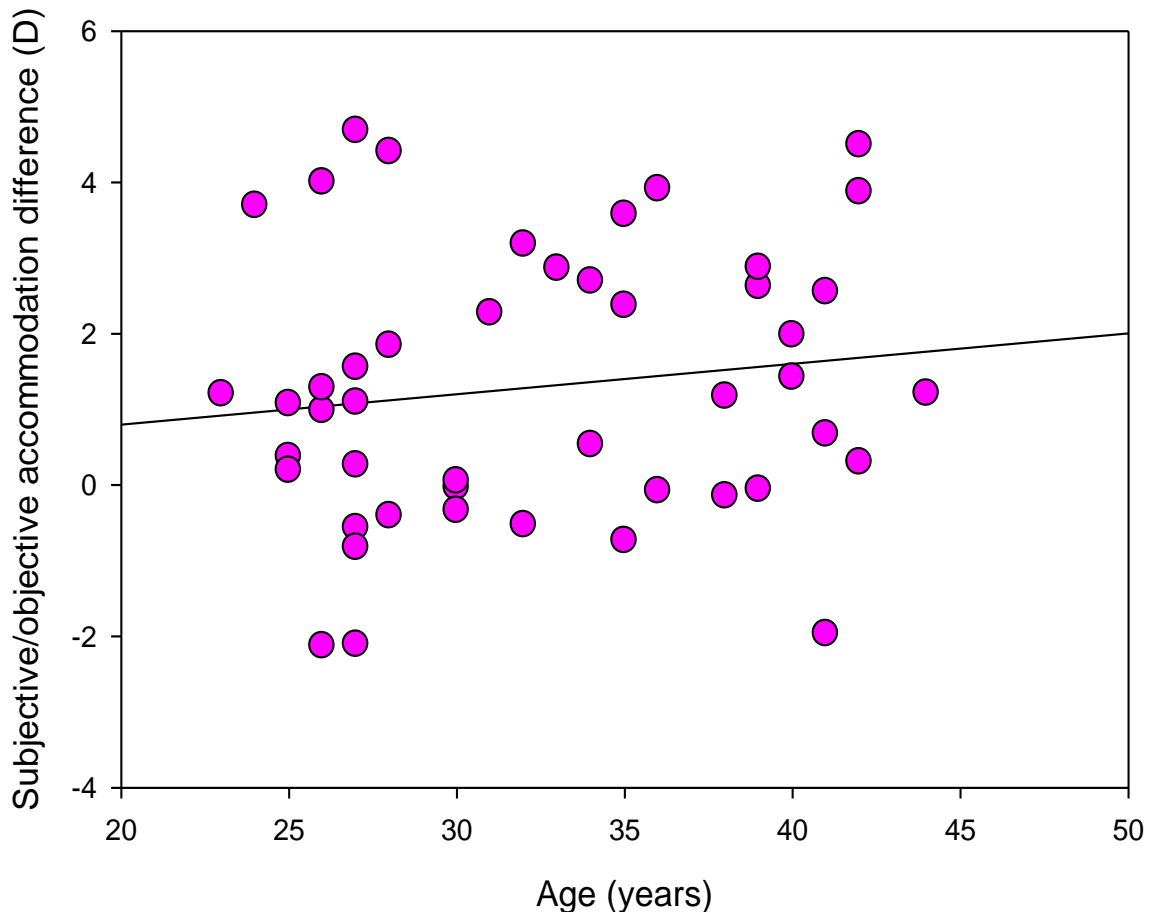
Figure 6.7: Subjective/objective accommodation difference increased with age.

Once the subject's maximum accommodation had been reached, the patient was instructed to continue focussing on an acuity chart through the remaining higher powered trial lenses. The accommodative response after this point was then evaluated and in most cases, once the limit of focusing ability had been reached, accommodation remained relatively steady with slight fluctuations about the maximum. A repeated measures ANOVA showed there to be no statistically significant difference in the

accommodative response of subjects once maximum accommodation had been stimulated (ANOVA: F-1.426, p=0.229; figure 6.8).
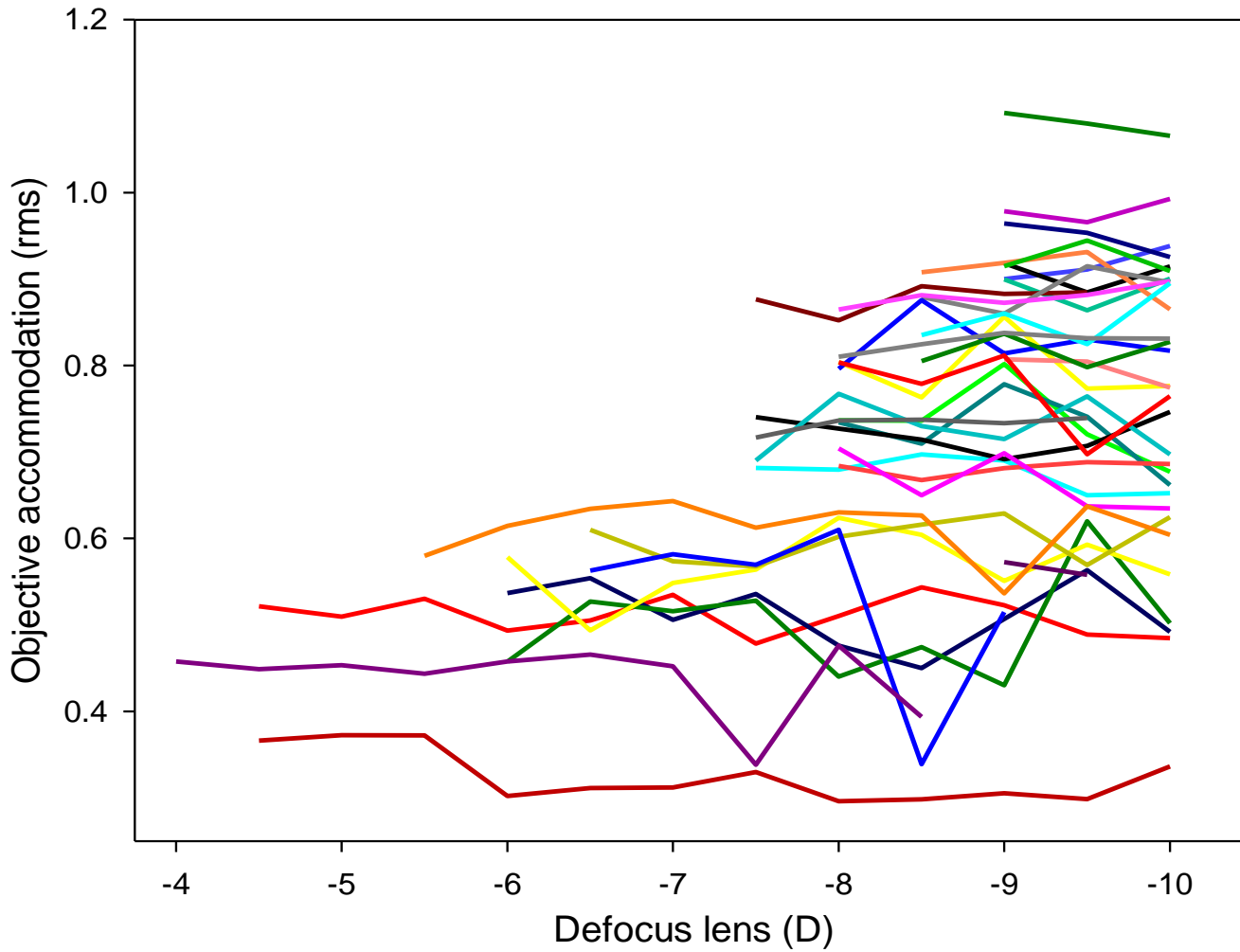
Figure 6.8: The objectively measured accommodative response, once maximum accommodation had been stimulated, is plotted. Data from subjects with an objective accommodative range ≤9.5D is included and in most cases accommodation remained relatively steady.

A statistically significant negative slope was found for change in pupil size per dioptre of defocus (t test: t=-2.253, p<0.05; figure 6.9).
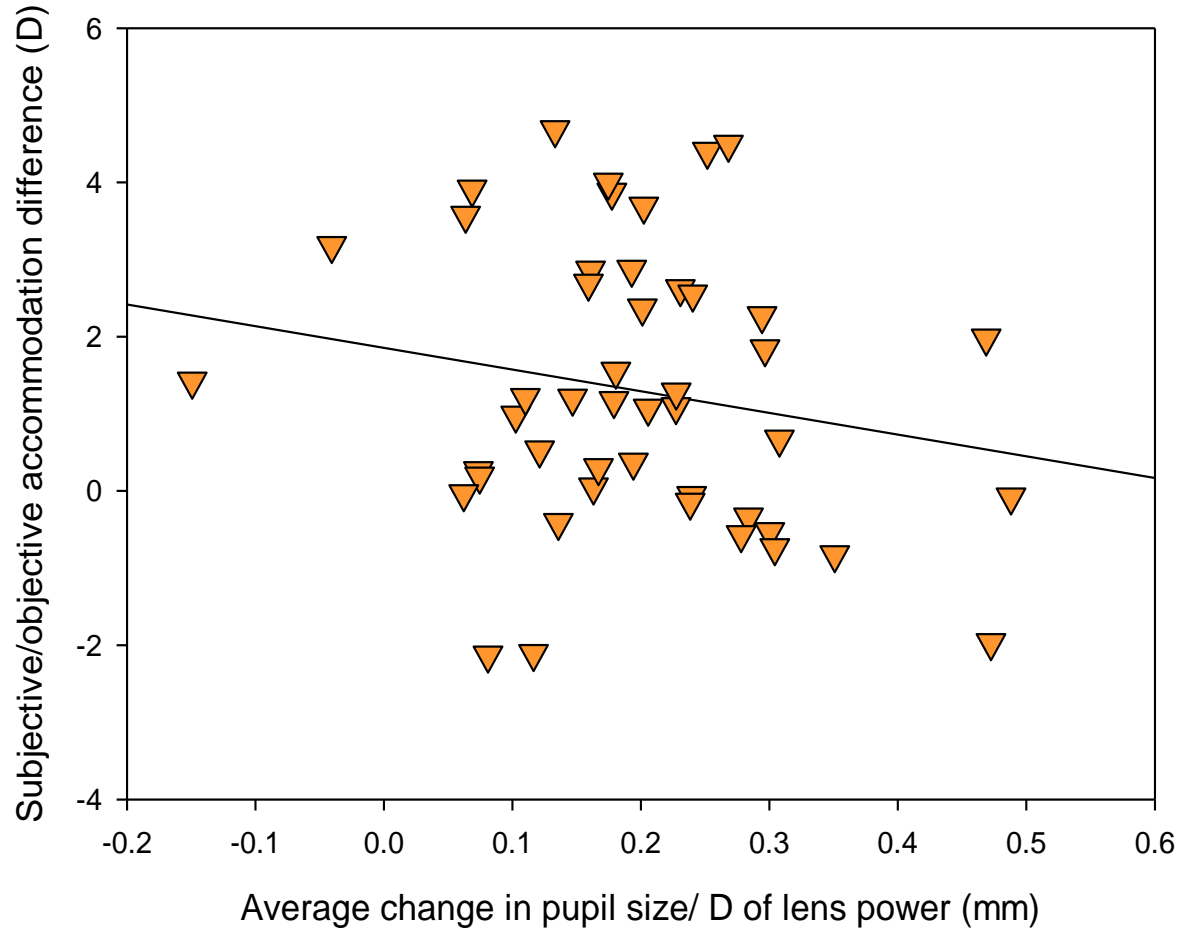
Figure 6.9: Difference between subjective and objective accommodation decreased as the average change in pupil size per dioptre of blur increased.

There was a statistically significant decrease (one way ANOVA: F=60.70, p<0.001) in

pupil size with lens induced defocus blur, as expected (figure 6.10).
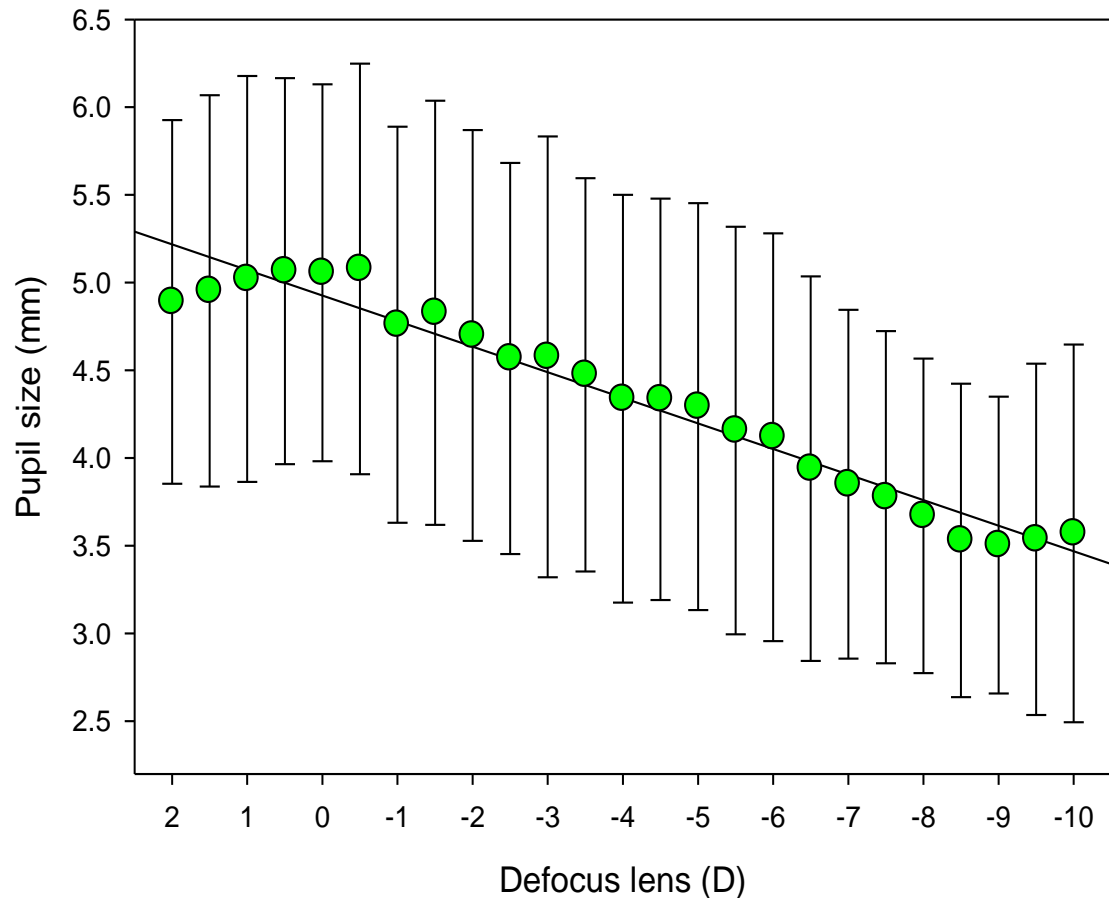
Figure 6.10: The pupil size with defocus lens is plotted here and shows that pupil miosis occurred with accommodative effort, which was an expected outcome.

6.10. Discussion

Cataract surgery involves removal of the cloudy natural crystalline lens and insertion of an artificial intraocular lens; a key goal of this surgery is for patients to attain spectacle independence post-operatively for distance vision, and a reduced reliance on spectacles for near and intermediate vision if implanted with a MIOL or AIOL. AIOLs are designed to increase the optical power of the eye by shifting within the capsular bag during near vision. However, many researchers have found there to be only a moderate benefit to near vision with these lenses (Wolffsohn *et al.*, 2006a;Wolffsohn *et al.*, 2006b;Cleary *et al.*, 2010;Sheppard *et al.*, 2010;Takakura *et al.*, 2010;Wolffsohn *et al.*, 2010b). It is hypothesised that only a limited amount of objective accommodation is needed to restore near visual function due to the eyes natural DOF. Therefore the objective of this study was to identify the key determinants of the subjective range of clear focus and to quantify their relative contribution to the difference between subjective and objective accommodation.

Blur tolerance was found to be the key factor driving subjective range of focus beyond objective measures in pre-presbyopes, with a greater tolerance to image blur linked to increased variability between subjective and objective measures. The dioptric effect of blur tolerance on increasing subjective range of accommodation should be evaluated and taken into consideration when selecting the optimum IOL design needed to overcome presbyopia for the patient. This study found a subjective DOF range of 8.60 ± 2.34D (absolute) compared to an objective DOF range of 8.02 ± 1.55D. This indicates an additional 0.58D of accommodative power is contributed principally as a result of the patient's ability to tolerate blur.

As anticipated, pupil size decreased with accommodative effort (one way ANOVA: $F=60.70$, $p<0.001$), however the absolute or change in pupil size was not found to be

an independent factor influencing the difference between subjective and objective accommodation in this study.

DOF has been found to increase with age and this is thought to occur due to a combination of pseudoaccommodative factors including pupil miosis, increased aberrations and an increased blur tolerance (Kline *et al.*, 1999b;McLellan *et al.*, 2001;Yi *et al.*, 2010;Atchison, 2012). In this study, subjects aged between 20 and 45 years were examined as residual accommodation was required and a positive correlation was found between age and the difference between subjective and objective accommodation ($p < 0.001$; figure 6.7). However, within this age group, there was no correlation between age and pupil size, aberrations or tolerance to blur ($p > 0.05$) suggesting other ageing factors may contribute, although this may have occurred due to the narrow age range of the subjects examined in this study.

It has been suggested that only one half of a person's amplitude of accommodation can be sustained for an extended period before CM fatigue manifests (Millodot *et al.*, 1989). However recent research has shown this value may be an underestimation. Wolffsohn *et al.* (2011b) found that up to 80% of accommodation could be used for prolonged near tasks without reports of asthenopia and without a reduction in the accuracy of objectively measured accommodation. Additionally, they noted an increase in this percentage with subject age and no evidence of a decrease in maximum accommodation level during prolonged tasks. This is in agreement with the findings of the present study which showed that the maximum accommodation level was maintained in most subjects beyond their point of blur, with only small fluctuations about the upper level (figure 6.8). This has implications for optimum MIOL selection since this, together with the effect of pseudo-accommodative factors such as blur tolerance, indicate that MIOLs may not need to provide such high levels of near

addition power to enable functional near vision. A stronger MIOL near addition power than required may in fact lead to patient dissatisfaction post-operatively, as this can produce a narrower range of clear vision (Wolffsohn *et al.*, 2011b). A study comparing visual acuity at different distances with a spherical MIOL with +4.00D add to aspheric MIOLs with a +4.00D add, a +3.75D add and a +3.00D found that all models produced good vision, however patients with the +3.00D add had statistically better corrected intermediate and near visual acuity than those with the other MIOLs (Alfonso *et al.*, 2010). Similar studies comparing outcomes with a +3.00D add MIOL to a +4.00D add MIOL have found the +3.00D IOL gave better intermediate vision than the +4.00D lens without compromising distance and near vision (Maxwell *et al.*, 2009;de Vries *et al.*, 2010;Santhiago *et al.*, 2010).

This is not the case for accommodating IOLs however. If on average 0.58D is contributed by blur tolerance, at a standard working distance of 33cm an additional 2.42D of power is required. If, as Wolffsohn *et al.* (2011b) suggests, around 80% of active focus can be used for sustained periods an AIOL would need to provide 3.00D of near power in order to provide this. Holladay (1993) investigated the effect of pseudophakic IOL movement on ocular power and stated a forward shift of 1.0mm of a posterior chamber IOL would effect a change in ocular refraction of approximately 1.90D. More recent studies measuring pseudophakic IOL shift have shown axial optic displacement of between 0.25mm and 1.0mm (Lesiewska-Junk *et al.*, 2000) which equates to between 0.3D and 1.9D of accommodating power (McLeod *et al.*, 2003). Langenbucher *et al.* (2003) used anterior chamber depth measurements together with data from Gullstrand's model eye to determine that forward movement of a single piece AIOL corresponded to a theoretical accommodating amplitude of between 1.13D and 1.40D. Similarly, Mcleod *et al.* (2003) found that a 1.0mm anterior displacement of a single optic IOL would produce a change in conjugate power of the eye of 1.2D, while a dual optic system would produce 2.2D of power for the same 1.0mm forward

movement. Thus providing 3.00D of accommodating power is beyond the theoretical limit of most hinge AIOLs and around the limit of dual optic AIOLs. Alternative options, such as shape changing IOLs (Fine *et al.*, 2007) which are reported to provide real accommodative restoration of as much as 8.00D (Alio Sanz *et al.*, 2008) may be more suitable. Having examined the factors affecting the range of clear focus in AIOLs, the next chapter explores how aberrometry might provide a more objective measure of the range of clear focus for MIOLs.

CHAPTER 7: Can Aberrometry Provide Rapid and Reliable Measures of Subjective Depth of Focus following Multifocal Intraocular Lens Implantation?

7.1. Evaluating Presbyopia correcting IOLs

7.1.1. Aberrometry

Surgical procedures such as cataract extraction and corneal refractive surgery necessitate deliberate modification of important ocular structures to improve or restore vision; however surgery in itself could be a potential source of superfluous ocular aberrations (Applegate *et al.*, 2003b;Chisholm *et al.*, 2003;Jimenez *et al.*, 2008). Measurement of a person's ocular aberrations after surgery can be used to provide an objective assessment of visual function (Ligabue *et al.*, 2009;Ravikumar, 2014).

There are two main categories of aberration: low and high order. Low order aberrations typically represent those aberrations which are correctable with spectacle or contact lenses whereas higher order aberrations (HOA), whose existence has been known for nearly 150 years, are generally lower in magnitude and not as easily corrected. The range of higher order aberrations that can occur in the human eye is extensive. It is generally accepted that no two people possess identical aberration profiles; instead every individual is thought to comprise both a unique pattern and quantity of different aberrations (Walsh *et al.*, 1984;Liang *et al.*, 1994;Liang *et al.*, 1997;Thibos *et al.*, 2002;Artal *et al.*, 2006;Piers *et al.*, 2007;Sawides *et al.*, 2011;Williams, 2011).

Ocular aberrations can be measured in a number of way including by comparing pairs of double pass retinal images and computing the wave aberration or more commonly, through the use of an aberrometer, as described later in this chapter and in more detail in the appendix (Vandenberg *et al.*, 1993;Liang *et al.*, 1997;Porter *et al.*, 2001;Kuroda *et al.*, 2002). Wavefront error maps are commonly used to convey information about

the pattern of aberrations present, and often incorporate colour to allow easier visual interpretation of the aberrometric information (Holladay, 2009;Ravikumar, 2014). In general, they are derived through the use of some form of topographic modelling system (Smolek *et al.*, 2007). However, such maps do not clearly describe which aberrations are present and in what quantity (Ravikumar, 2014).

The root mean square (RMS) wavefront error expresses the wavefront aberration more precisely since it provides a numerical value for the total amount of aberration present in that eye. However it does not specify the precise pattern of aberrations that constitute this total, which is a limitation since different aberrations tend to affect visual performance in distinctly different ways (Artal *et al.*, 2004;Sawides *et al.*, 2010). Hence two subjects with an identical total RMS wavefront error could have different visual experiences due to a disparity in the composition of each of their aberration profiles (Applegate *et al.*, 2002;Applegate *et al.*, 2003a;Charman, 2005).

To overcome this each wavefront aberration is arranged in terms of its Zernike polynomial. There are different indexing schemes for the Zernike polynomial sequence. As the polynomials depend on two parameters, their radial order and angular frequency, it is more convenient to arrange the polynomials in the form of a pyramid (Lakshminarayanan *et al.*, 2010). This allows all aberrations to be categorized precisely and the contribution of each aberration to the total RMS error to be determined (Applegate *et al.*, 2003a;Charman, 2005).

Zero and first order polynomials, which represent piston and prismatic tilt, do not affect image quality while second order modes describe spherical defocus and astigmatism, which are the most predominant type of aberration to occur in the general population and are amenable to sphero-cylindrical correction. Zernike polynomials of third order

and above are classified as higher order aberrations (Artal *et al.*, 2004;Charman, 2005;Lakshminarayanan *et al.*, 2010;Sawides *et al.*, 2011).

Visual performance is most commonly assessed using high contrast photopic assessment of visual acuity however on its own this provides an insufficient assessment of visual performance. The association between aberrations and visual performance is complex as some aberrations degrade visual quality more so than others and this formed the basis for the development of image quality metrics which are more highly correlated to measures of visual function (Ligabue *et al.*, 2009;Ravikumar, 2014).Visual quality metrics such as point spread function (PSF), modulation transfer function (MTF) and Strehl ratios can be used to assess visual performance and are discussed in more detail in the appendix.

The type of IOL implanted is important since IOL power, shape and refractive index can all affect aberrations. Taketani *et al.* (2005) established that IOLs with a higher refractive index were associated with a greater incidence of HOAs. They also found that a more posteriorly curved IOL was more effective in reducing glare and surface reflections when implanted. An equivalent anteriorly curved IOL was purported to show less spherical-like aberrations and was therefore recommended as the IOL of choice in patients with large pupils, such as children with congenital cataracts (Taketani *et al.*, 2005b).

7.1.2. Defocus curves

It is estimated that several million IOLs are routinely implanted into the eye following cataract extraction every year (Simpson, 1992). The range of clear vision achievable with different presbyopia correcting IOLs is most commonly evaluated using lengthy subjective defocus curves (Gupta *et al.*, 2008;Buckhurst *et al.*, 2012). Since MIOLs are designed to provide good vision at multiple distances this is reflected in their defocus

curve profiles as more than one peak of good acuity (Buckhurst *et al.*, 2012) and the depth and range of good acuity can indicate the strength of the presbyopic correction.

As summarised in chapter 6, depth of focus can be measured both objectively and subjectively and there is general agreement that subjective measures of accommodation tend to overestimate accommodation compared to objective measures (Marcos *et al.*, 1999b;Wold *et al.*, 2003;Wang *et al.*, 2006a;Wolffsohn *et al.*, 2006a;Vasudevan *et al.*, 2007;Win-Hall *et al.*, 2009). Subjective DOF may be influenced by a range of factors such as contrast, pupil size, higher order aberration, visual acuity, age, chromatic aberration, retinal eccentricity and target detail (Wang *et al.*, 2006a). In a previous study (chapter 6) we found that blur tolerance was a key factor driving subjective range of focus beyond objective measures in pre-presbyopes. Thus an objective defocus curve testing procedure would be preferable in allowing a more accurate assessment of near visual function to be obtained following implantation of a presbyopia correcting IOL.

Subjective defocus curve testing times can be prolonged and potentially tiring for the patient especially if there are numerous defocus lenses to be tested. Wolffsohn *et al.* (2013) investigated the effect of reducing the number of steps between defocus trial lenses on quality of results. They used trial lenses from +1.50 to -5.00D in the traditional 0.50D step size and compared this against 1.00D and 1.50D steps. Larger step sizes were found to produce distorted results indicating defocus step sizes cannot be increased in order to speed up testing time. As a result, it is often not possible to fully assess the visual capability of patients, for example under different levels of illumination as the optics in front of the pupil change, with subjectively measured defocus curves.

7.2. Study purpose

A faster defocus curve testing procedure would allow additional measurements to be conducted which could help improve our understanding of MIOLs. Objective measures of accommodation, such as aberrometry, tend to be quicker however there is a disparity between subjective and objective measures of accommodation. In the previous chapter we found this was largely attributed to blur tolerance, which accounted for approximately 0.60D of the difference. Taking this into account, this study will simultaneously measure objective and subjective defocus curves using the Aston aberrometer in order to determine whether reliable defocus curves can be predicted from faster objective through focus measurements in patients implanted with different types of presbyopia correcting IOL.

7.3. Method

Subjects (7 male, 17 females) aged between 46-79 years (mean age 62.9 ± 8.9 years) who had been successfully implanted with either the Oculentis Mplus segmented IOL(n=10), Tetraflex accommodating IOL (n=6) and a Rayner Mflex or Acrysof concentric ring design IOL (n=8) were recruited from Midland Eye, Solihull, UK.

To take part in this study, participants were required to:

- have corrected visual acuity in the eye being tested of at least 6/7.5
- be free of any active eye disease
- not currently taking ocular medications or systemic medications with known ocular side effects
- have had no history of ocular surgery within the previous 3 months
- Be willing to participate in the study.

All patients gave informed consent to take part in the study. The study adhered to the tenets of the Declaration of Helsinki and was approved by the Institutional Ethics Committee and the research conformed to the tenets of the Declaration of Helsinki. A breakdown of the subject demographics is detailed in Table 7.1.

IOL type	Segmented	Accommodating	Concentric
Age, years (mean ± SD)	60.7±9.3	56.5±6.5	69.3±5.4
Gender (F:M)	8:2	5:1	4:4

Table 7.1: Subject demographic for each IOL group.

The cataract extraction procedure was performed by the same experienced surgeon on all subjects using either topical or local anaesthetic. A 2.85mm clear corneal incision, widening to 3.2mm before IOL insertion, was positioned along the steepest corneal meridian to reduce residual postoperative astigmatism. Phacoemulsification, aspiration and irrigation were performed through a 5.5mm diameter curvilinear capsulorhexis using the Millennium phacoemulsification system (Bausch & Lomb). All presbyopia-correcting IOLs were then implanted in the capsular bag.

Subjects were invited to attend the Ophthalmic Research Group's laboratories a year after their surgery. A sphero-cylindrical refractive examination was conducted by the same UK-qualified optometrist (S.K.D) in which positive power was maximised whilst maintaining optimum distance vision in order to ensure subjects were wearing the most accurate distance prescription. A measurement of the best corrected visual acuity (VA) for each eye was taken at this point using a new digital test chart at four metres (Aston EyeTech, Birmingham, UK; Figure 7.3). Simultaneous monocular subjective and objective defocus curves were then measured using randomised trial lenses from +1.50 to -5.00DS in -0.50 steps. Objective measurements were taken using the miniaturized Aston open field Hartman-Shack aberrometer (Bhatt *et al.*, 2013) which

also measured pupil size and higher order aberrations (a combination of the patient's and the defocus inducing lens aberrations) at each level of defocus blur.

7.3.1. The Aston Aberrometer

The Aston open-field aberrometer is a miniaturized aberrometer designed to be slit-lamp mountable and based on the Hartmann-Shack principle (Bhatt *et al.*, 2013). A near infrared (840nm) super luminescent diode (SLD) beam of light is transmitted onto the retina and reflects back becoming aberrated by the optics of the eye on its return. The reflected beam of light is focused by a 47 by 47 lenslet array into 2209 spots and captured by a complementary-symmetry metal oxide semiconductor (CMOS) pixel camera (Micron Technology, Inc). The pattern and displacement of the reflected spots from the optical axis of each lenslet indicates the shape of the wavefront, which can be measured mathematically using Zernike coefficients. Zernike terms up to the 6th order are displayed in microns. A second CMOS sensor uses a 940nm light emitting diode (LED) to provide an image of the anterior eye which aids with alignment and pupil measurement. Beam-splitting dichroic prisms are positioned in the path of both incoming and returning light. Dichroic mirrors 1 and 2 (figure 7.1) allow visible light and certain bands of the infra red spectrum to pass through in order to aid viewing of the target and in anterior eye imaging. They reflect other bands of the near infrared light range for measurement and wavefront sensing purposes (Bhatt *et al.*, 2013).

Aston University

Illustration removed for copyright restrictions

*SHWS: Shack Hartmann wavefront sensor
**Light source 1 refers to the 840nm SLD needed for wavefront sensing
***Light source 2 to the 940nm LED required for imaging the anterior eye.

Figure 7.1: Schematic of the Aston aberrometer from (Bhatt *et al.*, 2013).

The Aston aberrometer can be attached to a slit lamp base (figure 7.2) and has an open-field and so can measure aberrations over a range of different focal distances (Bhatt *et al.*, 2013).

.
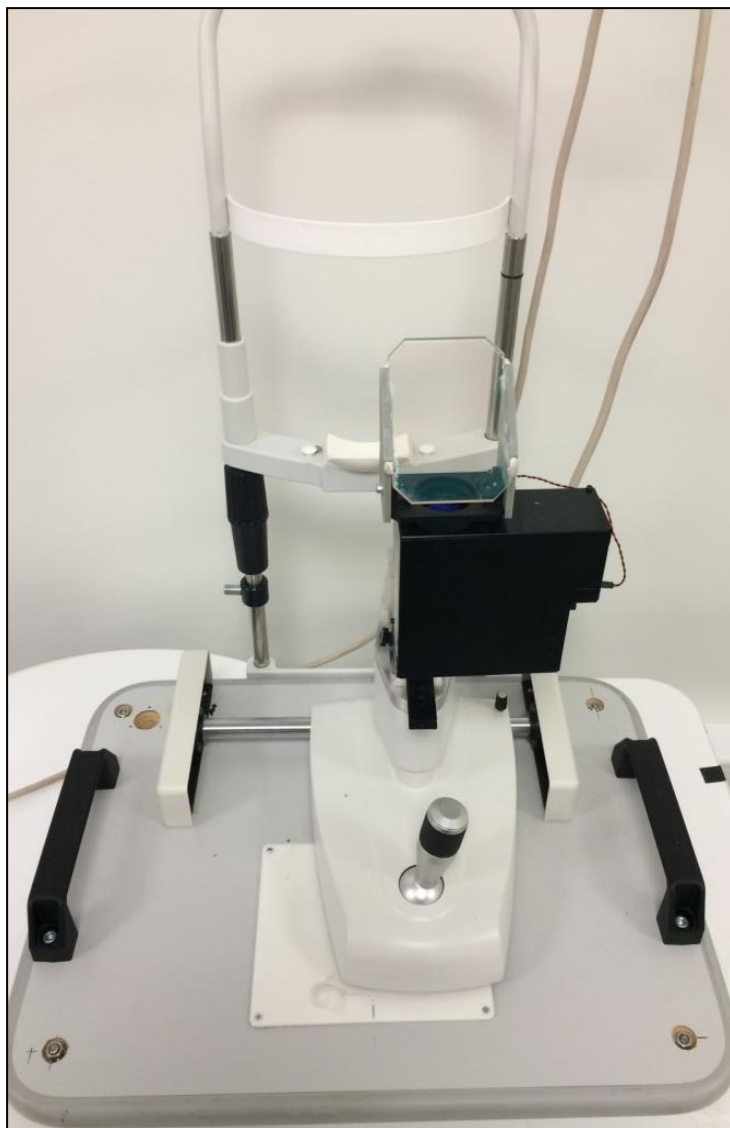
Figure 7.2: Aston aberrometer mounted on a slit lamp base.

Subjective DOF was measured by assessing best visual acuity with each defocus trial lens. The manifest refraction along with each defocus lens was placed in an Oculus Universal Trial Frame (Keeler Ltd., Windsor, UK) which had been adjusted to ensure trial lenses were held 12mm from the corneal plane. A new remote test chart application called the Aston EyeTech Ipad app was connected from the hand-held device to a 23 inch display screen placed four metres away using the Wi-Fi network (Figure 7.3). A digital logarithmic progression chart was projected onto this screen using the app which allowed letter randomisation to help overcome memory and learning effects.
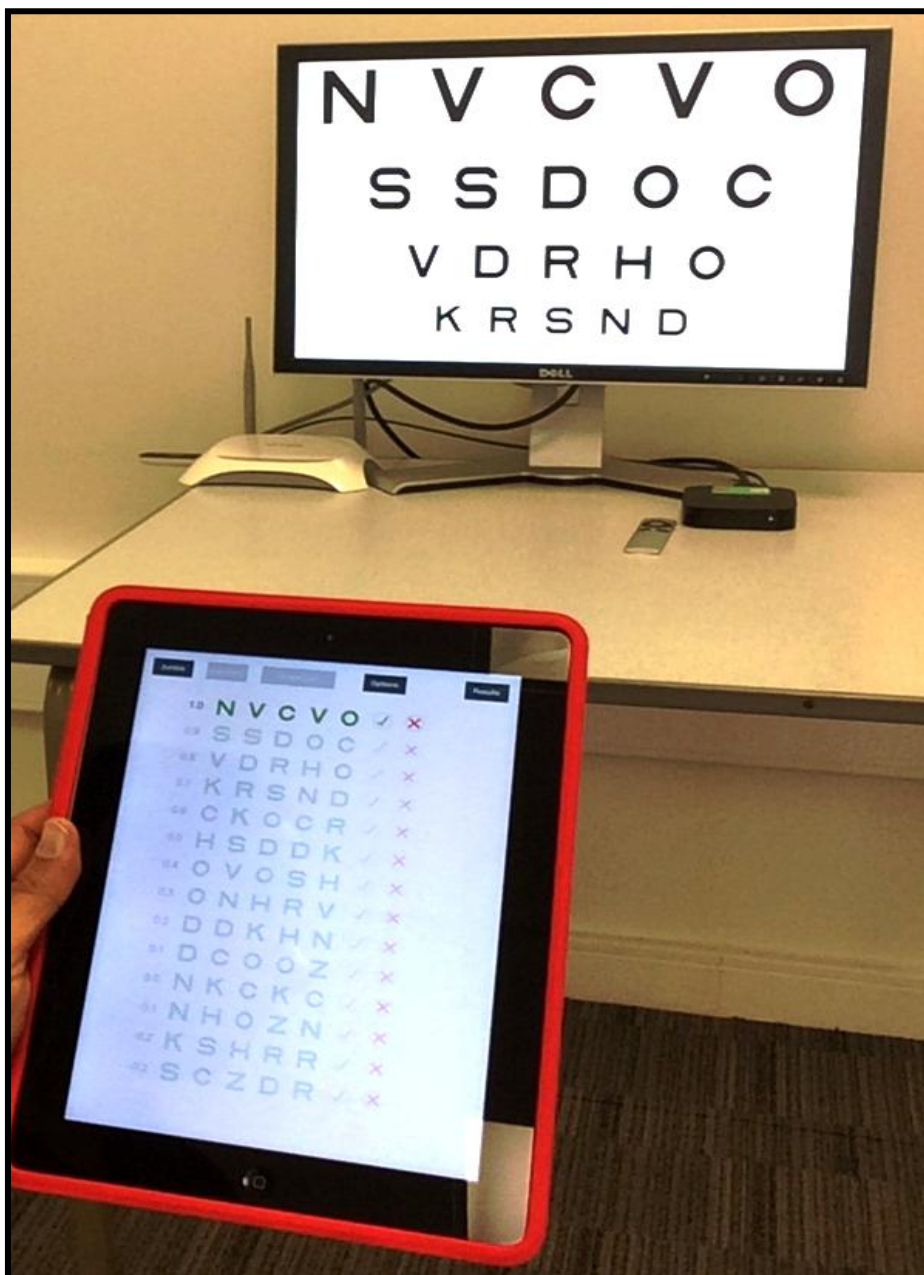
Figure 7.3: remote Ipad acuity application.

Letter sequences on the computerised test chart were randomised for each trial lens and subjects requested to read the lowest line on the test chart in order to obtain subjective DOF measurements. When they stopped reading they were asked if they could read any more letters on the line below to ensure the best visual acuity was

measured as recommended by Gupta *et al.* (2008). Each correctly read letter scored 0.02logMAR. The study set up is illustrated below (Figure 7.4).

Figure 7.4: Diagram illustrating the study set-up for the MIOL group. Defocus trial lenses in addition to the patient's prescription were housed in an Oculus trial frame 12mm from the corneal plane. Subjects viewed a distance logMAR chart at 4 meters through the aberrometer, which measured pupil size and HOAs at each defocus level simultaneously to the subjective measurement.

7.4. Statistical analysis

7.4.1. Testing for Normality

A one-sample Kolmogorov-Smirnov test was used to test for normality. Parametric analysis was used for normally distributed data and non-parametric tests for data that didn't follow a normal distribution (Armstrong *et al.*, 2011).

7.4.2. Analysis method

A one-sample Kolmogorov-Smirnov test revealed that the data was normally distributed (Kolmogorov-Smirnov $Z = 1.056$, $P=0.215$). A repeated measures ANOVA was conducted in SPSS version 21.0 (SPSS Inc., Chicago, USA) with post-hoc testing conducted using paired t-tests at each defocus level. Pearson's bivariate correlation coefficient was also conducted to investigate the correlation between the two measures for each MIOL. Predicted logMAR acuity was calculated using the LogVSX image quality metric.

7.4.2.1. LogVSX visual quality metric

Snellen acuity indicates the eyes ability to resolve detail and the recorded value for this is commonly used to measure a person's quality of vision. However this type of high contrast visual acuity assessment does not indicate the level of photic phenomena, such as halos and glare, that is experienced and so on its own provides an insufficient assessment of visual performance. Image quality metrics can provide a greater insight regarding visual function and thus may be more useful (Ligabue *et al.*, 2009). They can objectively predict optimum sphero-cylindrical correction (Thibos *et al.*, 2004;Martin *et al.*, 2011) as well as help improve the design of wavefront guided refractive corrections such as contact lenses and IOLs (Ravikumar, 2014).

VSX refers to the visual Strehl ratio computed in the spatial domain (Martin *et al.*, 2011) and takes into account optical components of visual processing, such as the effect of diffraction and wavefront aberrations, as well as neural effects and shares a linear relationship with logMAR acuity (Ravikumar *et al.*, 2011). It can be calculated from the optical transfer function (OTF) where the OTF is weighted by the neural contrast sensitivity function (CSFN) normalized to the diffraction-limited case (Thibos *et al.*, 2004;Ravikumar *et al.*, 2011) as shown in equation 7.1 (Ravikumar *et al.*, 2011).

$$\mathbf{LogVSX = log} \; \frac{\iint_{-\infty}^{\infty} \mathbf{CSF_N}\left(\mathbf{f_x, f_y}\right) \times \mathbf{OTF}\left(\mathbf{f_x, f_y}\right)\mathbf{df_x df_y}}{\iint_{-\infty}^{\infty} \mathbf{CSF_N}\left(\mathbf{f_x, f_y}\right) \times \mathbf{OTF_{DL}}\left(\mathbf{f_x, f_y}\right)\mathbf{df_x df_y}}$$

Equation 7.1

Where CSFN is the neural contrast sensitivity function, OTF is the measured optical transfer function and OTFDL is the diffraction-limited OTF.

Ravikumar *et al.* (2011) concluded that the LogVSX was a effective metric with numerous uses such as objectively assessing the likelihood of new intraocular lenses, designed to increase the depth of focus, producing noticeable blur to the patient. It was also determined that when optical errors are reduced, age does not significantly alter the correlation between change in logMAR acuity and change in LogVSX, which was thought to occur due to stability of the neural contrast sensitivity function, from which LogVSX is calculated. This was therefore believed to further indicate the efficacy of such objective visual quality metrics in predicting acuity over a large subject age range (Ravikumar, 2014).

Ravikumar *et al.* (2011) found that change in logMAR acuity was highly correlated with six image quality metrics, indicating the use of these metrics to objectively model acuity with refractive corrections such as IOLs. Cheng *et al.* (2004) stated that image quality

metrics which take into account the neural contrast sensitivity threshold, such as the VSX, are good predictors of visual acuity in through focus experiments. Therefore this, together with its strong reported correlation with logMAR (Cheng *et al.*, 2004;Marsack *et al.*, 2004;Thibos *et al.*, 2004;Ravikumar *et al.*, 2011;Shi *et al.*, 2013) was the reason why LogVSX was selected as the image quality metric with which to predict logMAR in this study. The relation between LogVSX and logMAR was presented by Ravikumar *et al.* (Ravikumar, 2014) and is defined as follows:

$$\text{LogMAR acuity} = -0.4029 \text{ x LogVSX} - 0.1579 \qquad \text{Equation 7.2}$$

7.4.3. Sample size calculation

Sample size for earlier studies that have investigated defocus curves in MIOL patients tend to vary with subject numbers ranging from 6 (Plakitsi *et al.*, 1995) to 60 and above (Buckhurst *et al.*, 2012). It is difficult to accurately calculate study sample sizes because of differences in defocus curve testing procedures and analysis as recognised by Buckhurst (2011). However, Armstrong and colleagues advised at least 15 degrees of freedom for repeated measure type statistics (Armstrong *et al.*, 2000), which was achieved.

7.5.   Results

Objectively measured predicted defocus curves for each IOL type are shown below in figure 7.5. Predicted acuity was optimal around plano, as expected, for all IOLs. There was a gradual reduction in acuity with increasing defocus lens power either side of plano. There appeared to be a slower deterioration in acuity between -3.00D and -4.50D for the concentric MIOL, around -3.00D for the Oculentis segmented MIOL and from -2.00D and -2.50D for the Tetraflex AIOL, signifying stimulation of the near portion of the presbyopia correcting IOLs.
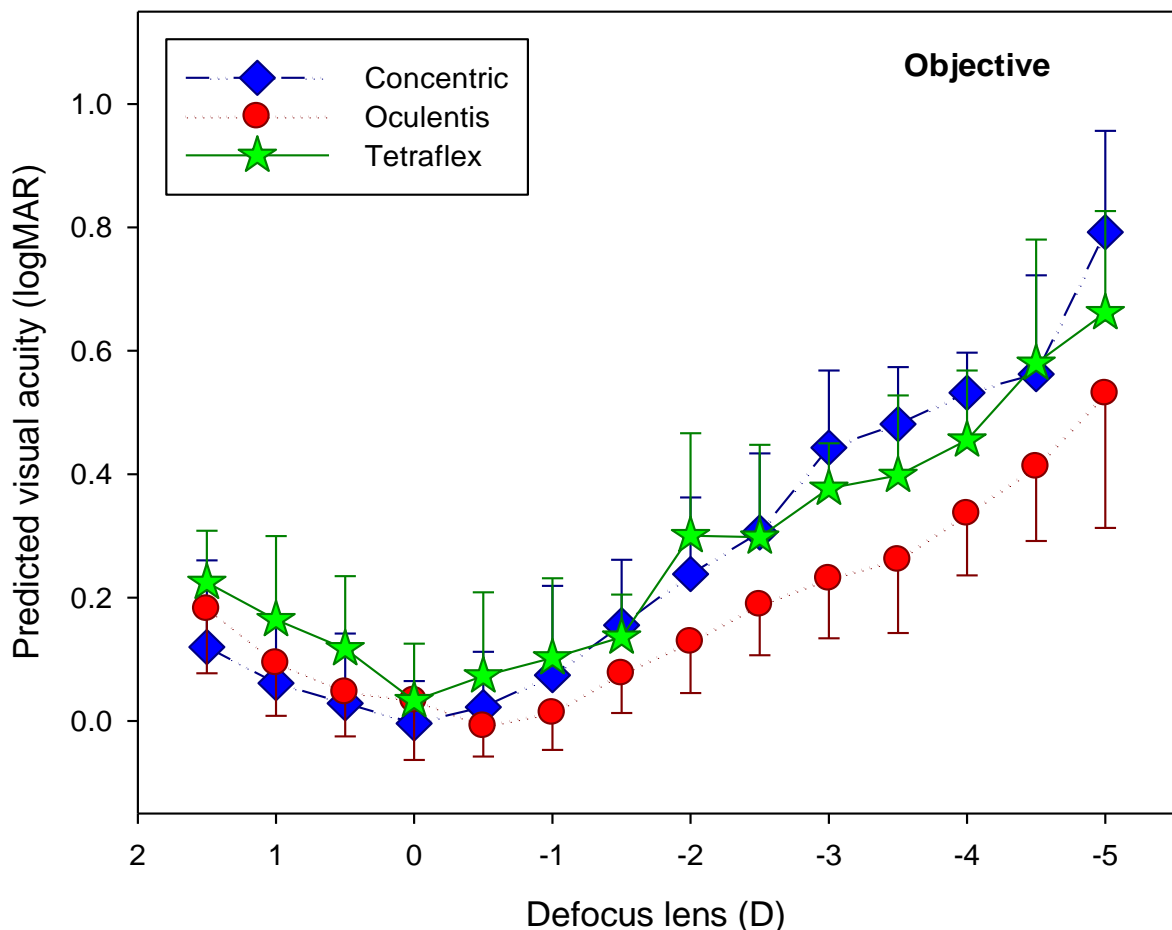
Figure 7.5: Average predicted defocus curves, measured using the Aston aberrometer, as a function of target vergences for lenses between +1.50DS and -5.00DS in 0.50 steps for patients implanted with the Oculentis segmented (n=10), Tetraflex accommodating IOL (n=6) and Concentric ring design IOL(n=8).

A more noticeable double dip occurred at the near point with subjectively measured defocus curves (figure 7.6), especially for the concentric (figure 7.7) and segmented IOLs (figure 7.8), indicating an overestimation of intermediation vision and underestimation of the near focusing ability with objective measures. This is not the case for the Tetraflex AIOL, which instead appears to perform better overall with objective compared to subjective measures (figure 7.9).
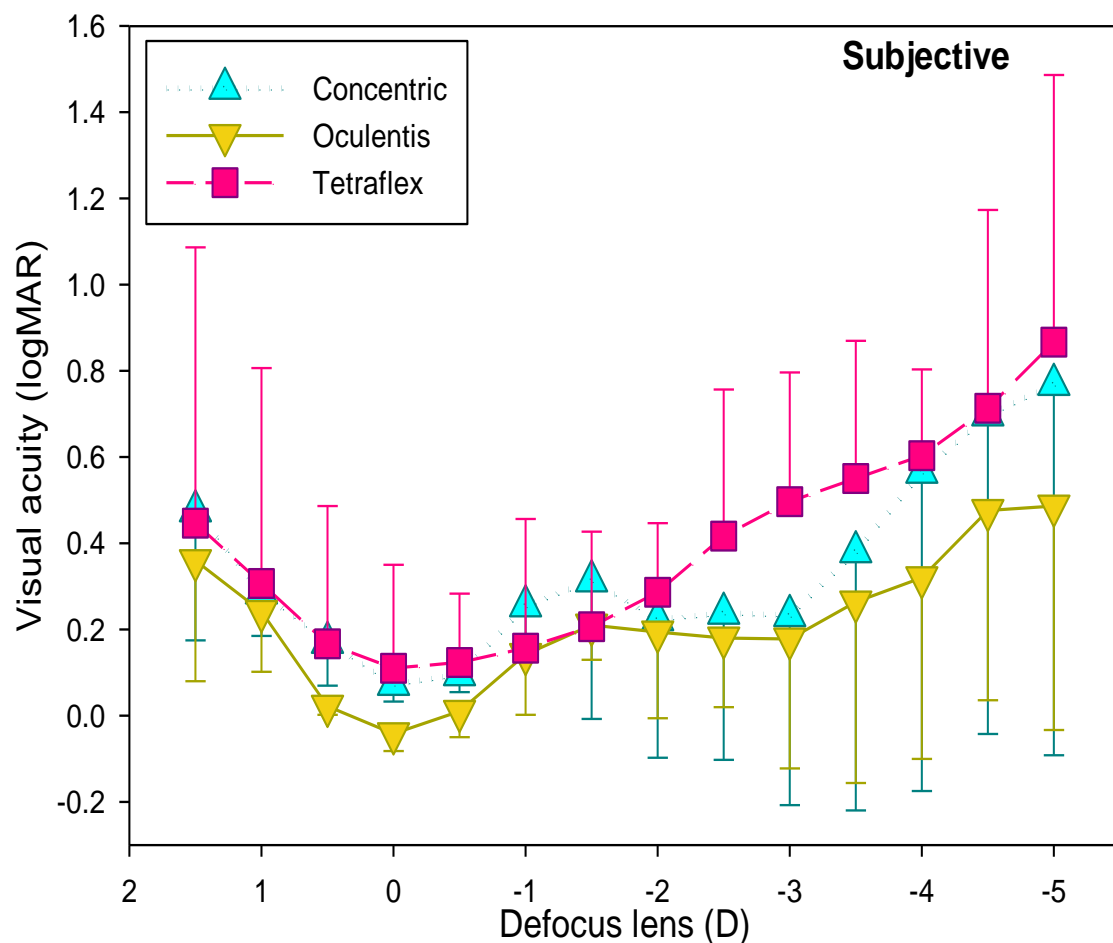
Figure 7.6: Subjectively measured defocus curves for lenses between +1.50DS to -5.00DS for each IOL design type.

A repeated measures ANOVA showed a difference in visual acuity between the three IOL types, (ANOVA F=15.506, P=0.001) and also between subjective and objective defocus curve measures (F=6.685, P=0.049). This was investigated further using a series of paired t-tests, which showed that on the whole subjective and objective

measures related well with each other for minus defocus lenses, with discrepancies mainly found between the two measures for positive defocus lenses. There was no statistically significant difference between subjective and objective defocus curves with lenses from +0.50DS to -5.00DS in the Oculentis segmented MIOL group (Paired t-test: p>0.05). A difference was found with this MIOL for +1.50DS (p= 0.022) and +1.00DS (p=0.017). Similarly there was no statistically significant difference between the two measures for lenses between +1.00DS and -5.00DS in the Tetraflex AIOL group (Paired t-test: p>0.05) with the only statistically significant difference found with a +1.50DS lens (p=0.018). For the concentric ring group, the two measures related well with each other for most lenses between -0.50DS and -5.00DS (p>0.05). A difference was found between subjective and objective measures at -1.00DS (p=0.010) and -3.00DS (p=0.015). There was again a discrepancy with positive defocus with differences found at +1.50DS (p=0.002), +1.00DS (p=0.002), +0.50DS (p=0.007) and plano (P=0.022).
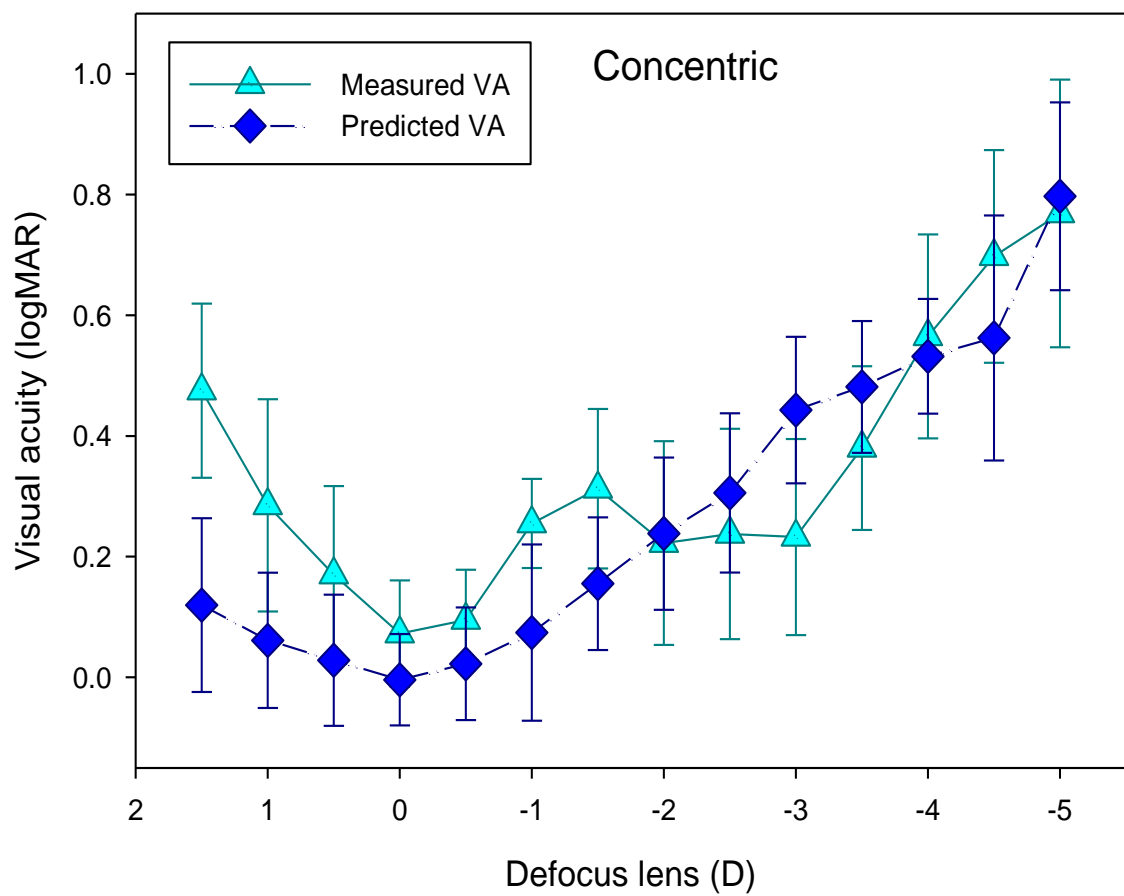
Figure 7.7: Predicted versus measured logMAR acuity with the concentric ring MIOL.
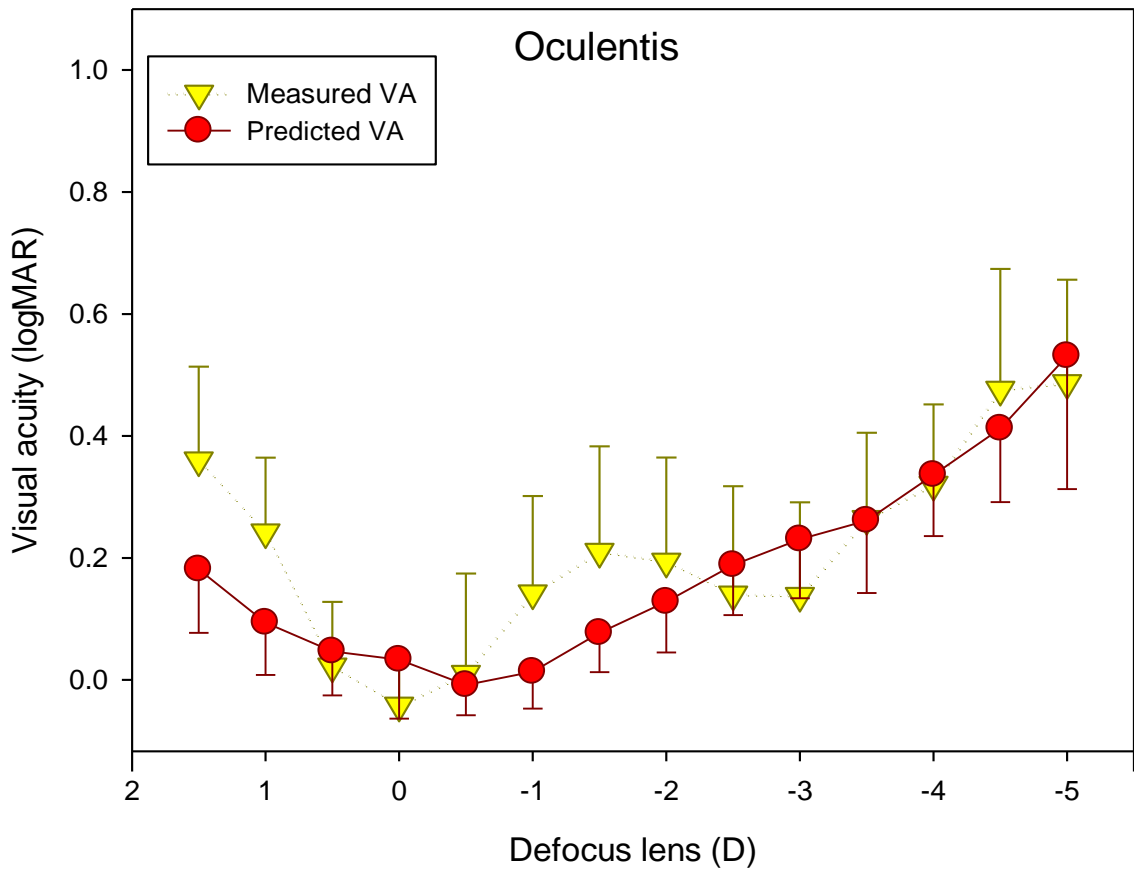
Figure 7.8: Predicted versus measured logMAR acuity for the Oculentis segmented lens.
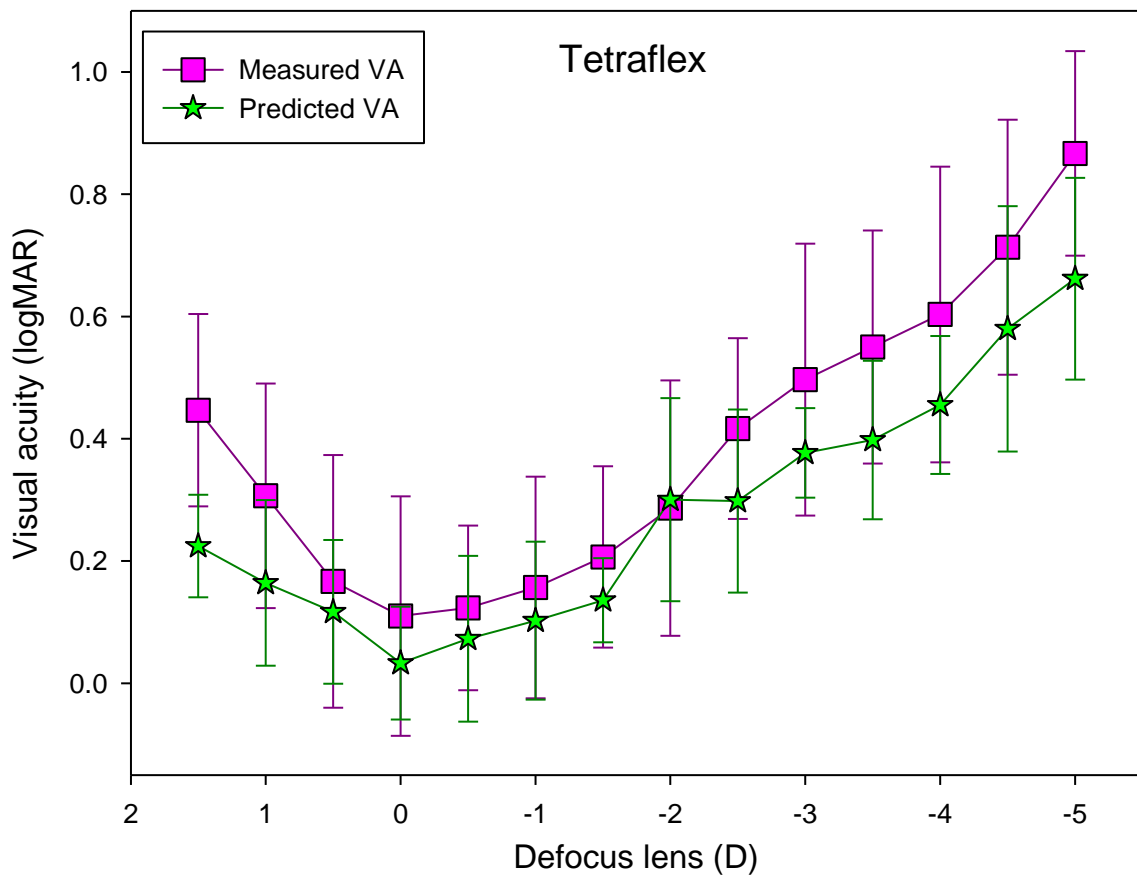
Figure 7.9: Predicted versus measured logMAR acuity for the Tetraflex AIOL.

Delta logMAR, which refers to the mean predicted acuity minus mean measured acuity, for all target vergences was -0.06 ± 0.21 logMAR. Therefore, on average across all defocus lenses and for all IOLs, the average predicted logMAR was three letters better than average measured acuity (figure 7.10).
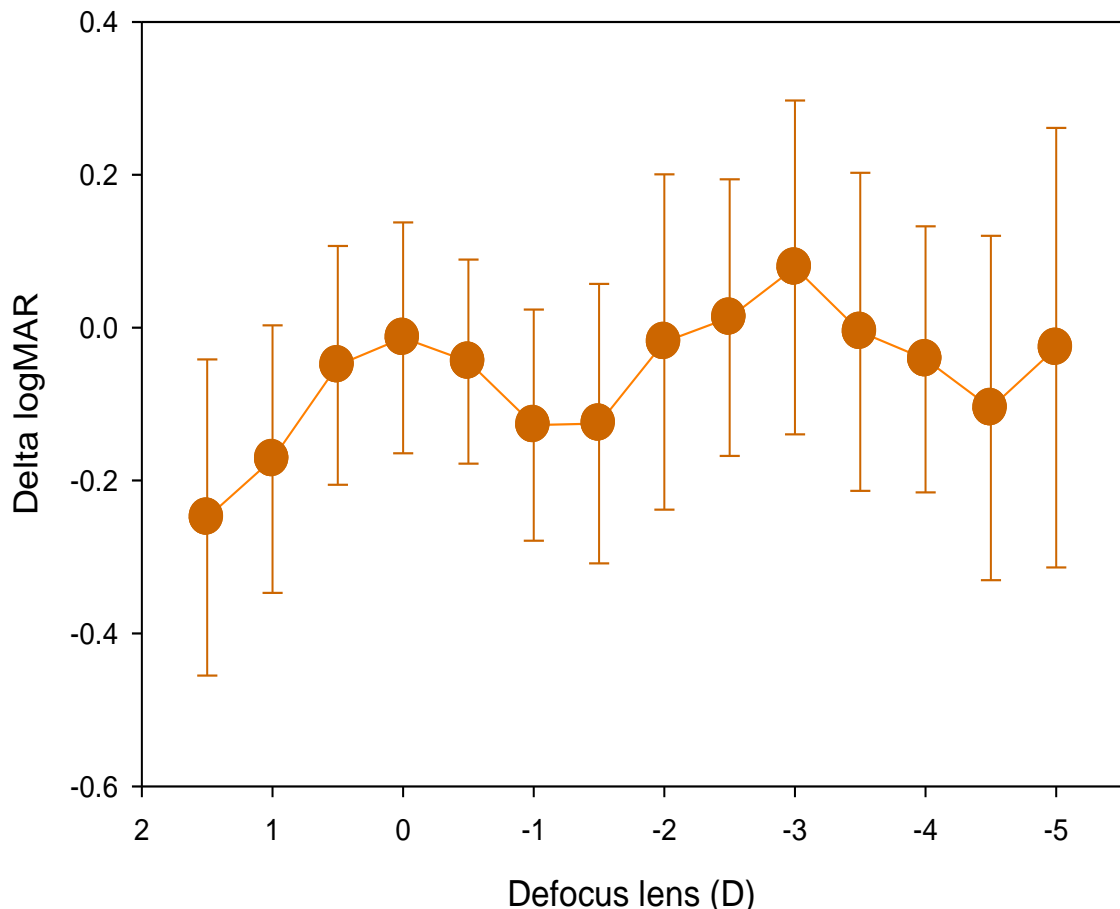
Figure 7.10: Mean Delta logMAR data (Predicted logMAR – Measured logMAR) for all IOLs, as a function of target vergences.

This can be reduced to 0.00 ± 0.22 logMAR by steepening the slope of the model used to predict acuity as follows:

$$\text{logMAR acuity} = -0.462 \times \text{LogVSX} - 0.1579 \qquad \text{Equation 7.4}$$

Ravikumar *et al.* (2014) used average data obtained from a cohort of largely young subjects with good visual acuity. Subjects participating in the present study were principally recruited from an older age range. Although the correlations between change in logMAR acuity and change in LogVSX were reported to remain true regardless of variation in starting acuity (Ravikumar, 2014), the slope of the model used to predict acuity could be adjusted to account for this difference in subject age range and is the subject of future research.

A strong positive correlation was found between measured and predicted logMAR for all three types of IOL (table 7.2, figure 7.11).

		Concentric objective	Oculentis objective	Tetraflex objective
Concentric subjective	**Pearson Correlation**	.812**	.906**	.861**
	Sig. (2-tailed)	.000	.000	.000
	N	14	14	14
Oculentis subjective	**Pearson Correlation**	.759**	.860**	.831**
	Sig. (2-tailed)	.002	.000	.000
	N	14	14	14
Tetraflex subjective	**Pearson Correlation**	.948**	.988**	.973**
	Sig. (2-tailed)	.000	.000	.000
	N	14	14	14

Table 7.2: Pearson's correlation between subjective and objective depth of focus measures for the three different presbyopia correcting IOL types.
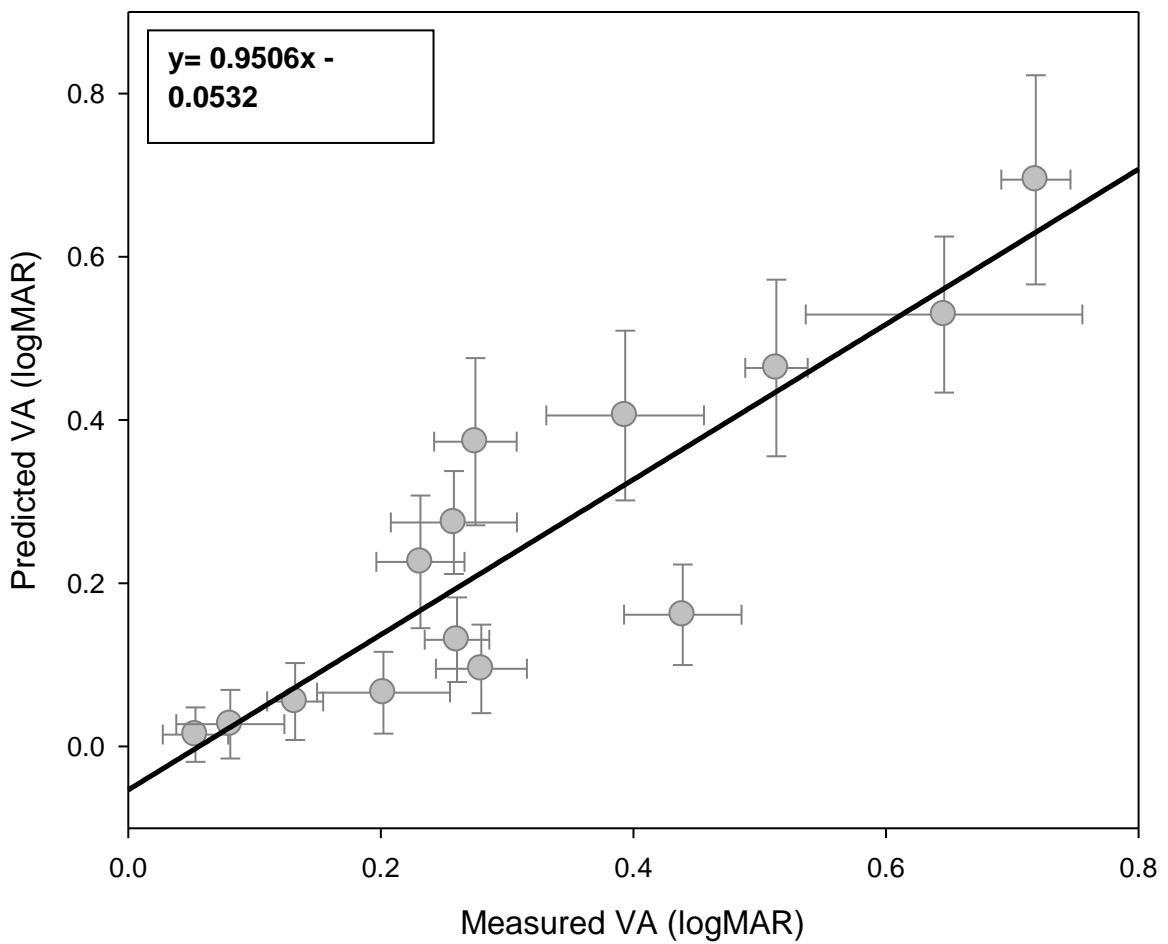
Figure 7.11: Predicted visual acuity as a function of measured acuity.

7.6.   Discussion

Simultaneous subjective and objective defocus curves were conducted in patients implanted with two different types of MIOL and an AIOL to determine whether objective defocus measurements can reliably predict patient clear range of focus, as measured by subjective visual acuity at different levels of defocus. Current subjective procedures are lengthy and do not enable important additional measures such as defocus curves under different luminance or contrast levels to be assessed. This, therefore, may limit our understanding of these advanced technology IOLs especially their performance in sub-optimal conditions. This is especially important since there is often a mismatch between the visual performances achievable in a relatively well-lit testing room compared to the real-world.

In general, the segmented MIOL wearers benefitted from better vision compared to the concentric ring and AIOL groups and this was true for both subjectively and objectively measured acuity (figure 7.5-7.6). Subjective defocus curves with MIOLs usually show a double dip corresponding to maximum visual acuity at distance and near vision (Maxwell *et al.*, 2009;Buckhurst *et al.*, 2012;Berrow *et al.*, 2014). For the concentric ring (figure 7.7) and segmented MIOLs (figure 7.8) this classic double dip was present, with maximum vision at 0D corresponding to optimal distance vision and around - 3.00D corresponding to near vision, for both lenses. As expected, there was no double dip in the subjective defocus curve with the AIOL (figure 7.9), which seemed to perform moderately better at intermediate distances. There is some evidence that there is a reduction in accommodative ability with AIOLs (Hancox *et al.*, 2006;Wolffsohn *et al.*, 2006b) as soon as six months post-implantation (Wolffsohn *et al.*, 2006b) and a high incidence of anterior and posterior capsule opacification (Mastropasqua *et al.*, 2007) which may have contributed to the comparative under-performance of this IOL type.

Paired t-tests showed that in general, subjective and objective measures related well with each other for minus defocus lenses, especially for the segmented MIOL and

AIOL, with discrepancies between the two measures mostly found with positive defocus. For the concentric ring design MIOL, objective measures over-estimated visual acuity compared to subjective measures at intermediate distances and under-estimated at near. While objectively predicted visual acuity and subjective measurement across a range of levels of defocus were strongly correlated (figure 7.11), the profile of the defocus curve was largely masked by the objective prediction of acuity. Hence objective measures cannot currently reliably predict patient clear range of focus as measured by subjective visual acuity at different levels of defocus. This could be due to the spot size of the aberrometer not detecting the multifocal optics of the lenses, although this seems unlikely with the dense array of the Aston aberrometer and the large area of the segment in the Oculentis IOL. The alternative is the metrics do not fully account for the neural factors, especially under blurred viewing conditions as they were developed to predict optimum refraction for clear vision. Hence future research will be needed to see whether these metrics can be further developed for this purpose.

CHAPTER 8: Conclusions

8.1. General conclusions

Premium IOLs can provide better visual outcomes compared to standard monofocal IOL designs leading to greater levels of spectacle independence and better vision post-operatively (Leyland *et al.*, 2003;Bi *et al.*, 2008;Alio *et al.*, 2011a;Ong *et al.*, 2014). The central experimental theme of the thesis has been to evaluate techniques to enhance the assessment of and visual performance with premium or advanced technology IOLs specifically toric, multifocal and accommodating IOLs.

The first part of the thesis concerned IOLs designed to correct astigmatism. Rotation of an implanted toric IOL can significantly diminish visual acuity therefore precise IOL alignment is vital to attaining good levels of vision in astigmats. The development of IOLs has evolved rapidly and new lens design features have been incorporated in order to minimise intracapsular rotation (Buckhurst *et al.*, 2010b;Ale *et al.*, 2012b). However it appears that toric IOL rotation is still an inevitable outcome, as studies have shown small amounts of rotation occur despite advances in current IOL designs. Thus an alternative avenue focussing on the development of an optical mechanism to increase the patient's ability to accept small amounts of rotation was instead proposed. A novel toric IOL design idea was devised and its potential to improve patient tolerance to toric IOL misalignment, without significantly detracting from distance visual acuity, was tested. The proposed idea involved splitting the astigmatic power of a toric IOL across both surfaces and misaligning their axes slightly. However, splitting toric power in this way was found to have no statistically significant improvement on visual acuity retention compared to a standard toric design. Toric IOL rotation is one of the main sources of patient dissatisfaction (Ale *et al.*, 2012b) especially with higher cylinder powers; a faster and larger drop in visual acuity was observed with lens rotation in this

study, as expected. Therefore compensating for the effect of lens rotation is crucial in order to maximise visual performance.

Like rotation, tilt can also decrease the effectiveness of an IOL and limit visual success post-operatively, although its visual impact is not reported to be as visually debilitating (Taketani *et al.*, 2004;Kumar *et al.*, 2011;Madrid-Costa *et al.*, 2012). Current methods of assessing lens tilt can be quite lengthy and require the use of specialist equipment. Therefore a new, faster and more cost-effective objective method of IOL tilt assessment was proposed using equipment that is readily accessible in the majority of optometry and ophthalmology clinics. This new method requires photographic assessment of an implanted IOL, followed by measurement of the width to height ratio of the central lens optic using imaging software. From this the angle of tilt can be solved using the cosine trigonometric function. The validity and repeatability of the technique was investigated *in vitro* using an IOL placed on a custom made stand and imaged using a high resolution digital camera. This technique was found to give accurate calculated tilt measurements and also shown to be highly repeatable.

While the link between IOL tilt and decentration has been studied in depth, the relationship between tilt, decentration and rotation is not so clear, therefore the next part of the thesis aimed to investigate this. An IOL was implanted and imaged digitally at set intervals after surgery. Tilt was assessed in this large cohort of patients using the new, objective tilt evaluation technique described earlier. Rotation was analysed from the position of the toric markings and lens decentration was measured in relation to the pupil. A link was anticipated between these three factors due to similarities in their potential cause, however linear regression analysis revealed a poor correlation between IOL tilt, decentration and rotation indicating they occur independently of each

other. The relationship between IOL tilt, rotation and tilt was examined with just one type of IOL design, a closed loop aspheric lens, and this may have limited our ability to fully investigate the association between these factors. Future studies will investigate the link between these IOL alignment factors with multiple different lens designs featuring varying haptics.

Hence the chapters in the first part of the thesis focussed on toric IOLs and showed the importance of correcting even low levels of corneal astigmatism in order to optimise vision. These investigations also demonstrated that objective analysis of digital retro-illumination images following surgery can allow IOL stability to be assessed relatively easily and precisely using standard ophthalmic equipment.

The remaining chapters examined the other principal form of premium IOLs, those designed to overcome presbyopia. The first of these investigated the distribution of light by the optics of different types of MIOL and an AIOL, in order to determine whether there were measureable differences in the retinal projection of light between these lenses. Visual field examination was performed using the Humphrey visual field analyzer in order to determine the efficacy of this test in identifying retinal threshold differences created as a result of the mechanism of action of each lens type. Depending on how test points were divided during the analysis, a difference in threshold loss in the superior section of the visual field could be detected using this technique. However this was not thought to be related to the IOL optics but instead attributed to natural differences in the function of the superior visual field compared to the inferior field (Previc, 1990;Danckert et al., 2003;Silva et al., 2008). Anticipated differences in perimetry thresholds between IOLs were not found. Therefore it was concluded that perimetry was not a useful technique with which to map and compare

the retinal projection of different presbyopia correcting IOLs in order to gain a greater insight into their mechanism of action and to inform optimal MIOL design.

The final part of the thesis examined the influence of pseudoaccommodative factors (Legge *et al.*, 1987;Atchison *et al.*, 1997;Ciuffreda *et al.*, 2007b), such as blur tolerance and higher order aberrations, on the observed difference between subjective and objective measures of accommodation (Marcos *et al.*, 1999b;Wold *et al.*, 2003;Macsai *et al.*, 2006;Wolffsohn *et al.*, 2006b) in order to ascertain how much additional objective power would be needed to restore the eye's focus with AIOLs. Blur tolerance was found to be the key factor driving subjective range of focus beyond objective measures in pre-presbyopes, with an approximate dioptric contribution of 0.60D. As anticipated, pupil size decreased with accommodative effort but was not found to be a key factor influencing the difference between subjective and objective accommodation. Axis shift AIOLs are designed to increase the optical power of the eye by moving within the capsular bag during near vision. However, many researchers have found there to be only a moderate benefit to near vision with these lenses (Wolffsohn *et al.*, 2006a;Wolffsohn *et al.*, 2006b;Cleary *et al.*, 2010;Sheppard *et al.*, 2010;Takakura *et al.*, 2010;Wolffsohn *et al.*, 2010b). Given blur tolerance contributes 0.60D, in order to provide adequate near focussing ability at a standard 33cm reading distance, 2.40D of additional power would be required. Given that Wolffsohn *et al.* (2011b) found approximately 80% of accommodation can be used for sustained near tasks, an AIOL would need to provide 3.00D of near power at this working distance, which is beyond the theoretical limit of most hinge AIOLs and around the limit of dual optic AIOLs. This therefore, may explain the observed underperformance of AIOLs at near compared to MIOLs.

Having examined the factors affecting the range of clear focus in AIOLs, the next chapter explored how aberrometry might provide a more objective measurement of the range of clear focus for MIOLs. Current subjective procedures are long and do not enable important additional measures to be undertaken such as defocus curves under different luminance or contrast levels which may limit our understanding of MIOLs. The use of faster objective techniques was thus examined. Simultaneous subjective and objective defocus curves were conducted in patients implanted with two different types of MIOL and an AIOL, to determine whether objective defocus curve measurements taken with an aberrometer, could reliably predict range of clear focus as compared to subjective measures. In general, although subjective and objective measures related well with each other, the peaks of the defocus curve profile of the two MIOLs was largely hidden in the objective prediction of acuity. Hence at present, objective measures are not able to reliably predict the range of clear focus as measured by subjective visual acuity at different defocus levels. This could be because the metrics do not fully account for the neural factors, as they were developed to predict optimum refraction in young observers with clear vision. Future research would therefore need to focus on developing these visual metrics further for this purpose.

8.2.   Main limitations

In the first study, the potential of a new split power toric IOL design in increasing patient tolerance to lens rotation was evaluated. High contrast visual acuity was used to measure visual performance in this study; however this test alone may not have been sufficient to detect subtle changes in vision with this novel design idea. Therefore additional studies incorporating a battery of visual assessment tests, including more sensitive measures of visual function such as low contrast visual acuity and reading speed (Watanabe *et al.*, 2013) may improve the ability to ascertain whether there is any visual benefit to a split surface design approach for toric correction. Another

limitation of this study was the absence of any trial frame verification techniques to ensure consistency in orientation of the trial frame and trial lenses, and so should be adopted for future studies.

The next chapter evaluated a new, simplified mathematical technique for measuring IOL tilt using more readily available ophthalmic equipment. Imaging software was used to calculate IOL measurements; however the objectivity of the technique could be improved by the development of an automated process to determine these IOL dimensions.

In the succeeding chapter, this new tilt evaluation technique was utilised to measure IOL tilt *in vivo*, in a large cohort of subjects. Good quality digital images are important in obtaining accurate and valid measurements of IOL position. Accurate set up of ophthalmic and imaging equipment as well as correctly directing the subject's gaze is therefore essential to prevent erroneous measurements. Use of reference markers to ensure consistent eye position during photography is recommended however as this is determined using subjective judgement there is potential for human error. Therefore development of an automated system to identify key anatomical features would be advantageous and further increase the objectivity of the new IOL tilt technique. The new method presented is also susceptible to the effects of corneal astigmatism, which if uncorrected, could make an imaged IOL appear more tilted than it truly is. Although the theoretical impact of uncorrected astigmatism on tilt error was estimated, no refractive information was available for the *in vivo* study which is a limitation of the study since true IOL tilt may have been masked to some extent. For the *in vivo* study, regression analysis showed that the majority of IOL tilt occurred within 48 hours of surgery however the study did not measure IOL position intra-operatively which may

be beneficial in future studies to further understand the mechanisms behind IOL mal-position.

The potential for perimetry to assess the retinal light projection through an implanted, advanced technology IOL was evaluated in chapter 5. In order to minimise patient fatigue due to the multiple testing required with distance and near correction, the SITA-fast strategy was selected. This calculates the threshold sensitivity of a primary point located in each of the four visual field quadrants using a double reversal strategy in order to predict the starting stimulus intensity of neighbouring test points, which are measured using a single reversal strategy (Bengtsson *et al.*, 1998a).It is ideally used on reliable patients; however given that subjects were older, SITA fast may not have been the most appropriate threshold testing strategy for this cohort. Such advanced technology IOLs consist of complex optics within a very small area and so small changes in head and eye position during testing could have affected testing accuracy. Head and eye position was monitored by the examiner using the internal camera; however the use of reference markers should perhaps have been employed to ensure consistency in head and eye position during testing.

The next chapter investigated the impact of pseudoaccommodation on driving subjective measures of accommodation beyond objective measures as it was envisaged that this information could help inform the level of additional objective power an AIOL would need in order to restore the eye's focus. It is difficult to accurately calculate study sample sizes because of differences in defocus curve testing procedures and analysis as recognised by Buckhurst (2011). The sample size in the present study, as well as in the next study, was relatively small and so larger sample sizes are recommended in future studies.

The final chapter explored whether aberrometry could provide accurate and repeatable objective measurement of the range of clear focus with MIOLs. However the prediction metrics used had been developed to predict optimum refraction in clear vision which may explain why they were not able to reliably predict the defocus curve profile. This was therefore a limitation of the study and future research will need to focus on further developing these visual metrics.

8.3. Concluding statement

The investigations detailed in the thesis have explored methods of improving visual performance with and assessment of premium IOLs. Toric IOLs are effective in correcting corneal astigmatism with generally good levels of patient satisfaction reported postoperatively (Ahmed *et al.*, 2010;Agresta *et al.*, 2012;Waltz *et al.*, 2014). However a potential complication of toric IOL implantation is lens misalignment which can reduce the effectiveness of the toric correction (Langenbucher *et al.*, 2009;Jin *et al.*, 2010;Kim *et al.*, 2010;Ale *et al.*, 2012a;Visser *et al.*, 2013). The development of innovative toric IOL design ideas aimed at enhancing the patient's ability to tolerate toric IOL rotation may be beneficial as small amounts of rotating motion are unavoidable with current toric IOLs.

The development of toric, multifocal and accommodating IOLs have provided surgeons with greater flexibility and given rise to the potential for patients to benefit from superior quality of vision compared to standard monofocal IOLs. However, to achieve optimum vision with premium IOLs, it is crucial for the lens to both attain and maintain a stable position within the capsular bag, which is not always the case.

While IOL designs have evolved rapidly in order to prevent misalignment of an implanted lens, the techniques used to assess IOLs have not progressed as rapidly. There is a need for faster objective methods of vision assessment with premium IOLs,

as this could provide greater insight into several aspects of their optical performance that are not yet fully understood, such as performance under different lighting conditions. These evaluations could provide useful information to help improve future lens designs and more crucially further enhance patient satisfaction post-operatively.

References

Aaron, M. T., Applegate, R. A., Porter, J., Thibos, L. N., Schallhorn, S. C., Brunstetter, T. J. and Tanzer, D. J. (2010). Why preoperative acuity predicts postoperative acuity in wavefront-guided LASIK. *Optometry and Vision Science.* **87,** 861-866.

Abrams, J., Nizam, A. and Carrasco, M. (2012). Isoeccentric locations are not equivalent: the extent of the vertical meridian asymmetry. *Vision Research.* **52,** 70-78.

Agresta, B., Knorz, M. C., Donatti, C. and Jackson, D. (2012). Visual acuity improvements after implantation of toric intraocular lenses in cataract patients with astigmatism: a systematic review. *BMC Ophthalmology.* **12,** 41.

Ahmed, I. I. K., Rocha, G., Slomovic, A. R., Climenhaga, H., Gohill, J., Gregoire, A. and Ma, J. (2010). Visual function and patient experience after bilateral implantation of toric intraocular lenses. *Journal of Cataract and Refractive Surgery.* **36,** 609-616.

Al-Ghoul, K. J., Nordgren, R. K., Kuszak, A. J., Freel, C. D., Costello, M. J. and Kuszak, J. R. (2001). Structural evidence of human nuclear fiber compaction as a function of ageing and cataractogenesis. *Experimental Eye Research.* **72,** 199-214.

Ale, J. B., Power, J., Zohs, K. and Cunningham, F. (2012a). Refractive and visual outcome of toric intraocular lens implantation following cataract surgery. *Nepalese Journal of Ophthalmology.* **4,** 37-44.

Ale, J. B., Power, J., Zohs, K. and Cunningham, F. (2012b). Refractive and visual outcome of toric intraocular lens implantation following cataract surgery. *Nepal J Ophthalmol.* **4,** 37-44.

Alfonso, J. F., Fernandez-Vega, L., Blazquez, J. I. and Montes-Mico, R. (2012). Visual function comparison of 2 aspheric multifocal intraocular lenses. *Journal of Cataract and Refractive Surgery.* **38,** 242-248.

Alfonso, J. F., Fernández-Vega, L., Puchades, C. and Montés-Micó, R. (2010). Intermediate visual function with different multifocal intraocular lens models. *Journal of Cataract and Refractive Surgery.* **36,** 733-739.

Alfonso, J. F., Fernandez-Vega, L., Valcarcel, B. and Montes-Mico, R. (2008). Visual performance after AcrySof ReSTOR aspheric intraocular lens implantation. *Journal of Optometry.* **1,** 30-35.

Alió, J. L., Ben-Nun, J., Rodríguez-Prats, J. L. and Plaza, A. B. (2009). Visual and accommodative outcomes 1 year after implantation of an accommodating intraocular lens based on a new concept. *Journal of Cataract and Refractive Surgery.* **35,** 1671-1678.

Alio, J. L., Pinero, D. P., Plaza-Puche, A. B. and Chan, M. J. (2011a). Visual outcomes and optical performance of a monofocal intraocular lens and a new-generation multifocal intraocular lens. *Journal of Cataract and Refractive Surgery.* **37,** 241-250.

Alió, J. L., Piñero, D. P., Tomás, J. and Plaza, A. B. (2011). Vector analysis of astigmatic changes after cataract surgery with implantation of a new toric multifocal intraocular lens. *Journal of Cataract and Refractive Surgery.* **37,** 1217-1229.

Alio, J. L., Plaza-Puche, A. B., Javaloy, J. and Ayala, M. J. (2012a). Comparison of the visual and intraocular optical performance of a refractive multifocal IOL with rotational asymmetry and an apodized diffractive multifocal IOL. *Journal of Refractive Surgery.* **28,** 100-105.

Alio, J. L., Plaza-Puche, A. B., Javaloy, J., Ayala, M. J., Moreno, L. J. and Pinero, D. P. (2012b). Comparison of a new refractive multifocal intraocular lens with an inferior segmental near add and a diffractive multifocal intraocular lens. *Ophthalmology.* **119,** 555-563.

Alió, J. L., Plaza-Puche, A. B., Montalban, R. and Ortega, P. (2012). Near visual outcomes with single-optic and dual-optic accommodating intraocular lenses. *Journal of Cataract and Refractive Surgery.* **38,** 1568-1575.

Alio, J. L., Plaza-Puche, A. B., Pinero, D. P., Javaloy, J. and Ayala, M. J. (2011b). Comparative analysis of the clinical outcomes with 2 multifocal intraocular lens models with rotational asymmetry. *Journal of Cataract and Refractive Surgery.* **37,** 1605-1614.

Alio Sanz, J. and Ben-Nun, J. (2008). Innovative IOL accommodative technologies: NuLens and TekClear. *Acta Ophthalmologica* **86,** 0.

Anderson, D. R. and Patella, M. V. 1992. *Automated static perimetry,* St. Louis, Mosby Year Book Inc.

Anderson, R. S., Mcdowell, D. R. and Ennis, F. A. (2001). Effect of localized defocus on detection thresholds for different sized targets in the fovea and periphery. *Acta Ophthalmologica Scandinavica.* **79,** 60-63.

Ang, R. E. T., Samano, A. a. J., Reyes, M. R. M. M. and Cruz, E. M. (2013). Incidence, Indications, and Outcomes of Yag Capsulotomy In Eyes Implanted with an Accommodating Intraocular Lens. *Philippine Journal of Ophthalmology.* **38,** 13-20.

Apple, D. J. and Sims, J. (1996). Harold Ridley and the Invention of the Intraocular lens. *Survey of Ophthalmology.* **40,** 279-292.

Applegate, R., Ballentine, C., Gross, H., Sarver, E. and Sarver, C. (2003a). Visual acuity as a function of Zernike mode and level of root mean square error. *American Academy of Ophthalmology.* **80,** 97-105.

Applegate, R., Marsack, J., Ramos, R. and Sarver, E. (2003b). Interaction betwen aberrations to improve or reduce visal performance. *Journal of Cataract and Refractive Surgery.* **29,** 1487-1495.

Applegate, R., Sarver, E. and Khemsara, V. (2002). Are all aberrations equal? *Journal of Refractive Surgery.* **18,** 556-562.

Applegate, R. A., Donnelly, W. J., Marsack, J. D., Koenig, D. E. and Pesudovs, K. (2007). Three-dimensional relationship between high-order root-mean-square

wavefront error, pupil diameter, and aging. *Journal of the Optical Society of America a-Optics Image Science and Vision.* **24,** 578-587.

Armstrong, R. A., Davies, L. N., Dunne, M. C. and Gilmartin, B. (2011). Statistical guidelines for clinical studies of human vision. *Ophthalmic and Physiological Optics.* **31,** 123-136.

Artal, P. (2000). Understanding aberrations by using double-pass techniques. *Journal of Refractive Surgery.* **16,** S560-S562.

Artal, P., Benito, A. and Tabernero, J. (2006). The human eye is an example of robust optical design. *Journal of Vision.* **6,** 1-7.

Artal, P., Berrio, E., Guirao, A. and Piers, P. (2002). Contribution of the cornea and internal surfaces to the change of ocular aberrations with age. *Journal of the Optical Society of America.* **19,** 137-143.

Artal, P., Chen, L., Fernandez, E. J., Singer, B., Manzanera, S. and Williams, D. R. (2004). Neural compensation for the eye's optical aberrations. *Journal of Vision.* **4,** 281-287.

Artal, P., Marcos, S., Navarro, R. and Williams, D. R. (1995). Odd aberrations and double-pass measurements of retinal image quality. *Journal of the Optical Society of America.* **12,** 195-201.

Artal, P. and Navarro, R. (1994). Monochromatic modulation transfer function of the human eye for different pupil diameters:an analytical expression. *Journal of the Optical Society of America.* **11,** 246-249.

Artal, P., Santamaria, J. and Bescos, J. (1988). Retrieval of wave aberration of human eyes from actual point spread function data. *Journal of the Optical Society of America.* **5,** 1201-1206.

Artes, P. H., Iwase, A., Ohno, Y., Kitazawa, Y. and Chauban, B. C. (2002). Properties of perimetric threshold estimates from full threshold, SITA standard, and SITA fast strategies. *Investigative Ophthalmology and Visual Science.* **43,** 2654-2659.

Asbell, P., Dualan, I., Mindel, J., Brocks, D., Ahmad, M. and Epstein, S. (2005). Age-related cataract. *The Lancet.* **365,** 599-609.

Aslam, S. A., Kashani, S., Jones, E. and Claoué, C. (2009). Pilot study and functional results following implantation of the M-flex 630F multifocal intraocular lens. *Journal of Cataract and Refractive Surgery.* **35,** 792.

Atchison, D. A. (1995). Accommodation and presbyopia. *Ophthalmic and Physiological Optics.* **15,** 255-272.

Atchison, D. A. (1996). Calculating relative retinal image sizes of eyes. *Ophthalmic and Physiological Optics.* **16,** 532-538.

Atchison, D. A. (2012). Depth of Focus of the Human Eye. *Presbyopia: Origin, Effects, and Treatment.* 21-28.

Atchison, D. A., Capper, E. J. and Mccabe, K. L. (1994). Critical subjective measurement of amplitude of accommodation. *Optometry and Vision Science.* **71,** 699-706.

Atchison, D. A., Charman, W. N. and Woods, R. L. (1997). Subjective depth-of-focus of the eye. *Optometry and Vision Science.* **74,** 511-520.

Atchison, D. A., Fisher, S. W., Pedersen, C. A. and Ridall, P. G. (2005). Noticeable, troublesome and objectionable limits of blur. *Vision Research.* **45,** 1967-1974.

Auran, J. D., Koester, C. J. and Donn, A. (1990). In vivo measurement of posterior chamber intraocular lens decentration and tilt. *Archives of Ophthalmology.* **108,** 75-79.

Aychoua, N., Junoy Montolio, F. G. and Jansonius, N. M. (2013). Influence of multifocal intraocular lenses on standard automated perimetry test results. *Journal of the American Medical Association Ophthalmology.* **131,** 481-485.

Bachernegg, A., Ruckl, T., Riha, W., Grabner, G. and Dexl, A. K. (2013). Rotational stability and visual outcome after implantation of a new toric intraocular lens for the correction of corneal astigmatism during cataract surgery. *Journal of Cataract and Refractive Surgery.* **39,** 1390-1398.

Bali, S. J., Hodge, C., Lawless, M., Roberts, T. V. and Sutton, G. (2012). Early experience with the femtosecond laser for cataract surgery. *Ophthalmology.* **119,** 891-899.

Barisic, A., Dekaris, I., Gabric, N., Bohac, M., Romac, I., Mravicic, I. and Lazic, R. (2008). Comparison of Diffractive and Refractive Multifocal Intraocular Lenses in Presbyopia Treatment. *Collegium Antropologicum.* **32,** 27-31.

Bauer, N. J., De Vries, N. E., Webers, C. A., Hendrikse, F. and Nuijts, R. M. (2008). Astigmatism management in cataract surgery with the AcrySof toric intraocular lens. *Journal of Cataract and Refractive Surgery.* **34,** 1483-1488.

Baumeister, M., Neidhardt, B., Strobel, J. and Kohnen, T. (2005). Tilt and decentration of three-piece foldable high-refractive silicone and hydrophobic acrylic intraocular lenses with 6-mm optics in an intraindividual comparison. *American Journal of Ophthalmology.* **140,** 1051-1058.

Bayramlar, H. H., Daglioglu, M. C. and Borazan, M. (2003). Limbal relaxing incisions for primary mixed astigmatism and mixed astigmatism after cataract surgery. *Journal of Cataract and Refractive Surgery.* **29,** 723-728.

Becker, K. A., Auffarth, G. U. and Volcker, H. E. (2004). Measurement method for the determination of rotation and decentration of intraocular lenses. *Ophthalmologe.* **101,** 600-603.

Ben-Nun, J. and Alió, J. L. (2005). Feasibility and development of a high-power real accommodating intraocular lens. *Journal of Cataract and Refractive Surgery.* **31,** 1802-1808.

Bengtsson, B. and Heijl, A. (1998a). SITA Fast, a new rapid perimetric threshold test. Description of methods and evaluation in patients with manifest and suspect glaucoma. *Acta Ophthalmologica Scandinavica.* **76,** 431-437.

Bengtsson, B. and Heijl, A. (1999). Comparing significance and magnitude of glaucomatous visual field defects using the SITA and Full Threshold strategies. *Acta Ophthalmologica Scandinavica.* **77,** 143-146.

Bengtsson, B., Heijl, A. and Olsson, J. (1998b). Evaluation of a new threshold visual field strategy, SITA, in normal subjects. *Acta Ophthalmologica Scandinavica.* **76,** 165-169.

Bengtsson, B., Olsson, J., Heijl, A. and Rootzen, H. (1997). A new generation of algorithms for computerized threshold perimetry, SITA. *Acta Ophthalmologica Scandinavica.* **75,** 368-375.

Bernal-Molina, P., Montés-Micó, R., Legras, R. and López-Gil, N. (2014). Depth-of-Field of the Accommodating Eye. *Optometry and Vision Science.* **91,** 1208-1214.

Berrio, E., Tabernero, J. and Artal, P. (2010). Optical aberrations and alignment of the eye with age. *Journal of Vision.* **10,** 34.

Berrow, E. J., Wolffsohn, J. S., Bilkhu, P. S. and Dhallu, S. (2014). Visual performance of a new bi-aspheric, segmented, asymmetric multifocal IOL. *Journal of Refractive Surgery.* **30,** 584-588.

Bhartiya, S., Sethi, S., Bhargava, S. and Lakhotia, S. (2009). History of intraocular lenses:Triumphs and Tribulations. *Delhi Journal of Ophthalmology.* **20,** 71-76.

Bhatt, U. K., Sheppard, A. L., Shah, S., Dua, H. S., Mihashi, T., Yamaguchi, T. and Wolffsohn, J. S. (2013). Design and validity of a miniaturized open-field aberrometer. *Journal of Cataract and Refractive Surgery.* **39,** 36-40.

Bhogal, G. and Wolffsohn, J. S. (2011). Intraocular lenses: A Review of Technolgical Developments and the Optometrist's Role. *Optometry in Practice.* **12,** 1-10.

Bi, H., Cui, Y., Ma, X., Cai, W., Wang, G., Ji, P. and Xie, X. (2008). Early clinical evaluation of AcrySof ReSTOR multifocal intraocular lens for treatment of cataract. *Ophthalmologica.* **222,** 11-16.

Biber, J. M., Sandoval, H. P., Trivedi, R. H., Fernández De Castro, L. E., French, J. W. and Solomon, K. D. (2009). Comparison of the incidence and visual significance of posterior capsule opacification between multifocal spherical, monofocal spherical, and monofocal aspheric intraocular lenses. *Journal of Cataract and Refractive Surgery.* **35,** 1234-1238.

Bland, J. M. and Altman, D. G. (1986). Statistical methods for assessing agreement between two methods of clinical measurement. *Lancet.* **1,** 307-310.

Bland, J. M. and Altman, D. G. (1999). Measuring agreement in method comparison studies. *Statistical methods in medical research.* **8,** 135-160.

Bogdan, N., Allison, R. and Suryakumar, R. (2010). Infrared Tracking of the Near Triad. *Journal of Vision* **10,** 507.

Bohorquez, V. and Alarcon, R. (2010). Long-term reading performance in patients with bilateral dual-optic accommodating intraocular lenses. *Journal of Cataract and Refractive Surgery.* **36,** 1880-1886.

Bradbury, J. A., Hillman, J. S. and Cassells-Brown, A. (1992). Optimal postoperative refraction for good unaided near and distance vision with monofocal intraocular lenses. *British Journal of Ophthalmology.* **76,** 300-302.

Brunette, I., Bueno, J. M., Parent, M., Hamam, H. and Simonet, P. (2003). Monochromatic aberrations as a function of age, from childhood to advanced age. *Investigative Ophthalmology and Visual Science.* **44,** 5438-5446.

Buckhurst, P. (2011). Evaluation of modern intraocular lenses. PhD thesis, Aston University, Birmingham, UK, Ch. 6, pp. 214-234.

Buckhurst, P. J., Wolffsohn, J. S., Davies, L. N. and Naroo, S. A. (2010a). Surgical correction of astigmatism during cataract surgery. *Clinical and Experimental Optometry.* **93,** 409-418.

Buckhurst, P. J., Wolffsohn, J. S., Naroo, S. A. and Davies, L. N. (2010b). Rotational and centration stability of an aspheric intraocular lens with a simulated toric design. *Journal of Cataract and Refractive Surgery.* **36,** 1523-1528.

Buckhurst, P. J., Wolffsohn, J. S., Naroo, S. A., Davies, L. N., Bhogal, G. K., Kipioti, A. and Shah, S. (2012). Multifocal Intraocular Lens Differentiation Using Defocus Curves. *Investigative Ophthalmology and Visual Science.* **53,** 3920-3926.

Bueno, J. M., Acosta, E., Schwarz, C. and Artal, P. (2010). Wavefront measurements of phase plates combining a point-diffraction interferometer and a Hartmann-Shack sensor. *Applied Optics.* **49,** 450-456.

Campbell, F. W. (1957). The depth of field of the human eye. *Optica Acta.* **4,** 157-164.

Cazal, J., Lavin-Dapena, C., Marín, J. and Vergés, C. (2005). Accommodative Intraocular Lens Tilting. *American Journal of Ophthalmology.* **140,** 341-344.

Cervino, A., Hosking, S. L., Ferrer-Blasco, T., Montes-Mico, R. and Gonzalez-Meijome, J. M. (2008). A pilot study on the differences in wavefront aberrations between two ethnic groups of young generally myopic subjects. *Ophthalmic Physiol Opt.* **28,** 532-537.

Cezon Prieto, J. and Bautista, M. J. (2010). Visual outcomes after implantation of a refractive multifocal intraocular lens with a +3.00 D addition. *Journal of Cataract and Refractive Surgery.* **36,** 1508-1516.

Chandra Sekhar, G., Naduvilath, T. J., Lakkai, M., Jayakumar, J., Thanga Pandi, G., Mandal, A. K. and Honavar, S. G. (2000). Sensitivity of Swedish Interactive Threshold Algortihm compared with standard full threshold algorithm in Humphrey visual field testing. *American Academy of Ophthalmology.* **107,** 1303-1308.

Chang, D. F., Dell, S. J., Hill, W. E., Lindstrom, R. L. and Waltz, K. L. (eds.) 2008. *Mastering refractive IOLs: the art and science,* U.S.A: SLACK Incorporated.

Chang, Y., Wu, H. M. and Lin, Y. F. (2007). The axial misalignment between ocular lens and cornea observed by MRI (I) - At fixed accommodative state. *Vision Research.* **47,** 71-84.

Charbel Issa, P., Helb, H. M., Rohrschneider, K., Holz, F. G. and Scholl, H. P. (2007). Microperimetric assessment of patients with type 2 idiopathic macular telangiectasia. *Investigative Ophthalmology and Visual Science.* **48,** 3788-3795.

Charman, W. N. (2005). Wavefront technology:Past, present and future. *British Contact Lens Association.* **28,** 75-92.

Charman, W. N. (2008). The eye in focus: accommodation and presbyopia. *Clinical and Experimental Optometry.* **91,** 207-225.

Charman, W. N. (2014). Developments in the correction of presbyopia II: surgical approaches. *Ophthalmic and Physiological Optics.* **34,** 397-426.

Chauhan, B. C., House, P. H., Mccormick, T. A. and Leblanc, R. P. (1999). Comparison of conventional and high-pass resolution perimetry in a prospective study of patients with glaucoma and healthy controls. *Archives of Ophthalmology.* **117,** 24-33.

Cheng, X., Bradley, A. and Thibos, L. N. (2004). Predicting subjective judgment of best focus with objective image quality metrics. *Journal of Vision.* **4,** 310-321.

Cheng, X., Himebaugh, N. L., Kollbaum, P. S., Thibos, L. N. and Bradley, A. (2003). Validation of a clinical Shack-Hartmann aberrometer. *Optometry and Vision Science.* **80,** 587-595.

Chernyak, D. A. (2004). Cyclotorsional eye motion occurring between wavefront measurement and refractive surgery. *Journal of Cataract and Refractive Surgery.* **30,** 633-638.

Chiam, P. J. T., Chan, J. H., Haider, S. I., Karia, N., Kasaby, H. and Aggarwal, R. K. (2007). Functional vision with bilateral ReZoom and ReSTOR intraocular lenses 6 months after cataract surgery. *Journal of Cataract and Refractive Surgery.* **33,** 2057-2061.

Chisholm, C. M., Evans, A. D. B., Harlow, J. A. and Barbur, J. L. (2003). New test to assess pilot's vision following refractive surgery. *Aviation, Space and Environmental Medicine.* **74,** 551-559.

Ciuffreda, K. J., Wang, B. and Vasudevan, B. (2007a). Conceptual model of human blur perception. *Vision Research.* **47,** 1245-1252.

Ciuffreda, K. J., Wang, B. and Vasudevan, B. (2007b). Depth-of-focus: control system implications. *Computers in Biology and Medicine.* **37,** 919-923.

Cleary, G., Spalton, D. J. and Marshall, J. (2010). Pilot study of new focus-shift accommodating intraocular lens. *Journal of Cataract and Refractive Surgery.* **36,** 762-770.

Conrad-Hengerer, I., Al Juburi, M., Schultz, T., Hengerer, F. H. and Dick, H. B. (2013). Corneal endothelial cell loss and corneal thickness in conventional compared

with femtosecond laser-assisted cataract surgery: three-month follow-up. *Journal of Cataract and Refractive Surgery.* **39,** 1307-1313.

Coppens, J. E., Van Den Berg, T. J. T. P. and Budo, C. J. (2005). Biometry of phakic intraocular lens using Scheimpflug photography. *Journal of Cataract and Refractive Surgery.* **31,** 1904-1914.

Crnej, A., Hirnschall, N., Nishi, Y., Gangwani, V., Tabernero, J., Artal, P. and Findl, O. (2011). Impact of intraocular lens haptic design and orientation on decentration and tilt. *Journal of Cataract and Refractive Surgery.* **37,** 1768-1774.

Crossland, M., Jackson, M.-L. and Seiple, W. H. (2012). Microperimetry: a review of fundus related perimetry. *Optometry Reports.* **2,** 11-15.

Cufflin, M. P., Mankowska, A. and Mallen, E. A. (2007). Effect of blur adaptation on blur sensitivity and discrimination in emmetropes and myopes. *Investigative Ophthalmology and Visual Science.* **48,** 2932-2939.

Cumming, J. S. (1993). Postoperative complications and uncorrected acuities after implantation of plate haptic silicone and three-piece silicone intraocular lenses. *Journal of Cataract and Refractive Surgery.* **19,** 263-274.

Cumming, J. S. and Kammann, J. (1996). Experience with an accommodating IOL. *Journal of Cataract and Refractive Surgery.* **22,** 1001.

Curcio, C. A. and Allen, K. A. (1990). Topography of ganglion cells in human retina. *Journal of Comparative Neurology.* **300,** 5-25.

Danckert, J. A. and Goodale, M. A. (2003). Ups and downs in the visual control of action. *Taking action: Cognitive neuroscience perspectives on intentional acts.* 29-64.

Davison, J. A. (2000). Positive and negative dysphotopsia in patients with acrylic intraocular lenses. *Journal of Cataract and Refractive Surgery.* **26,** 1346-1355.

Davison, J. A. and Simpson, M. J. (2006). History and development of the apodized diffractive intraocular lens. *Journal of Cataract and Refractive Surgery.* **32,** 849-858.

De Castro, A., Rosales, P. and Marcos, S. (2007). Tilt and decentration of intraocular lenses in vivo from Purkinje and Scheimpflug imaging. Validation study. *Journal of Cataract and Refractive Surgery.* **33,** 418-429.

De Silva, S. R., Riaz, Y. and Evans, J. R. (2014). Phacoemulsification with posterior chamber intraocular lens versus extracapsular cataract extraction (ECCE) with posterior chamber intraocular lens for age-related cataract. *Cochrane Database of Systematic Reviews.* **1**.

De Vries, N. E., Webers, C. a. B., Montés-Micó, R., Ferrer-Blasco, T. and Nuijts, R. M. M. A. (2010). Visual outcomes after cataract surgery with implantation of a +3.00 D or +4.00 D aspheric diffractive multifocal intraocular lens: Comparative study. *Journal of Cataract and Refractive Surgery.* **36,** 1316-1322.

Diaz-Douton, F., Benito, A., Pujol, J., Arjona, M., Guell, J. L. and Artal, P. (2006). Comparison of the retinal image quality with a Hartmann-Shack wavefront

sensor and a double-pass instrument. *Investigative Ophthalmology and Visual Science.* **47,** 1710-1716.

Dirani, M., Chamberlain, M., Couper, T. A., Guymer, R. H. and Baird, P. N. (2009). Role of genetic factors in lower- and higher-order aberrations--the genes in myopia twin study. *Ophthalmic Research.* **41,** 142-147.

Donaldson, K. E., Braga-Mele, R., Cabot, F., Davidson, R., Dhaliwal, D. K., Hamilton, R., Jackson, M., Patterson, L., Stonecipher, K. and Yoo, S. H. (2013). Femtosecond laser-assisted cataract surgery. *Journal of Cataract and Refractive Surgery.* **39,** 1753-1763.

Duane, A. (1925). Are the current theories of accommodation correct? *American Journal of Ophthalmology.* **8,** 196-202.

Dubbelman, M., Van Der Heijde, G. L. and Weeber, H. A. (2001). The thickness of the aging human lens obtained from corrected Scheimpflug images. *Optometry and Vision Science.* **78,** 411-416.

Dunne, M. C., Davies, L. N. and Wolffsohn, J. S. (2007). Accuracy of cornea and lens biometry using anterior segment optical coherence tomography. *Journal of Biomedical Optics.* **12,** 064023.

Durak, A., Oner, H. F., Kocak, N. and Kaynak, S. (2001). Tilt and decentration after primary and secondary transsclerally sutured posterior chamber intraocular lens implantation. *Journal of Cataract and Refractive Surgery.* **27,** 227-232.

El-Maghraby, A., Marzouky, A., Gazayerli, E., Van Der Karr, M. and Deluca, M. (1992). Multifocal versus monofocal intraocular lenses. Visual and refractive comparisons. *Journal of Cataract and Refractive Surgery.* **18,** 147-152.

Elgohary, M. A. and Beckingsale, A. B. (2008). Effect of posterior capsular opacification on visual function in patients with monofocal and multifocal intraocular lenses. *Eye (Lond).* **22,** 613-619.

Eppig, T., Scholz, K., Loffler, A., Messner, A. and Langenbucher, A. (2009). Effect of decentration and tilt on the image quality of aspheric intraocular lens designs in a model eye. *Journal of Cataract and Refractive Surgery.* **35,** 1091-1100.

Ferreira, T. B., Marques, E. F., Rodrigues, A. and Montés-Micó, R. (2013). Visual and optical outcomes of a diffractive multifocal toric intraocular lens. *Journal of Cataract and Refractive Surgery.* **39,** 1029-1035.

Ferrer-Blasco, T., Montés-Micó, R., Peixoto-De-Matos, S. C., González-Méijome, J. M. and Cerviño, A. (2009). Prevalence of corneal astigmatism before cataract surgery. *Journal of Cataract and Refractive Surgery.* **35,** 70-75.

Filkorn, T., Kovacs, I., Takacs, A., Horvath, E., Knorz, M. C. and Nagy, Z. Z. (2012). Comparison of IOL power calculation and refractive outcome after laser refractive cataract surgery with a femtosecond laser versus conventional phacoemulsification. *Journal of Refractive Surgery.* **28,** 540-544.

Findl, O., Hirnschall, N., Nishi, Y., Maurino, V. and Crnej, A. (2015). Capsular bag performance of a hydrophobic acrylic 1-piece intraocular lens. *Journal of Cataract and Refractive Surgery.* **41,** 90-97.

Fine, I. H., Hoffman, R. S. and Packer, M. (2007). Refractive lens exchange: the quadruple win and current perspectives. *Journal of Refractive Surgery.* **23,** 819-824.

Fledelius, H. C. and Stubgaard, M. (1986). Changes in refraction and corneal curvature during growth and adult life. A cross-sectional study. *Acta Ophthalmologica.* **64,** 487-491.

Ford, J., Werner, L. and Mamalis, N. (2014). Adjustable intraocular lens power technology. *Journal of Cataract and Refractive Surgery.* **40,** 1205-1223.

Frisen, L. (1993). High-pass resolution perimetry. A clinical review. *Documenta Ophthalmologica.* **83,** 1-25.

Fujikado, T., Kuroda, T., Ninomiya, S., Maeda, N., Tano, Y., Oshika, T., Hirohara, Y. and Mihashi, T. (2004). Age-related changes in ocular and corneal aberrations. *American Journal of Ophthalmology.* **138,** 143-146.

Fujita, H., Tsai, D. Y., Itoh, T., Doi, K., Morishita, J., Ueda, K. and Ohtsuka, A. (1992). A Simple Method for Determining the Modulation Transfer-Function in Digital Radiography. *IEEE Transactions on Medical Imaging.* **11,** 34-39.

Garzón, N., Poyales, F., De Zárate, B., Ruiz-García, J. and Quiroga, J. (2015). Evaluation of rotation and visual outcomes after implantation of monofocal and multifocal toric intraocular lenses. *Journal of Refractive Surgery.* **31,** 90-97.

Gaviola, E. (1936). On the Quantitative Use of the Foucault Knife-Edge Test. *Journal of the Optical Society of America.* **26,** 163-163.

Gerten, G., Michels, A. and Olmes, A. (2001). Toric intraocular lenses. Clinical results and rotational stability. *Ophthalmologe.* **98,** 715-720.

Gilmartin, B. (1995). The Etiology of Presbyopia - a Summary of the Role of Lenticular and Extralenticular Structures. *Ophthalmic and Physiological Optics.* **15,** 431-437.

Gimbel, H. V., Sanders, D. R. and Raanan, M. G. (1991). Visual and refractive results of multifocal intraocular lenses. *Ophthalmology.* **98,** 881-887; discussion 888.

Glasser, A. (2006). Accommodation: mechanism and measurement. *Ophthalmology Clinics of North America.* **19,** 1-12.

Glasser, A. and Campbell, M. C. (1999). Biometric, optical and physical changes in the isolated human crystalline lens with age in relation to presbyopia. *Vision Research.* **39,** 1991-2015.

Glasser, A. and Campbell, M. C. W. (1998). Presbyopia and the Optical Changes in the Human Crystalline Lens with Age. *Elsevier Science Ltd.* **38,** 209-229.

Graether, J. M. (2009). Simplified system of marking the cornea for a toric intraocular lens. *Journal of Cataract and Refractive Surgery.* **35,** 1498-1500.

Green, D. G., Powers, M. K. and Banks, M. S. (1980). Depth of focus, eye size and visual acuity. *Vision Research.* **20,** 827-835.

Grewal, D. S. and Grewal, S. P. (2012). Clinical applications of Scheimpflug imaging in cataract surgery. *Saudi Journal of Ophthalmology.* **26,** 25-32.

Gualtieri, M., Feitosa-Santana, C., Lago, M., Nishi, M. and Ventura, D. F. (2013). Early visual changes in diabetic patients with no retinopathy measured by color discrimination and electroretinography. *Psychology and Neuroscience.* **6,** 227-234.

Gullstrand, A. 1924. Mechanism of accommodation. *Helmholtz's treatise on physiological optics, Vol 1 (Trans. from the 3rd German ed.).* Rochester, NY, US: Optical Society of America.

Gupta, N., Naroo, S. A. and Wolffsohn, J. S. (2007). Is randomisation necessary for measuring defocus curves in pre-presbyopes? *Contact Lens & Anterior Eye.* **30,** 119-124.

Gupta, N., Wolffsohn, J. S. and Naroo, S. A. (2008). Optimizing measurement of subjective amplitude of accommodation with defocus curves. *Journal of Cataract and Refractive Surgery.* **34,** 1329-1338.

Guyton, D. L. (1977). Prescribing cylinders: the problem of distortion. *Survey of Ophthalmology.* **22,** 177-188.

Guyton, D. L., Uozato, H. and Wisnicki, H. J. (1990). Rapid Determination of Intraocular Lens Tilt and Decentration Through the Undilated Pupil. *Ophthalmology.* **97,** 1259-1264.

Hammett, S. T., Georgeson, M. A. and Gorea, A. (1998). Motion blur and motion sharpening: temporal smear and local contrast non-linearity. *Vision Research.* **38,** 2099-2108.

Hancox, J., Spalton, D., Heatley, C., Jayaram, H. and Marshall, J. (2006). Objective measurement of intraocular lens movement and dioptric change with a focus shift accommodating intraocular lens. *Journal of Cataract and Refractive Surgery.* **32,** 1098-1103.

Hancox, J., Spalton, D., Heatley, C., Jayaram, H., Yip, J., Boyce, J. and Marshall, J. (2007). Fellow-eye comparison of posterior capsule opacification rates after implantation of 1CU accommodating and AcrySof MA30 monofocal intraocular lenses. *Journal of Cataract and Refractive Surgery.* **33,** 413-417.

Hansen, S. O., Tetz, M. R., Solomon, K. D., Borup, M. D., Brems, R. N., O'morchoe, D. J., Bouhaddou, O. and Apple, D. J. (1988). Decentration of flexible loop posterior chamber intraocular lenses in a series of 222 postmortem eyes. *Ophthalmology.* **95,** 344-349.

Hayashi, K., Harada, M., Hayashi, H., Nakao, F. and Hayashi, F. (1997). Decentration and tilt of polymethyl methacrylate, silicone, and acrylic soft intraocular lenses. *Ophthalmology.* **104,** 793-798.

Hayashi, K., Hayashi, H., Nakao, F. and Hayashi, F. (1999). Intraocular lens tilt and decentration after implantation in eyes with glaucoma. *Journal of Cataract and Refractive Surgery.* **25,** 1515-1520.

Hayashi, K., Hayashi, H., Nakao, F. and Hayashi, F. (2001). Correlation between pupillary size and intraocular lens decentration and visual acuity of a zonal-progressive multifocal lens and a monofocal lens1. *Ophthalmology.* **108,** 2011-2017.

He, J. C., Burns, S. A. and Marcos, S. (2000). Monochromatic aberrations in the accommodated human eye. *Vision Research.* **40,** 41-48.

Helmholtz, H. V. (1855). Uber die akkommodation des auges. *Archives of Ophthalmology.* **1,** 1-74.

Hengerer, F. H., Dick, H. B. and Conrad-Hengerer, I. (2011). Clinical Evaluation of an Ultraviolet Light Adjustable Intraocular Lens Implanted after Cataract Removal: Eighteen Months Follow-up. *Ophthalmology.* **118,** 2382-2388.

Herse, P. R. (1992). Factors influencing normal perimetric thresholds obtained using the Humphrey Field Analyzer. *Investigative Ophthalmology and Visual Science.* **33,** 611-617.

Hess, R. F., Pointer, J. S. and Watt, R. J. (1989). How are spatial filters used in fovea and parafovea? *Journal of the Optical Society of Am A- Optics and Image Science.* **6,** 329-339.

Hirnschall, N., Maedel, S., Weber, M. and Findl, O. (2014). Rotational stability of a single-piece toric acrylic intraocular lens: a pilot study. *American Journal of Ophthalmology.* **157,** 405-411.

Hofer, H., Artal, P., Singer, B., Aragon, J. L. and Williams, D. R. (2001). Dynamics of the eye's wave aberration. *Journal of the Optical Society of America.* **18,** 497-506.

Hoffer, K. J. (1980). Biometry of 7,500 cataractous eyes. *American Journal of Ophthalmology.* **90,** 360-368.

Hoffmann, P. C. and Hutz, W. W. (2010). Analysis of biometry and prevalence data for corneal astigmatism in 23,239 eyes. *Journal of Cataract and Refractive Surgery.* **36,** 1479-1485.

Holladay, J. T. (1993). Refractive power calculations for intraocular lenses in the phakic eye. *American Journal of Ophthalmology.* **116,** 63-66.

Holladay, J. T. (2009). Keratoconus Detection Using Corneal Topography. *Journal of Refractive Surgery.* **25,** S958-S962.

Holladay, J. T., Piers, P., Koranyi, G., Van Der Mooren, M. and Norrby, S. (2002). A New Intraocular Lens Design to Reduce Spherical Aberration of Pseudophakic Eyes. *Journal of Refractive Surgery.* **18,** 683-691.

Hollick, E. J., Spalton, D. J., Ursell, P. G., Meacock, W. R., Barman, S. A. and Boyce, J. F. (2000). Posterior capsular opacification with hydrogel, polymethylmethacrylate, and silicone intraocular lenses: two-year results of a randomized prospective trial. *American Journal of Ophthalmology.* **129,** 577-584.

Horn, J. D. (2007). Status of toric intraocular lenses. *Current Opinion in Ophthalmology.* **18,** 58-61.

Horvath, K., Constantinescu, D., Vultur, F. and Muhlfay, G. (2014). Premium Intraocular Lenses: Patient Satisfaction. *Acta Medica Transilvanica.* **19,** 228-230.

Huang, C. Q., Townshend, J. R. G., Liang, S. L., Kalluri, S. N. V. and Defries, R. S. (2002). Impact of sensor's point spread function on land cover characterization: assessment and deconvolution. *Remote Sensing of Environment.* **80,** 203-212.

Hudson, C., Wild, J. M. and O'neill, E. C. (1994). Fatigue effects during a single session of automated static threshold perimetry. *Investigative Ophthalmology and Visual Science.* **35,** 268-280.

Hung, G. K. 2001. *Models of oculomotor control,* River Edge, NJ, World Scientific Pub.

Hwang, I. P., Clinch, T. E., Moshifar, M., Malmquist, L., Cason, M. and Crandall, A. S. (1998). Decentration of 3-piece versus plate-haptic silicone intraocular lenses. *Journal of Cataract and Refractive Surgery.* **24,** 1505-1508.

Iglesias, I., Berrio, E. and Artal, P. (1998a). Estimates of the ocular wave aberration from pairs of doble-pass retinal images. *Journal of the Optical Society of America.* **15,** 2466-2476.

Iglesias, I., Lopez-Gil, N. and Artal, P. (1998b). Reconstruction of the point-spread function of the human eye from two double-pass retinal images by phase-retrieval algorithms. *Journal of the Optical Society of America.* **15,** 326-339.

International Organisation for Standardisation 2014. Ophthalmic Implants- Part 2: Optical Properties and Test methods. Geneva, Switzerland: ISO 11979-2.

Iovieno, A., Yeung, S. N., Lichtinger, A., Alangh, M., Slomovic, A. R. and Rootman, D. S. (2013). Cataract Surgery with Toric Intraocular Lens for Correction of High Corneal Astigmatism. *Canadian Journal of Ophthalmology / Journal Canadien d'Ophtalmologie.* **48,** 246-250.

Jaffe, N. S. (1996). History of cataract surgery. *Ophthalmology.* **103,** S5-S16.

Jakel, F. and Wichmann, F. A. (2006). Spatial four-alternative forced-choice method is the preferred psychophysical method for naive observers. *Journal of Vision.* **6,** 1307-1322.

Jampaulo, M., Olson, M. D. and Miller, K. M. (2008). Long-term Staar toric intraocular lens rotational stability. *American Journal of Ophthalmology.* **146,** 550-553.

Jimenez, J. R., Ortiz, C., Hita, E. and Soler, M. (2008). Correlation between image quality and visual performance. *Journal of Modern Optics.* **55,** 783-790.

Jin, H. Y., Limberger, I. J., Ehmer, A., Guo, H. K. and Auffarth, G. U. (2010). Impact of axis misalignment of toric intraocular lenses on refractive outcomes after cataract surgery. *Journal of Cataract and Refractive Surgery.* **36,** 2061-2072.

Johnson, C. A., Adams, C. W. and Lewis, R. A. (1988). Fatigue effects in automated perimetry. *Applied Optics.* **27,** 1030-1037.

Johnson, C. A., Keltner, J. L. and Balestrery, F. (1978). Effects of target size and eccentricity on visual detection and resolution. *Vision Research.* **18,** 1217-1222.

Jung, C. K., Chung, S. K. and Baek, N. H. (2000). Decentration and tilt: silicone multifocal versus acrylic soft intraocular lenses. *Journal of Cataract and Refractive Surgery.* **26,** 582-585.

Jung, G. H. and Kline, D. W. (2010). Resolution of blur in the older eye: Neural compensation in addition to optics? *Journal of Vision.* **10,** 1-9.

Kaemmerer, M., Mrochen, M., Mierdal, P., Krinke, H.-E. and Seiler, T. (2000). Clinical experience with the Tscherning Aberrometer. *Journal of Refractive Surgery.* **16,** 584-587.

Kasthurirangan, S. and Glasser, A. (2006). Age related changes in the characteristics of the near pupil response. *Vision Research.* **46,** 1393-1403.

Kaufmann, C., Peter, J., Ooi, K., Phipps, S., Cooper, P. and Goggin, M. (2005). Limbal relaxing incisions versus on-axis incisions to reduce corneal astigmatism at the time of cataract surgery. *Journal of Cataract and Refractive Surgery.* **31,** 2261-5.

Keates, R. H., Pearce, J. L. and Schneider, R. T. (1987). Clinical results of the multifocal lens. *Journal of Cataract and Refractive Surgery.* **13,** 557-560.

Kermani, O., Oberheide, U. and Gerten, G. (2013). Rotation stability of the cachet angle-supported phakic intraocular lens. *Journal of Refractive Surgery.* **29,** 390-394.

Kershner, R. M. (2003). Retinal image contrast and functional visual performance with apsheric, silicone and acrylic intraocular lenses. *Journal of Cataract and Refractive Surgery.* **29,** 1684-1694.

Khanna, R., Pujari, S. and Sangwan, V. (2011). Cataract surgery in developing countries. *Current Opinion in Ophthalmology.* **22,** 10-14.

Kim, J. S. and Shyn, K. H. (2001a). Biometry of 3 types of intraocular lenses using Scheimpflug photography. *Journal of Cataract and Refractive Surgery.* **27,** 533-536.

Kim, J. S. and Shyn, K. H. (2001b). Biometry of 3 types of intraocular lenses using Scheimpflug photography. *J Cataract Refract Surg.* **27,** 533-6.

Kim, M. H., Chung, T. Y. and Chung, E. S. (2010). Long-term efficacy and rotational stability of AcrySof toric intraocular lens implantation in cataract surgery. *Korean J Ophthalmol.* **24,** 207-212.

Kline, D. W., Buck, K., Sell, Y., Bolan, T. L. and Dewar, R. E. (1999a). Older observers' tolerance of optical blur: age differences in the identification of defocused text signs. *Human Factors.* **41,** 356-364.

Kline, D. W., Buck, K., Sell, Y., Bolan, T. L. and Dewar, R. E. (1999b). Older observers' tolerance of optical blur: age differences in the identification of defocused text signs. *Hum Factors.* **41,** 356-64.

Kobashi, H., Kamiya, K., Shimizu, K., Kawamorita, T. and Uozato, H. (2012). Effect of axis orientation on visual performance in astigmatic eyes. *Journal of Cataract and Refractive Surgery.* **38,** 1352-1359.

Kocabeyoglu, S., Uzun, S., Mocan, M. C., Bozkurt, B., Irkec, M. and Orhan, M. (2013). Comparison of visual field test results obtained through Humphrey matrix frequency doubling technology perimetry versus standard automated perimetry in healthy children. *Indian Journal of Ophthalmology.* **61,** 576-579.

Korynta, J., Bok, J., Cendelin, J. and Michalova, K. (1999). Computer modeling of visual impairment caused by intraocular lens misalignment. *Journal of Cataract and Refractive Surgery.* **25,** 100-105.

Kothari, M., Mody, K., Walinjkar, J., Madia, J. and Kaul, S. (2009). Paralysis of the near-vision triad in a child. *Journal of Aapos.* **13,** 202-203.

Kozaki, J. and Takahashi, F. (1995). Theoretical analysis of image defocus with intraocular lens decentration. *Journal of Cataract and Refractive Surgery.* **21,** 552-555.

Kozaki, J., Tanihara, H., Yasuda, A. and Nagata, M. (1991a). Tilt and decentration of the implanted posterior chamber intraocular lens. *Journal of Cataract and Refractive Surgery.* **17,** 592-595.

Kozaki, J., Tanihara, H., Yasuda, A. and Nagata, M. (1991b). Tilt and decentration of the implanted posterior chamber intraocular lens. *J Cataract Refract Surg.* **17,** 592-5.

Kranitz, K., Takacs, A., Mihaltz, K., Kovacs, I., Knorz, M. C. and Nagy, Z. Z. (2011). Femtosecond laser capsulotomy and manual continuous curvilinear capsulorrhexis parameters and their effects on intraocular lens centration. *Journal of Refractive Surgery.* **27,** 558-563.

Kriechbaum, K., Findl, O., Koeppl, C., Menapace, R. and Drexler, W. (2005). Stimulus-driven versus pilocarpine-induced biometric changes in pseudophakic eyes. *Ophthalmology.* **112,** 453-459.

Krueger, R. R., Mrochen, M., Kaemmerer, M. and Seiler, T. (2001). Understanding refraction and accommodation through 'retinal imaging' aberrometry - A case report. *Ophthalmology.* **108,** 674-678.

Kumar, D. A., Agarwal, A., Prakash, G., Jacob, S. and Saravanan, Y. (2011). Evaluation of intraocular lens tilt with anterior segment optical coherence tomography. *American Journal of Ophthalmology.* **151,** 406-412.

Kuroda, T., Fujikado, T., Ninomiya, S., Maeda, N., Hirohara, Y. and Mihashi, T. (2002). Effect of aging on ocular light scatter and higher order aberrations. *Journal of Refractive Surgery.* **18,** 598-602.

Kwartz, J. and Edwards, K. (2010). Evaluation of the long-term rotational stability of single-piece, acrylic intraocular lenses. *British Journal of Ophthalmology.* **94,** 1003-1006.

Lakshminarayanan, V. and Fleck, A. (2010). Zernike polynomials: a guide. *Journal of Modern Optics.* **58,** 545-561.

Langenbucher, A., Huber, S., Nguyen, N. X., Seitz, B., Gusek-Schneider, G. C. and Kuchle, M. (2003). Measurement of accommodation after implantation of an accommodating posterior chamber intraocular lens. *Journal of Cataract and Refractive Surgery.* **29,** 677-685.

Langenbucher, A., Viestenz, A., Szentmary, N., Behrens-Baumann, W. and Viestenz, A. (2009). Toric Intraocular Lenses-Theory, Matrix Calculations, and Clinical Practice. *Journal of Refractive Surgery.* **25,** 611-622.

Legge, G. E., Mullen, K. T., Woo, G. C. and Campbell, F. W. (1987). Tolerance to visual defocus. *Journal of the Optical Society of Am A- Optics and Image Science.* **4,** 851-863.

Lesiewska-Junk, H. and Kaluzny, J. (2000). Intraocular lens movement and accommodation in eyes of young patients. *Journal of Cataract and Refractive Surgery.* **26,** 562-565.

Leyland, M. and Zinicola, E. (2003). Multifocal versus monofocal intraocular lenses in cataract surgery: a systematic review. *Ophthalmology.* **110,** 1789-1798.

Leyland, M., Zinicola, E., Bloom, P. and Lee, N. (2001). Prospective evaluation of a plate haptic toric intraocular lens. *Eye (Lond).* **15,** 202-205.

Li, Y.-J., Choi, J., Kim, H., Yu, S.-Y. and Joo, C.-K. (2011). Changes in ocular wavefront aberrations and retinal image quality with objective accommodation. *Journal of Cataract and Refractive Surgery.* **37,** 835-841.

Liang, J., Grimm, B., Goelz, S. and Bille, J. F. (1994). Objective measurement of wave aberrations of th human eye with the use of a Hartmann-Shack wave-front sensor. *Journal of the Optical Society of America.* **11,** 1949-1957.

Liang, J. and Williams, D. R. (1997). Aberrations and retinal image quality of the normal human eye. *Journal of the Optical Society of America.* **14,** 2873-2883.

Lichtinger, A. and Rootman, D. S. (2012). Intraocular lenses for presbyopia correction: past, present, and future. *Current Opinion in Ophthalmology.* **23,** 40-46.

Ligabue, E. A. and Giordano, C. (2009). Assessing visual quality with the point spread function using the NIDEK OPD-Scan II. *Journal of Refractive Surgery.* **25,** S104-S109.

Linebarger, E. J., Hardten, D. R., Shah, G. K. and Lindstrom, R. L. (1999). Phacoemulsification and modern cataract surgery. *Survey of Ophthalmology.* **44,** 123-147.

Lopez-Gil, N. and Artal, P. (1997). Comparison of double-pass estimates of the retinal-image quality obtained with green and near-infrared light. *Journal of the Optical Society of America.* **14,** 961-971.

Lopez-Gil, N., Iglesias, I. and Artal, P. (1998). Retinal image quality in the human eye as a function of the accommodation. *Vision Research.* **38,** 2897-2907.

Luck, J. (2010). Customized ultra-high-power toric intraocular lens implantation for pellucid marginal degeneration and cataract. *Journal of Cataract and Refractive Surgery.* **36,** 1235-1238.

Ludbrook, J. (2010). Confidence in Altman–Bland plots: a critical review of the method of differences. *Clinical and Experimental Pharmacology and Physiology.* **37,** 143-149.

Lung, J. C. Y., Swann, P. G., Wong, D. S. H. and Chan, H. H. L. (2012). Global flash multifocal electroretinogram: early detection of local functional changes and its correlations with optical coherence tomography and visual field tests in diabetic eyes. *Documenta Ophthalmologica.* **125,** 123-135.

Ma, J. J. K. and Tseng, S. S. (2008). Simple method for accurate alignment in toric phakic and aphakic intraocular lens implantation. *Journal of Cataract and Refractive Surgery.* **34,** 1631-1636.

Macsai, M. S., Padnick-Silver, L. and Fontes, B. M. (2006). Visual outcomes after accommodating intraocular lens implantation. *Journal of Cataract and Refractive Surgery.* **32,** 628-633.

Madrid-Costa, D., Ruiz-Alcocer, J., Perez-Vives, C., Ferrer-Blasco, T., Lopez-Gil, N. and Montes-Mico, R. (2012). Visual simulation through different intraocular lenses using adaptive optics: effect of tilt and decentration. *Journal of Cataract and Refractive Surgery.* **38,** 947-958.

Mamalis, N., Omar, O., Veiga, J., Tanner, D., Pirayesh, A. and Fernquist, D. S. (1996). Comparison of two plate-haptic intraocular lenses in a rabbit model. *Journal of Cataract and Refractive Surgery.* **22 Suppl 2,** 1291-1295.

Marchini, G., Mora, P., Pedrotti, E., Manzotti, F., Aldigeri, R. and Gandolfi, S. A. (2007). Functional assessment of two different accommodative intraocular lenses compared with a monofocal intraocular lens. *Ophthalmology.* **114,** 2038-2043.

Marcos, S., Moreno, E. and Navarro, R. (1999a). The depth-of-field of the human eye from objective and subjective measurements. *Vision Res.* **39,** 2039-49.

Marcos, S., Moreno, E. and Navarro, R. (1999b). The depth-of-field of the human eye from objective and subjective measurements. *Vision Research.* **39,** 2039-2049.

Marsack, J. D., Thibos, L. N. and Applegate, R. A. (2004). Metrics of optical quality derived from wave aberrations predict visual performance. *Journal of Vision.* **4,** 322-328.

Martin, J., Vasudevan, B., Himebaugh, N., Bradley, A. and Thibos, L. (2011). Unbiased estimation of refractive state of aberrated eyes. *Vision Research.* **51,** 1932-1940.

Mastropasqua, L., Toto, L., Falconio, G., Nubile, M., Carpineto, P., Ciancaglini, M., Di Nicola, M. and Ballone, E. (2007). Longterm results of 1 CU accommodative intraocular lens implantation: 2-year follow-up study. *Acta Ophthalmologica Scandinavica.* **85,** 409-414.

Maxwell, W. A., Cionni, R. J., Lehmann, R. P. and Modi, S. S. (2009). Functional outcomes after bilateral implantation of apodized diffractive aspheric acrylic intraocular lenses with a +3.0 or +4.0 diopter addition power Randomized multicenter clinical study. *Journal of Cataract and Refractive Surgery.* **35,** 2054-2061.

Mayer, W. J., Klaproth, O. K., Hengerer, F. H. and Kohnen, T. (2014). Impact of crystalline lens opacification on effective phacoemulsification time in femtosecond laser-assisted cataract surgery. *American Journal of Ophthalmology.* **157,** 426-432.

Mcalinden, C. and Moore, J. E. (2011). Multifocal intraocular lens with a surface-embedded near section: Short-term clinical outcomes. *Journal of Cataract and Refractive Surgery.* **37,** 441-445.

Mclellan, J., Marcos, S., Prieto, P. and Burns, S. A. (2002). Imperfect optics may be the eye's defence against chromatic blur. *Nature.* **417,** 174-176.

Mclellan, J. S., Marcos, S. and Burns, S. A. (2001). Age-related changes in monochromatic wave aberrations of the human eye. *Investigative Ophthalmology and Visual Science.* **42,** 1390-1395.

Mcleod, S. D., Portney, V. and Ting, A. (2003). A dual optic accommodating foldable intraocular lens. *British Journal of Ophthalmology.* **87,** 1083-1085.

Mencucci, R., Ponchietti, C., Virgili, G., Giansanti, F. and Menchini, U. (2006). Corneal endothelial damage after cataract surgery: Microincision versus standard technique. *Journal of Cataract and Refractive Surgery.* **32,** 1351-1354.

Mendicute, J., Irigoyen, C., Aramberri, J., Ondarra, A. and Montes-Mico, R. (2008). Foldable toric intraocular lens for astigmatism correction in cataract patients. *Journal of Cataract and Refractive Surgery.* **34,** 601-607.

Mendicute, J., Irigoyen, C., Ruiz, M., Illarramendi, I., Ferrer-Blasco, T. and Montes-Mico, R. (2009). Toric intraocular lens versus opposite clear corneal incisions to correct astigmatism in eyes having cataract surgery. *Journal of Cataract and Refractive Surgery.* **35,** 451-458.

Messias, A., Messias, K., Arcieri, R., Castro, V., Siqueira, R. and Jorge, R. (2013). Chromatic Full-field Stimulus Threshold (FST) in Retinitis Pigmentosa-Relationships with electroretinography and visual field outcomes. *Investigative Ophtalmology and Visual Science.* **54,** 5112.

Mester, U., Sauer, T. and Kaymak, H. (2009). Decentration and tilt of a single-piece aspheric intraocular lens compared with the lens position in young phakic eyes. *Journal of Cataract and Refractive Surgery.* **35,** 485-490.

Michael, R. and Bron, A. J. (2011). The ageing lens and cataract: a model of normal and pathological ageing. *Philos Trans R Soc Lond B Biol Sci.* **366,** 1278-1292.

Milazzo, S., Grenot, M. and Benzerroug, M. (2014). [Posterior capsule opacification]. *Journal francais d'ophtalmologie.* **37,** 825-830.

Millodot, M. 2009. Dictionary of Optometry and Visual Science. 7th ed.: Butterworth-Heinemann.

Millodot, M. and Millodot, S. (1989). Presbyopia correction and the accommodation in reserve. *Ophthalmic and Physiological Optics.* **9,** 126-132.

Mingo-Botin, D., Munoz-Negrete, F. J., Kim, H. R. W., Morcillo-Laiz, R., Rebolleda, G. and Oblanca, N. (2010). Comparison of toric intraocular lenses and peripheral corneal relaxing incisions to treat astigmatism during cataract surgery. *Journal of Cataract and Refractive Surgery.* **36,** 1700-1708.

Miranda, M. A., O'donnell, C. and Radhakrishnan, H. (2009). Repeatability of corneal and ocular aberration measurements and changes in aberrations over one week. *Clinical and Experimental Optometry.* **92,** 253-266.

Mojzis, P., Piñero, D., Ctvrteckova, V. and Rydlova, I. (2013). Analysis of internal astigmatism and higher order aberrations in eyes implanted with a new diffractive multifocal toric intraocular lens. *Graefes Archive for Clinical and Experimental Ophthalmology.* **251,** 341-348.

Molebny, V. V., Panagopoulou, S. I., Molebny, S. V., Wakil, Y. S. and Pallikaris, I. G. (2000). Principles of Ray Tracing Aberrometry. *Journal of Refractive Surgery.* **16,** 572-575.

Moreno-Barriuso, E., Marcos, S., Navarro, R. and Burns, S. A. (2001). Comparing laser ray tracing, the spatially resolved refractometer, and the Hartmann-Shack sensor to measure the ocular wave aberration. *Optometry and Vision Science.* **78,** 152-156.

Morris, C., Werner, L., Barra, D., Liu, E., Stallings, S. and Floyd, A. (2014). Light scattering and light transmittance of cadaver eye-explanted intraocular lenses of different materials. *Journal of Cataract and Refractive Surgery.* **40,** 129-137.

Moshirfar, M., Churgin, D. S. and Hsu, M. (2011). Femtosecond laser-assisted cataract surgery: a current review. *Middle East African Journal of Ophthalmology.* **18,** 285-291.

Mrochen, M., Kaemmerer, M., Mierdal, P., Krinke, H.-E. and Seiler, T. (2000). Principle of Tscherning Aberrometry. *Journal of Refractive Surgery.* **16,** 570-571.

Muftuoglu, O., Dao, L., Cavanagh, H. D., Mcculley, J. P. and Bowman, R. W. (2010). Limbal relaxing incisions at the time of apodized diffractive multifocal intraocular lens implantation to reduce astigmatism with or without subsequent laser in situ keratomileusis. *Journal of Cataract and Refractive Surgery.* **36,** 456-464.

Mutlu, F. M., Erdurman, C., Sobaci, G. and Bayraktar, M. Z. (2005). Comparison of tilt and decentration of 1-piece and 3-piece hydrophobic acrylic intraocular lenses. *Journal of Cataract and Refractive Surgery.* **31,** 343-347.

Nagy, Z., Takacs, A., Filkorn, T. and Sarayba, M. (2009). Initial clinical evaluation of an intraocular femtosecond laser in cataract surgery. *Journal of Refractive Surgery.* **25,** 1053-1060.

Nagy, Z. Z., Ecsedy, M., Kovacs, I., Takacs, A., Tatrai, E., Somfai, G. M. and Cabrera Debuc, D. (2012). Macular morphology assessed by optical coherence tomography image segmentation after femtosecond laser-assisted and

standard cataract surgery. *Journal of Cataract and Refractive Surgery.* **38,** 941-946.

Nakazawa, M. and Ohtsuki, K. (1984). Apparent accommodation in pseudophakic eyes after implantation of posterior chamber intraocular lenses: optical analysis. *Investigative Ophthalmology and Visual Science.* **25,** 1458-1460.

Nanavaty, M. A., Spalton, D. J. and Marshall, J. (2010). Effect of intraocular lens asphericity on vertical coma aberration. *Journal of Cataract and Refractive Surgery.* **36,** 215-221.

Nanavaty, M. A., Vasavada, A. R., Patel, A. S., Raj, S. M. and Desai, T. H. (2006). Analysis of patients with good uncorrected distance and near vision after monofocal intraocular lens implantation. *Journal of Cataract and Refractive Surgery.* **32,** 1091-1097.

Naranjo-Tackman, R. (2011). How a femtosecond laser increases safety and precision in cataract surgery? *Current Opinion in Ophthalmology.* **22,** 53-57.

Narendran, R., Vyas, A. and Bacon, P. 2009. Centration, rotational stability and outcomes of Rayner T-flexTM toric lens implantation: 2 year results. *Proceedings of the XXVII congress of the ESCRS, Barcelona.*

Nishi, Y., Hirnschall, N., Crnej, A., Gangwani, V., Tabernero, J., Artal, P. and Findl, O. (2010). Reproducibility of intraocular lens decentration and tilt measurement using a clinical Purkinje meter. *Journal of Cataract and Refractive Surgery.* **36,** 1529-1535.

Nishimoto, H., Shimizu, K., Ishikawa, H. and Uozato, H. (2007). New approach for treating vertical strabismus: decentered intraocular lenses. *Journal of Cataract and Refractive Surgery.* **33,** 993-998.

Novis, C. (2000). Astigmatism and toric intraocular lenses. *Current Opinion in Ophthalmology.* **11,** 47-50.

O'donnell, C., Hartwig, A. and Radhakrishnan, H. (2011). Correlations between refractive error and biometric parameters in human eyes using the LenStar 900. *Contact Lens & Anterior Eye.* **34,** 26-31.

Ohlendorf, A., Tabernero, J. and Schaeffel, F. (2011a). Neuronal adaptation to simulated and optically-induced astigmatic defocus. *Vision Research.* **51,** 529-534.

Ohlendorf, A., Tabernero, J. and Schaeffel, F. (2011b). Visual acuity with simulated and real astigmatic defocus. *Optometry and Vision Science.* **88,** 562-569.

Ong, H. S., Evans, J. R. and Allan, B. D. (2014). Accommodative intraocular lens versus standard monofocal intraocular lens implantation in cataract surgery. *Cochrane Database of Systematic Reviews.* **5**.

Ortiz, S., Perez-Merino, P., Gambra, E., De Castro, A. and Marcos, S. (2012). In vivo human crystalline lens topography. *Biomedical Optics Express.* **3,** 2471-2488.

Oshika, T., Kawana, K., Hiraoka, T., Kaji, Y. and Kiuchi, T. (2005). Ocular higher-order wavefront aberration caused by major tilting of intraocular lens. *American Journal of Ophthalmology.* **140,** 744-746.

Oshika, T., Nagata, T. and Ishii, Y. (1998). Adhesion of lens capsule to intraocular lenses of polymethylmethacrylate, silicone, and acrylic foldable materials: an experimental study. *British Journal of Ophthalmology.* **82,** 549-553.

Ostrin, L. A. and Glasser, A. (2004). Accommodation measurements in a prepresbyopic and presbyopic population. *Journal of Cataract and Refractive Surgery.* **30,** 1435-1444.

Packer, M. (2014). Enhancements After Premium IOL Cataract Surgery: Tips, Tricks, and Outcomes. *Current Ophthalmology Reports.* **2,** 34-40.

Pascolini, D. and Mariotti, S. P. (2012). Global estimates of visual impairment: 2010. *British Journal of Ophthalmology.* **96,** 614-618.

Patel, C. K., Ormonde, S., Rosen, P. H. and Bron, A. J. (1999). Postoperative intraocular lens rotation: A randomized comparison of plate and loop haptic implants. *Ophthalmology.* **106,** 2190-2196.

Pershing, S. and Kumar, A. (2011). Phacoemulsification versus extracapsular cataract extraction: where do we stand? *Current Opinion in Ophthalmology.* **22,** 37-42.

Peterson, R. C. and Wolffsohn, J. S. (2005). The effect of digital image resolution and compression on anterior eye imaging. *British Journal of Ophthalmology.* **89,** 828-830.

Petrova, K. and Wentura, D. (2012). Upper-lower visual field asymmetries in oculomotor inhibition of emotional distractors. *Vision Research.* **62,** 209-219.

Phillips, P., Perez-Emmanuelli, J., Rosskothen, H. D. and Koester, C. J. (1988). Measurement of intraocular lens decentration and tilt in vivo. *Journal of Cataract and Refractive Surgery.* **14,** 129-135.

Piers, P. A., Manzanera, S., Prieto, P. M., Gorceix, N. and Artal, P. (2007). Use of adaptive optics to determine the optimal ocular spherical aberration. *Journal of Cataract and Refractive Surgery.* **33,** 1721-1726.

Pierscionek, B. K. and Weale, R. A. (1995). Presbyopia- a maverick of human aging. *Archives of Gerontology and Geriatrics.* **20,** 229-240.

Plakitsi, A. and Charman, W. N. (1995). Comparison of the depths of focus with the naked eye and with three types of presbyopic contact lens correction. *Journal of the British Contact Lens Association.* **18,** 119-125.

Pollreisz, A. and Schmidt-Erfurth, U. (2010). Diabetic cataract-pathogenesis, epidemiology and treatment. *Journal of Ophthalmology.* **2010,** 1-8.

Porter, J., Guirao, A., Cox, I. G. and Williams, D. R. (2001). Monochromatic aberrations of the human eye in a large population. *Journal of the Optical Society of America.* **18,** 1793-1803

Previc, F. H. (1990). Functional specialization in the lower and upper visual fields in humans: Its ecological origins and neurophysiological implications. *Behavioral and Brain Sciences.* **13,** 519-542.

Prieto, P., Vargas-Martin, F., Goelz, S. and Artal, P. (2000). Analysis of the performance of the Hartmann-Shack sensor in the human eye. *Journal of the Optical Society of America.* **17,** 1388-1398.

Prinz, A., Neumayer, T., Buehl, W., Vock, L., Menapace, R., Findl, O. and Georgopoulos, M. (2011). Rotational stability and posterior capsule opacification of a plate-haptic and an open-loop-haptic intraocular lens. *Journal of Cataract and Refractive Surgery.* **37,** 251-257.

Queiros, A., González-Méijome, J. M., Jorge, J. and Franco, S. Year. Ocular components data in young adults and their correlation with the refractive error. *In:* EVER, 2005.

Queiros, A., Villa-Collar, C., Gonzalez-Meijome, J. M., Jorge, J. and Gutierrez, A. R. (2010). Effect of pupil size on corneal aberrations before and after standard laser in situ keratomileusis, custom laser in situ keratomileusis, and corneal refractive therapy. *American Journal of Ophthalmology.* **150,** 97-109

Rabiu, M. M. (2001). Cataract blindness and barriers to uptake of cataract surgery in a rural community of northern Nigeria. *British Journal of Ophthalmology.* **85,** 776-780.

Rabsilber, T. M., Rudalevicius, P., Jasinskas, V., Holzer, M. P. and Auffarth, G. U. (2013). Influence of +3.00 D and +4.00 D near addition on functional outcomes of a refractive multifocal intraocular lens model. *Journal of Cataract and Refractive Surgery.* **39,** 350-357.

Ram, J., Agarwal, A., Kumar, J. and Gupta, A. (2014). Bilateral implantation of multifocal versus monofocal intraocular lens in children above 5 years of age. *Graefes Archives of Clinical and Experimental Ophthalmology.* **252,** 441-447.

Ravalico, G., Parentin, F., Pastori, G. and Baccara, F. (1998). Spatial resolution threshold in pseudophakic patients with monofocal and multifocal intraocular lenses. *Journal of Cataract and Refractive Surgery.* **24,** 244-248.

Ravikumar, A. (2014). Predicting change in visual acuity from change in image quality metric for normal and keratoconic wavefront errors. PhD thesis, University of Houston, Houston, USA.

Ravikumar, A., Applegate, R. A., Shi, Y. and Bedell, H. E. (2011). Six just-noticeable differences in retinal image quality in 1 line of visual acuity: toward quantification of happy versus unhappy patients with 20/20 acuity. *Journal of Cataract and Refractive Surgery.* **37,** 1523-1529.

Read, S. A., Collins, M. J. and Carney, L. G. (2007). A review of astigmatism and its possible genesis. *Clinical and Experimental Ophthalmology.* **90,** 5-19.

Read, S. A., Vincent, S. J. and Collins, M. J. (2014). The visual and functional impacts of astigmatism and its clinical management. *Ophthalmic and Physiological Optics.* **34,** 267-294.

Ridley, H. (1952). Intra-ocular acrylic lenses after cataract extraction. *Lancet.* **1,** 118-121.

Roberts Jr, L., Perrin, M., Marchis, F., Sivaramakrishnan, A., Makidon, R. B., Christou, J., Macintosh, B., Poyneer, L., Van Dame, M. and Troy, M. (2004). Is that really your Strehl ratio? *Advancements in Adaptive optics.* **5490,** 504-515.

Roberts, T. V., Lawless, M., Bali, S. J., Hodge, C. and Sutton, G. (2013). Surgical outcomes and safety of femtosecond laser cataract surgery: a prospective study of 1500 consecutive cases. *Ophthalmology.* **120,** 227-233.

Rocha, K. M. and Krueger, R. R. (2009a). The future: Adaptive optics visual simulation. *Ophthalmology Times.* 35-38.

Rocha, K. M., Vabre, L., Chateau, N. and Krueger, R. R. (2009b). Expanding depth of focus by modifying higher-order aberrations induced by an adaptive optics visual simulator. *Journal of Cataract and Refractive Surgery.* **35,** 1885-1892.

Ronchi, L. and Molesini, G. (1975). Depth of focus in peripheral vision. *Ophthalmic Research.* **7,** 152-157.

Roorda, A. (2011). Adaptive optics for studying visual function: A comprehensive review. *Journal of Vision.* **11,** 1-21.

Rosales, P., De Castro, A., Jimenez-Alfaro, I. and Marcos, S. (2010). Intraocular lens alignment from purkinje and Scheimpflug imaging. *Clinical and Experimental Ophthalmology.* **93,** 400-408.

Rosales, P. and Marcos, S. (2006). Phakometry and lens tilt and decentration using a custom-developed Purkinje imaging apparatus: validation and measurements. *Journal of the Optical Society of America A- Optics and Image Science.* **23,** 509-520.

Rosales, P. and Marcos, S. (2009). Pentacam Scheimpflug quantitative imaging of the crystalline lens and intraocular lens. *Journal of Refractive Surgery.* **25,** 421-428.

Rosen, R., Lundstrom, L. and Unsbo, P. (2011). Influence of optical defocus on peripheral vision. *Investigative Ophthalmology and Visual Science.* **52,** 318-323.

Rosenfield, M., Logan, N. and Edwards, K. 2009. *Optometry: Science, Techniques and Clinical Management,* Oxford, Butterworth-Heinemann Elsevier.

Rubenstein, J. B. and Raciti, M. (2013). Approaches to corneal astigmatism in cataract surgery. *Current Opinion in Ophthalmology.* **24,** 30-34.

Ruhswurm, I., Scholz, U., Zehetmayer, M., Hanselmayer, G., Vass, C. and Skorpik, C. (2000). Astigmatism correction with a foldable toric intraocular lens in cataract patients. *Journal of Cataract and Refractive Surgery.* **26,** 1022-1027.

Saiki, M., Negishi, K., Dogru, M., Yamaguchi, T. and Tsubota, K. (2010). Biconvex posterior chamber accommodating intraocular lens implantation after cataract surgery: long-term outcomes. *Journal of Cataract and Refractive Surgery.* **36,** 603-608.

Sample, P. A. and Johnson, C. A. (2001). Functional Assessment of Glaucoma. *Journal of Glaucoma.* **10,** S49-S52.

Santhiago, M. R., Netto, M. V., Espindola, R. F., Mazurek, M. G., Gomes, B. D. a. F., Parede, T. R. R., Harooni, H. and Kara-Junior, N. (2010). Comparison of reading performance after bilateral implantation of multifocal intraocular lenses with +3.00 or +4.00 diopter addition. *Journal of Cataract and Refractive Surgery.* **36,** 1874-1879.

Sasaki, K., Sakamoto, Y., Shibata, T., Nakaizumi, H. and Emori, Y. (1989). Measurement of postoperative intraocular lens tilting and decentration using Scheimpflug images. *Journal of Cataract and Refractive Surgery.* **15,** 454-457.

Sawides, L., De Gracia, P., Dorronsoro, C., Webster, M. A. and Marcos, S. (2011). Vision Is Adapted to the Natural Level of Blur Present in the Retinal Image. *Plos One.* **6,** e27031.

Sawides, L., Marcos, S., Ravikumar, S., Thibos, L., Bradley, A. and Webster, M. (2010). Adaptation to astigmatic blur. *Journal of Vision.* **10,** 1-15.

Saxena, R. C. (1965). Couching and its hazards (a review of 62 cases). *Indian Journal of Ophthalmology.* **13,** 100-104.

Schachar, R. A. (2006). The mechanism of accommodation and presbyopia. *Int. Ophthalmol. Clin.* **46,** 39-61.

Schaumberg, D. A., Dana, M. R., Christen, W. G. and Glynn, R. J. (1998). A systematic overview of the incidence of posterior capsule opacification. *Ophthalmology.* **105,** 1213-1221.

Schaumberger, M., Schafer, B. and Lachenmayr, B. J. (1995). Glaucomatous visual fields. *Investigative Ophthalmology and Visual Science.* **36,** 1390-1397.

Schemann, J.-F., Bakayoko, S. and Coulibaly, S. (2000). Traditional couching is not an effective alternative procedure for cataract surgery in Mali. *Ophthalmic Epidemiology.* **7,** 271-283.

Schimiti, R. B., Avelino, R. R., Kara-Jose, N. and Costa, V. P. (2002). Full threshold versus Swedish Interactive Threshold Algorithm (SITA) in normal individuals undergoing automated perimetry for the first time. *American Academy of Ophthalmology.* **109,** 2084-2092.

Schmid, K. L., Robert Iskander, D., Li, R. W., Edwards, M. H. and Lew, J. K. (2002). Blur detection thresholds in childhood myopia: single and dual target presentation. *Vision Research.* **42,** 239-247.

Schor, C. M. (2009). Charles F. Prentice award lecture 2008: surgical correction of presbyopia with intraocular lenses designed to accommodate. *Optometry and Vision Science.* **86,** E1028-1041.

Schwiegerling, J., Mccafferty, S. and Duncan, W. (2013). Curvature Changing Accommodating IOL. *Investigative Ophthalmology and Visual Science.* **54,** 837.

Shah, G. D., Praveen, M. R., Vasavada, A. R., Rampal, N. V., Vasavada, V. A., Asnani, P. K. and Pandita, D. (2009). Software-based assessment of

postoperative rotation of toric intraocular lens. *Journal of Cataract and Refractive Surgery.* **35,** 413-418.

Shah, G. D., Praveen, M. R., Vasavada, A. R., Vasavada, V. A., Rampal, G. and Shastry, L. R. (2012). Rotational stability of a toric intraocular lens: influence of axial length and alignment in the capsular bag. *Journal of Cataract and Refractive Surgery.* **38,** 54-59.

Sheppard, A. L., Bashir, A., Wolffsohn, J. S. and Davies, L. M. (2010). Accommodating intraocular lenses: a review of design concepts, usage and assessment methods. *Clinical and Experimental Optometry.* **6,** 441-452.

Sheppard, A. L., Dunne, M. C. M., Wolffsohn, J. S. and Davies, L. N. (2008). Theoretical evaluation of the cataract extraction-refraction-implantation techniques for intraocular lens power calculation. *Ophthalmic and Physiological Optics.* **28,** 568-576.

Sheppard, A. L., Wolffsohn, J. S., Bhatt, U., Hoffmann, P. C., Scheider, A., Hutz, W. W. and Shah, S. (2013). Clinical outcomes after implantation of a new hydrophobic acrylic toric IOL during routine cataract surgery. *Journal of Cataract and Refractive Surgery.* **39,** 41-47.

Shi, Y., Queener, H. M., Marsack, J. D., Ravikumar, A., Bedell, H. E. and Applegate, R. A. (2013). Optimizing wavefront-guided corrections for highly aberrated eyes in the presence of registration uncertainty. *Journal of Vision.* **13,** 1-15.

Shimizu, K., Misawa, A. and Suzuki, Y. (1994). Toric intraocular lenses: correcting astigmatism while controlling axis shift. *Journal of Cataract and Refractive Surgery.* **20,** 523-526.

Signes-Soler, I., Javaloy, J., Montes-Mico, R. and Munoz, G. (2012). Cataract surgery in West Africa: is couching still a choice? *Acta Ophthalmologica.* **90,** e488-489.

Silva, M. F., Maia-Lopes, S., Mateus, C., Guerreiro, M., Sampaio, J., Faria, P. and Castelo-Branco, M. (2008). Retinal and cortical patterns of spatial anisotropy in contrast sensitivity tasks. *Vision Research.* **48,** 127-135.

Simpson, M. J. (1992). Diffractive multifocal intraocular lens image quality. *Optical Society of America.* **31,** 3621-3626.

Sivak, J. G., Kreuzer, R. O. and Hildebrand, T. (1985). Intraocular lenses, tilt and astigmatism. *Ophthalmic Research.* **17,** 54-59.

Smirnov, M. S. (1961). Measurement of the wave aberration of the human eye. *Biofizika.* **6,** 776-795.

Smolek, M. K. and Klyce, S. D. (2007). Absolute color scale for improved diagnostics with wavefront error mapping. *American Academy of Ophthalmology.* **114,** 2022-2030.

Spalton, D. J. (1999). Posterior capsular opacification after cataract surgery. *Eye (Lond).* **13,** 489-492.

Springer, C., Bultmann, S., Volcker, H. E. and Rohrschneider, K. (2005). Fundus perimetry with the micro-perimeter 1 in normal individuals. *American Academy of Ophthalmology.* **112,** 848-854.

Steinert, R. F., Aker, B. L., Trentacost, D. J., Smith, P. J. and Tarantino, N. (1999). A prospective comparative study of the AMO ARRAY zonal-progressive multifocal silicone intraocular lens and a monofocal intraocular lens. *Ophthalmology.* **106,** 1243-1255.

Strenk, S. A., Semmlow, J. L., Strenk, L. M., Munoz, P., Gronlund-Jacob, J. and Demarco, J. K. (1999). Age-related changes in human ciliary muscle and lens: a magnetic resonance imaging study. *Investigative Ophthalmology and Visual Science.* **40,** 1162-1169.

Strenk, S. A., Strenk, L. M. and Guo, S. (2006). Magnetic resonance imaging of aging, accommodating, phakic, and pseudophakic ciliary muscle diameters. *Journal of Cataract and Refractive Surgery.* **32,** 1792-1798.

Takakura, A., Iyer, P., Adams, J. R. and Pepin, S. M. (2010). Functional assessment of accommodating intraocular lenses versus monofocal intraocular lenses in cataract surgery: metaanalysis. *Journal of Cataract and Refractive Surgery.* **36,** 380-388.

Taketani, F., Matuura, T., Yukawa, E. and Hara, Y. (2004). Influence of intraocular lens tilt and decentration on wavefront aberrations. *Journal of Cataract and Refractive Surgery.* **30,** 2158-2162.

Taketani, F., Yukawa, E., Ueda, T., Sugie, Y., Kojima, M. and Hara, Y. (2005a). Effect of tilt of 2 acrylic intraocular lenses on high-order aberrations. *Journal of Cataract and Refractive Surgery.* **31,** 1182-1186.

Taketani, F., Yukawa, E., Yoshii, T., Sugie, Y. and Hara, Y. (2005b). Influence of intraocular lens optical design on high-order aberrations. *Journal of Cataract and Refractive Surgery.* **31,** 969-972.

Taylor, H. R. (2000). Cataract: how much surgery do we have to do? *British Journal of Ophthalmology.* **84,** 1-2.

Tester, R., Pace, N. L., Samore, M. and Olson, R. J. (2000). Dysphotopsia in phakic and pseudophakic patients: incidence and relation to intraocular lens type(2). *Journal of Cataract and Refractive Surgery.* **26,** 810-816.

Thibos, L. N., Bradley, A. and Hong, X. (2002). A statistical model of the aberration structure of normal, well-corrected eyes. *Ophthalmic and Physiological Optics.* **22,** 427-433.

Thibos, L. N., Hong, X., Bradley, A. and Applegate, R. A. (2004). Accuracy and precision of objective refraction from wavefront aberrations. *Journal of Vision.* **4,** 329-351.

Trikha, S., Turnbull, A. M., Morris, R. J., Anderson, D. F. and Hossain, P. (2013). The journey to femtosecond laser-assisted cataract surgery: new beginnings or a false dawn? *Eye (Lond).* **27,** 461-473.

Uozato, H., Okada, Y., Hirai, H. and Saishin, M. (1988). What is the tolerable limits of the IOL tilt and decentration? *Jpn Rev Clin Ophthalmol.* **82,** 2308-2311.

Ursell, P. G., Spalton, D. J., Pande, M. V., Hollick, E. J., Barman, S., Boyce, J. and Tilling, K. (1998). Relationship between intraocular lens biomaterials and posterior capsule opacification. *Journal of Cataract and Refractive Surgery.* **24,** 352-360.

Uy, H. S., Hill, W. and Edwards, K. (2011). Refractive results after laser anterior capsulotomy. *Investigative Ophthalmology and Visual Science.* **52,** E-abstract 5695.

Van Der Linden, J. W., Van Velthoven, M., Van Der Meulen, I., Nieuwendaal, C., Mourits, M. and Lapid-Gortzak, R. (2012). Comparison of a new-generation sectorial addition multifocal intraocular lens and a diffractive apodized multifocal intraocular lens. *Journal of Cataract and Refractive Surgery.* **38,** 68-73.

Vandenberg, D. E., Humbel, W. D. and Wertheimer, A. (1993). Quantitative-Evaluation of Optical-Surfaces by Means of an Improved Foucault Test Approach. *Optical Engineering.* **32,** 1951-1954.

Vasudevan, B., Ciuffreda, K. J. and Wang, B. (2007). Subjective and objective depth-of-focus. *Journal of Modern Optics.* **54,** 1307-1316.

Venter, J. and Pelouskova, M. (2013). Outcomes and complications of a multifocal toric intraocular lens with a surface-embedded near section. *Journal of Cataract and Refractive Surgery.* **39,** 859-866.

Viestenz, A., Seitz, B. and Langenbucher, A. (2005). Evaluating the eye's rotational stability during standard photography: effect on determining the axial orientation of toric intraocular lenses. *Journal of Cataract and Refractive Surgery.* **31,** 557-561.

Villegas, E. A., Alcón, E., Mirabet, S., Yago, I., Marín, J. M. and Artal, P. (2014). Extended Depth of Focus With Induced Spherical Aberration in Light-Adjustable Intraocular Lenses. *American Journal of Ophthalmology.* **157,** 142-149.

Visser, N., Bauer, N. J. and Nuijts, R. M. (2013). Toric intraocular lenses: historical overview, patient selection, IOL calculation, surgical techniques, clinical outcomes, and complications. *Journal of Cataract and Refractive Surgery.* **39,** 624-637.

Visser, N., Berendschot, T. T. J. M., Bauer, N. J. C., Jurich, J., Kersting, O. and Nuijts, R. M. M. A. (2011a). Accuracy of toric intraocular lens implantation in cataract and refractive surgery. *Journal of Cataract and Refractive Surgery.* **37,** 1394-1402.

Visser, N., Ruíz-Mesa, R., Pastor, F., Bauer, N. J. C., Nuijts, R. M. M. A. and Montés-Micó, R. (2011b). Cataract surgery with toric intraocular lens implantation in patients with high corneal astigmatism. *Journal of Cataract & Refractive Surgery.* **37,** 1403-1410.

Walsh, G., Charman, W. N. and Howland, H. C. (1984). Objective technique for the determination of monochromatic aberrations of the human eye. *Journal of the Optical Society of America.* **1,** 987-992.

Waltz, K. L., Featherstone, K., Tsai, L. and Trentacost, D. (2014). Clinical Outcomes of TECNIS Toric Intraocular Lens Implantation after Cataract Removal in Patients with Corneal Astigmatism. *Ophthalmology.*

Wang, B. and Ciuffreda, K. J. (2005a). Blur discrimination of the human eye in the near retinal periphery. *Optometry and Vision Science.* **82,** 52-58.

Wang, B. and Ciuffreda, K. J. (2006a). Depth-of-focus of the human eye: theory and clinical implications. *Survey of Ophthalmology.* **51,** 75-85.

Wang, B., Ciuffreda, K. J. and Vasudevan, B. (2006b). Effect of blur adaptation on blur sensitivity in myopes. *Vision Research.* **46,** 3634-3641.

Wang, L. and Koch, D. D. (2003a). Ocular higher-order aberrations in individuals screened for refractive surgery. *Journal of Cataract and Refractive Surgery.* **29,** 1896-1903.

Wang, L. and Koch, D. D. (2005b). Effect of decentration of wavefront-corrected intraocular lenses on the higher-order aberrations of the eye. *Archives of Ophthalmology.* **123,** 1226-1230.

Wang, L. I., Misra, M. and Koch, D. D. (2003b). Peripheral corneal relaxing incisions combined with cataract surgery. *Journal of Cataract and Refractive Surgery.* **29,** 712-722.

Wang, Z., Glazowski, C. E. and Zavislan, J. M. (2007). Modulation transfer function measurement of scanning reflectance microscopes. *Journal of Biomedical Optics.* **12,** 051802.

Watanabe, K., Negishi, K., Kawai, M., Torii, H., Kaido, M. and Tsubota, K. (2013). Effect of Experimentally Induced Astigmatism on Functional, Conventional, and Low-Contrast Visual Acuity. *Journal of Refractive Surgery.* **29,** 19-24.

Watanabe, K., Negishi, K., Torii, H., Saiki, M., Dogru, M. and Tsubota, K. (2012). Simple and accurate alignment of toric intraocular lenses and evaluation of their rotation errors using anterior segment optical coherence tomography. *Japanese Journal of Ophthalmology.* **56,** 31-37.

Wei, X. and Thibos, L. (2010). Design and validation of a scanning Shack Hartmann aberrometer for measurements of the eye over a wide field of view. *Optical Society of America.* **18,** 1134-1143.

Weinand, F., Jung, A., Stein, A., Pfutzner, A., Becker, R. and Pavlovic, S. (2007). Rotational stability of a single-piece hydrophobic acrylic intraocular lens: new method for high-precision rotation control. *Journal of Cataract and Refractive Surgery.* **33,** 800-803.

Weinreb, R. N. and Perlman, J. P. (1986). The effect of refractive correction on automated perimetric thresholds. *American Journal of Ophthalmology.* **101,** 706-709.

Who. 2007. Vision 2020. The Right to Sight. Global Initiative for the Elimination of Avoidable Blindness Action Plan 2006-2011. [Accessed December 17th 2014; Available at: http://www.who.int/blindness/Vision2020_report.pdf].

Williams, D. R. (2011). Imaging single cells in the living retina. *Vision Research.* **51,** 1379-1396.

Williams, D. R., Brainard, D. H., Mcmahon, M. J. and Navarro, R. (1994). Double-pass and interferometric measures of the optical quality of the eye. *Journal of the Optical Society of America.* **11,** 3123-3135.

Win-Hall, D. M. and Glasser, A. (2009). Objective accommodation measurements in pseudophakic subjects using an autorefractor and an aberrometer. *Journal of Cataract and Refractive Surgery.* **35,** 282-290.

Wold, J. E., Hu, A., Chen, S. and Glasser, A. (2003). Subjective and objective measurement of human accommodative amplitude. *Journal of Cataract and Refractive Surgery.* **29,** 1878-1888.

Wolffsohn, J. S., Bhogal, G. and Shah, S. (2011a). Effect of uncorrected astigmatism on vision. *Journal of Cataract and Refractive Surgery.* **37,** 454-460.

Wolffsohn, J. S. and Buckhurst, P. J. (2010a). Objective analysis of toric intraocular lens rotation and centration. *Journal of Cataract and Refractive Surgery.* **36,** 778-782.

Wolffsohn, J. S. and Davies, L. N. (2007). Advances in ocular imaging. *Expert Reviews in Ophthalmology.* **2,** 755-767.

Wolffsohn, J. S., Davies, L. N., Gupta, N., Naroo, S. A., Gibson, G. A., Mihashi, T. and Shah, S. (2010b). Mechanism of Action of the Tetraflex Accommodative Intraocular Lens. *Journal of Refractive Surgery.* **26,** 858-862.

Wolffsohn, J. S., Hunt, O. A., Naroo, S. A., Gilmartin, B., Shah, S., Cunliffe, I. A., Benson, M. T. and Mantry, S. (2006a). Objective accommodative amplitude and dynamics with the 1CU accomodative intraocular lens. *Investigative Ophthalmology and Visual Science.* **47,** 1230-1235.

Wolffsohn, J. S., Jinabhai, A. N., Kingsnorth, A., Sheppard, A. L., Naroo, S. A., Shah, S., Buckhurst, P., Hall, L. A. and Young, G. (2013). Exploring the optimum step size for defocus curves. *Journal of Cataract and Refractive Surgery.* **39,** 873-880.

Wolffsohn, J. S., Naroo, S. A., Motwani, N. K., Shah, S., Hunt, O. A., Mantry, S., Sira, M., Cunliffe, I. A. and Benson, M. T. (2006b). Subjective and objective performance of the Lenstec KH-3500 "accommodative" intraocular lens. *British Journal of Ophthalmology.* **90,** 693-696.

Wolffsohn, J. S., Sheppard, A. L., Vakani, S. and Davies, L. N. (2011b). Accommodative amplitude required for sustained near work. *Ophthalmic and Physiological Optics.* **31,** 480-486.

Woods, R. L., Colvin, C. R., Vera-Diaz, F. A. and Peli, E. (2010). A relationship between tolerance of blur and personality. *Investigative Ophthalmology and Visual Science.* **51,** 6077-6082.

Woolliams, P. D. and Tomlins, P. H. (2011). The modulation transfer function of an optical coherence tomography imaging system in turbid media. *Physics in Medicine and Biology.* **56,** 2855-2871.

Xi, L., Liu, Y., Zhao, F., Chen, C. and Cheng, B. (2014). Analysis of glistenings in hydrophobic acrylic intraocular lenses on visual performance. *International Journal of Ophthalmology.* **7,** 446-451.

Yang, H. C., Chung, S. K. and Baek, N. H. (2000). Decentration, tilt, and near vision of the array multifocal intraocular lens. *Journal of Cataract and Refractive Surgery.* **26,** 586-589.

Yeh, L. K., Chiu, C. J., Fong, C. F., Wang, I. J., Chen, W. L., Hsiao, C. K., Huang, S. C., Shih, Y. F., Hu, F. R. and Lin, L. L. (2007). The genetic effect on refractive error and anterior corneal aberration: twin eye study. *Journal of Refractive Surgery.* **23,** 257-265.

Yi, F., Iskander, D. R. and Collins, M. J. (2010). Estimation of the depth of focus from wavefront measurements. *Journal of Vision.* **10,** 3 1-9.

Yoshida, S., Obara, Y., Nishio, M., Fujikake, F. and Chikuda, M. (1998). Clinical results of three types of intraocular lenses for small incision surgery. *Nihon Ganka Gakkai Zasshi.* **102,** 678-684.

Yu, X., Dai, Y., Rao, X., Wang, C., Xue, L., Jiang, W. and Xiong, Y. (2010). A wavefront aberrometer for dynamic high-order aberration measurement. *Elsevier Science Ltd.* 1405-1411.

Zelichowska, B., Rekas, M., Stankiewicz, A., Cervino, A. and Montes-Mico, R. (2008). Apodized diffractive versus refractive multifocal intraocular lenses: Optical and visual evaluation. *Journal of Cataract and Refractive Surgery.* **34,** 2036-2042.

Zhe, D., Ning-Li, W. and Jun-Hong, L. (2010). Vision, subjective accommodation and lens mobility after TetraFlex accommodative intraocular lens implantation. *Chinese Medical Journal.* **123,** 2221-2224.

Zuberbuhler, B., Signer, T., Gale, R. and Haefliger, E. (2008). Rotational stability of the AcrySof SA60TT toric intraocular lenses: a cohort study. *BMC Ophthalmology.* **8,** 8.

Appendices

A1.   Ocular aberrations

The human eye is not a perfect, diffraction-limited optical system (Cervino *et al.*, 2008). Irregularities in ocular structures, particularly the cornea, give rise to higher order aberrations (Liang *et al.*, 1997;He *et al.*, 2000;McLellan *et al.*, 2002;Charman, 2005). Although it is generally accepted that aberrations degrade retinal image quality and therefore restrict the eye's visual capability (Queiros *et al.*, 2010), some reports suggest certain aberrations may in fact be beneficial to vision (Liang *et al.*, 1997;Rocha *et al.*, 2009b). Smirnov (1961) was one of the first to recognize the potential to enhance human vision by modifying the eye's aberrations.

The range of higher order aberrations that can occur in the human eye is extensive. It is generally accepted that no two people possess identical aberration profiles; instead every individual is thought to comprise both a unique pattern and quantity of different aberrations (Walsh *et al.*, 1984;Liang *et al.*, 1994;Liang *et al.*, 1997;Thibos *et al.*, 2002;Artal *et al.*, 2006;Piers *et al.*, 2007;Sawides *et al.*, 2011;Williams, 2011). Whilst there is much inter-subject variability with regards to the specific pattern and quantity of ocular aberrations present, there is little intra-subject variability. In fact there appears to be a positive correlation in the aberration pattern between a person's right and left eye, which implies that aberrations are not just random imperfections, but fulfil a role in human vision that has yet to be fully understood (Walsh *et al.*, 1984;Liang *et al.*, 1997;Thibos *et al.*, 2002;Charman, 2005;Artal *et al.*, 2006). Yeh *et al.* (2007) enrolled monozygotic and dizygotic twin pairs in a study in order to investigate the role of genetics in determining refractive error, corneal curvature and anterior corneal aberrations. They found a moderate correlation between the right and left eyes for vertical coma, secondary vertical coma, spherical aberration and secondary spherical aberration in monozygotic twins and between vertical coma, secondary horizontal coma and spherical aberration for dizygotic twins. They concluded that corneal aberrations, specifically spherical aberration and corneal astigmatism had a higher genetic predisposition compared with refractive error and other aberrations. This is in agreement with Dirani *et al.* (2009) who also identified a potential genetic component for HOAs.

Wavefront error maps can be used to convey information about the pattern of aberrations present (Holladay, 2009;Ravikumar, 2014) but generally do not clearly express the visually debilitating effect of wavefront error or which aberrations are present and in what quantity (Ravikumar, 2014). The root mean square (RMS) wavefront error provides a numerical value for the total ocular aberration but also does not specify the precise pattern of aberrations that constitute this total (Artal *et al.*, 2004;Sawides *et al.*, 2010). Wavefront aberration can also be arranged in terms of its Zernike polynomial which allows all aberrations to be categorized precisely and determination of the contribution of each aberration to the total RMS error (Applegate *et al.*, 2003a;Charman, 2005). Aberrations in the Zernike pyramid degrade visual acuity (VA) differently and therefore some impact on visual performance more so than others. Applegate *et al.* (2002) studied second, third and fourth order aberrations and found that aberrations towards the centre of the Zernike pyramid, with a lower angular frequency, produced a greater loss in VA compared to more peripherally located aberrations with higher angular frequencies. Thus defocus was found to degrade the visual image more so than astigmatism, likewise coma impacted on VA more than trefoil, and both spherical aberration and secondary astigmatism were found to be more detrimental to VA than tetrafoil (Applegate *et al.*, 2002).

Visual performance is most commonly assessed using high contrast photopic assessment of visual acuity. The association between aberrations and visual performance is complex as some aberrations degrade visual quality more so than others and this formed the basis for the development of image quality metrics which are more highly correlated to measures of visual performance (Ravikumar, 2014).

A1.1. Visual quality metrics

While Snellen acuity is used to evaluate the eyes ability to resolve detail, on its own it provides an insufficient assessment of visual performance. Image quality metrics can provide a greater insight regarding visual function and thus may be more useful (Ligabue *et al.*, 2009).

A1.1.1. Modulation Transfer Function

Visual quality metrics such as point spread function (PSF), modulation transfer function (MTF) and Strehl ratios can be used to assess visual performance. The MTF (see figure A1.1) illustrates how a point of light is distorted by the optics of the eye (Thibos *et al.*, 2004;Ligabue *et al.*, 2009).

Figure A1.1: Example of the MTF taken from a subject implanted with a concentric ring design MIOL. When the area beneath the MTF is maximised, better image quality is achieved (Ligabue *et al.*, 2009).

The MTF characterizes the resolution capability of an optical system or lens (Fujita *et al.*, 1992) and is a commonly used measure of image quality (Wang *et al.*, 2007;Roorda, 2011;Woolliams *et al.*, 2011). In general, measurement of the MTF utilizes the relationship between the spatial frequency of an image and modulation amplitude. Spatial frequency describes the rate of change in image luminance as a function of length and is usually expressed in cycles per degree, a unit which describes the number of cycles of a grating that subtend a one degree angle at the eye. Modulation amplitude is a measure of the difference in the maximum and minimum luminance of a grating. For a certain spatial frequency the modulation amplitude will be zero, at which point image intensity is uniformly spread. With increasing lens quality, there is a concurrent increase in the spatial frequency at which this point is reached, and this forms the basis of assessing lens quality using MTFs (Millodot, 2009).

Lopez-Gil *et al.* (1998) developed a near-infrared double pass imaging device in order to better understand the changes that occur to HOAs in the accommodated eye. They used a 784nm infrared light as opposed to the 632nm laser light that is typically used, in order to reduce dazzle and enable a truer measure of the effect of accommodation on aberrations to be obtained. Lopez-Gil *et al.* (1998) computed and then compared the MTF for the accommodated and unaccomodated eye and found that the MTFs were similar but generally slightly worse in the accommodated eye; this is consistent with the drop in image quality that occurs with accommodation (He *et al.*, 2000). The eye's natural response when focusing at close distances is characterized by the near vision triad, the components of which include binocular convergence, pupil miosis and accommodation (Kothari *et al.*, 2009;Bogdan *et al.*, 2010). The similarity in the MTFs between the unaccommodated and accommodated eye was attributed in part to this near vision triad due to the constricted pupil present in the accommodated eye. Defocus due to accommodative error is considered to be the main cause of image quality degradation during accommodation (Artal, 2000). A smaller pupil can help to negate some of this loss in image quality resulting in a similar MTF between the two accommodative states (Lopez-Gil *et al.*, 1998).

A1.1.2. Point Spread function

A point spread function provides a mathematical description of the distribution of light that has been emitted from a point source. It essentially characterizes the response of an imaging system to a point source (Huang *et al.*, 2002;Roorda, 2011). Objects may be considered an amalgamation of several point sources of light. The process by which all these points are overlapped to form an object is known as a convolution and from this the PSF can be calculated (Ligabue *et al.*, 2009). The shape and spread of the PSF is influenced by factors such as pupil size. As pupil size increases so too do the levels of wavefront aberrations which directly impact on the PSF. The point spread function that would be produced in a perfect, diffraction limited optical system, is commonly known as an Airy disk (Millodot, 2009). In highly aberrated eyes, an infinitely located point source would neither be imaged as a point nor a rotationally symmetric blurred point, instead the PSF would take on a more complex form (Ravikumar, 2014).

A1.1.3. Strehl ratio

The Strehl ratio is an example of a visual quality metric and is given by the ratio of the peak height of the PSF being measured to the peak height in a perfect optical system (Thibos *et al.*, 2004). It ranges from 0 to 1 with greater Strehl ratios indicating better image quality (Hofer *et al.*, 2001;Roberts Jr *et al.*, 2004;Ligabue *et al.*, 2009) and can be calculated as shown in equation A1.1.

$$\text{Strehl ratio} = \frac{\text{max PSF}}{\text{max PSF DL}}$$

<div align="right">Equation A1.1</div>

Where DL is the PSF in a diffraction-limited system, for the same pupil diameter.

A1.1.4. LogVSX

As alluded to in chapter 7, VSX shares a linear relationship with logMAR acuity (Ravikumar *et al.*, 2011) and can be calculated as shown in equation 7.1. Ravikumar *et al.* (2011) concluded that the LogVSX was an effective metric with numerous uses such as objectively assessing the likelihood of new intraocular lenses, designed to increase the depth of focus, producing noticeable blur to the patient.

A1.2. Factors affecting ocular aberrations

Ocular aberrations do not remain constant throughout life; instead they are dynamic and change with pupil size, age and accommodation (Artal *et al.*, 2002;Holladay *et al.*, 2002;Artal *et al.*, 2004;Ferrer-Blasco *et al.*, 2009;Queiros *et al.*, 2010;Li *et al.*, 2011).

A1.2.1. Pupil size

Liang *et al.* (1997) found that ocular aberrations vary with pupil size, with dilated eyes typically found to be more susceptible to aberration associated visual degradation than smaller pupils. This was corroborated by Applegate *et al.*, (2007) who measured ocular aberrations in 146 subjects aged between 20 and 80 years, with pupil diameters of 3, 4, 5, 6 and 7mm and found that the RMS wavefront error increased with larger pupil diameters for any given age group. It was also established that fourth order aberrations and above did not impact greatly on retinal image quality when pupil size was small, yet the same aberrations had a considerable impact on image quality in a dilated pupil (Liang *et al.*, 1997).

A1.2.2. Age

With age, there occurs a gradual rise in ocular aberrations (McLellan *et al.*, 2001;Brunette *et al.*, 2003;Fujikado *et al.*, 2004) particularly those originating from the crystalline lens (Wang *et al.*, 2003a;Ferrer-Blasco *et al.*, 2009) in addition to a measured and systematic fall in both retinal image quality (Artal *et al.*, 2002;Holladay *et al.*, 2002;Charman, 2005) and contrast sensitivity (McLellan *et al.*, 2001). Berrio *et al.* (2010) found that the higher order aberrations of the complete eye increased at a rate of approximately 0.032µm/year with relative increases in SA of about 0.0011µm/year and horizontal coma of approximately 0.0017 µm/year.

A1.2.3. Accommodation

As mentioned previously, age-related lenticular changes are known to affect the overall wavefront aberration of the eye by generating increased aberrations. Similarly lenticular changes due to accommodation also affect the total wavefront aberration of the eye. A young eye is able to bring into clear focus objects at close distances

because of its ability to accommodate; this ability declines gradually with age in a process termed presbyopia (Gilmartin, 1995). As the eye accommodates the crystalline lens undergoes significant changes to both its shape and location within the eye, in order to focus objects at varying distances. Both of these changes occur in response to ciliary muscle contraction (Helmholtz, 1855;Glasser *et al.*, 1998). For near objects the ciliary muscle contracts forcing the young and flexible crystalline lens to adopt a more convex form, with a greater positive refractive power. This enables close objects to be precisely focused onto the retina to produce a sharp image. It is the misalignment of the crystalline lens in relation to other ocular structures that is thought to initiate the change in high order aberrations during accommodation (He *et al.*, 2000).

Artal (2000) suggested that on the whole ocular aberrations decreased with accommodation. Li *et al.* (2011) stated that spherical aberration, which reportedly decreases in relation to accommodative effort, changes more than any other aberration during accommodation. Other aberrations such as defocus and coma are also known to change with accommodation; however the precise direction of this change is less certain and appears to vary considerably from one individual to the next (Lopez-Gil *et al.*, 1998;He *et al.*, 2000;Charman, 2005;Li *et al.*, 2011).

In summary, there is much ambiguity as to the exact nature of the change in ocular aberrations that occur during accommodation with trends appearing to vary significantly between subjects.

A1.3. Measurement of ocular aberrations

Ocular aberrations can be measured in a number of ways. One of the earliest methods used for this purpose was the Foucault knife edge test, which is a simple and inexpensive test first described by Léon Foucault in 1858. In this test light is directed onto a knife edge either at or close to the centre of the mirror's radius of curvature, in doing so surface defects are amplified (Gaviola, 1936;Vandenberg *et al.*, 1993).

In recent times two different methods of assessing the wavefront aberration of the eye have evolved; the first technique involves comparing pairs of double pass retinal images and computing the wave aberration. The second more popular method is through the use of an aberrometer (Vandenberg *et al.*, 1993;Liang *et al.*, 1997;Porter *et al.*, 2001;Kuroda *et al.*, 2002).

A1.3.1. Double pass retinal imaging

This retinal imaging technique involves directing a point source, such as an infra red laser light, onto the retina and capturing images after retinal reflection and double pass through the ocular media. From these double pass images the modulation transfer function (MTF), which indicates the optical performance of the human eye and point spread function (PSF) can be calculated (Artal, 2000;Diaz-Douton *et al.*, 2006). The wavefront aberration of the eye can also be measured from this using phase-retrieval techniques (Artal *et al.*, 1995;Lopez-Gil *et al.*, 1997;Prieto *et al.*, 2000).

Originally, red 632nm light was used in this system, however, it was later shown that substituting this for a green 543nm light potentially reduced light scatter at the retina, which in turn improved the quality of the retinal images allowing more accurate estimates of the ocular MTF to be obtained (Williams *et al.*, 1994;Lopez-Gil *et al.*, 1997). The first double pass setup used equal entrance and exit pupil sizes, however this proved to be a major limitation of the system since it enabled only even aberrations to be imaged; important information about odd aberrations such as coma were lost. Without this vital phase information, although the MTF could be computed correctly,

the shape of the PSF was difficult to determine and consequently the wave aberration of the eye could not be accurately judged. To overcome this asymmetrical, sized entrance and exit pupils were used and was found to be an effective solution since it allowed the shape of the PSF to be accurately ascertained and this could then be used to recover accurate information about the wavefront aberration in the eye (Artal *et al.*, 1988;Artal *et al.*, 1995;Iglesias *et al.*, 1998a;Iglesias *et al.*, 1998b). While there is no doubt that double pass retinal imaging is a useful technique, it is known to underestimate retinal image quality. As such it has largely been superseded by other more accurate methods of wavefront assessment such as aberrometry (Artal *et al.*, 1994;Williams *et al.*, 1994;Artal *et al.*, 1995;Prieto *et al.*, 2000).

A1.3.2. Aberrometry

There are several types of aberrometer currently available to measure ocular aberrations; all are based upon slightly different measurement principles. The three leading types of aberrometer include the Hartmann-Shack objective wavefront sensor (Cheng *et al.*, 2003;Charman, 2005;Miranda *et al.*, 2009;Bueno *et al.*, 2010;Yu *et al.*, 2010) (Cheng *et al.*, 2003), the Tscherning objective aberrometer (Kaemmerer *et al.*, 2000;Mrochen *et al.*, 2000) and the Ray tracing aberrometer (Molebny *et al.*, 2000;Moreno-Barriuso *et al.*, 2001). Of the three, the Hartmann-Shack is currently the preferred aberrometer since it is thought to allow a faster and more accurate evaluation of the eye's higher order aberrations (Prieto *et al.*, 2000;Cheng *et al.*, 2003;Miranda *et al.*, 2009;Bueno *et al.*, 2010;Yu *et al.*, 2010).

A1.3.2.1. Hartmann-Shack aberrometer

A Hartmann-Shack wavefront sensor provides a relatively simple but accurate method of measuring the aberrations of the human eye. A spot of coherent light approximately 1mm wide is directed onto the fovea and reflects back from the retina. The Hartmann-Shack wavefront sensor uses this emerging spot of light alongside wave-front estimation with Zernike polynomials to measure the actual wavefront of that eye (Liang *et al.*, 1994;Charman, 2005). This system generally consists of identical microlenses also known as lenslets, set in a regular pattern. These lenslets, typically around 1024 in current commercially available devices, bring to a focus any of the reflected light that reaches them. In an aberration free eye, the lenslets will focus light at its precise focal point and a charged couple device (CCD) camera is carefully placed to coincide with the plane of ideally focused points that would be produced in such an eye. A focusing target is incorporated into the system and often also a means of correcting the subjects existing refractive error (Charman, 2005;Rocha *et al.*, 2009a).

In a perfect eye, the reflected light would be composed of parallel light rays, in other words a plane wavefront. These parallel light rays would be focused by the lenslets at their focal point on the optical axis which would fall perfectly onto the camera sensor to produce perfectly positioned point images, set in an identical pattern to that of the array of microlenses. In an aberrated eye however the returning wavefronts would not be plane and therefore when focused would fall less uniformly onto the carefully placed camera sensor producing a distorted replication of the lenslet array as shown in figure A1.2 The degree of displacement of these distorted point images from their ideal location would be governed by the degree of tilt of the emerging wavefront, which would in turn be influenced by the amount of aberration existing in the eye. From this, the Hartmann-Shack wavefront sensor is able to deduce important information about the type and intensity of aberrations present in an eye (Cheng *et al.*, 2003;Charman, 2005;Yu *et al.*, 2010).
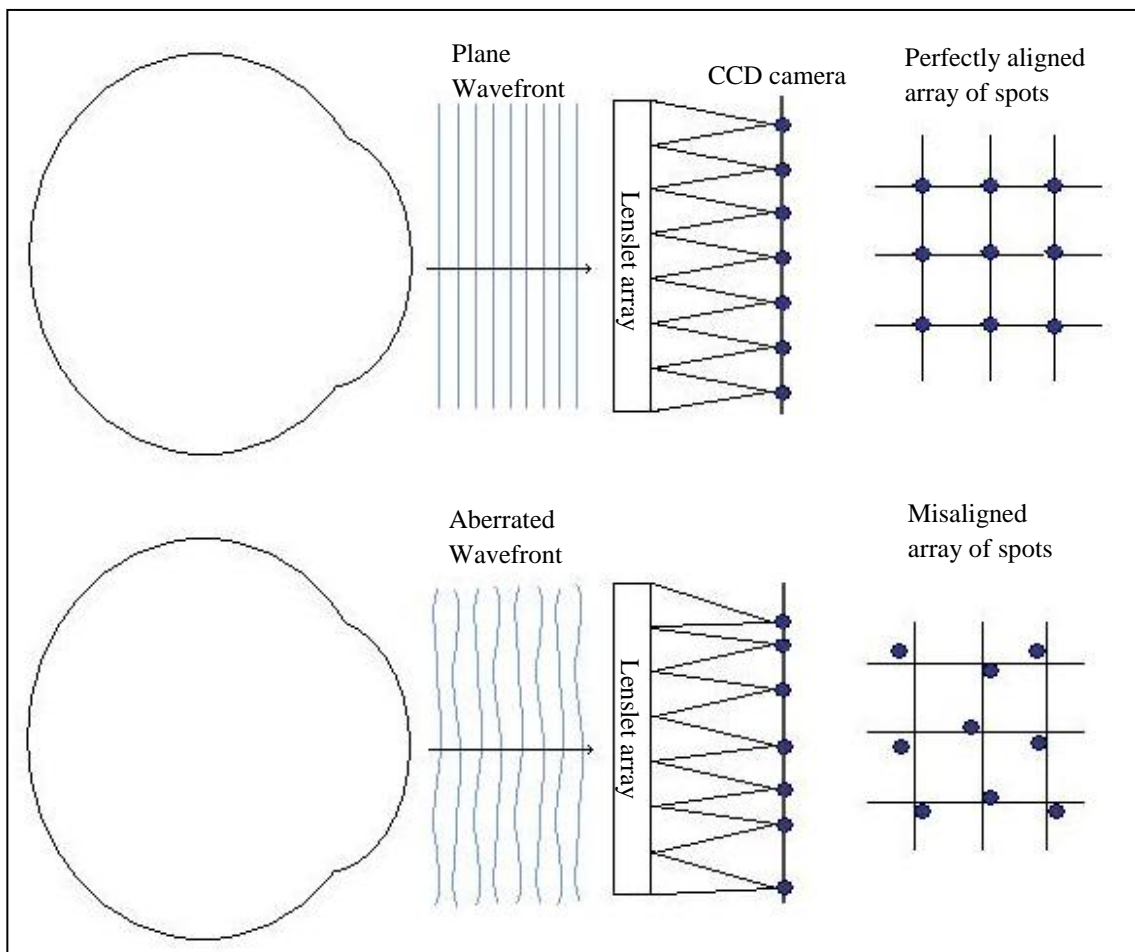
Figure A1.2: Simplified diagram of the mechanism of action of the Hartmann-Shack aberrometer.

A1.3.2.2. The Aston Aberrometer

The Aston open-field aberrometer is a miniaturized aberrometer designed to be slit-lamp mountable and is based on the Hartmann-Shack principle (Bhatt *et al.*, 2013). It is described in more detail in chapter 7.

A1.3.2.3. Tscherning aberrometer

The Tscherning aberrometer measures aberrations by projecting a regular lattice of spots onto the retina and using the distortions that are created in the pattern of spots, as a result of the eye's imperfections, to determine the HOAs present in that eye. A Nd: YAG (neodymium-doped yttrium aluminium garnet) laser beam, which has been frequency doubled so that it emits green light at a wavelength of 532nm as opposed to infrared light at a wavelength of 1064nm, is used to illuminate a 10mm grid pattern onto the retina, typically for 40 milliseconds. The returning spot pattern is imaged by indirect ophthalmoscopy onto a camera sensor that is linked to a computer. A comparison is then made of each spot in the imaged grid against the equivalent spot location in an ideal grid and from this the wavefront aberration can be calculated (Mrochen *et al.*, 2000;Krueger *et al.*, 2001) as shown in figure A1.3.

A target is usually used to aid alignment and an infrared tracking system can be used to monitor fixation (Kaemmerer *et al.*, 2000). One of the drawbacks of this particular aberrometer is its need for optically clear ocular media to facilitate accurate evaluation of the eye's aberrations (Kaemmerer *et al.*, 2000;Mrochen *et al.*, 2000;Krueger *et al.*, 2001;Yu *et al.*, 2010).
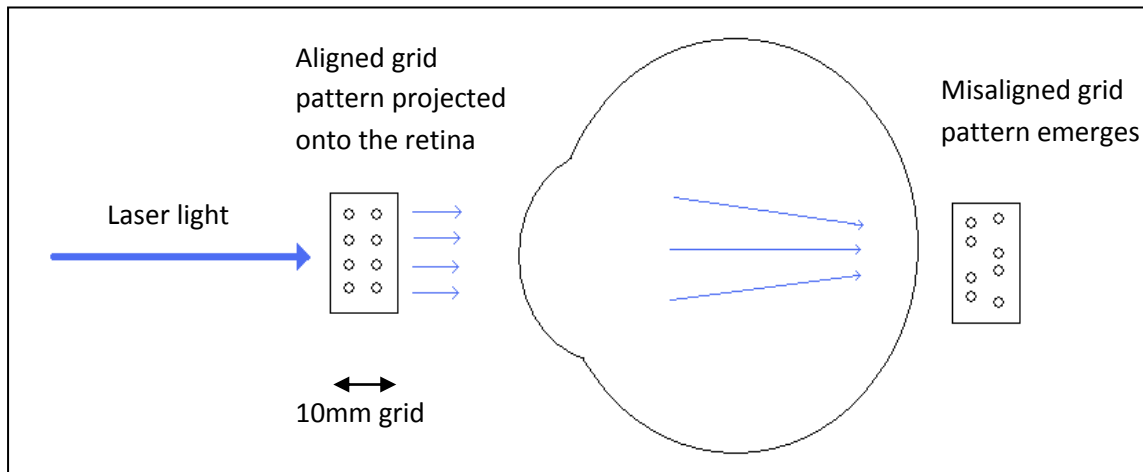

Figure A1.3: Simple diagram of the mechanism of action of the Tscherning aberrometer. A grid pattern is projected onto the retina using a laser light. The grid pattern is then imaged by a CCD and compared against the original to measure the wavefront aberration in that eye.

A1.3.2.4.Ray tracing aberrometry

A ray tracing aberrometer directs multiple parallel laser beams onto the retina via numerous points in the pupil. Each laser beam is usually 0.3mm wide with a wavelength of around 650nm. These light spots are then imaged onto a detector using an objective lens to create a map from which the wavefront aberrations are measured (Molebny *et al.*, 2000). One commercially available device, the Tracey ray tracing aberrometer, may incorporate an accommodative fixation target thereby permitting dynamic evaluation of aberrations. Previously, one of the problems encountered with this type of system was its sensitivity to a subject's eye movements. To overcome this, the length of time over which the eye is irradiated has been reduced in addition to the use of video tracking which only allows irradiation to occur when the eye and instrument are in perfect alignment (Molebny *et al.*, 2000;Moreno-Barriuso *et al.*, 2001;Yu *et al.*, 2010).

A2: Aston University Life and Health Sciences Ethics Committee acceptance of amendment to project AO2010.14 JW.

Aston University
Birmingham

Aston Triangle
Birmingham B4 7ET
United Kingdom
Tel +44 (0)121 204 3000

www.aston.ao.uk

MEMORANDUM

DATE: 24 January 2013

TO: Prof James Wolffsohn
           Cc: Rachel Giles, administrator to the Life and Health Sciences Research Ethics
           Committee

FROM: Dr. Robert Morse
           Chair of the Life and Health Sciences Research Ethics Committee

SUBJECT: Project AO2010.14 JW. "Assessment of visual function and optics of intraocular lenses"

I am writing to inform you that the following minor proposed changes to the above project as
described in your letter of December 14th 2012 and subsequent email of 14th January 2013 have
been approved:

- Postgraduate student Sandeep Dhallu added to the list of investigators.
- Ethics approval extended to end of December 2015.
- 300 new participants to be tested across 6 new intraocular lens.

No documents have been amended.

The Ethic Committee's approval applies only to research conducted in accordance with the
amended protocol and documentation approved by the LHS REC, any change to the protocol must
be approved by the Committee prior to its implementation.

The details of the investigation will be placed on file. You should notify me of any difficulties
experienced by the volunteer subjects, and any significant changes which may be planned for this
project in the future.

Yours sincerely

Dr Robert Morse
Chair of the LHS Research Ethics Committee

A3: Aston University Life and Health Sciences Ethics Committee Decision letter for project 606.

Aston University
Birmingham

Aston Triangle
Birmingham B4 7ET
United Kingdom
Tel +44 (0)121 204 3000

www.aston.ac.uk

Memo

Life and Health Sciences Research Ethics Committee's Decision Letter

To: Professor James Wolffsohn

           Cc: Rachel Giles, administrator to the Life and Health Sciences Research Ethics Committee

From: Dr Corinne M. Spickett

           Chair of the Life and Health Sciences Research Ethics Committee

Date: 20/2/2014

Subject: Project #606: Evaluating visual acuity with different levels of induced spherical and astigmatic blur and ocular aberrations and pupil size using an aberrometer

Thank you for your resubmission. The additional information for the above proposal has been considered by the Chair of the LHS Ethics Committee.

Please see below for details of the decision and the approved documents that have been uploaded on the LHS Ethics website.

Reviewer's recommendation: Approved

Please see the tabled list below of approved documents:

Documentation	Version/s	Date	Approved
Participant information sheet	participant_information_sheet-v2-amended_5-2-14	17-02-2014	√
Response to queries	ethics_amendments	17-02-2014	√

After starting your research please notify the LHS Research Ethics Committee of any of the following:

Substantial amendments. Any amendment should be sent as a Word document, with the amendment highlighted. The amendment request must be accompanied by all amended documents, e.g. protocols, participant information sheets, consent forms etc. Please include a version number and amended date to the file name of any amended documentation (e.g. "Ethics Application #100 Protocol v2 amended 17/02/12.doc").

**New Investigators**

The end of the study

Please email all notifications and reports to lhs_ethics@aston.ac.uk and quote the original project reference number with all correspondence.

Ethics documents can be downloaded from: http://www.ethics.aston.ac.uk/documents-all. Please note that these documents can ONLY be opened using Mozilla Firefox or the latest Internet Explorer version (IE9).

Statement of Compliance

The Committee is constituted in accordance with the Government Arrangements for Research Ethics Committees (July 2001) and compiles fully with the Standard Operating Procedures for Research Ethics Committees in the UK. In accord with University Regulation REG/11/203(2), this application was considered to have low potential risk and was reviewed by three appropriately qualified members, including the Chair of the Life and Health Sciences Ethics Committee.

Yours sincerely,
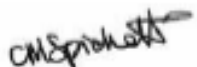
CMSpickett

Dr Corinne M Spickett
Chair of the LHS Ethics Committee

A4:   Patient Information sheet and consent form for experimental participants at Aston University.

A.4.1: Reducing the effect of toric intraocular lens misalignment using a split surface approach.

PATIENT INFORMATION SHEET

Research workers, school and subject area responsible
Professor James Wolffsohn, School of Life & Health Sciences, Aston University
Dr Amy Sheppard, School of Life & Health Sciences, Aston University
Miss Sandeep Dhallu, School of Life & Health Sciences, Aston University

Project Title
Reducing the effect of toric intraocular lens misalignment using a split surface approach.

Invitation
You are being invited to take part in a research study. Before you decide whether you wish to participate, please take the time to read this information sheet detailing why the research is being done and what it will involve.

What is the purpose of the study?
To investigate whether splitting toric lens power results in greater patient tolerance to lens rotation.

Where will the study take place?
Ophthalmic Research Group laboratories, Vision Sciences, Aston University, Birmingham, B4 7ET.

Inclusion and Exclusion Criteria
To take part in this study, you must be at least 18 years of age and have refractive astigmatism of no more than -3.50DC. You must also have best corrected visual acuity of at least 6/9 or better in the eye being tested, be free of any active eye disease, not on ocular medications or systemic medications with known ocular side effects and have no history of eye surgery within the last 3 months. If you are a contact lens wearer, you must remove your contact lenses before any tests are carried out but you may re-insert them after testing.

What will happen to me if I take part?
By volunteering to participate in this study, you will be invited to attend the Ophthalmic Research Group's laboratories to sit for a non-contact, non-invasive test.

Data collection will start with you being asked to wear a trial frame with your distance correction in place. The prescription will be refined to ensure it is accurate and up to date and your visual acuity will be checked at this point.

After this one of two things will happen, depending on your prescription. Either an additional cylindrical lens will be added to the trial frame in order to induce astigmatism followed by a further two cylindrical lenses of half the power to correct this astigmatism. Or, if you have a toric component to your prescription of between -1.00DC to -3.50DC then two cylindrical lenses, each of half the power will be used to correct your own astigmatism. The orientation and separation of these two correcting cylinders will be altered numerous times throughout the test, and each time you will be asked to read a distance letter chart and your visual acuity will be recorded.

All measurements will be taken on one eye only and the visit is expected to last approximately 30minutes.

Are there any potential risks in talking part in the study?
There are no known risks involved with the instruments or techniques listed above. All measurements will be taken in accordance with the manufacturers' guidelines by a GOC (General Optical Council) registered Optometrist.

Do I have to take part?
No, you do not have to participate if you do not wish to do so. You are free to withdraw at any time from the project. Your decision to participate (or not) will not influence your ability to participate in any future research.

Expenses and payments
Your participation in this study is voluntary. No expenses or payments will be offered.

Will my taking part in this study be kept confidential?
Privacy and confidentiality will be protected vigorously to the extent permissible by law. Your name will be turned into a code, the details of which will be kept on a separate database which will only be accessed by the investigators. Analysis of data by others, including the internal project examiner, will only be undertaken in the coded format to prevent a breach of confidentiality. We cannot, however, guarantee privacy or confidentiality.

What will happen to the results of the research study?
We aim to publish the results of this project. However, there will be no reference to any individual's performance in any publication. A copy of the entire thesis (that this study will contribute to) will be available from the British Library.

Who is organising and funding the research?
The project is being conducted by a research team at Aston University and is funded by Lenstec, Florida.

Who has reviewed the study?
The research has been submitted to the LHS Research Ethics Committee, Aston University.

Who do I contact if something goes wrong or I need further information
Please contact the principal investigator, Professor James Wolffsohn J.S.W.Wolffsohn@aston.ac.uk .

Please email Sandeep Dhallu at dhallus@aston.ac.uk if you are interested in taking part in this study.

CONSENT FORM

Title of Project
Reducing the effect of toric IOL misalignment using a split surface approach.

Research Venue
Ophthalmic Research Group laboratories, Vision Sciences, Aston University, Birmingham, B4 7ET.

Name of Investigators
Miss Sandeep Dhallu, Professor James Wolffsohn and Dr Amy Sheppard.

Please initial inside each box:

1.   I confirm that I have read and understand the information sheet
        for this study and have had the opportunity to ask questions.   ☐

2.   I understand that my participation is voluntary and that I am free
        to withdraw at any time without giving any reason, without my legal   ☐
        rights being affected.

                                                                               ☐

3.   I agree to take part in the above study.

_____   _____   _____
Name of Research Participant   Date   Signature

_____   _____   _____
Name of Person taking Consent   Date   Signature

                        1 copy for research participant
                        1 copy for investigator

A.4.2: Evaluating visual acuity with different levels of induced spherical and astigmatic blur and ocular aberrations and pupil size using an aberrometer.

PATIENT INFORMATION SHEET

Research workers, school and subject area responsible
Professor James Wolffsohn, School of Life & Health Sciences, Aston University
Dr Amy Sheppard, Optometry, School of Life & Health Sciences, Aston University
Miss Sandeep Dhallu, Optometry, School of Life & Health Sciences, Aston University

Proposed Project Title
Evaluating visual acuity with different levels of induced spherical and astigmatic blur and ocular aberrations and pupil size using an aberrometer.

Invitation
You are being invited to take part in a research study. Before you decide whether you wish to participate, please take the time to read this information sheet about why the research is being done and what it will involve.

What is the purpose of the study?
The aim of this study is to determine how different levels of blur affect visual perception, ocular aberrations (which occur due to small imperfections in the eye's optics) and pupil size.

Where will the study take place?
Ophthalmic Research Group laboratories, Vision Sciences, Aston University, Birmingham, B4 7ET.

Inclusion and Exclusion Criteria
In order to participate in the study subjects will need to:

- be aged 18 years and over
- have good corrected visual acuity in the eye being tested
- be willing to wear a daily disposable contact lenses for the duration of the test if vision without spectacles does not meet the required standard
- be free of any active eye disease
- be free of ocular medications or systemic medications with known ocular side effects and
- have had no history of eye surgery within the last 3 months.

What will happen to me if I take part?
You will be invited to attend the Ophthalmic Research Group's laboratories to sit for a test. A basic refractive examination will be conducted by a qualified optometrist to ensure you are wearing the most accurate distance prescription for the study. Your subjective visual acuity, which is a measure of how clearly you can see, will be taken with different levels of induced blur. Astigmatic blur is caused by the eye's inability to focus an image to a sharp point and occurs due to the irregular curvature of the cornea

or lens. With spherical blur, the image is focused to a sharp point however this point does not fall on the retina, it falls either in front (termed myopia) or behind the retina (termed hyperopia) and also causes blur. Astigmatic blur between 0 and -3.00DC at axes between 0 and 180° and increasing levels of spherical blur between +2.00 to -10.00DS in -0.50 steps will be induced as subjective visual acuity is measured using a digital test chart that is placed four metres away. While you are doing this an instrument you will be look through will assess the optics of your eyes and measure your pupil size. We will also ask you to identify which out of several images displayed on a computer screen are blurred and test how close we can bring some letters to you before you can no longer focus on them clearly. Your field of vision will also be measured using the Humphrey visual field analyzer. This test will be done monocularly; therefore the eye not being tested will be covered with an eye patch. This will be conducted twice, once when corrected for close distances and once when corrected for far distances.

Are there any potential risks in talking part in the study?
There are no known risks involved with the instruments or techniques listed above. All measurements will be taken in accordance with the manufacturers' guidelines by a GOC registered Optometrist.

Do I have to take part?
No, you do not have to participate if you do not wish to do so. You are free to withdraw at any time from the project. Your decision to participate (or not) will not influence your ability to participate in any future research.

Will my taking part in this study be kept confidential?
Privacy and confidentiality will be protected vigorously to the extent permissible by law. Your name will be turned into a code, the details of which will be kept on a separate database which will only be accessed by the investigators. Analysis of data by others, including the internal project examiner, will only be undertaken in the coded format to prevent a breach of confidentiality. We cannot, however, guarantee privacy or confidentiality.

What will happen to the results of the research study?
We aim to publish the results of this project. However, there will be no reference to any individual's performance in any publication. A copy of the entire thesis (that this study will contribute to) will be available from the British Library.

Who is organising and funding the research?
The project is being conducted by a research team at Aston University and is funded by Lenstec, Florida.

Who has reviewed the study?
The research has been submitted to the LHS Research Ethics Committee, Aston University.

Who do I contact if something goes wrong or I need further information
Please contact the principal investigator, Professor James Wolffsohn at J.S.W.Wolffsohn@aston.ac.uk or telephone on 0121 204 4140.

Who do I contact if I wish to make a complaint about the way in which the research is conducted?

If you have any concerns about the way in which the study has been conducted, then you should contact the Secretary of the University Research Ethics Committee at j.g.walter@aston.ac.uk or telephone 0121 204 4665.

Please email Sandeep Dhallu at dhallus@aston.ac.uk if you are interested in taking part in this study.

CONSENT FORM

Proposed Title of Project

Evaluating visual acuity with different levels of induced spherical and astigmatic blur, ocular aberrations and pupil size using an aberrometer.

Research Venue
ORG laboratories, Vision Sciences, Aston University, Birmingham, B4 7ET

Name of Investigators
Miss Sandeep Dhallu, Professor James Wolffsohn and Dr Amy Sheppard.

Please initial box

1. I confirm that I have read and understand the information sheet for this study and have had the opportunity to ask questions. ☐

2. I understand that my participation is voluntary and that I am free to withdraw at any time without giving any reason, without my legal rights being affected. ☐

3. I agree to take part in the above study. ☐

_____   _____   _____
Name of Research Participant   Date   Signature

_____   _____   _____
Name of Person taking Consent   Date   Signature

1 copy for research participant
1 copy for investigator

A5: **Supporting Publications**

Dhallu, S. K., Wolffsohn, J. S., Sheppard, A. L. (2014). Evaluating the effect of splitting cylindrical power on improving patient tolerance to toric lens misalignment. *Contact Lens and Anterior Eye.* **37**, 191-195.

Berrow, E. J., Wolffsohn, J. S., Bilkhu, P. S. and Dhallu, S. (2014). Visual performance of a new bi-aspheric, segmented, asymmetric multifocal IOL. *J Refract Surg.* **30,** 584-588.